Laboratoire de **T**ribologie et
Dynamique des **S**ystèmes
UMR 5513

N° 2009-17

Année 2009

THESE

présentée devant

L'ECOLE CENTRALE DE LYON

pour obtenir le grade de DOCTEUR

Spécialité : Matériaux

par

Dabing LUO

Master Université Jiaotong du Sud-Ouest (Chine)

SELECTION OF COATINGS FOR TRIBOLOGICAL APPLICATIONS

CHOIX DES REVETEMENTS POUR APPLICATIONS TRIBOLOGIQUES

Soutenue le 23 septembre 2009 devant la commission d'examen composée de

Léo VINCENT	Professeur, Ecole Centrale de Lyon	Président de jury
Amílcar RAMALHO	Professeur, Universidade de Coimbra, Portugal	Rapporteur
Cécile LANGLADE	Professeur, Université de Technologie de Belfort-Montbéliard	Rapporteur
Christine BOHER	Docteur, Ecole des Mines d'Albi Carmaux	Membre
Vincent FRIDRICI	Docteur, Ecole Centrale de Lyon	Co-directeur de thèse
Philippe KAPSA	Directeur de Recherche CNRS, Ecole Centrale de Lyon	Directeur de thèse

ACKNOWLEDGEMENT

First, I express my sincere gratitude to Prof. Philippe KAPSA, my supervisor of the thesis, for giving me the opportunity of studying in his group and supporting me during the whole thesis work. His wide knowledge in the tribology field has broadened my mind.

I address my special appreciation to Dr. Vincent FRIDRICI, my co-supervisor of the thesis. During the last three years, he gave me many valuable suggestions to promote the advance of the work, and he also patiently and critically proofread the manuscript.

I would like to thank Prof. Léo VINCENT for acting as the president of the jury. His achievements in tribology field are admirable. I want to thank the reviewers of the thesis, Prof. Amilcar RAMALHO and Prof. Cécile LANGLADE, for their hard work during the hot summer. Prof. Amilcar RAMALHO gave me many interesting suggestions when he was visiting LTDS in 2008, and his kindness left me a deep impression. I also thank Dr. Christine BOHER as a member of the jury.

I am so grateful to Prof. Zhongrong ZHOU, professor of Tribology Research Institute in Southwest Jiaotong University, for being my supervisor in China. He opened the first door for me towards the tribology field and recommended me to study in LTDS.

I address my appreciation to Gérard MEILLE, Jean-Christophe ABRY, Sophie PAVAN, Sandrine BEC, Denis MAZUYER, Bernard BEAUGIRAUD, Gaëtan BOUVARD, Jing ZHAO, Imen LAHOUIJ, Juliette CAYER-BARRIOZ, Romain CHARPENAY, Pierre-Henri CORNUAULT, Florian BREMOND, Francois-Pierre NINOVE, Maxime RUET ... all the colleagues in the laboratory LTDS for their generous help.

I wish to thank China Scholarship Council and le Groupe des Ecoles Centrales. Due to their financial support, the thesis became possible.

At the end, I must appreciate my wife, my daughter and my parents. I cannot finish the thesis without their support and understanding.

Contents

CHAPTER 5: EFFECT OF TEST CONDITIONS ON TRIBOLOGICAL PERFORMANCE OF COATINGS: EXTENSION OF THE DISSIPATED ENERGY APPROACH

CHAPTER 6: EFFECT OF COATING PROPERTIES ON TRIBOLOGICAL PERFORMANCE: COATING SELECTION PROCESS

INTRODUCTION

The objectives of this thesis are to systemically discuss the selection process of tribological coatings, and to propose some approaches to evaluate and compare coatings, sequentially to help the selection of tribological coatings.

Background

In tribological applications, using coatings is an effective and relatively economical measure to reduce friction and protect the substrate surface from wear. However, selecting the appropriate coating for a given tribological application is still difficult and complicated because the tribological response of a coating system depends on many factors (coating properties, counterpart, substrate, interface and running conditions). There is no general rule to help the coating selection.

Additionally, many new deposition techniques and new coatings are being continuously developed, which provides a wide range for the selection of tribological coatings. At the same time, it also brings the coating users a problem: how to find the most suitable coating from numerous possibilities for a specific tribological application? The current method is trial and error, which is time-consuming and expensive, and some better coatings are probably missed.

Objectives and research approaches

The objectives of the thesis are to systemically discuss the coating selection process, to develop a coating pre-selection tool (based on analysis of contact and use of coating database), and to propose some approaches for evaluating and comparing coatings, sequentially to help the selection of tribological coatings.

Around the objectives, the following research approaches will be realized. At first, literature study and case studies will be carried out to investigate the research progress in the field and general coating selection process. Based on the investigation, a coating pre-selection tool will be developed, comprehensively considering factors from various aspects, to select candidate coatings for further tests. Then, two kinds of experiments (one coating under different conditions and 5 coatings under the same conditions) will be performed for understanding the relationships between the tribological behaviors of coatings and coating properties and running conditions. Finally, according to the experiments, some approaches will be proposed to predict coating lifetime, or evaluate and compare coatings.

Organization of the manuscript

The manuscript is organized as presented in Figure 1.

In Chapter 1, literature study will be summarized, including the common deposition methods and coating types and structures used in tribological applications, tribological response of coating systems, important parameters influencing the tribological behaviors, coating selection methods and the prediction of coating lifetime.

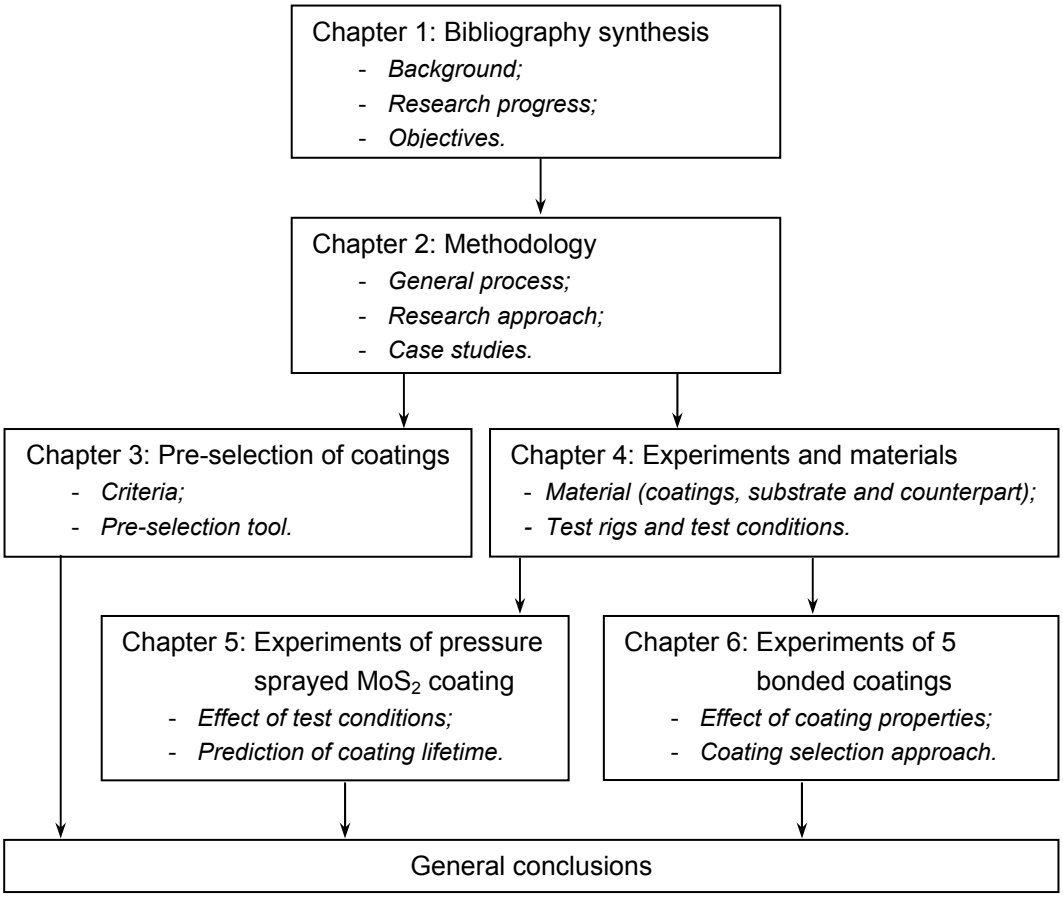

Figure 1: Organization of the manuscript.

Methodology of coating selection will be discussed in Chapter 2. Three case studies will be performed to understand the general coating selection process and difference requirements for the coatings under different tribological conditions.

Pre-selection criteria and strategies of coatings will be discussed and a relevant pre-selection tool will be developed in Chapter 3.

Chapter 4 will introduce the relevant experiments and materials. 6 solid lubrication coatings (pressure sprayed MoS_2 coating and 5 bonded commercial coatings) will be investigated by fretting tests, sliding tests and simple evaluation techniques.

In Chapter 5, the effect of test conditions on tribological performance of coatings will be investigated through the experiments of a pressure sprayed MoS_2 coating under different contact configurations (ball-on-disk sliding, cylinder-on-flat fretting and ball-on-flat fretting). The prediction of coating lifetime will be discussed.

In Chapter 6, coating properties of the 5 bonded solid lubricant coatings will be investigated by simple evaluation techniques, and the relationships between coating properties and tribological performance will be discussed. According to the experiments, a systemic approach will be put forward to comprehensively evaluate and compare the coatings and help the coating selection.

CHAPTER 1

BIBLIOGRAPHY SYNTHESIS

CHAPTER 1: BIBLIOGRAPHY SYNTHESIS

CHAPTER 1: BIBLIOGRAPHY SYNTHESIS

In this chapter, literature study is summarized to understand the research context, including deposition methods, coating structures, wear mechanisms of coating systems, important parameters influencing tribological performance of coating systems, coating selection methods and wear prediction.

1 Introduction

1.1 Why are coatings used in tribological applications?

The energy losses due to friction in the industrialized countries represent an annual cost estimated at between 5 and 7% of their Gross Domestic Product, and approximate one-third of the world's energy resources in present use appear as friction in one form or another [1]. Every year, hundreds of thousands of components in industries are disused due to excessive wear. On the other hand, it has been estimated that 10% of oil consumption in the United States is used simply to overcome friction [2]. In a vehicle, a reduction of friction among components of engines could annually reduce about 5% (i.e., 30 billion liters of fuel) global consumption of fuel accompanied by an annual decrease of 250 million tons of CO_2 emissions. Therefore, from the viewpoint of both energy saving and environmental protection, it is a considerable issue to reduce friction and control wear through applying tribological principles (the suitable use of materials, lubricants, coatings, surface treatments and special structure designs).

Surface engineering, including surface treatments and coatings, is one of the most effective and flexible solutions for tribological problems. Coatings change tribological systems by inducing residual compressive stresses, decreasing the friction coefficient, increasing the surface hardness, altering the surface chemistry, changing the surface roughness [3]. So, they improve the wear resistance of surfaces and extend the lifetime of relevant components. During last several decades, numerous coatings and deposition methods have been successfully developed, and used to reduce friction or/and to protect surfaces from damage in mechanical systems. The increasing use of coatings in tribological applications is mainly based on the following reasons:

- More and more scientists recognize that the surface is the most important part in many engineering components, and most failures have a relationship with the properties of the surface area.

- Many other functionally important properties depend on the surface area, such as electronic, magnetic, optical, bio-compatible characteristics.

- Higher and higher performance is required for mechanical components and tools, which cannot be realized just by selecting materials or improving structures. The use of coatings can improve the performance of surface regions for friction reduction, wear resistance, corrosion resistance and other functionally attributes; at the same time, the substrate remains its original properties, responsible for the strength and toughness.

- In some special situations, the systems cannot normally function without advanced tribological coatings; for example, devices and bearing systems in space mechanisms operating under near-vacuum conditions, or engineering components in aero-turbines running under corrosive or erosive conditions.

- Development of technologies produces some new deposition processes, which gives the possibility of depositing coatings with high performance that was previously unachievable.

However, with the development of surface engineering, there are several problems. It is impossible to deposit coatings with all of the desired properties, such as low shear strength, high hardness, excellent bonding strength, high toughness, etc. because some of them are in conflict with each other. For example, high hardness will sacrifice toughness and bonding strength. Therefore, we need to select the most suitable one from hundreds of thousands of coatings for a specific application, but how can we realize it? The use of coatings is a very complex situation, and there is no general rule to help the selection of coatings for various tribological applications.

The current selection method is usually based on two processes. One is to try a coating, and if it works it will be used; so some more suitable coatings will be neglected. The other is trial and error, which is time consuming and expensive. The objective of this thesis is to propose some approaches and develop a tool to help the coating selection for tribological applications.

1.2 Coating deposition

1.2.1 Deposition methods

1.2.1.1 Classification of deposition methods

The applications of deposition techniques in industrial areas rapidly increase since the successful application of decorative coatings in the late 1950s; especially during the last two decades, the rapid development of microelectronic resulted in many new deposition processes.

Facing so many deposition methods, some schemes were devised to classify or categorize coating processes, none of which are very satisfying because some processes overlap different categories. For example, Kern and Schuegraf [4] grouped thin-film deposition technologies according to evaporative, glow-discharge, gas-phase chemical, and liquid-phase chemical processes. Chapman and Anderson [5] suggested to group deposition processes into conduction and diffusion processes, chemical processes, wetting processes, and spraying processes. The classifications proposed by Holmberg and Matthews [6] and Bunshah [7] are clearer. Holmberg and Matthews divided the processes into four groups (gaseous, solution, molten and semi-molten, and solid) according to the state of deposition phase, as shown in Figure 1. Bunshah gave a classification of deposition methods based on the dimensions of the depositing specie, e.g., whether it is atoms/molecules, liquid droplets or bulk quantities, as shown in Table 1.

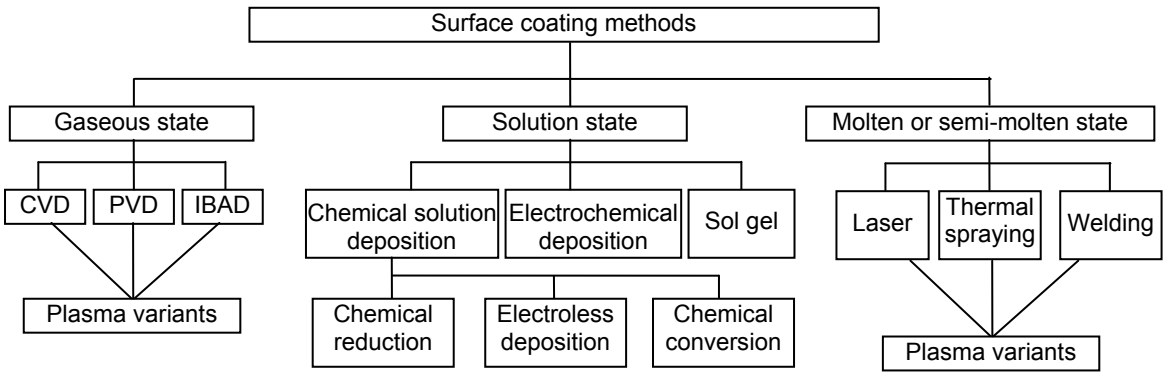

Figure 1: A general classification of surface engineering techniques [6].

Table 1: Methods of fabricating coatings [7].

Atomistic Deposition	Particulate deposition	Bulk coating	Surface modification
Electrolytic environment - Electroplating - Electroless plating - Fused salt electrolysis - Chemical displacement ***Vacuum environment*** - Vacuum evaporation - Ion Beam Deposition - Molecular beam epitaxy ***Plasma environment*** - Sputter deposition - Activated reactive evaporation - Plasma polymerization - Ion plating ***Chemical vapor environment*** - Chemical vapor deposition -- Reduction -- Decomposition -- Plasma enhanced - Spray pyrolysis ***Liquid phase epitaxy***	***Thermal spraying*** - Plasma spraying - D-gun - Flame spraying ***Fusion coatings*** - Thick film ink - Enameling - Electrophoretic ***Impact plating***	***Wetting process*** - Painting - Dip coating ***Electrostatic spraying*** - Printing - Spin coating ***Cladding*** - Explosive - Roll bonding ***Overlaying*** - Weld coating	***Chemical conversion*** - Electrolytic -- Anodization - Fused salts ***Chemical-liquid*** ***Chemical-vapor*** - Thermal - Plasma ***Leaching Mechanical*** - Shot peening ***Thermal surface enrichment*** - Diffusion from bulk ***Sputtering Ion implantation***

1.2.1.2 Common deposition methods for tribological coatings

There are many coating deposition methods, but not all of them are suitable for tribological applications due to their poor bonding strength, thin achievable thickness, etc. Some of them are developed for electronic, optical or decorative applications. The common deposition methods for tribological coatings include bonding, electrochemical deposition, thermal spraying, chemical vapor deposition, physical vapor deposition, welding, etc.

▪ Bonding

Solid lubricant coatings usually cover the substrate surfaces through a bonding process, where the solid lubricant particles are mixed into organic or inorganic binding agents, and then the liquid mixture is applied on the substrate surface by immersion, brushing, or spraying, etc. It is an efficient and inexpensive process, the coating performances depend on the following factors [8]:

- *Pretreatment of substrate surfaces*: before being applied the coatings, the substrate surfaces should be thoroughly degreased and roughened by ultrasonic cleaning, sand blasting or phosphatizing to improve the bonding strength of the coatings on the substrates.

- *Drying and hardening*: depending on the used binding agent, a bonded coating should be dried and hardened at suitable temperature during an appropriate period, which also influences the bonding strength between the coatings and the substrates.

- *Coating thickness*: every bonded coating has an optimum thickness range, and an excessively thick coating will result in poor bonding strength or excessive brittleness.

▪ Electrochemical deposition

Electrochemical deposition, also called electroplating, is the process of depositing a thin metal or alloy coating on an electrode (electrically conductive substrate) by an electrolysis process under external electrical current, as shown in Figure 2. The electrode made of coating material works as the

anode, and the part plated is the cathode in the circuit, where they are connected to an external direct current supply. Both the anode and cathode are immersed in an electrolyte bath, which contains dissolved metal salts and other ions to permit the flow of electricity. Under the effect of electrical current, ions in the bath are continuously deposited on the cathode, and the anode slowly dissolves to supply ions into the bath. In some electroplating processes, a nonconsumable anode like lead may be used, where ions to be plated must be periodically putted into the bath.

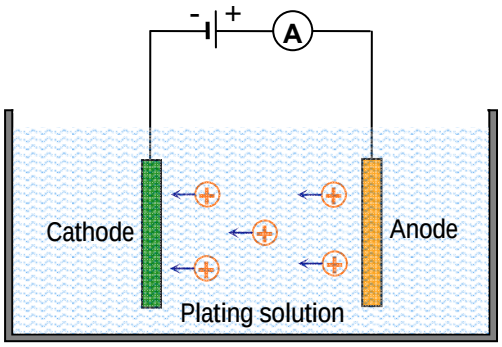

Figure 2: Scheme of electroplating process.

In engineering, electroplating is primarily used for enhancing surface performance (e.g., abrasion and wear resistance, corrosion protection, lubricity, etc.) through depositing a layer of material to a surface. Another application of electroplating is to repair worn parts and to make them rework with a less expensive cost.

Hard chromium plating is the most successfully applied electroplating process due to its excellent bonding strength, high hardness, good thermal conductivity and corrosion resistance, and the retention of the lubricating film resulting from its porosity. It is widely applied in industrial products, such as piston rings, shock absorbers, struts, brake pistons, engine valve stems, cylinder liners, hydraulic rods, aircraft landing gears, textile and gravure rolls, plastic rolls, and dies and molds [9].

- **Thermal spraying**

In thermal spraying processes, the deposited materials, in the form of powder, wire or rod, are fed to a torch or gun and are heated to near or somewhat above their melting point. The molten or nearly molten droplets of material are accelerated in a gas stream and projected on the substrate surface, as shown in Figure 3. On impact, the droplets flow into thin lamellar particles adhering to the surface, overlapping and interlocking as they solidify [9]. Thermal spraying processes include: flame spraying, electric arc spraying, plasma spraying, detonation gun spraying, and HVOF (High Velocity Oxygen Fuel) spraying.

One of the main objectives of thermal sprayed coatings is wear resistance. They are used to resist all forms of wear, including abrasion, erosion, and adhesion, in virtually every type of industry. Generally, the wear resistance of the coatings increases with their density, cohesive strength and bonding strength, so the higher-velocity coatings, such as plasma spraying, HVOF, and detonation gun coatings, provide the greater wear resistance for a given composition.

The materials used in thermal spraying processes are extremely wide, ranging from soft metals to hard metal alloys to refractory ceramics and cermets, such as WC/Co, Cr_3C_2/NiCr, Cr_2O_3, and Al_2O_3. At the same time, the thermal spraying processes can deposit coatings at a very high deposition rate without a large substrate distortion (the substrate does not need to be directly heated). The main

disadvantage of thermal spraying process is its line of sight nature, which results that the process is unsuitable for complex-shaped substrates.

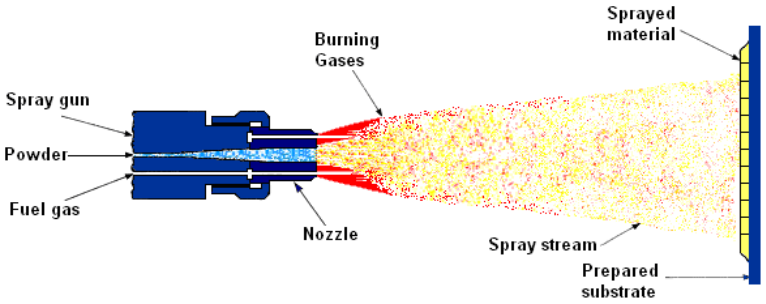

Figure 3: Scheme of wire flame spraying [9].

- **Chemical vapor deposition (CVD)**

Chemical vapor deposition technique is to deposit a solid layer on a heated surface via a chemical reaction from the vapor or gas phase, as shown in Figure 4. It is a versatile process that can be used to deposit layers of metals, nonmetallic elements (such as carbon and silicon), compounds (such as carbides, nitrides, and oxides), intermetallics, as well as many other materials. According to the operating pressure and environment, CVD can be classified as atmospheric pressure CVD (APCVD), low-pressure CVD (LPCVD) and plasma-enhanced CVD (PECVD).

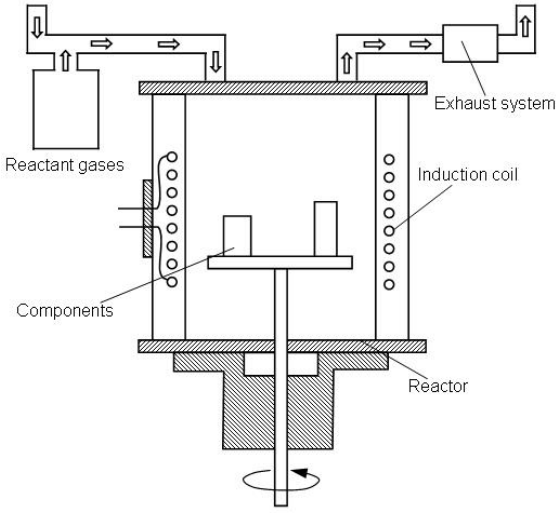

Figure 4: Principle of CVD technique.

A remarkable advantage of the CVD technique is its excellent throwing power. It can produce coatings with uniform thickness and low porosity even on complex-shaped substrates. Its main shortcoming is the high substrate temperature (except PECVD), which induces distortion of the substrates and limits the applications where the substrate materials have poor thermal resistance.

The first commercial application of CVD technique is titanium nitride (TiN) coatings on high speed steel tools for metal cutting. Now, CVD process has been extended to wear, erosion, and corrosion resistance applications, such as metal forming, molding tools, pump and valve parts, machine elements (e.g., gears, bearings and blades), etc. It is also employed in microelectronics, optical films, and high-temperature superconductors.

▪ **Physical vapor deposition (PVD)**

Physical vapor deposition is an atomistic deposition process, in which material is vaporized from a solid source in the form of atoms or molecules, transported in the form of a vapor through a vacuum or low pressure gaseous (or plasma) environment to the substrate where it condenses to form a coating. Typically, PVD processes are used to deposit films with thickness in the range of a few nanometers to several microns. The PVD technique can be mainly divided into three groups: evaporation PVD, sputtering PVD and ion plating [7].

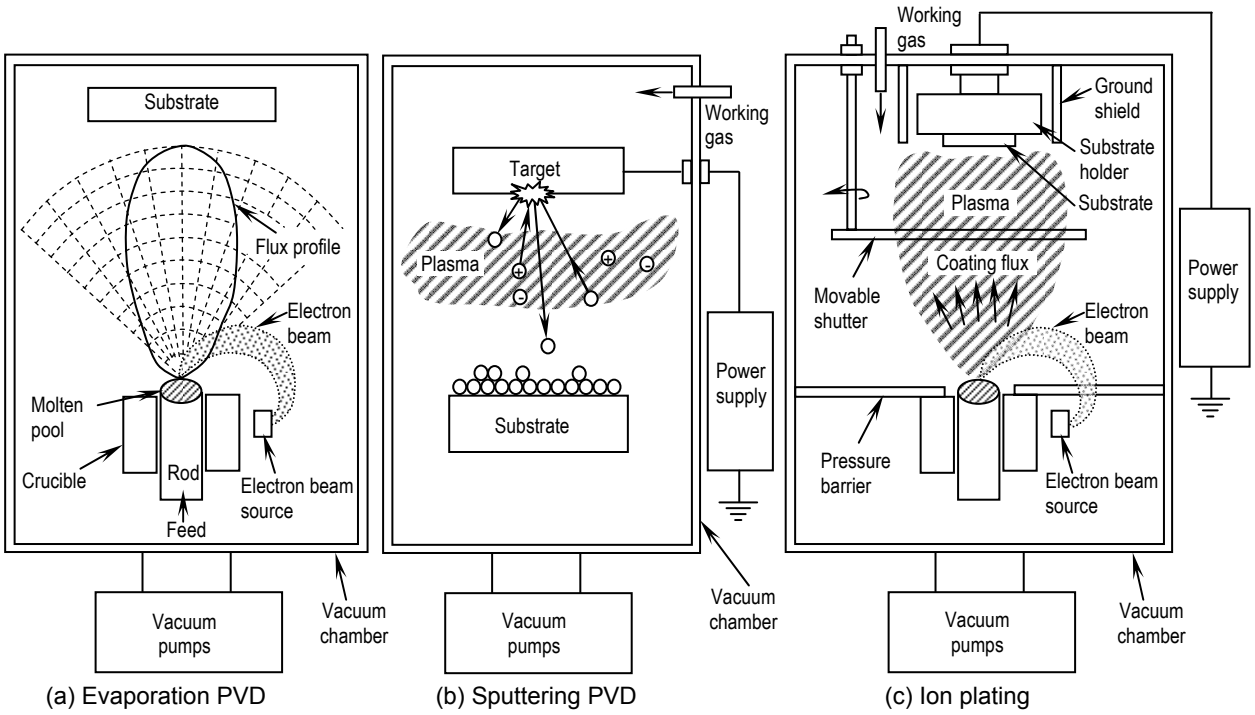

Figure 5: Scheme of physical vapor deposition technologies [7].

In the evaporation process (Figure 5a), the coating materials are heated to vaporize by direct resistance, radiation, induction, electron beam, laser beam or an arc discharge. The evaporated atoms are transported by a line of sight way without collision before condensation on the substrate because the process is usually carried out in vacuum.

In the sputtering process (Figure 5b), gas (usually argon) is ionized by a glow discharge to produce positive ions (gas pressure: 20 to 150 mTorr). The ions bombard the target material to dislodge groups of atoms which then pass into the vapor phase and deposit onto the substrate. Sputtering process can improve the adhesion of the coating, but its deposition rate and energy efficiency is very low.

In the ion-plating process (Figure 5c), the evaporization of coating material is similar to that in the evaporation process, but it passes through a gaseous glow discharge on the way to the substrate, thus some of the vaporized atoms are ionized. The glow discharge is produced by biasing the substrate to a high negative potential (-2 to -5 kV) and admitting a gas (usually argon) at a pressure of 5 to 200 mTorr into the chamber. The material on the substrate surface is sputtered off by the bombardment of high-energy gas ions. This ion bombardment results in better adhesion and lower impurity content due to a constant cleaning of the substrate. It also causes a modification in the microstructure and residual stresses in the deposit. On the other hand, it induces a decrease of the deposition rate since some of the deposited film is sputtered off, and causes a considerable heating of the substrate due to the ion bombardment of the intense gas.

PVD process can be employed to deposit virtually any metal, alloy, refractory or intermetallic compound materials on low temperature substrates with excellent bonding strength and structure controllability. The limit of PVD process is its achievable thickness, usually lower than 10 microns. PVD coatings have been used in many industrial areas, such as aerospace, automotive, surgical/medical, dies and moulds, cutting tools, and semiconductors.

1.2.1.3 Comparing the characteristics of common deposition methods

In practical applications, when a deposition method is employed, several important characteristics must be considered, such as bonding strength, deposition rate, substrate temperature, achievable coating thickness, cost, etc. Figure 6 shows the typical ranges of achievable coating thickness and processing temperature for some surface technologies.

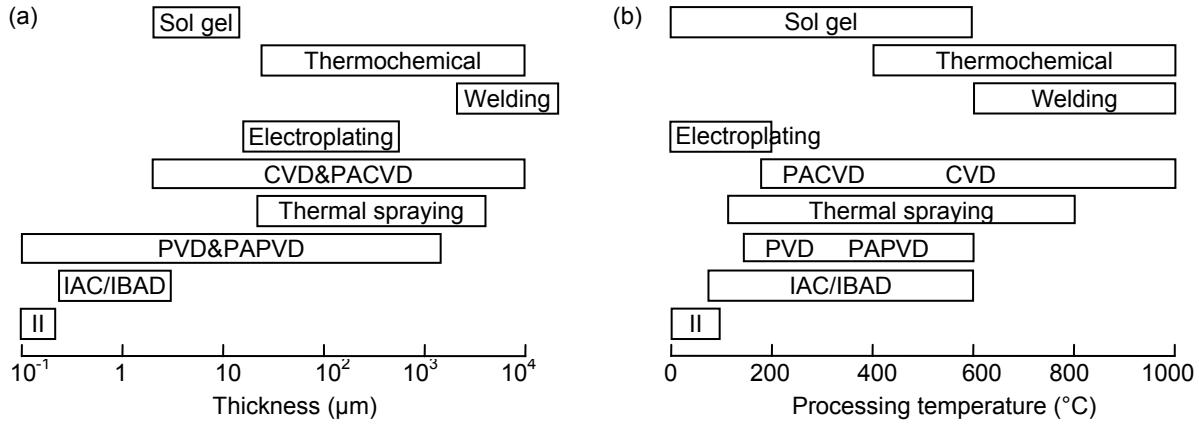

Figure 6: Typical ranges for (a) thickness of coatings, and (b) processing temperature for some surface technologies [6]. II: Ion implantation.

Holmberg and Matthews [6] and Bunshah [7] also summarized the characteristics of some common deposition methods from different aspects, as shown respectively in Table 2 and Table 3.

Table 2: Comparative characteristics of some of the main coating methods [6].

	Gaseous state processes					Solution processes		Molten or semi-molten state processes		
	PVD	PAPVD	CVD	PACVD	Ion implantation	Sol-gel	Electro-plating	Laser	Thermal spraying	Welding
Deposition rate(kg/hr)	Up to 0.5	Up to 0.2	Up to 1	Up to 0.5		0.1-0.5	0.1-0.5	0.1-1	0.1-10	3.0-5.0
Component size	Limited by chamber size					Limited by solution bath		May be limited by chamber size		
Substrate material	Wide choice	Wide choice	Limited by deposition temperature	Some restrictions	Some restrictions	Wide choice	Some restrictions	Wide choice	Wide choice	Mostly steels
Pre-treatment	Mechanical/ chemical plus ion bombardment	Mechanical/ chemical plus ion bombardmen	Mechanical/ chemical	Mechanical/ chemical plus ion bombardmen	chemical plus ion bombardmen	Grit blast and/or chemical cleaning	chemical cleaning and etching	Mechanical and chemical cleaning		
Post-treatment	None	None	Substrate stress relief	None	None	High temperature calcine	None/thermal treatment	None/substrate stress relief		None
Control of deposit thickness	Good	Good	Fair/good	Fair/good	Good	Fair/good	Fair/good	Fair/good	Manual-variable automated-good	Poor
Uniformity of coating	Good	Good	Very good	Good	Line of sight	Fair/good	Fair/good	Fair	Variable	Variable
Bonding mechanism	Atomic	Atomic plus diffusion	Atomic	Atomic plus diffusion	Integral	Surface forces		Mechanical/chemical		Metallurgical
Distortion of substrate	Low	Low	Can be high	Low/ moderate	Low	Low	Low	Low/ moderate	Low/ moderate	Low/ moderate

Table 3: Some characteristics of deposition processes [7].

	Evaporation	Ion plating	Sputtering	CVD	Electro-deposition	Thermal spraying
Mechanism of production of deposition species	Thermal energy	Thermal energy	Momentum transfer	Chemical reaction	Deposition from solution	From flames or plasmas
Deposition rate	Can be very high (up to 750,000 Å/min)	Can be very high (up to 250,000 Å/min)	Low except for pure metals (e.g. Cu-10,000 Å/min)	Moderate (200-2,500 Å/min)	Low to high	Very high
Deposition specie	Atoms to ions	Atoms to ions	Atoms to ions	Atoms	Ions	Droplets
Throwing powder for: a. complex shaped object	Poor line-of-sight coverage	Good, but nonuniform thickness distributions	Good, but nonuniform thickness distributions	Good	Good	No
b. into small blind holes	Poor	Poor	Poor	Limited	Limited	Very limited
Metal deposition	Yes	Yes	Yes	Yes	Yes, limited	Yes
Alloy deposition	Yes	Yes	Yes	Yes	Quite limited	Yes
Refractory compound deposition	Yes	Yes	Yes	Yes	Yes, limited	Yes
Energy of deposition species	Low	Can be high	Can be high	Can be high with PACD	Can be high	Can be high
Bombardment of substrate/deposit by inert gas ions	Not normally	Yes	Yes or no depending on geometry	possible	No	Yes
Growth interface perturbation	Not normally	Yes	Yes	Yes (by rubbing)	No	No
Substrate heating (by external means)	Yes, normally	Yes or no	Not generally	Yes	No	Not normally

In Table 2 and Table 3, each deposition process shows its own advantages and disadvantages. In actual applications, it is difficult for a single deposition process to meet the higher and higher requirements for tribological performance. In order to cancel out the disadvantages of different surface treatments and improve surface performances of coatings, some hybrid technologies by combining at least two traditional coating deposition processes are becoming prevalence. For example, the combination of electron beam surface hardening for soft substrate (like steel) and PVD hard coatings (like Ti(C)N, TiAlN, Cr_xN_y and DLC) can result in a significant improvement of the substrate material's load carrying for the hard coatings, and high hardness and high critical loads in scratch tests are obtained [10]. Another example is the laser assisted plasma spraying technology (a combination of plasma spraying and laser remelting). Plasma spraying is a versatile and high efficiency deposition method; however, the as-sprayed coatings are porous and inadequately adherent to the substrate, which decreases their wear and corrosion resistance. Laser remelting for the as-sprayed coatings may lead to the elimination of porosity and improvement of mechanical properties [11]. These technologies are being used for industrial components.

1.2.2 Effect of deposition parameters on coating properties

For given coating materials and deposition methods, different tribological performances are often found in literature due to the use of different deposition parameters. For example, in the deposition process of MoCu(N) films by reactive dc magnetron sputtering, Joseph *et al.* [12] found coating properties and tribological performance are quite different by changing the N_2 flow rates into the deposition chamber, as shown in Figure 7.

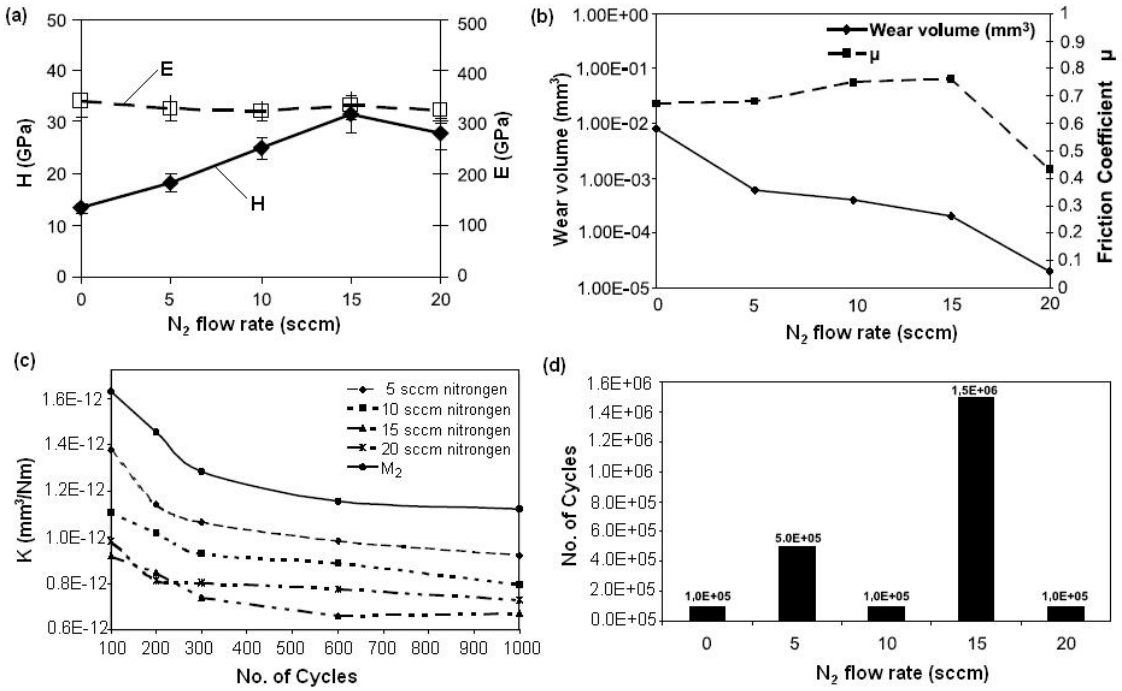

Figure 7: Effect of N_2 flow rate on coating properties and tribological performance: (a) hardness *H* and elastic modulus *E*, (b) reciprocating sliding test results, (c) wear rate *K* in micro-abrasive tests, (d) coating lifetime (No. of cycles) in impact tests [12].

In general, the change of coating properties and tribological performance is attributed to the effect of process parameters on coating microstructure. Thornton [13] investigated the influences of deposition temperature and argon pressure during the sputtering PVD deposition process of thick coatings (~25 μm) of various metals (Mo, Cr, Ti, Fe, Cu, and Al-alloy) on glass and metallic substrates. He found that, as increasing substrate temperature, coating microstructures generally transfer from an open columnar arrangement (Zone 1), to a dense columnar formation (Zone T), to a second dense columnar microstructure (Zone 2), and, finally, to dense equiaxed grain structure (Zone 3), as shown in Figure 8 (where T is the substrate temperature and T_m is the melting point of the substrate material).

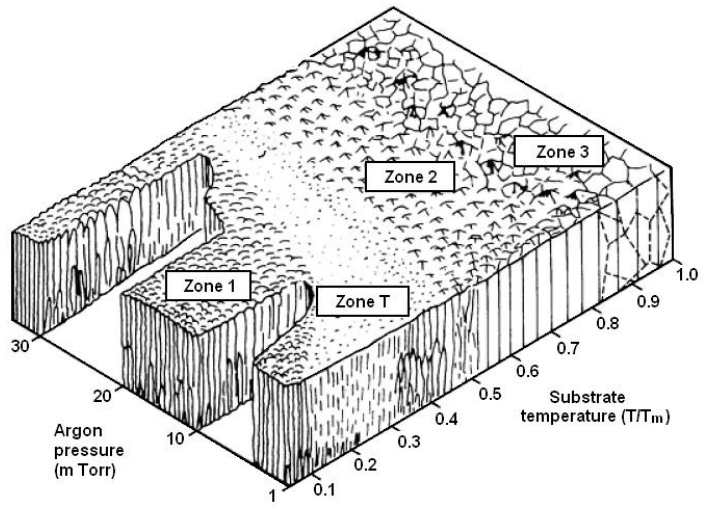

Figure 8: Microstructural dependence of sputtered coatings on substrate temperature and argon pressure [13].

1.3 Coating types and structures

Since the successful application of titanium nitride (TiN) and titanium carbide (TiC) coatings on cutting tools, there are a huge variety of available coatings applied in tribological applications. In literature, coatings are commonly classified as soft coatings and hard coatings according to the hardness lower or higher than 10 GPa, because the hardness is generally looked as the most important parameter for the tribological response of a coating system. Soft coatings, such as polymers, soft metals, some carbon-based compositions (like a-C:H DLC) and lamellar solids (including transition-metal dichalcogenides and graphite), are usually used to reduce friction, while hard coatings, such as oxides, carbides, nitrides, borides, and some carbon-based compositions (like diamond, a-C DLC), are believed with a good wear resistance, especially the ultra-hard coatings with an excellent abrasion resistance. Sometimes, coatings are also classified by thickness, as thin coatings and thick coatings. For thin coatings, the substrate will carry a large part of the load; therefore, the tribological response of coating systems depends on the properties of interface and substrate. When a coating is thick enough, it will support the whole load and work like a bulk material [6].

After several decades of development, structures of tribological coatings go through an enormous change, from simple single-layer, to multi-layer, to gradient and to advanced adaptative coatings, as shown in Figure 9. Donnet and Erdemir [14] reviewed the developments and new trends of tribological and solid lubricant coatings, and grouped the development of coating structure as four generations: single component coatings; multilayer and multicomponent coatings; gradient, superlattice and nanostructured coatings; smart (adaptative or chameleon) coatings. The advantages of combining several structures and compositions within one coating include achievement of various individual physical properties (e.g., diffusion barrier + low friction), reduction of the mismatch in mechanical and chemical properties between the substrate and the coating (mainly to enhance adhesion), control of the residual stress within the coatings, the ability to stop cracks during operation under severe conditions, the adaptability with the change of operating conditions, and enhancement of hardness and/or toughness.

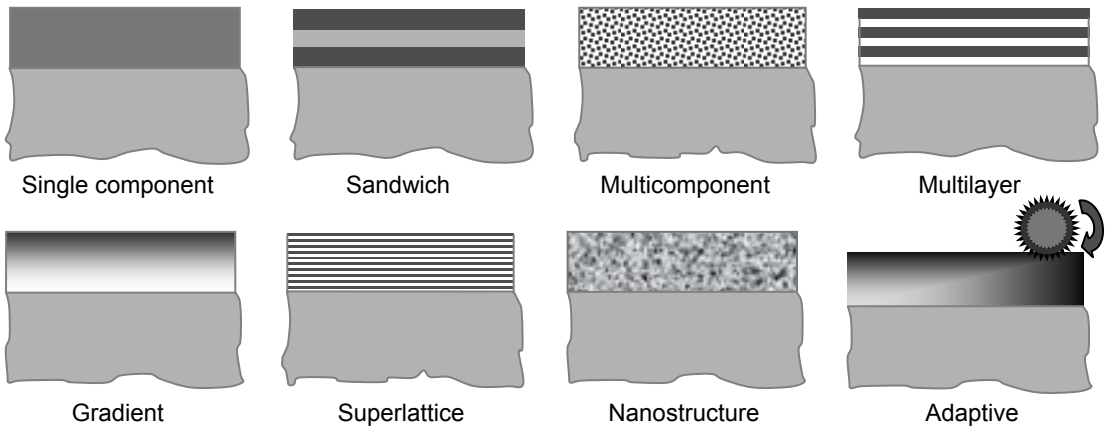

Figure 9: Structures of coatings [14, 15].

▪ **Single component coatings**

Single component coatings are the simplest coatings, which prevail on the market and continue to be favorites. For example, most commercial PVD and CVD coatings consist of one single layer, such as TiC, TiN, CrN, CrC, Al_2O_3, TiAlN, TiCN, DLC, W_2C, MoS_2, diamond, soft metals or some polymers. Sometimes, in order to enhance the bonding strength with substrates, an adhesion interlayer is employed. However, for some special applications, where a combination of low friction, high wear

resistance and some other functions is required, single component coatings cannot cope with these situations, so coatings with complex structures must be employed.

- **Multi-component coatings**

Multi-component coatings are made up of two or more constituents in the form of grains, particles or fibers, which offer a wide range of possibilities to improve the tribological properties. The research of multi-component coatings focuses on mixed ceramics, which exhibit much improved properties, such as high-temperature hardness, oxidation resistance and impact resistance, so the coatings are suitable for interrupted cutting applications [16].

- **Multilayer coatings**

Multilayer coatings include two types: several successive layers of different composition (sandwich coatings) and periodically repeated structure of lamellae of two or more materials. In sandwich structure, the interlayers can reduce the mismatch in mechanical or chemical properties between coatings and substrates, and improve the adhesion of the coating. In periodically repeated structure, alternating layers can act as crack-stoppers either by introducing layer boundaries to stop cracks or providing a tough medium through which propagation is mitigated.

- **Nanostructure coatings**

Nanostructure coatings include nanocrystallized films (with grain sizes in the nanometer range) and nanocomposite films including structures that combine amorphous phases with crystallized ones [14]. According to the well-known Hall–Petch relation, the yield strength, hardness and toughness of polycrystalline materials are generally improved with decreasing grain size, which is also suitable for nanostructure coatings. Jeong *et al.* [17] investigated the effect of grain size (from 90 μm to 13 nm) in nanocrystalline nickel coatings by electrodeposition on coating hardness and wear resistance, and found that the hardness and wear resistance increase with the decrease of grain size, as shown in Figure 10.

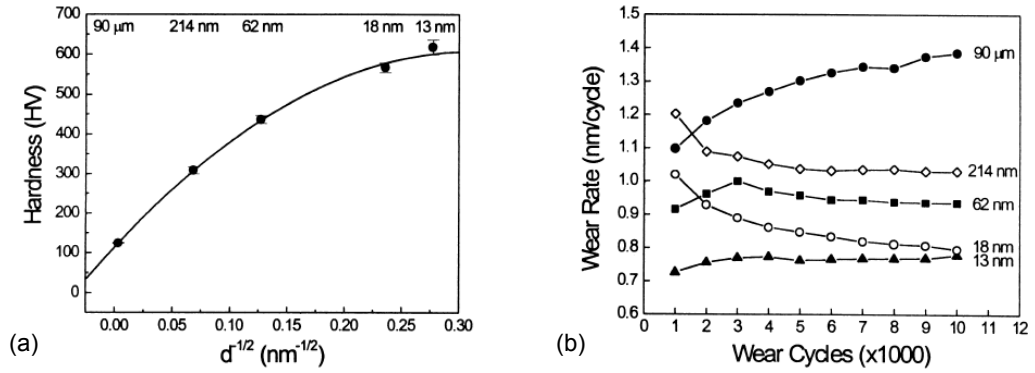

Figure 10: Effect of grain size on the properties of electrodeposited nanocrystalline nickel coatings: (a) hardness, (b) ware rate [17].

- **Gradient coatings**

The idea of functionally gradient coating is a logical development of multilayer concept to tailor the microstructure of coatings. A sharp change of mechanical, physical and chemical properties between layers and the substrate can induce high residual stresses at the interfaces, then formation of cracks and detachment of coatings. Therefore, a gradient transition from the substrate to different layers is expected [18]. For example, in order to improve the load carrying capacity of low friction DLC coating

on low-cost steel substrates under a high normal load, Voevodin *et al.* [19] designed the functionally gradient metal-ceramic Ti-TiN-TiCN supporting interlayers, as shown in Figure 11. Low friction coefficients in combination with low wear rate were obtained in ball-on-disk experiments against steel and cemented tungsten carbide balls.

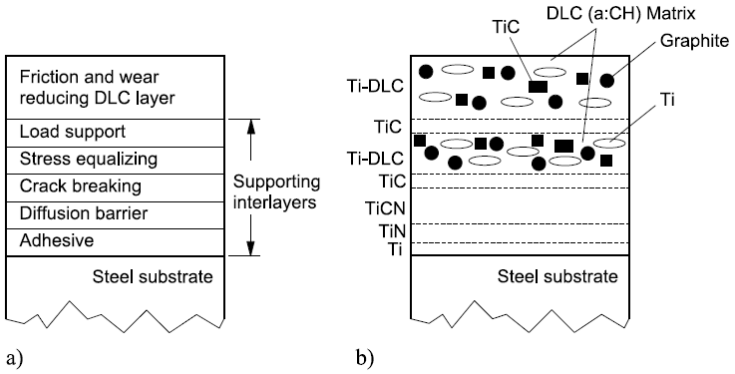

Figure 11: Gradient multilayer coating with an upper DLC layer on a steel substrate: (a) theoretical constitution of supporting interlayer; (b) coating developed for sliding wear applications [19].

▪ Superlattice

Superlattice coatings are periodically repeated multilayer coatings with a thickness of individual layers in the range of 5~50 nm [14]. Some researchers found that the superlattice coatings, especially TiN-based superlattice coatings (such as TiN/WN, TiN/CrN, TiN/TaN, TiN/MoN and TiN/AlN), can improve hardness, toughness and thermal stability in comparison to single layers [20]. For example, Yang and Zhao [21] deposited TiN/CrN superlattice coatings (consisting of alternating TiN and CrN layers, 6.4~12.6 nm) by reactive magnetron sputtering, and they found the superlattice coatings exhibit lower friction coefficient and much higher wear resistance than a commercial TiN hard coating rubbed against WC–Co counterpart, as shown in Figure 12.

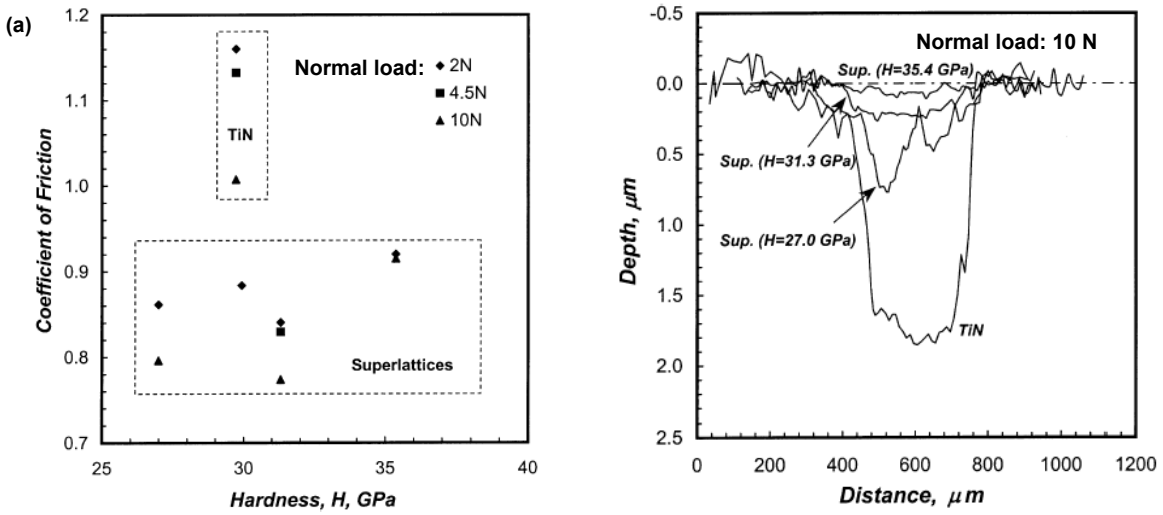

Figure 12: Comparison of tribological performance for TiN and TiN/CrN superlattice coatings (sliding against WC–Co counterpart): (a) effect on coefficient of friction, (b) surface profile perpendicular to wear tracks [21].

▪ Adaptive coatings

Adaptive (or chameleon) coatings are able to change their properties to adapt to the change of running conditions. The first adaptive coatings were solid lubricant composites made of oxides and

dichalcogenides (PbO/MoS_2, ZnO/MoS_2, ZnO/WS_2), which could operate in a broad temperature range: dichalcogenides can only work well below 500°C, while oxides have a better lubricating ability under high temperatures, 500~800°C [22, 23]. Recently, Voevodin and Zabinski [24] developed novel self-adaptive coatings, which combine nanocrystalline carbides (TiC, WC), dichalcogenides (MoS_2, WS_2), and amorphous hydrogen-free DLC into nanocomposite structures. First, the coatings had a high hardness, between 27~32 GPa, to resist wear. Second, based on the large volume of boundaries available, TiC/DLC and WC/DLC nanocomposites could provide self-regulation of surface mechanical properties from hard to ductile, because grain boundary sliding under a load exceeding the elastic strength prevents brittle fracture and distributes contact load onto larger areas. Finally, the introduction of the WS_2 phase provided friction self-adaptation of the operating environment: DLC phase was used for lubrication in humid environments and the WS_2 phase was used for lubrication in dry nitrogen and vacuum. Their friction coefficients were about 0.1 in humid air, 0.03 in vacuum, and 0.007 in dry nitrogen. So, the surface chemistry, structure and mechanical behavior of these nanocomposite coatings could change depending on applied loads and operational environment to maintain outstanding tribological performances.

2 Tribological response of coating systems

When a coating is used in a tribological application, the tribological requirements usually include two main aspects: friction reduction and wear resistance.

2.1 Friction reduction

Bowden and Tabor [25] first demonstrated that thin soft metallic films coated on hard substrates can induce a low friction coefficient. In their opinion, the frictional force between unlubricated surfaces arises from two main factors [26, 27]. One is the adhesion which occurs at the regions of real contact. These adhesions, welds or junctions have to be sheared if sliding is to occur. The other is the deformation arising from the ploughing, grooving or cracking of one surface by asperities of the other. So the frictional force can be expressed as:

$$F = F_{adhesion} + F_{deformation} = A \cdot s + F_{deformation} \qquad (1\text{-}1)$$

where A is the real area of contact, $A=P/p$, s and p are respectively the shear strength and the yield pressure of the softer material, P is the normal load. In most situations, the first part is more important. If the deformation force is neglected, then friction coefficient is:

$$\mu = F/P = s/p \qquad (1\text{-}2)$$

So, in order to obtain a low friction coefficient μ, a low s and a high p are expected. In Figure 13a with a low s and a low p, and in Figure 13b with a high s and a high p, μ is high. When a soft coating with low shear strength is deposited on a hard substrate material, the normal load is mainly carried by the substrate, so in Figure 13c with a low s and a high p, μ is low. A low friction can also be achieved with a hard coating if a microfilm with low shear strength can be formed on the top of the coating [6].

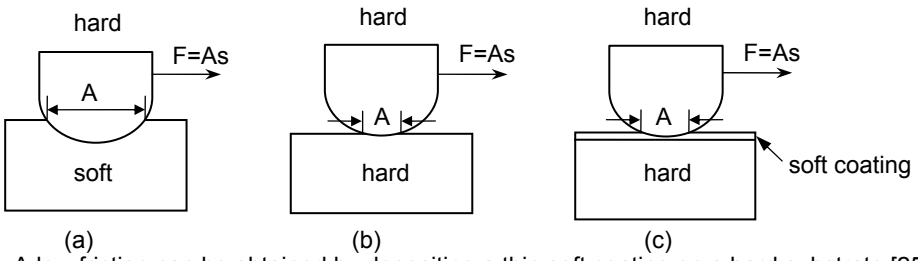

Figure 13: A low friction can be obtained by depositing a thin soft coating on a hard substrate [25].

2.2 Wear resistance

Wear resistance is the main objective of tribological coatings, especially for mechanical components and cutting tools. Except for the problems resulting from the discontinuity of properties between the coating and the substrate, the wear mechanisms of coatings are similar to those of bulk materials.

2.2.1 Wear mechanisms for bulk materials

Wear is the phenomenon of material removal from a surface due to interaction with another contacting surface. Wear rate can drastically change in a large range, depending on operating conditions and contact materials, which result in different wear mechanisms and modes. There are many terms used to describe wear, including abrasion, adhesion, galling, scuffing, scoring, pitting, flaking, mild wear, severe wear, erosion, impact, seizure, oxidational wear, fretting wear, detachment, spalling, delamination, etc. Some of these wear concepts are similar, which make the understanding of wear mechanisms confusing. In order to achieve greater clarity for wear mechanisms, Kato and Adachi [28] summarized the interrelations of some wear terms from contact types, deformation states and material removal principles, as shown in Figure 14.

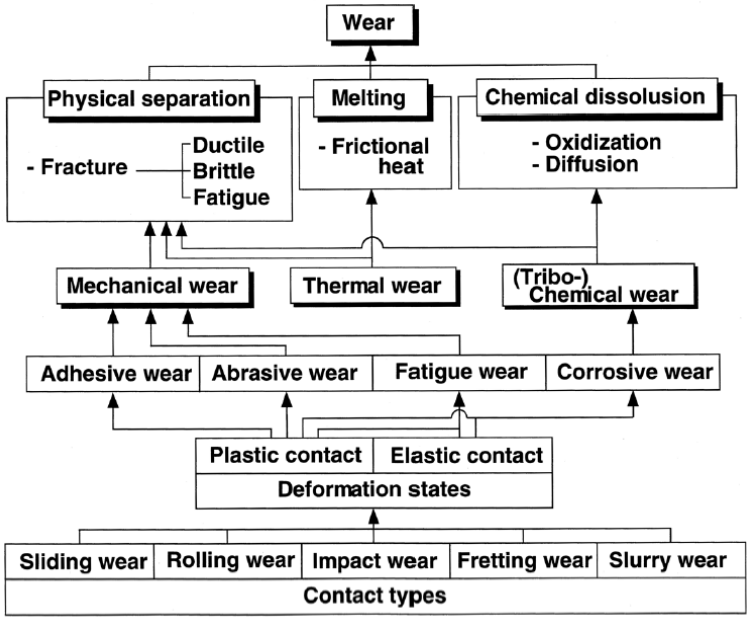

Figure 14: Descriptive key words of wear and their interrelations [28].

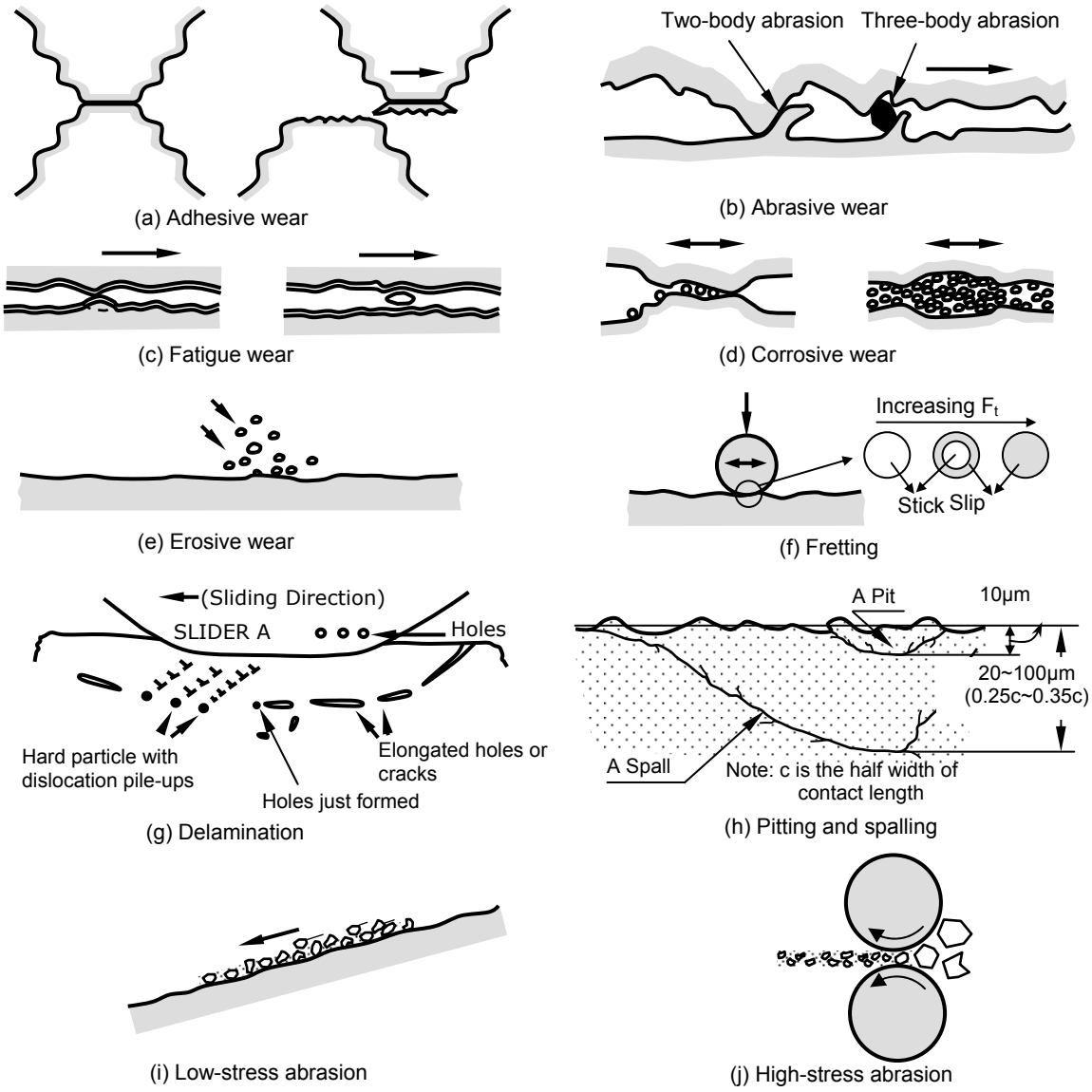

Figure 15: Scheme of wear mechanisms and modes [6, 29-31].

Despite many wear modes, the classification of wear mechanisms based on Strang and Burwell [32, 33] is most widely cited, in which there are four principal types of mechanical wear, i.e., adhesive wear (scoring, galling, scuffing, seizure), abrasive wear, fatigue wear and corrosive wear, as well as several minor types. So, it is generally recognized that most common types of wear include abrasive wear, adhesive wear, fatigue wear, corrosion wear, erosion wear and fretting wear [31], and each type includes some subclasses. For example, abrasive wear includes two-body abrasion, three-body abrasion, high-stress abrasion, gouging abrasion, low-stress abrasion; adhesive wear includes mild wear, severe wear (galling and seizure) and scuffing. The scheme of some wear types is shown in Figure 15.

2.2.2 Damage mechanisms of coating systems

The use of coatings induces discontinuity of mechanical properties and mismatch of physical parameters on the interface of coatings and substrates, which leads to high interfacial stresses. The main difference of damage mechanisms between coating systems and bulk material systems is the

damage of the interface, such as detachment, delamination, spalling, cracking. Based on the research of thin hard coatings, Hogmark *et al.* [34] brought forward an all-around classification, in which the surface damage included the following three groups:

- *Damage without exchange of material.* There are two aspects: one is the change of component geometry due to insufficient elastic modulus, hardness and coating thickness; the other is change of topography such as roughness and waviness because of deficiency hardness or ductility of coatings. In some forming tools, even small change of topography is unacceptable.

- *Wear (Damage with loss of material).* The loss of coating materials includes two main categories: detachment and gradual removal. Detachment, a special wear of coating systems, is the result of poor bonding strength between coatings and substrates (i.e., fracture in the coating/substrate interface). Therefore, the adhesion between the coating and the substrate is very important for preventing the detachment of coating; however, the practical adhesion depends on many factors, such as materials, deposition methods, surface preparation, and deposition parameters. Gradual removal of coating material is similar to the wear mechanisms of bulk materials, including abrasion, adhesion, contact fatigue, fretting, particle erosion, and wear by chemical dissolution or degradation.

- *Damage with material pick up.* This is a kind of special failure for coatings applied in the manufacturing industry, like sheet forming tools. The adhesion of material picked up from the counterpart on the coatings of tools can cause the quality problem of products. To prevent it, the coating should have a smooth topography and low chemical reactivity with the counter material [35].

In order to help understanding the wear of coatings, Holmberg *et al.* [36] comprehensively summarized contact mechanisms of tribological coating systems from different scales: macromechanical, material transfer, micromechanical, tribochemical and nanomechanical contact, as shown in Figure 16.

- *Macromechanical friction and wear mechanisms.* In contacts between two surfaces of which one or both are coated, the tribological contact behavior controlled by four main parameters: the coating-to-substrate hardness relationship, the thickness of the coating, the surface roughness, and the size and hardness of any debris in the contact. According to the change of these four parameters, there are 12 typical tribological contacts when a hard sphere slides on a coated flat surface, as shown in Figure 17.

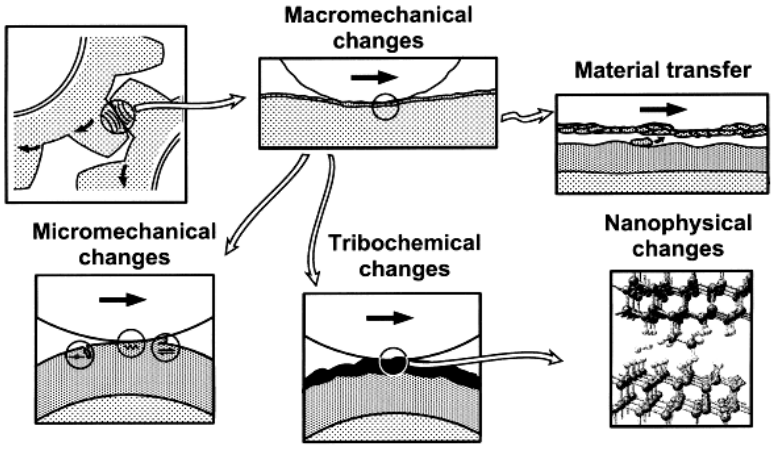

Figure 16: Tribological contact mechanisms [36].

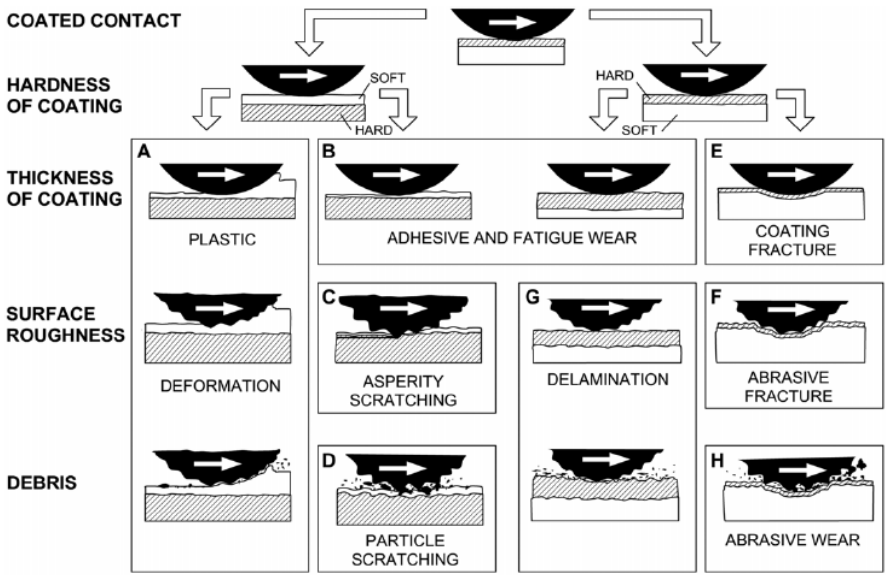

Figure 17: Macromechanical contact conditions for different mechanisms [6].

- *Micromechanical tribological mechanisms.* The micromechanical tribological mechanisms describe the stress and strain formation, the crack nucleation and propagation, material liberation and particle formation at an asperity-to-asperity level. In typical engineering contacts, these phenomena are at a size level of about 1 μm or less, down to the nanometer range.

- *Tribochemical mechanisms of coated surfaces.* During sliding contact and the periods between repeated contacts, the chemical reactions taking place at the surfaces change the composition of the outermost surface layer and its mechanical properties. The chemical reactions on the surfaces are strongly influenced by the high local pressures and the flash temperatures. Tribochemical mechanisms may involve two main aspects: oxidation of soft coatings and formation of thin microfilms on hard coatings.

- *Nanomechanical contact mechanisms.* The emergence of some new technologies (like the atomic force microscope) provide the possibility of studying friction and wear phenomena on a molecular scale and measuring frictional forces between contacting molecules at the nano Newton level.

- *Mechanisms of material transfer.* When wear particles have been liberated from the surface, some of them may attach to the counterface to form a transfer layer and significantly change the tribological properties of the counterface (like forming a new counterface).

3 Important parameters of coating systems

3.1 Introduction

The control of the tribological response in a coating system is very difficult, because the friction and wear are influenced by many parameters, which are interactional. A tribological coating system is made of two first bodies (one or both is/are coated), solicitation (kinematics, contact configuration, load, speed, frequency, etc.) and environment (temperature, lubrication, relative humidity, atmosphere, etc.). In general, the relationships between the tribological response and the parameters are complicated. Various friction tests have to be performed to investigate the tribological performance of coatings.

To meet the tribological requirements, the coated surface must possess a suitable combination of properties. Holmberg and Matthews [6] pointed out that different properties from four different zones must be considered, as shown in Figure 18. Strafford and co-workers [37, 38] considered two interfaces as the critical areas of a coating system for tools and dies applications: interface1 (between the coating and the environment or work material) and interface2 (between the coating and the substrate), as shown in Figure 19. Excellent coating adhesion is required at interface2 whereas at interface1 no adhesion (or welding) of work material to the tool (coating) is desirable. In order to develop “ideal” coatings, they have broadly identified key coatings’ properties and requirements about mechanical, physical and chemical properties.

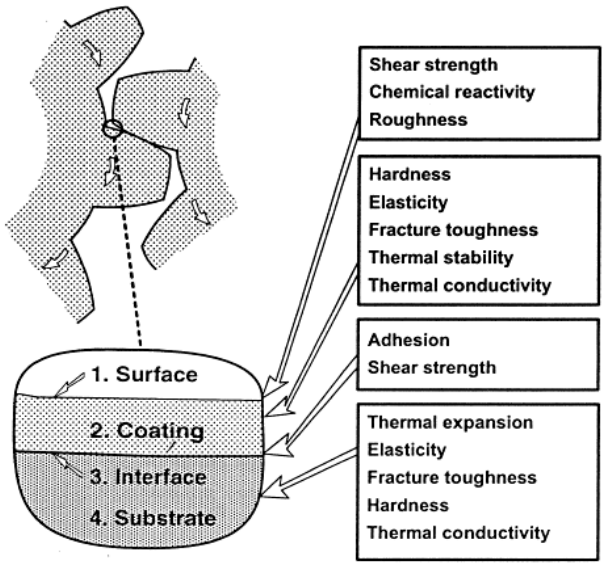

Figure 18: Tribologically important properties in different zones of the coated surface [6].

The research group of Hogmark [15, 34, 35] also discussed the evaluation of some important parameters and their effect on tribological response of thin hard coatings, such as elastic modulus, residual stresses, hardness and ductility, fracture strength, topography, toughness, adhesion, etc., and the relationship between characteristics and properties of thin coatings and their substrates and tribological response was suggested, as shown in Table 4.

The important parameters of coating systems emphasized by several research groups are listed in Table 5. In fact, the tribological response depends on the whole system, including coating, substrate, counterpart, solicitation and running environment, but more attention was focused on coating and substrate.

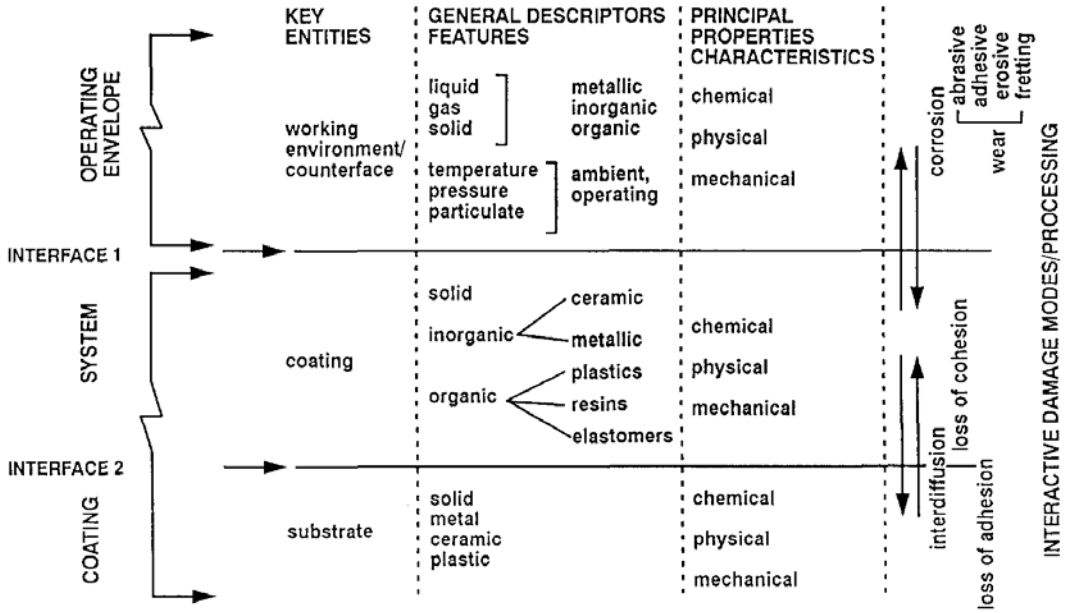

Figure 19: Generalized features of a working coating system [37].

Table 4: Characteristics and basic properties of thin hard coatings and their substrates decisive for tribological response [34].

Characteristics and basic properties	Tribological response				
	Friction	Surface damage			
		Deformation	Detachment	Gradual wear	Pick up
Coating					
Topography	×	×	-	×	×
Thickness	-	×	×	×	-
Elastic modulus	-	×	×	×	-
Residual stress	-	×	×	×	-
Hardness	×	×	×	×	-
Ductility	×	×	×	×	-
Fracture strength	-	×	-	×	-
Fatigue strength	-	×	-	×	-
Chemical properties	×	×	×	×	×
Thermal properties	-	×	×	×	×
Substrate					
Shape	-	×	×	×	-
Topography	×	×	×	×	×
Elastic modulus	-	×	×	×	-
Hardness	-	×	×	×	-
Ductility	-	×	×	×	-
Chemical properties	-	-	×	×	-
Thermal properties	-	×	×	×	-

× denotes a relatively strong influence.

Table 5: Important parameters of a coating system according to different research groups.

Parameters	Holmberg [6]	Hogmark [34]	Strafford [37]	Carton[39]
Counterface	×	×	×	
Coating				
Shear strength	×			×
Thickness	×	×	×	×
Roughness / Topography	×	×	×	
Microstructure/ Morphology	×		×	
Composition	×		×	
Hardness	×	×	×	×
Elastic modulus	×	×	×	×
Fracture toughness	×	×	×	
Ductility		×	×	
Yield strength			×	×
Fatigue strength		×		×
Cohesion			×	
Density			×	
Chemical properties	×	×		
Thermal stability	×	×		
Thermal conductivity	×	×	×	
Thermal expansion	×	×	×	
Internal stress	×	×	×	×
Interface				
Adhesion	×	×	×	×
Substrate				
Shape		×		
Topography	×	×		
Elastic modulus	×	×	×	×
Fracture toughness	×			
Ductility		×		
Hardness	×	×	×	×
Chemical properties		×		
Thermal conductivity	×	×	×	
Thermal expansion	×	×	×	

3.2 Important parameters for friction coefficient

3.2.1 Friction models

The fundamental experimental laws of friction are usually called Coulomb laws, which were built on earlier work by Leonardo da Vinci and Amontons. The laws include the following aspects:

- Static friction is greater than kinetic friction
- Kinetic friction is independent of sliding velocity
- Friction force is directly proportional to the applied load, i.e., $F=\mu P$, where μ is the friction coefficient.
- Friction force is independent of the apparent contact area.

Coulomb suggested that friction was caused by mechanical interlocking of asperities. The “interlocking” model had many limitations, and there were some objections to this theory, then adhesion, cohesion, atomic attraction, molecular attraction, and similar terms were used to explain friction [28].

Leonhard Euler first studied theoretically the mechanism of friction and distinguished between static and dynamic friction. Considering a sliding block on an inclined plane (inclination angle α), he obtained the first mathematic formula of static friction coefficient: $\mu_s=\tan\alpha$.

In 1950, Bowden and Tabor [27] assumed the friction force is proportional to the real contact area, presented the classical adhesion model, where plastic deformation from the adhesion shearing and the ploughing caused by asperities contact is the origin of friction, as mentioned in section 2.1. Friction coefficient is:

$$\mu=s/p+F_{deformation}/P= s/p+A/A' \quad (1\text{-}3)$$

where A' is the cross-section area of the groove, and A/A' depends on the shape and size of asperities or debris, namely the roughness of the surfaces. Therefore, to reduce the friction coefficient, low shear strength, high yield pressure (hardness) and small roughness are essential. Surface energy and mutual solubility of contact materials were considered as important factors, which influence the adhesion. Rabinowicz developed a compatibility chart of metals indicating which metals can safely slide against one another and which metal couples should be avoided [40].

In contrary to the assumption of fully plastic deformation of the asperities in the adhesion model, Archard [41] believed friction can also occur if the asperities are only elastically deformed. For a single elastic contact with a contact radius a, combining the equation of Bowden and Tabor with the Hertzian formula (replace the yield pressure by mean Hertzian contact pressure), the friction force was found to be proportional to 2/3 power of the normal load:

$$F = s\pi\left(\frac{3}{4}\frac{R}{E^*}\right)^{2/3} P^{2/3} \quad \Rightarrow \quad \mu=\frac{\pi\cdot s}{P^{1/3}}\left(\frac{3R}{4E^*}\right)^{2/3} \quad (1\text{-}4)$$

where E^* is the reduced elastic modulus of the contact materials and R is the curvature radius of the asperity. In this equation, the friction coefficient depends on the elastic modulus of two contact materials, the normal load (contact pressure), the shear strength of the softer material, and the roughness of the contact surfaces.

Based on a multiasperity model with Gaussian height distribution, Greenwood and Williamson [42] developed a criterion, "plasticity index" Ψ, to indicate whether the contact is elastic or plastic, where Ψ just depends on mechanical and topographic properties of the contact surfaces. Typically, the contact will be elastic if Ψ is low (Ψ<0.6), and plastic if it is high (Ψ >1).

$$\psi = \frac{E^*}{H}\sqrt{\frac{\sigma}{\beta}} \quad (1\text{-}5)$$

where H is the hardness of the softer material, σ is the standard deviation of the asperity height distribution, and β is the radius of the asperity tips.

In 1981, Suh and Sin [43] put forward a new theory, "the genesis of friction", where the friction force is affected by the sliding distance and the environment. They explained that the friction coefficient is composed of three components, $\mu= \mu_d + \mu_p + \mu_a$: μ_d due to the deformation of surface asperities; μ_p due to plowing by wear particles and hard asperities, μ_a due to the adhesion of the flat portions of the sliding surface. The contributions to the overall friction coefficient by plowing and asperity deformation can be greater than that by adhesion.

3.2.2 Effect of parameters

According to literature, the effect of coating system parameters on friction coefficient is summarized in Table 6. From the table, the effect of some parameters was investigated by many researchers,

such as coating thickness, surface roughness, normal load, velocity, relative humidity, so these parameters are important for friction coefficient. Despite few reports in literature, some other parameters are also important, such as the parameters of counterpart, shear strength of coating, chemical properties of coating, and hardness of substrate.

Table 6: Effect of parameters on friction coefficient.

Parameters	Effect on Friction in References
Counterpart	
Hardness	↘[44, 45]
Roughness	
Shear strength	
Chemical properties	×[44, 46-48]
Coating	
Thickness	∨[49] = [50-53] ↘[54]
Hardness	↗[55]
Elastic modulus	
Shear strength	↗[25, 27]
Microstructure	
Fracture toughness	
Residual stresses	
Chemical properties	×[48, 56-60]
Thermal properties	
Interface	
Bonding strength	
Substrate	
Hardness	↘[25, 27, 61]
Roughness	↗[46, 50, 54, 56, 62] ↘[63] =[63, 64]
Elastic modulus	↘[63, 65]
Chemical properties	
Thermal properties	
Running conditions	
Load	↗[3, 56, 66-68] ∧[44, 69] ↘[45, 58, 66, 67, 70-76] ∨[77]
Velocity	↘[69, 74, 78-81] ↗[47] ∨[68]
Slip amplitude	↗[77]
Lubrication	×[16]
Temperature	∨[82, 83]
Relative humidity	↘[3, 57, 84-86] <[57] ↗[85, 87] ×[84]
Ambience (air, vacuum, …)	Argon,air [3, 45] vacuum, nitrogen [87, 88]

(× means that the parameter influences friction coefficient, but it cannot be expressed in data.
↘ means that friction coefficient decreases with the increase of the parameter.
↗ means that friction coefficient increases with the increase of the parameter.
∧ means that friction coefficient first increases, then decreases with the increase of the parameter.
∨ means that friction coefficient first decreases, then increases with the increase of the parameter
< means that friction coefficient may increase or decrease with the increase of the parameter.
= means that friction coefficient does not change with the increase of the parameter.)

▪ Parameters of counterpart

Friction is the result of interaction of two contacting surfaces, so the parameters of the counterpart influence the friction coefficient as importantly as the ones of the coating and substrate. However, in most tests, researchers use hard and smooth counterparts or use the same coating as counterparts, so the comparison of counterpart is gotten rid of. Friction coefficient of a coating is different with employing different counterparts, because chemical properties of counterparts will influence the formation of transfer films, which are usually crucial for friction coefficient. When a friction reduction

coating is used, mechanical properties of counterpart are also important. In general, the harder was the mating material, the lower the friction coefficient was [44, 45].

▪ Coating thickness

Softer coatings have an optimum thickness for friction reduction. A soft metal indium coating with the thickness of 0.1 ~ 10 μm can obtain a low friction coefficient less than 0.1, and thinner or thicker coatings will lead to an increase of friction coefficient, as shown in Figure 20 [25]. For thinner coatings, the friction coefficient will be influenced by the roughness of substrate surface due to the penetration of asperities. On the other hand, the poor load carrying capacity of thicker soft coatings can result in a large real contact area, and an increase of friction coefficient. For the same reason, friction coefficient decreases with the increase of thickness for thinner hard coating, while there is no obvious thickness dependence of friction coefficient for thicker hard coating [50-53], as shown in Figure 21.

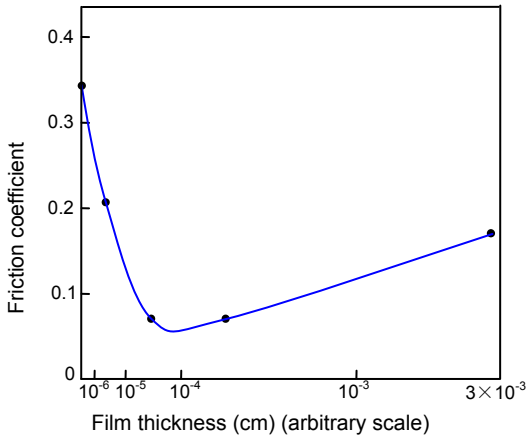

Figure 20: Effect of film thickness on friction coefficient for indium films deposited on tool steel [25].

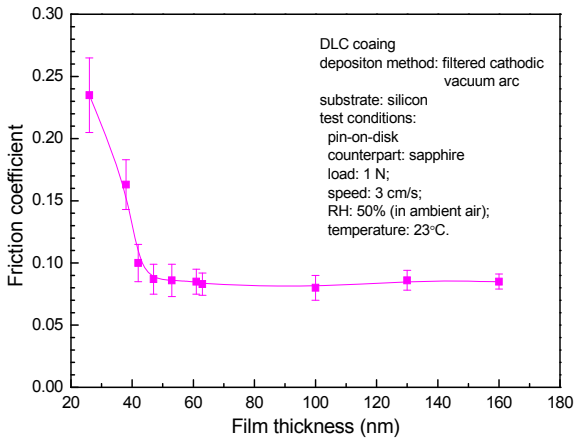

Figure 21: Effect of film thickness on friction coefficient for DLC coating [51].

▪ Surface roughness

The roughness of thin coatings mainly depends on the roughness of the substrate surface, while the roughness of thick coatings is influenced by the deposition process. In general, the friction coefficient increases with the surface roughness [46, 50, 54, 56, 62]. If the roughness is the same order of magnitude as the coating thickness, the increase of roughness will influence the friction coefficient more obviously due to the penetration of coating by asperities of the substrate. The effect of roughness on friction coefficient for soft coating is different from one for hard coating because the asperities of soft coatings are apt to plastic deformation, while for hard coating the plastic deformation is very limited [89]. So, there is usually higher requirement of surface finishes for hard coatings than for soft coatings. Below a certain value, the friction is less influenced by the surface roughness, as shown in Figure 22, while the cost of producing smoother surfaces increases exponentially [62]. In some situations, an optimum roughness maybe exists for low friction. In the investigation of sputtered MoS_2 coatings, Roberts and Price [90] found lower surface roughness maybe induced a higher friction coefficient, as shown in Figure 23. According to the investigation, Roberts [63] obtained the best tribological response when surface roughness was about 0.2 μm.

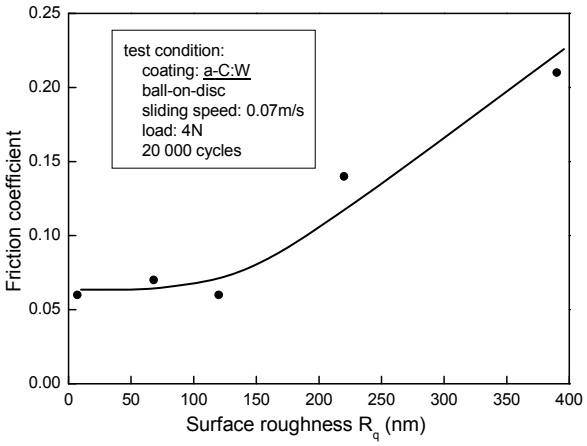

Figure 22: Effect of surface roughness on friction coefficient of DLC coatings [62].

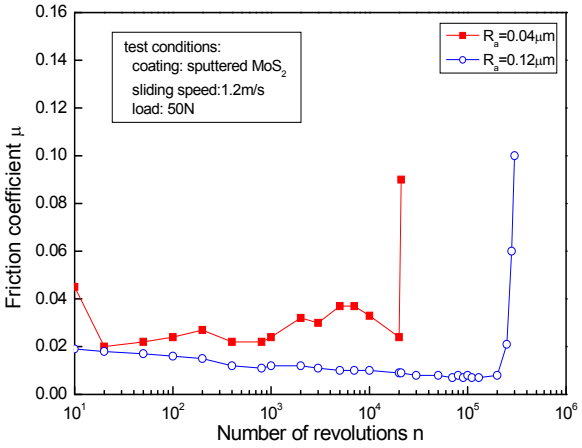

Figure 23: Effect of surface roughness on friction coefficient of sputtered MoS_2 coatings [90].

▪ Elastic modulus of substrate

When a thin coating is employed, the load is primarily supported by the substrate. Increasing the elastic modulus of the substrate can reduce the contact area, and result in a lower friction coefficient. For example, sputtered MoS_2 coatings on Si_3N_4 substrate presented a lower friction coefficient than on 440C steel and Ti6Al4V substrates, as shown in Figure 24 [91]. However, for thick hard coatings, friction coefficient is independent of the elastic modulus of substrate, because the load is mainly supported by the coatings.

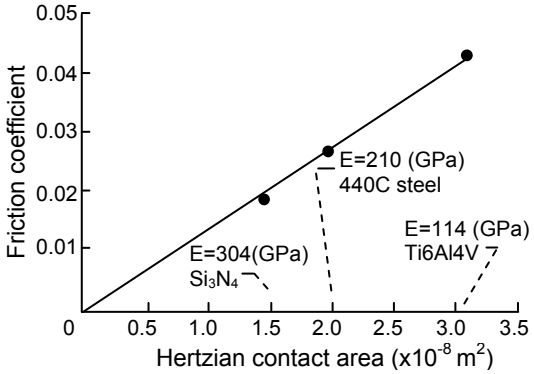

Figure 24: Friction coefficient as a function of contact area for sputtered MoS_2 films on different substrates [91].

▪ Normal load

From literature [25, 58, 66, 67, 70, 71, 75, 76], for soft coatings, such as MoS_2, PTFE and soft metal, the friction coefficient decreases with the increase of normal load or contact pressure. Based on the research of solid lubrication films, Towle [75] gave a reasonable explanation according to the pressure dependence of shear-strength, i.e., there is a linear relationship between the shear strength and the contact pressure.

$$s=s_0+\alpha \cdot p \qquad (1\text{-}6)$$

where s_0 and α are constants of material. Combining with Eq.1-2, we have:

$$\mu=s_0/p+\alpha \qquad (1\text{-}7)$$

So, the friction coefficient decreases with the increase of contract pressure. For hard coatings, the variation of friction coefficient with load is uncertain. At low load level, friction coefficient increases with

the load due to the increase of real contact area [44] and the ploughing effect [69], and then with a further increase of load, the friction coefficient may increase or decrease. If the increase of the load facilitates the formation of transfer films or oxide protective films with a low shear strength, then friction coefficient will decrease [44, 69]; or else it may continue increasing [68]. However, under some conditions, the friction coefficient of hard coatings decreases with the increase of the normal load due to the smoothening of coating asperities under the rising temperature [72], the slow increase of actual contact area with the increasing load [73] or the increase of tribolayer thickness [74].

- **Sliding speed**

In general, the trend of the average friction coefficient is to decrease with an increase in sliding speed [69, 74, 78-81]. This behavior can possibly be attributed to four factors. First, the plastic flow is easy to occur due to local melting under high flash temperatures by frictional heating. Second, high sliding speed promotes the formation of a low friction transfer layer [74, 79]. Third, frictional heating accelerates the transition of autolubrication phase, for example, the transition from sp^3 to sp^2 phase in diamond coatings [80]. Fourth, the increase of sliding speed accelerates the ejection of debris from the wear track between the coating and the counterpart, which will reduce the ploughing effect [69]. However, with the continuous increase of sliding speed, if large-scale melting occurs, the friction coefficient will rise because of the sharp increase in the real contact area [68].

- **Running environments**

The effects of running environments, such as lubrication, temperature, relative humidity and ambience, on friction coefficient are different for different coatings and counterparts.

In the applications with liquid lubricants, coatings are just used to reduce friction and wear for mixed lubricated situations. Liquid lubricants prevent the formation of junction between two surfaces and lead to low shear strength, so the friction coefficient is very low.

The effect of temperature on friction coefficient is complex, because the variation of temperature will influence the formation and composition of transfer films, the shear strength of interfaces, the real contact area, and the surface morphology. For example, graphite, MoS_2 or $MoSe_2$ can lubricate until 400°C, and at higher temperatures, they will be seriously oxidized. For magnetron sputtered MoS_2 and $MoSe_2$ coatings, the latter has more stable friction coefficient than the former up to 200 °C [83]. Oxide and fluoride-based solid lubricants (e.g., CaF_2, BaF_2 and PbO), as well as some soft metals (e.g., Ag, Au), can endure elevated temperature, but they present high friction at room temperature or a lower ambient temperature [28].

The effect of relative humidity and ambience on friction coefficient depends on the material of coating and counterpart. For example, sputtered MoS_2 coating presents much lower friction coefficient in vacuum or inert gas than in ambient air [87, 92] due to its humidity sensitivity, while co-deposition with small amounts of metal, the MoS_2 composite coating is less sensitive to relative humidity [66]. Friction coefficient of $MoSe_2$ coating is independent of relative humidity within the range of 0~50% [83]. For DLC (a-C:H) coatings, the increase of humidity results in the increase of friction coefficient, while the friction coefficient of DLC (a-C) coatings decreases with humidity [60]. Graphite coating relies on adsorbed moisture or water vapors to achieve low friction. PVD TiN coatings in fretting tests presented high friction at low relative humidity and low friction at high relative humidity, because the presence of moisture seemed to promote the formation of lubricious reaction layers such as TiO_{2-x} [93]. Atmosphere also has a great effect on friction coefficient for DLC and MoS_2 coatings, e.g., friction coefficient of r.f. magnetron sputtered MoS_2 coatings is below 0.003 in ultra-high vacuum and in dry nitrogen, 0.015 ~ 0.018 in high vacuum and 0.15~0.20 in ambient air (RH = 40%) [87].

3.3 Important parameters for wear resistance

3.3.1 Theory models of wear

▪ Archard model

The most widely used quantitative wear equation was formulated by Archard [94] as following:

$$V = K \cdot \frac{P \cdot L}{H} \tag{1-8}$$

where V is the wear volume, P is the normal load, L is the sliding distance, H is the hardness and K is named as "wear coefficient", which is strongly affected by the material properties and the operating conditions. Archard model can be used in many situations such as adhesive, erosive and abrasive wear of ductile materials [38]. In this model, hardness is an important parameter.

▪ Model for brittle materials

For wear of brittle materials, fracture toughness is an important parameter. Considering different failure forms, several models were developed.

- Lateral crack model:

Evans and Marshall [95] assumed that the wear is due to brittle fractures caused by initiation and propagation of lateral cracks. They gave the following model:

$$V = C \frac{P^{9/8}}{K_{Ic}^{1/2} H^{5/8}} \left(\frac{E}{H} \right)^{4/5} L \tag{1-9}$$

where C is a constant, E the elastic modulus, and K_{Ic} the fracture toughness. In this model, the wear strongly depends on hardness and toughness.

- Tensile crack model:

Wang and Hsu [96] considered that the tensile stress at the rear edge of the contact was the predominant stress which causes cracks and the subsequent wear.

$$V = C \frac{\sigma_{\max}}{\sigma_D} \frac{PL}{H(T)} \tag{1-10}$$

where σ_{max} is the maximum tensile stress, σ_D the critical damage stress from a fracture mechanics model, $H(T)$ the temperature-dependent hardness and T the temperature.

For severe wear with cracks and considering the effect of friction heat, Hsu and Shen [97] modified this model as:

$$V \propto \frac{\sigma_{\max} \sqrt{a}}{K_{1c}} \frac{T^*}{T_0} \frac{PL}{H(T^*)} \tag{1-11}$$

where T^* is the interfacial temperature, T_0 the ambient temperature, a the crack length that determines the stress intensity.

▪ Model for compound impact wear

Compound impact signifies that normal impact occurs with a component of sliding, or two bodies impact at a tangential direction, e.g., the seating of valves on their seat inserts in internal combustion

engines. Compound impact can lead to much higher wear rate than normal impact alone. Lewis [98] developed a model for predicting compound impact wear, as shown in the following equation.

$$V = \left(\frac{k\overline{P}N\delta}{H} + KN\left(\frac{1}{2}mv^2\right)^n \right)\left(\frac{A_i}{A}\right)^j \quad (1\text{-}12)$$

The first item of the equation comes from Archard model [94] of sliding wear, and the second item is the wear volume contribution of impact. In the equation, V is the wear volume, $\overline{P}$ the average load at the contact interface, N the number of cycles, H the hardness of the softer material, k the sliding wear coefficient, δ the slip at the interface, K, j and n wear constants determined from experimental data, m the mass of the impact body, v the impact velocity, A_i the initial contact area and A the contact area after N cycles. In this model, the kinetic energy of impact body is very important for impact wear.

▪ Models based on dissipated energy

In the Archard formula, the effect of friction coefficient is not taken into account, so sometimes the wear rate presents a poor stability. Mohrbacher *et al.* [99] introduced the concept of cumulated dissipated energy for bidirectional sliding (fretting) contact conditions, which is calculated from the tangential force and the linear displacement in the whole test. They believed that the wear of materials in sliding contacts is the result of energy dissipation due to friction of the contacting bodies. Then, Huq and Celis [86] applied the dissipated energy approach in ball-on-disk unidirectional sliding tests of TiN coatings, and got a linear relationship between wear volume and the cumulated dissipated energy. Ramalho and Miranda [100] extended the energy method to the experiments with crossed cylinder sliding contact. Larbi *et al.* [101] validated that wear is a function of the energy dissipated under cylinder-on-flat contact. Fouvry *et al.* [102-105] put forward the concept ″the maximum dissipated energy density″ to relate to the maximal wear depth.

3.3.2 Effect of parameters

According to literature, the effect of parameters of coating systems on different wear mechanisms is summarized in Table 7. According to the table, the effect of a parameter on various wear mechanisms is different.

▪ Coating hardness

According to Archard model, there is a linear relationship between wear volume and the inverse of hardness. Many researchers found that high hardness of coatings can result in a good wear resistance in their experiments [34, 106-114]. Therefore, coating hardness is generally looked as the most important parameter for wear resistance of a coating. However, recently, some experiment results show that high hardness does not always result in good wear resistance [48, 53, 107, 115], because the pursual of super- or ultra-hard coatings is usually at the cost of ductility and fracture toughness.

▪ Substrate hardness

When a thin coating is employed, the load is mainly carried by the substrate, so the contact area and the strain of the coating depend on the substrate hardness. For example, the experiments of sputtered MoS_2 coating on three substrates with different hardness indicated that the coating on the softest substrate (titanium alloy with a Vickers hardness of 310) presented the worst endurance, and the coating on the hardest substrate (silicon nitride with a Vickers hardness of 1995) led to a three

orders of magnitude higher lifetime, as shown in Figure 25 [63]. In fretting tests of TiN coating on several substrates, Shima *et al*. [61] also found that a harder substrate can result in a longer coating lifetime.

Table 7: Effects of parameters of coating systems on different wear mechanisms.

Parameters	Wear							
	Abrasion	Adhesion	Delamination	Fatigue wear	Corrosive wear	Impact wear	Erosion	Fretting wear
Coefficient of friction		↗[34]						
Counterpart								
Hardness		↘[44] ↗[116]						
Roughness	↗[36]							
Shear strength								
Chemical properties		×[34, 59]			×[34]			
Coating								
Thickness	∨[34, 51, 117] =[118] ↗[113]	∨[50, 109, 117, 119, 120] ∧[121] ↘[54, 110, 122]	↗[123] ∨[49, 124]	∧[121]		↗[121]	↘[125] <[6]	↘[8]
Hardness	↘[34, 106-108, 113, 114] <[115]	↘[109-111] ↗[126]	↗[107, 127] ↘[112, 114]	↗[126]		↗[32, 115]	↘[125]	↘[3]
Elastic modulus	↘[34]	↗[126]	∨[128] ↗[123]	↗[126]		∨[128]↗[106] ↘[129]		⟨[39]
H/E	↘[12, 106, 107, 111, 115, 130-136]	↗[126, 137, 138]		↗[126, 137, 138]		↘[12, 139, 140] ↗[129, 138, 141]		
Shear strength								
Fatigue strength				↘[34]				↘[39]
Yield strength								↘[39]
Microstructure	×[17, 108, 142]	×[48, 110, 126]	×[114]				×[125]	
Fracture toughness	↘[143]			↘[34, 135]		↘[32, 129]		
Residual stresses			↗[128]	↗[135]		↗[128]		↗[3, 39]
Chemical properties		×[34, 48, 57, 58, 119]			×[34, 64]			
Thermal properties		×[32, 34]						
Interface								
Bonding strength	↘[51, 117, 134]	↘[48, 53, 56, 62, 63, 109, 117]	↘[49]	↘[62]		↘[121]	↘[125]	↘[39]
Substrate								
Hardness	↘[34]							↘[8, 61]
Roughness	↗[46, 54] =[144]	↗[50, 54, 64, 89] =[62] ∨[63]	↘[128] ↗[124]	↗[62, 89]	↗[46]	↘[128]		<[3]↘[8]
Elastic modulus	↘[34]							
Chemical properties		×[63, 64]						
Thermal properties								
Running conditions								
Load	↗[69]	=[89] ∧[44] ↗[67, 76, 81, 145] ⟨[58]		↗[89]		↗[141]		↗[61, 146]
Velocity	↘[78]	↗[120, 147] ↘[53, 80, 148]∧[81, 149] ∨[150]						
Slip amplitude								↗[3, 61]
Lubrication	×[16]	×[32, 48]			×[34]			
Temperature		↗[32, 147] ∨[83]			↗[32, 82]			∨[8]
Relative humidity		↘[57, 151]						<[3] ↘∧ [86] ↘[93]↗[8]
Ambience (air, vacuum,…)			×[124]		×[32, 34, 69, 152]			air[3]

(× means that the parameter influences wear, but it cannot be expressed in data.
↘ means that wear decreases with the increase of the parameter.
↗ means that wear increases with the increase of the parameter.
∧ means that wear first increases, then decreases with the increase of the parameter.
∨ means that wear first decreases, then increases with the increase of the parameter
< means that wear may increase or decrease with the increase of the parameter.
= means that wear does not change with the increase of the parameter.)

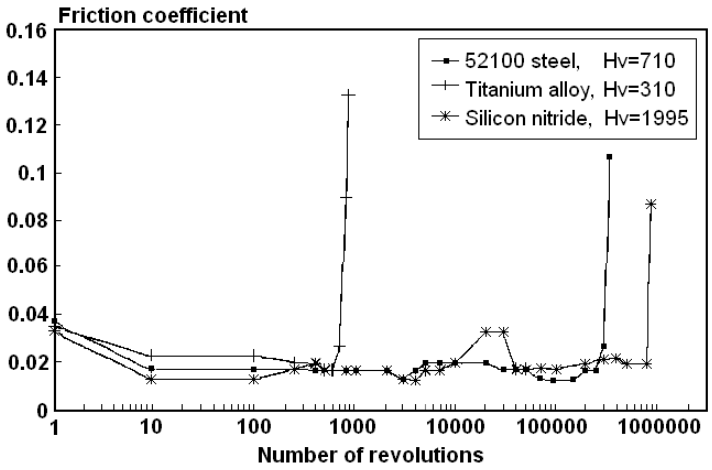

Figure 25: Variation of friction coefficient with sliding distance for 3 MoS_2 coated substrates of nominal roughness 0.2 µm [63].

▪ **Elastic modulus mismatch**

The use of coatings usually induces elastic modulus mismatch between coatings and substrates, which will cause residual stresses at the interface. Especially, hard coatings have higher elastic modulus than the substrates, and under heavy loads, the coatings cannot suit the deformation of the substrates, which leads to the nucleation and propagation of cracks in the coatings. Some researchers found that a low elastic modulus mismatch (E_c-E_s) is the most important parameter for impact wear [55, 106, 128], because high tensile stresses at the coating/substrate interface due to large elastic modulus mismatch can result in high wear, as shown in Figure 26.

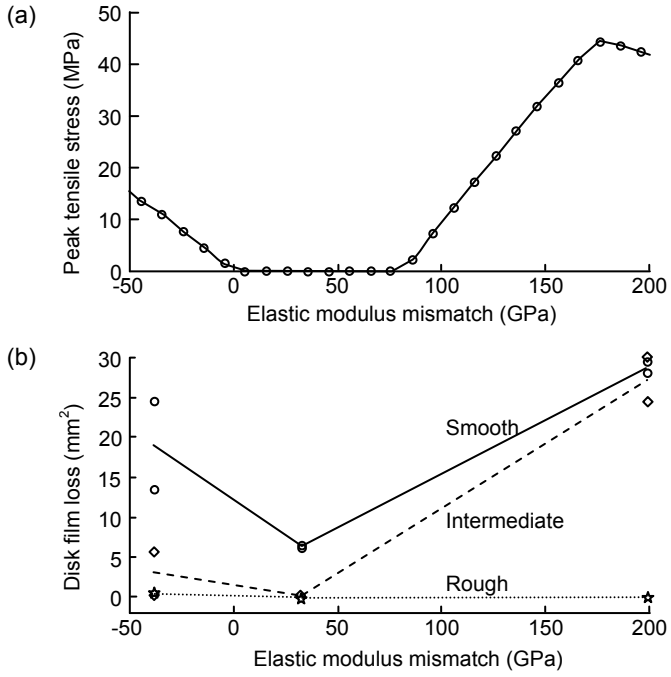

Figure 26: (a) peak tensile stress at the film/substrate interface and (b) area of disk film loss plotted against film/substrate elastic modulus mismatch for three different surface roughnesses [128].

- **Ratio of coating hardness to elastic modulus (*H*/*E*)**

For the contact of two cylinders or two balls, the maximal loads that the surface can sustain without plastic deformation are respectively proportional to H^2/E and H^3/E^2, so the combination of a high hardness and a low elastic modulus is expected to resist plastic deformation [153]. Oberle [130] pointed out that a truer measure of abrasive wear resistance is the amount of elastic deformation that the surface can sustain. The larger the elastic limit of strain (ε_{lim}), the better should the surface be able to resist damage by abrasive wear. And $\varepsilon_{lim}=\sigma_{lim}/E$, where σ_{lim} is the elastic limit of stress, empirically, $\sigma_{lim} \propto H$, so $\varepsilon_{lim} \propto H/E$. In other words, the higher the ratio of H/E, the better is the abrasive wear resistance of materials.

Recently, Leyland and Matthews [115] found that a high hardness and a low elastic modulus, i.e., a high ratio of H/E, which means improvement of the toughness and "elastic strain to failure", is a reliable indicator of wear resistance, which has been cited by many researchers [106, 131, 133, 134, 136, 140, 154, 155]. Using the same coating CrN as the surface coating, different thin films as the interlayer, Ni *et al.* [133] confirmed the effect of H/E on wear resistance, as shown in Figure 27, and rationalized the effect of H/E on wear caused by plastic deformation from the relationship between H/E and W_e/W_{tot}, h_f/h_{max}, "plasticity index" [42], where W_e and W_{tot} are respectively reversible work and total work of indentation tests, h_f and h_{max} are respectively final indentation depth and maximum indentation depth. More recently, some other researchers [156, 157] validated the relationship between H/E and $(W_{tot}-W_e)/W_{tot}$ and h_f/h_{max} by theoretical analysis, finite-element calculation and nanoindentation experiments.

However, some researchers put forward different viewpoints for the following situations.

i) For brittle coatings, a high H/E is unable to result in an elastic deformation; a high fracture toughness is more important [143].

ii) Under cavitation erosion, the H/E ratio was not found to be a reliable indicator of wear resistance [129].

iii) Under adhesive or adhesive-fatigue wear conditions (cutting tool), a high ductibility ($(W_{tot}-W_e)/W_{tot}$, i.e., a low value of H/E) leads to a good wear resistance [137, 138].

iv) H/E ratio as an indicator of wear resistance is unsuitable for nonhomogeneous coating [158].

Therefore, the H/E indicator just adapts to the wear caused by plastic deformation for some coatings.

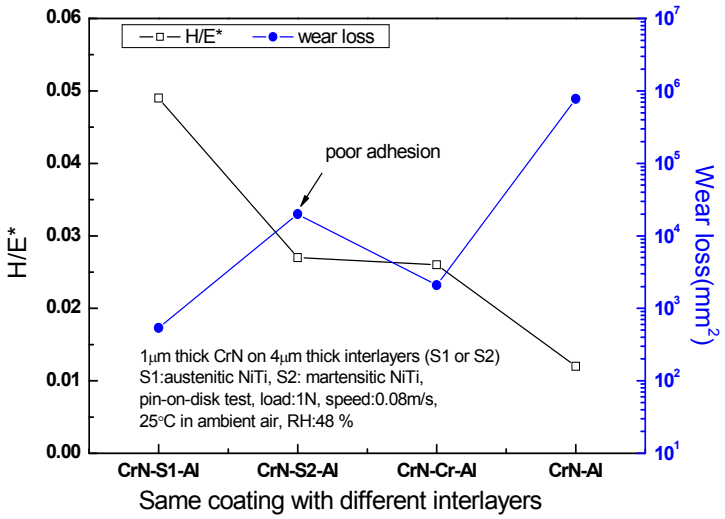

Figure 27: Effect of H/E^* on wear caused by plastic deformation [133].

▪ **Fracture toughness of coatings**

Fracture toughness is a very important parameter under fatigue wear, impact wear and erosion wear [32, 34, 129, 135, 138, 143, 159].

In indentation fracture tests, Lawn *et al.* [160] found a simple relationship between the fracture toughness and the length of the radial cracks, *c*:

$$K_c = \alpha\left(\frac{E}{H}\right)^{1/2}\left(\frac{P}{c^{3/2}}\right) \qquad (1\text{-}13)$$

where *P* is the indentation load and α is an empirical constant. According to this relationship, the Oliver–Pharr method which was used to determine the elastic modulus and hardness by nanoindentation tests can be used to measure the fracture toughness of coatings [161]. Zhang *et al.* [159] suggested that coating toughness is proportional to a "Scratch Crack Propagation Resistance" (CPRs) parameter, CPRs= $L_{c1}(L_{c2}\text{-}L_{c1})$, where L_{c1} and L_{c2} are respectively the critical load linked to first crack event and dramatic coating failure in scratch tests. This method can be used to quickly qualitatively compare the toughness of coatings.

▪ **Bonding strength**

Good adhesion between coating and substrate is the precondition of wear resistance, and poor bonding usually results in coating detachment and delamination. The bonding strength depends on the bonding mechanism and the internal stresses, which are influenced by several factors, such as the chemical composition of coating, the substrate material, the deposition method, the deposition parameters, the pretreatment of substrate surface, and the thickness of coating. Scratch test is the primary method for the evaluation of adhesion strength, in which a stylus is used to scratch the coating with a continuously increasing normal load until reaching a "critical load" at which adhesion failure occurs. Some measures can be employed to improve the bonding strength. For example, sandblasting is the most common method to roughen the substrate surface and improve the adhesion for thermal sprayed coatings [162]. Some interlayers can improve the bonding strength, such as Ti interlayer between TiN, TiB_2, VN or TaC coatings and tool steel substrates, Cr interlayer for DLC coatings and tool steel substrates [35]. Alternating multilayer of TiN with Ti interlayer can generate coatings thicker than 10 μm without adhesion problems [158].

▪ **Microstructure**

The tribological performance of a coating is closely connected to its microstructure. The microstructure (such as porosity, grain size, grain shape) depends on chemical composition, the deposition method and the deposition parameters. For example, in PVD deposition process, the microstructural evolution of the films strongly depends on gas pressure, deposition temperature and the substrate bias voltage. At a higher bias voltage, the film was composed of granular structures, while at a lower bias voltage, the films had columnar structures [38]. CVD TiN coatings deposited under temperatures from 850°C to 1150 °C presented different microstructures and wear resistance [163]. In [48], despite a higher hardness than $Ti_{10\%}$-C:H and $Ti_{20\%}$-C:H, the $Ti_{30\%}$-C:H coating showed a high friction coefficient and poor wear resistance due to the columnar microstructure and crystalline surface topology. Simply changing the substrate temperature during sputtering, the structure of sputtered MoS_2 films can change from crystalline to amorphous. When MoS_2 is sputtered on cold substrates (7°C down to -195°C), an amorphous structure is formed. These amorphous films are very brittle and do not display any lubricating properties, and are essentially abrasive. When sputtered at ambient or elevated temperatures, MoS_2 films exhibit the characteristic columnar structure

corresponding to crystallite growth in which the low-shear basal planes are aligned perpendicular to the substrate surface [92]. In addition, grain size strongly influences the hardness and wear resistance of a coating. According to classical Hall–Petch effect, for polycrystalline materials, reduced grain size results in the increase in hardness, however, further grain size reduction leads to an “inverse Hall–Petch effect”, as shown in Figure 28.

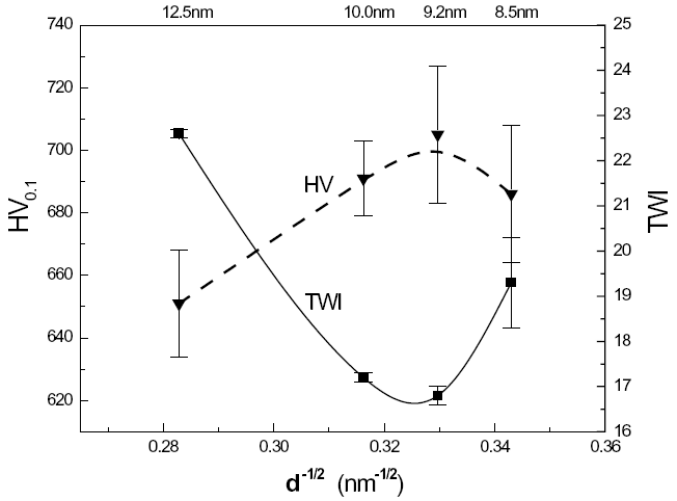

Figure 28: Hardness and Tabor wear index (TWI) as a function of grain size for nanocrystalline Ni-P coatings [108].

▪ Coating thickness

If there is only progressive wear, the thicker coating is certainly the better. In [164], a finite element model is used to predict the plastic deformation behavior for TiN coating-substrate system. According to Figure 29, a thicker coating has a higher threshold load of plasticity. However, for most coatings, there exists an optimum thickness for wear resistance, as shown in Figure 30 [50], because excessively thin coating can be easily penetrated or worn away and excessively thick coating usually induces adhesion problem due to poor flexibility and high residual stresses, as shown in Figure 31 [51]. Furthermore, for PVD deposition process, the coatings with the larger thickness present coarser superficial microstructures and weaken the mechanical properties due to the columns growth, as shown in Figure 32.

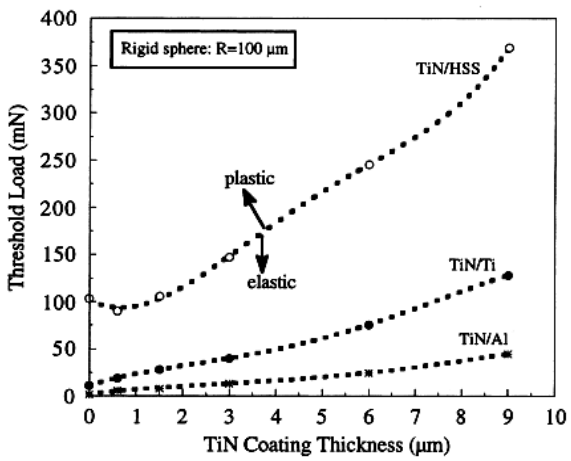

Figure 29: Deformation maps for various elastic–plastic TiN plating coating–substrate systems [164].

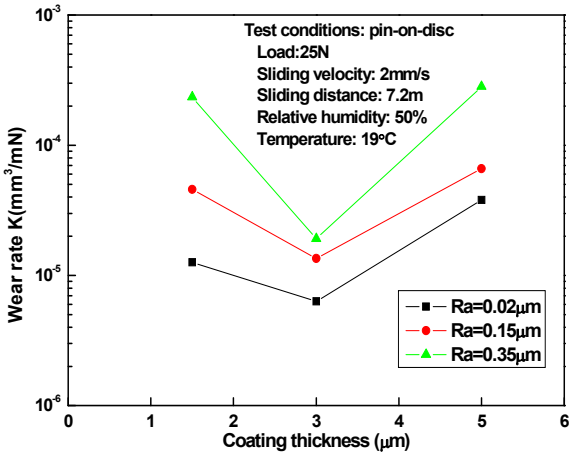

Figure 30: TiN coating deposited on steel by ion rubs against an alumina ball [50].

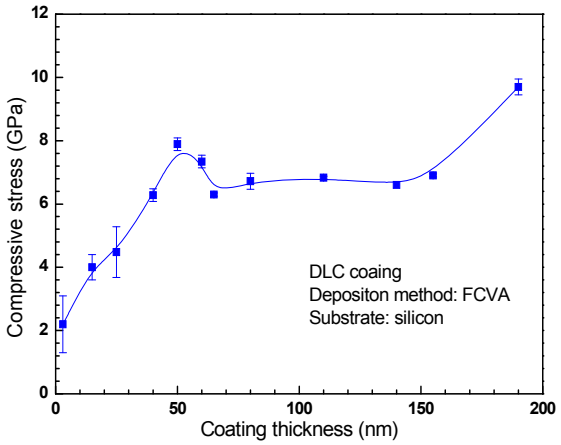

Figure 31: Effect of coating thickness on the interfacial residual stresses [51].

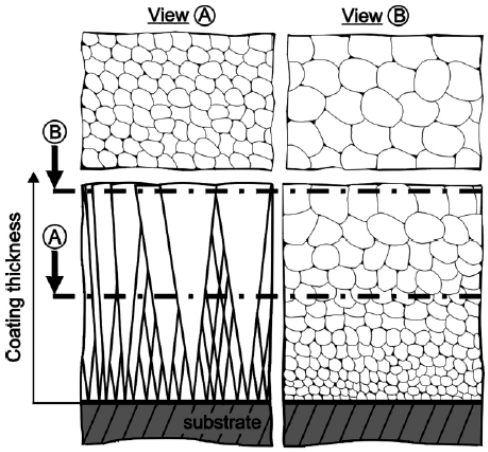

Figure 32: Microstructure of PVD coating at various thickness [110].

▪ Roughness of substrate surface

In general, the wear rate of coatings significantly increases with the increase of substrate surface roughness. Especially, the increase will be more rapid when the roughness exceeds a critical value, which results in a small contact area and plastic yield in local contact [89]. However, according to different coatings and contact conditions, there are some exceptions. For example, the a-C:Cr coating shows a much more pronounced influence of surface roughness on the coating wear rate than the a-C:W coating due to different wear mechanisms [62]. Sometimes, a smooth substrate surface can lead to delamination wear due to poor adhesion of coatings on the substrate [128]. A suitably rough surface induced by sandblasting or shot-peening usually improves the wear resistance [8], especially for thermal spraying processes.

▪ Normal load (contact pressure)

According to Archard model, wear volume is proportional to normal load and independent of the shape and size of contact surfaces. Many experiment results showed that wear increased with normal load [67, 69, 76, 89], and the influence of counterpart size on wear volume under a same normal load was also found [67]. In fact, contact pressure is a more important indicator than normal load for analyzing the wear behavior of coatings. In the wear map of Lim and Ashby [165], contact pressure and sliding speed were considered as the most important parameters, which determine the wear mechanisms. According to the Hertz theory, if the maximum contact pressure exceeds 1.6 times of the yield strength, Y, overall plastic yield will occur. However, Jiang and Arnell [89, 166] found that for DLC and MoS_2 coatings, the critical contact pressure under which wear modes change from a mild wear regime to a severe wear regime is $0.63Y_{DLC}$ and $0.57Y_{MoS2}$ respectively, lower than $1.6Y$, which is probably attributed to two reasons: one is that the fatigue limit of material is lower that the yield strength under cyclic load, the other is that the real contact stress of a rough surface is much higher that the calculation result of Hertz theory.

▪ Sliding speed

Sliding speed is the main influence factor of friction heating, and it will also result in the change of wear mechanism. According to data of literature, the evolution of wear rate with sliding speed includes several phases. When the sliding speed is very low, the coating is worn due to the stick-slip process, the increase of sliding speed will shorten the interval of contact between the given parts of two

surfaces, which will reduce the adhesion wear [81, 148, 150]. The further increase of the sliding speed will result in the increase of the wear rate owing to the brittle fracture of asperities for Cr_2O_3 coatings [81], the oxidization reactions and the graphite phase transformations for DLC coatings [150]. Above a critical value, the wear rate will decrease again with the increase of sliding speed because of the coating softening by friction heating [53, 81] or the formation of graphite lubricant phase in diamond coatings [80]. At very high sliding speed, the wear rate of coatings will increase rapidly by dissolution wear, severe-oxidation wear, especially the coatings deposited on cutting tools [120]. The influence of sliding speed on wear rate also depends on other parameters, such as normal load, materials of coating and counterpart, and running environments.

- **Running environments**

Running environments (lubrication, temperature, relative humidity, ambience, etc.) also influence the wear of coatings, but for different coatings, the effect is very different. For example, MoS_2 coatings are unsuitable to the environment of humid air because MoS_2 can be oxidized in air and the existence of water vapor and high temperature can speed up the oxidation process [167], while the size of the damaged surface area as well as the wear volume on the PVD TiN coatings were found to be larger at low relative humidity [93].

4 Coating selection

There is no general rule for coating selection, because the use of tribological coatings is a complicated situation. Tribological performance is not an intrinsic property of coatings, but depends on the whole system, which is influenced by many parameters. Additionally, the balance among tribological performance, non-tribological performance, cost and ecological effect should be considered.

Up to now, when tribological coatings need to be used in a new application, some experiments must be employed to evaluate the tribological behaviors of several coatings, which are empirically selected. This approach is often inefficient and the selected coating can be not the most suitable one. In order to solve this problem, researchers have put forward several approaches. Some are about the general selection process, some aim at several specific contact types, some focus on the selection according to experimental results.

4.1 Global selection methodology

Matthews [168-171], Franklin [172, 173] and Holmberg [6, 16] did much work in the field of coating tribology for a long time, and they provided a comprehensive consideration about the coating selection process, as shown in Figure 33. At first, according to the requirements of the application and the characteristics of coatings and deposition processes, a pre-selection process is realized to select 5~10 possible coatings. Following the first stage, some laboratory tests and bench/field tests will be carried out to select the best coating. In order to achieve the pre-selection, in early time, Matthews [168] and Franklin [172] developed knowledge-based expert systems to help the selection. Recently, Matthews and Holmberg [6] suggested selecting coatings according to different contact types, which include 7 typical contacts, as shown in Figure 34.

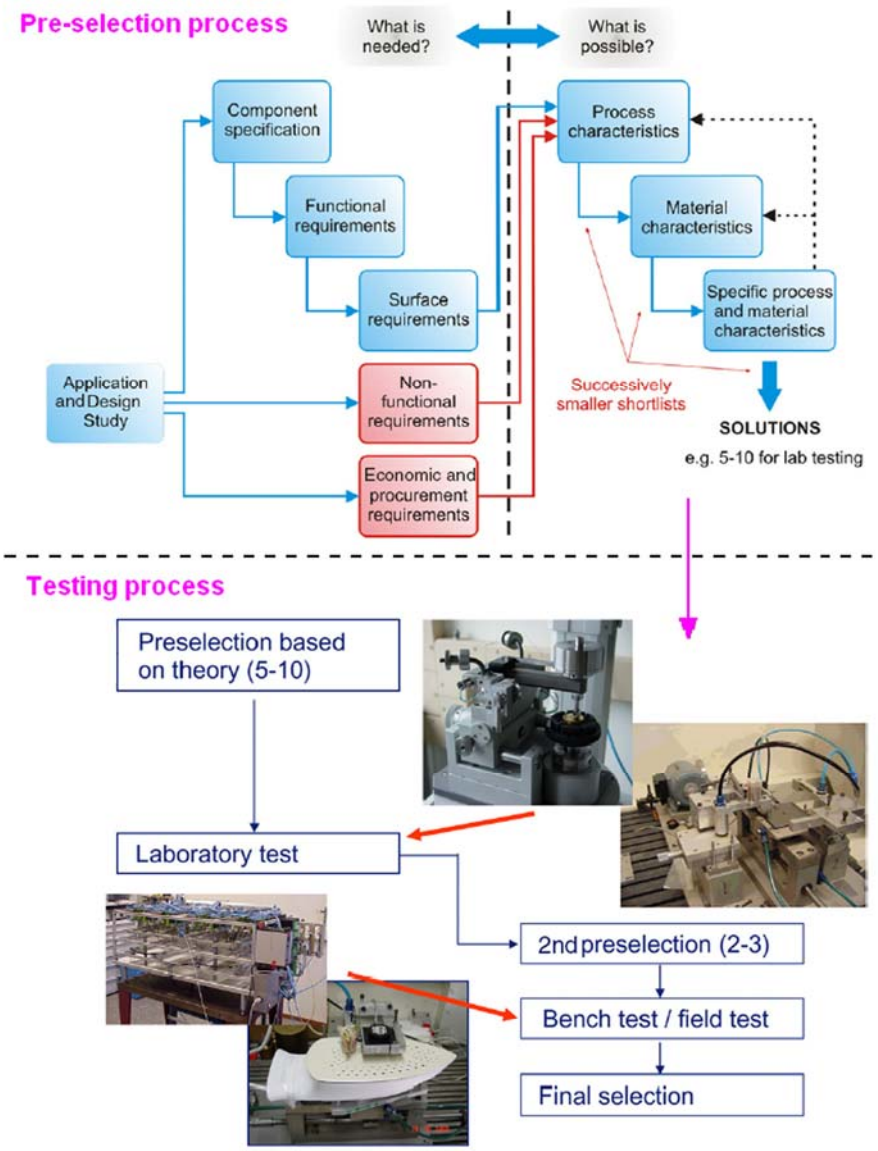

Figure 33: Coating selection process [171].

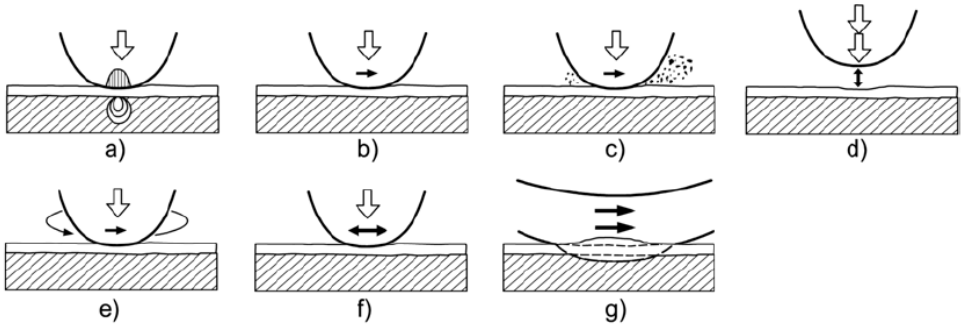

Figure 34: Typical contact conditions in tribological applications of coated surfaces: (a) contact stresses, (b) sliding, (c) abrasion, (d) impact, (e) surface fatigue, (f) fretting and (g) chemical dissolution [6].

For each contact type, Matthews and Holmberg [6] gave some brief suggestions.

(a) Static normal loading: Typical required properties of the surface are adequate yield strength and hardness. So, thermal hardening, thermochemical diffusion treatments can be employed.

(b) Sliding: The predominant wear is adhesion, so low shear strength at the top layer and good load carrying capacity are expected, and the possible coatings include DLC, MoS_2, diamond, (electroless) NiP-PTFE, (electrolytic) Co-Cr_3C_2 (at T >300°C), thermal sprayed WC-Co.

(c) Abrasion: When particles exist, the coatings should have good microtoughness and load carrying capacity, high hardness to resist plastic deformation, and sufficient coating thickness. Weld surfacing, hardfacing, thermal sprayed hard coatings, TiN, TiAlN, TiC, Al_2O_3, CrN, CrC, hard chromium, thermochemical diffusion treatments are possible selection.

(d) Impact: Good microtoughness and elasticity are very important. Thermochemical diffusion treatments, or tough resilient coatings (sandwich, graded, duplex, multilayer, nanocrystalline, multicomponent) are possibly useful.

(e) Surface fatigue: Good microtoughness and load carrying capacity are the favorable properties, and thermochemical diffusion treatments, or tough coatings (sandwich, graded, duplex, multilayer, nanocrystalline, multicomponent) can suit this situation.

(f) Fretting: Good elasticity, low shear strength surface layer, not producing hard wear debris and surface chemistry: inertness or lubricious reaction product is necessary. MoS_2, Cu-Ni-In multilayer, DLC can meet the requirements.

(g) Chemical dissolution (metal cutting): Non-soluble and thermally conductive are important aspects. Hard coatings are usually employed, such as TiN, TiAlN, TiC, WC, CrAlN, DLC, diamond.

In order to mitigate fretting wear by using coatings or surface treatments, Fu *et al.* [3] recounted a general coating selection process:

The first step is to identify the major failure modes on the surfaces (i.e., sliding wear, fretting wear or fretting fatigue), so a detailed investigation must be carried out, including the mechanical and material analysis at contact, the service conditions (such as contact nature, normal load, vibration, frequency, design requirement, etc.) and working conditions (such as working environments, temperature, liquid, etc.). Thus, guidelines can be obtained about looking for the suitable surface modification methods for the specific contact problems.

Table 8: Effects of surface modification technologies on fretting damage [3].

Surface modification methods	Decrease the friction coefficient	Introduce compressive stress	Increase in hardness	Increase in surface roughness	Durability or adhesion	Economy	Mitigation of fretting wear	Mitigation of fretting fatigue
Carburizing	✓	✓	✓	D	✓✓	✓	✓	✓
Nitriding	✓	✓✓	✓✓	D	✓✓	✓	✓	✓
Electroplating (Cr, Ni, etc.)	D	××	✓	D	×	✓	✓	××
Hard anodizing	D	×	✓	D	✓		✓	××
Shot-peening	×	✓	✓	✓✓	-	✓✓	✓✓	✓✓
Plasma sprayed coating	D	D	D	✓	××	✓	D	D
Solid lubricated coatings	✓✓	D	D	×	D	×	✓	✓
Ion implantation	✓	✓✓	✓	D	✓✓	×××	✓	✓
IBED hard films	✓	✓	✓	××	✓	××	✓✓	✓✓
PVD and CVD hard coatings	✓	D	✓	×	D	×	✓	D
Laser alloying or laser cladding	D	×	✓	✓	✓✓	✓	✓	D

D: depending on conditions; ×: bad effect; ✓: good effect

The next step is to choose the appropriate coating methods according to the previous investigation, considering the substrate, the coating properties, the non-functional requirements and economic,

procurement, fabrication cost, material costs, etc. In order to help the selection, a relationship table between some surface methods and tribological functions was summarized (Table 8).

Finally, quality control tests (basic physical, mechanical and fretting tests, such as thickness, adhesion, microhardness, chemistry, tribological tests, elastic modulus, yield strength, fracture toughness, etc.) are recommended in order to justify the effectiveness of the surface coatings.

4.2 Pre-selection methodology

Pre-selection process of coatings, selecting several coatings from hundreds of thousands of possibilities, is a complex work, so the best way is to utilize some tools: expert systems or information systems.

▪ The research group of Matthews [168, 174] developed a knowledge-based expert system "TRIBSEL" for tribological coating selection. In this system, selection criteria including the following 5 aspects were used: (1) operating constraints, (2) processing constraints, (3) geometrical constraints, (4) topographical constraints and (5) economic constraints.

▪ Franklin and Dijkman [172] developed another expert system "PRECEPT" to assist the coating selection during the initial stages of the engineering design process. Selection rules were suggested according to different situations, such as mechanical contact overloading, fretting, excessive material transfer, 3-body abrasion, 2-body abrasion, negligible wear, surface fatigue, and steady-state wear factor.

▪ Dobrzanski and Madejski [175] designed the prototype of an expert system to select coatings for metals, where a selection rule in terms of the total weight point was used. There are some requirements (K_1, K_2, ..., K_n) for the coatings in a specific application, and every requirement has a weight value "weight K_i". The coatings were scored according to the extent that the coatings meet the requirements, as the following equation. The higher the point is, the better the coating.

$$\text{total} = K_1 \times \text{weight } K_1 + \ldots + K_n \times \text{weight } K_n \qquad (1\text{-}14)$$

▪ Landru [176] developed a surface treatment selector in his thesis work to select coating for various objectives, such as decoration, protection and improvement of surface properties. In this system, a simple selection was carried out by designating the objectives and the substrate material, and a percentage was used to indicate the extent of a surface treatment meeting the requirements of an application. The percentage was the product of an objective point and a substrate point:

- If the objectives are the properties of a surface treatment, the objective point is 100%;
- If the parents of the objectives are the properties of a surface treatment, the objective point is 75%;
- If the children (d=1) or grandchildren (d=2) or great-grandchildren (d=3) of the objectives are the properties of a surface treatment, the objective point is 100%/(1+d);
- If there is no relationship between the objectives and the properties of a surface treatment, the objective point is 0;
- If the substrate just suits the treatment process, the substrate point is 100%;
- If a parent set of the substrate suits the treatment process, the substrate point is 90%;
- If a child set of the substrate suits the treatment process, the substrate point is 100%/(1+d);

▪ Schiffmann *et al.* [177] developed a web-based information system for coating selection, which included the content of the German OSTec research program of the last 10 years available. Up to now, only PVD and CVD coatings have been considered. In this system, a qualitative, fuzzy classification

scale was introduced to describe material properties and functional coating characteristics. It consisted of a point scale from 1 to 10, corresponding to very low and very high. The coatings could be searched by keywords, material properties, coating functions, chemical composition, and combinations of properties. The best match coating was selected by the root-mean-square deviation between the target value and the coating value of properties.

$$\min Q = \frac{1}{n}\sqrt{\sum_{i=1}^{n}\left[T(i)-C(i)\right]^2 \cdot W(i)} \qquad (1\text{-}15)$$

where *W(i)* is the weight factor of property *i*, *T(i)* and *C(i)* are the target value and coating value of property *i*.

4.3 Selection methodology according to experiments

▪ In the research of anti-friction coatings for fretting applications, Langlade *et al.* [178] believed Wöhler-like curves (contact pressure vs. number of cycles) is a promising method for coating selection. However, a basic superposition of Wöhler-like curves for different coatings leads to a quite confused presentation, as shown in Figure 35a. So, they used another method, i.e., comparing all the tested coatings to a reference coating. For example, choosing coating A as the reference coating whose endurance life is L_{ref}, and each other coating X was compared to the coating A and obtained a performance index I_x ($I_x=L_{ref}/L_x$, L_x is the lifetime of coating X), as shown in Figure 35b. According to this definition, all coatings exhibiting $I_x<1$ may be considered as better solutions than the coating A and the coating with the lowest I_x value is the best solution. This method can only be used under given running conditions because the performance index of a coating depends on running conditions, for example, the coating E1 is the best one under a maximal contact pressure of 1000 MPa, while the coating D3 is the best one under a maximal contact pressure of 1250 MPa.

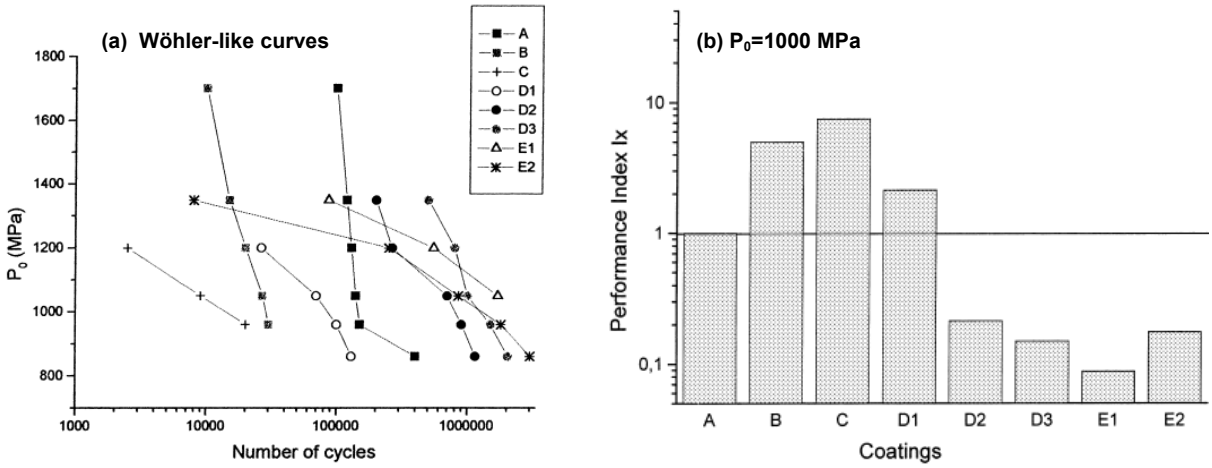

Figure 35: (a) Superposition of the Wöhler-like curves for all tested coatings, (b) Performance Index for all coatings considering coating A as a reference under different contact pressures [178].

▪ According to the fretting tests of several surface treatments and coatings, Carton [39, 179] used a polar diagram to give an overview of the fretting behavior of each coating being compared with the corresponding uncoated substrate. In this polar diagram, 12 parameters were considered, which were grouped as four sets plotted in four sectors:

- *Intrinsic properties of the coating*: elastic modulus (*E*), yield strength (σ_Y), fatigue strength (σ_D);
- *Properties at the coating-substrate interface*: residual stresses (p_r), binding strength (σ_{adh});

- *Running conditions*: load rate (T), width of stick plus partial slip domains on running condition fretting map (Δ), friction coefficient (μ);
- *Material response*: minimum duration of steady running conditions (n_S), minimum crack nucleation time (n_A), maximum crack depth (Z_F) and maximum wear depth (Z_U).

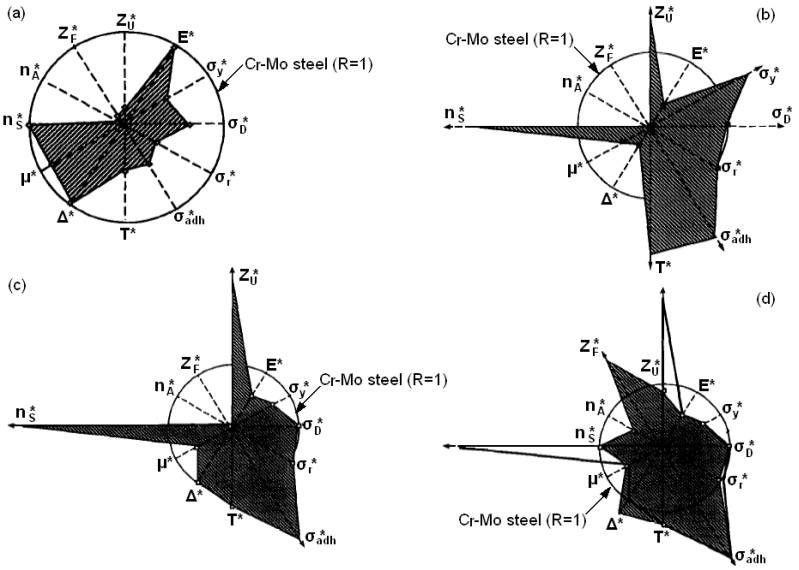

Figure 36: Polar diagrams for different surface treatments: (a) Gas nitriding, (b) Electrolytically deposited cadmium coating, (c) Plasma sprayed chromium carbide coating and (d) Chromium carbide coating after transfer of the coating on the 52100 steel counterface [39].

Each parameter on the polar diagram was written as the ratio X^* of the coating value X and the reference material value X_{ref}, i.e., $X^*=X/X_{ref}$ or $X^*=X_{ref}/X$. The ratio was defined so that an improvement in fretting behavior was associated with a ratio value less than 1.

A reference circle of radius 1 was drawn so that the plane was divided into two parts: an inner disk was associated with an improvement and an outer part associated with a worsening of the reference parameter. The polar diagrams of four coatings are shown in Figure 36, where the overview about the surface treatments can be easily obtained. Gas nitriding induced a general improvement of the mechanical properties, but running conditions were not modified. Although electrolytically deposited cadmium coating resulted in a low friction, it was rapidly removed due to the poor adhesion strength. The endurance of the plasma sprayed coating was also poor due to a high wear rate. Debris was transferred on the counterface which favored partial slip regime and consequently cracking.

5 Wear prediction

Wear prediction is a very important aspect in tribological applications, which means to forecast the service lifetime of relative components. However, it is a complex and tough task because the wear of contact surfaces is not an intrinsic material property but a complex system function. There are many models proposed to predict wear, but most of them are based on the specific materials and specific applications. Meng and Ludema [180] investigated wear equations in literature, and they found 182 equations, 28 of which are for erosion by solid particle impingement. 33 variables from particle, target and erosive condition were used in the equations, and the using frequency of each variable is listed in Figure 37. Additionally, 1~10 constants were used in the equations. Therefore, it is very difficult to use these equations; even under a specific condition the wear mechanisms evolve with the wear process. The following several simple models are the more popular.

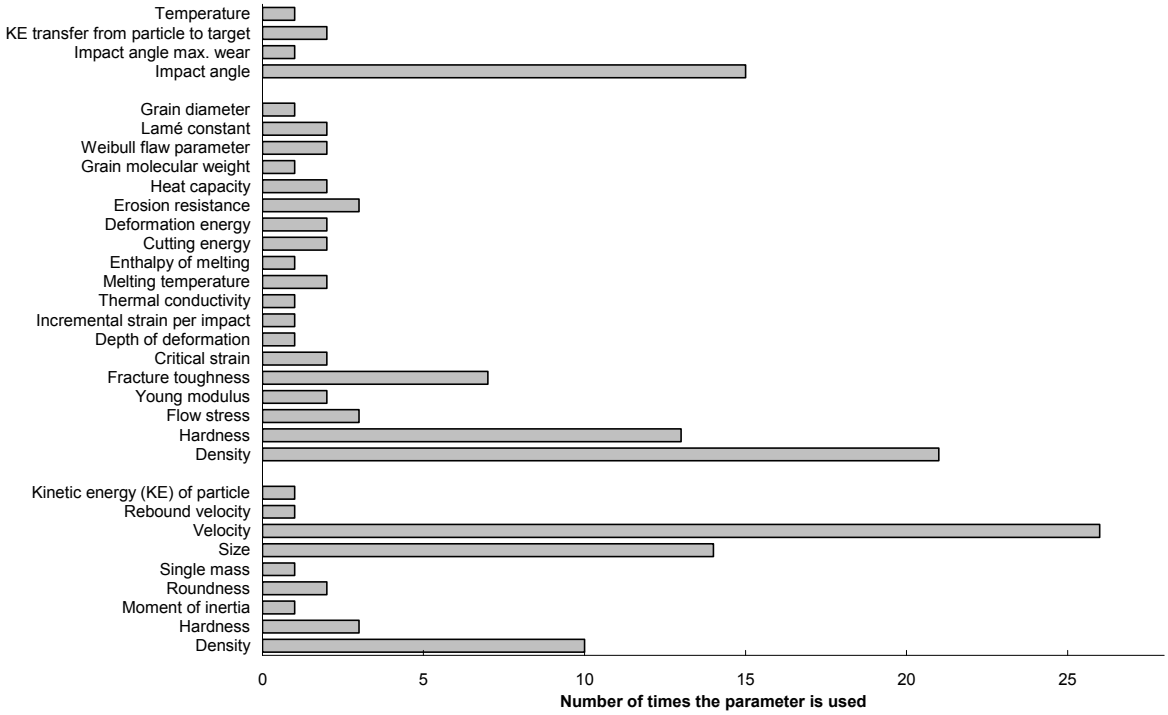

Figure 37: Using frequency of variables in 28 erosion equations [180, 181].

5.1 Wear maps

In order to find the relationship between wear mechanisms and running conditions, Lim and Ashby [165] developed a wear map (Figure 38) for steel to predict wear mechanism according to sliding velocity and contact pressure, and thought that asperity temperature was the underlying key to the various wear mechanisms. The wear mechanisms and modes involved in the map include ultra-mild wear, delamination wear, mild oxidational wear, severe oxidational wear, melt wear and seizure, which were related to the four basic wear mechanisms of Strang and Burwell by Holmberg and Matthews [6], as shown in Table 9.

Table 9: Relationship between wear mechanisms of Lim and Ashby and four basic mechanisms [6].

Wear mechanisms	Adhesion	Abrasion	Fatigue	Chemical wear
Seizure	×	×		
Melt wear	×			
Severe oxidational wear	×			×
Mild oxidational wear	×			×
Delamination wear	×		×	
Ultra-mild wear	×			

In this map, sliding velocity and contact pressure were normalized as:

$$\widetilde{V} = \frac{Vr_0}{a}, \qquad \widetilde{F} = \frac{F}{A_n H_0}$$

where V is sliding velocity, r_0 is radius of the apparent contact area, a is thermal diffusivity, F is normal force, A_n is apparent contact area and H_0 is room temperature hardness.

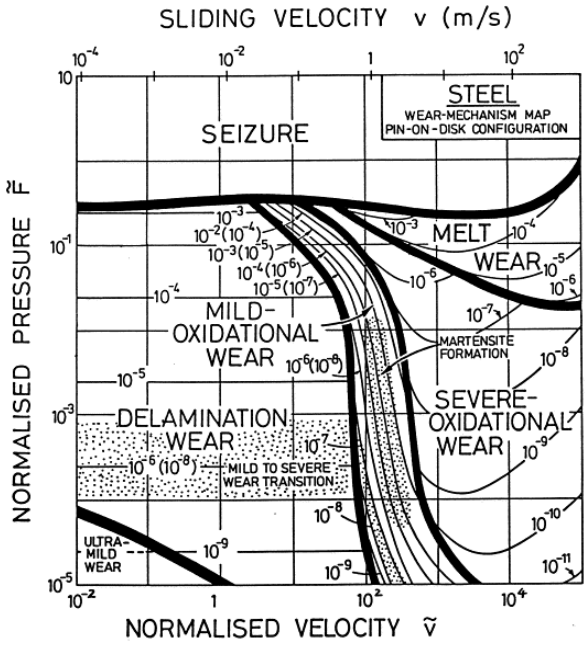

Figure 38: Wear map for steel under unlubricated pin-on-disk conditions [165].

According to this idea, wear maps of other materials were also developed. Alcock *et al.* [182] used the contours of logarithm of wear rate in the wear map of tungsten carbide pins against silicon carbide disks tests (Figure 39). According to the research of silicon nitride materials under unlubricated sliding between 22~1000°C, Skopp *et al.* [183] gave wear maps based on ambient temperature and sliding velocity (Figure 40). During the development of the wear map of magnesium alloy AZ91 in dry block-on-ring tests, Chen and Alpas [184] found that the surface temperature is a function of $F^{1/4}V^{1/2}$, and the transition from mild wear to severe wear is controlled by a critical surface temperature criterion (Figure 41). Hsu and Shen [185] developed 3D wear maps of several ceramic materials under different lubricated conditions (Figure 42).

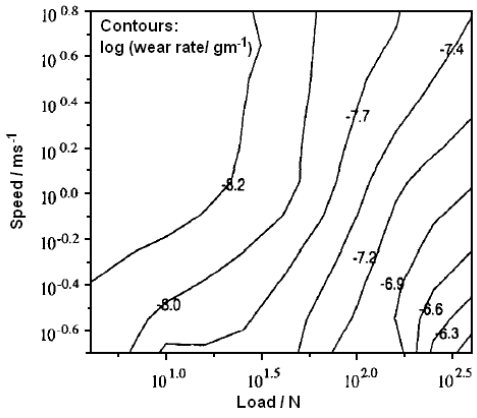

Figure 39: Wear map of tungsten carbide / silicon carbide [182].

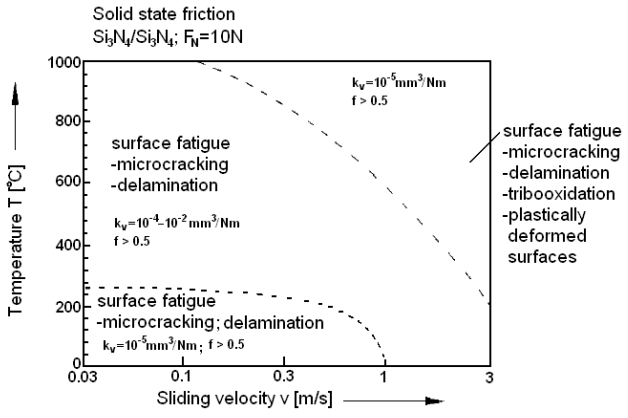

Figure 40: Wear map of Si_3N_4 / Si_3N_4 based sliding velocity and ambient temperature [183].

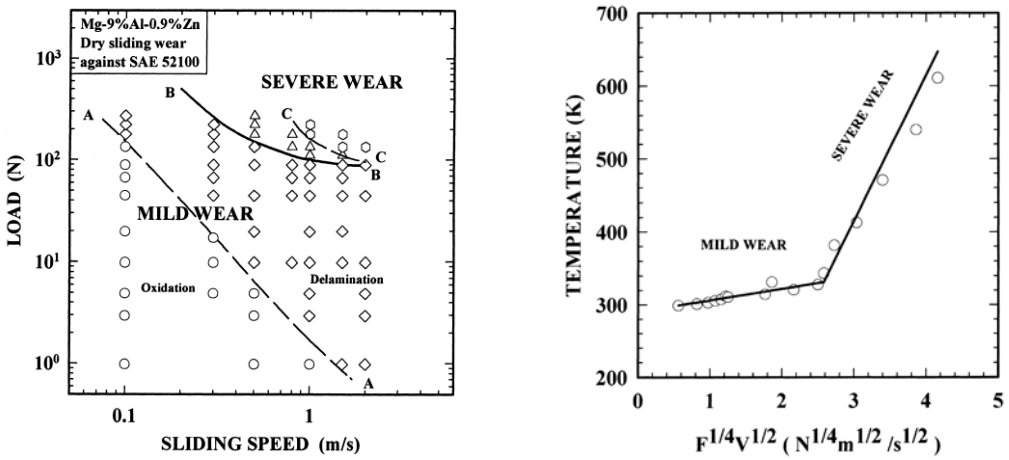

Figure 41: Wear map of magnesium alloy AZ91 in dry block on-ring tests [184].

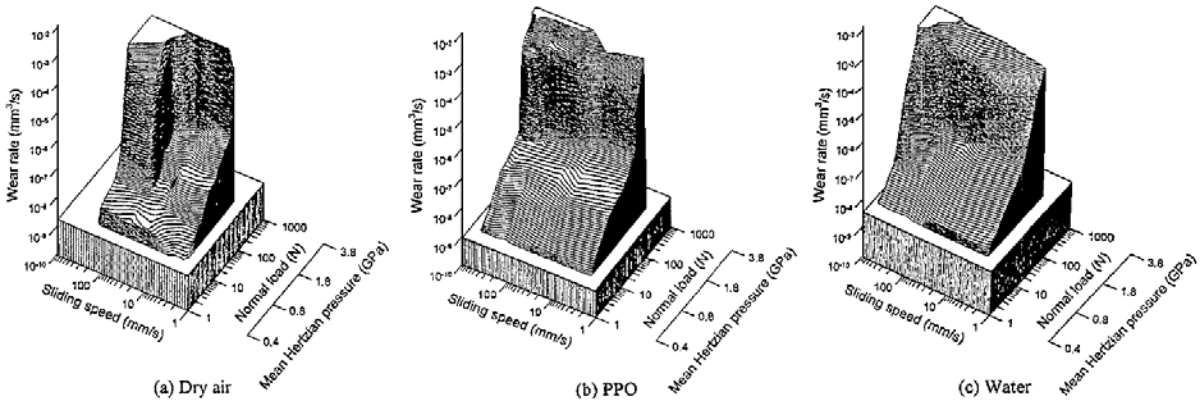

Figure 42: Wear maps of Al_2O_3 under (a) dry air, (b) PPO, (c) water lubricated conditions [185].

Wear of coatings can also be expressed by wear maps. For example, Wilson and Alpas [186] researched the wear of PVD TiN coating under dry pin-on-disk sliding contact at a low contact load and various sliding speed between 25°C and 500°C. The wear map in Figure 43 includes three regimes (oxidation, polishing, and ductile deformation and failure) based on different sliding speed and ambient temperature.

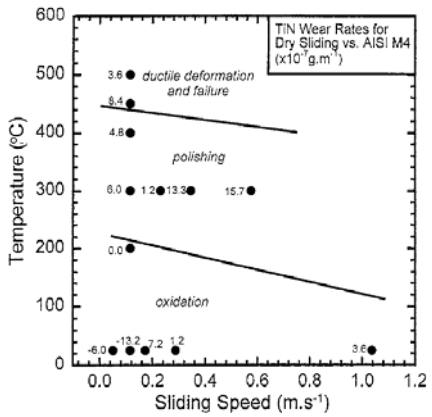

Figure 43: Wear map showing TIN coating wear rates at different sliding speeds and temperature conditions [186].

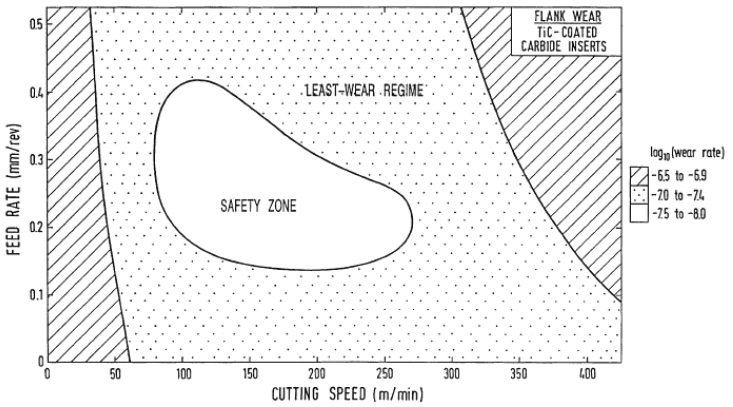

Figure 44: Map for flank wear of TiC-coated carbide inserts during single-point dry turning [187].

In the studies of cutting tools, Lim and Lim [187] found that machining conditions (feed rate and cutting speed) played a critical role in determining the wear extent. So, they developed a wear map of

coated tools based on feed rate and cutting speed, as shown in Figure 44. Actually, this wear map is similar to that of bulk materials under sliding conditions, because feed rate and cutting speed respectively reflect contact load and sliding velocity.

Wear map is a simple approach to predict wear extent, which is just based on two parameters (normal load and sliding speed). However, each wear map is only suitable for a specific material under a specific running condition, and many tests must be performed in order to obtain one wear map, which is time consuming.

5.2 Archard model

Archard model, as mentioned in section 3.3.1, is probably the most widely cited quantitative wear model. In this model, the sliding speed in wear map was replaced by the sliding distance *L*, and a material parameter (hardness) was considered. The "wear coefficient" *K* is widely used for wear resistance comparisons of materials. However, *K* is also dependent on running conditions. Under different lubricated conditions, the difference of wear coefficient for the same couple of materials can reach to seven orders of magnitude [188]. Even more confusing is that, the Archard wear coefficient can vary by two orders of magnitude just due to a change in load or speed [189].

5.3 Models based on dissipated energy

Neither the product of sliding speed and normal load in wear map approach nor that of sliding distance and normal load in the Archard model has any physical significance, while the products of tangential force and sliding speed or sliding distance respectively signify frictional power and frictional work. In fact, wear processes in sliding contacts can be attributed to the frictional energy in the contact zone, which can only be dissipated in heat and wear debris generation and flow. The temperatures achieved in the contact induce the oxidation of the surfaces, the transformation of microstructure, the formation or breakdown of lubricant films or other tribochemical films, and melting of the surface or thermal stress.

The frictional energy is generated by the combination of normal load, sliding speed, and friction coefficient. So, it is very important to introduce friction coefficient in the wear prediction models.

▪ Friction power intensity

The friction power intensity presented by Matveevsky [190] is defined as the energy dissipated of unit contact area as the rubbing surfaces pass through the contact zone.

$$Q_F = \frac{\mu P v_s}{A} \qquad (1\text{-}16)$$

where μ is friction coefficient, P normal load (N), v_s relative sliding velocity (m/s), and A real contact area (mm^2). This concept did not take into account the timescale over which the energy can be lost to the contacting materials.

▪ Energy pulse

Energy pulse combined friction power intensity and the contact transit time, as the following equation [191]:

$$EP = \frac{Q_F t_t}{2} = \frac{\mu P v_s t_t}{2A} \ (J/mm^2) \qquad (1\text{-}17)$$

where t_t is the contact transit time, and the energy generated in the contact area zone is equally split on the two surfaces. This concept can only be applied in contacts where the contact point is moved relative to both surfaces, such as gear teeth and automotive engine valve trains.

▪ Cumulated dissipated energy

Mohrbacher *et al.* [99] introduced the concept of cumulated dissipated energy, *Ed*, for fretting contact conditions. *Ed* is calculated from the real-time tangential force and displacement in cycles and is expressed as follows:

$$Ed = \sum F_t d \qquad (1\text{-}18)$$

where F_t is the tangential force, and *d* is the linear displacement. In ball-on-disk unidirectional sliding tests of TiN coatings, Huq and Celis [192] used the following equation and found a linear relationship between wear volume and cumulated dissipated energy.

$$Ed = F_t d = \mu P v_s t \qquad (1\text{-}19)$$

where *t* is the duration of the sliding test. In their tests, the real-time tangential force was used.

▪ Locally dissipated energy

Fouvry and co-workers [102, 105, 193] suggested that the wear depth is more important than the wear volume in evaluating the wear resistance of a coating. So, they developed a concept as “locally dissipated energy” (or dissipated energy density), which is linked to the local wear depth. Coating lifetime is related to number of cycles when the substrate is reached, thus the interest is focused on the maximum depth, which should be related to the maximum local cumulated interfacial shear work.

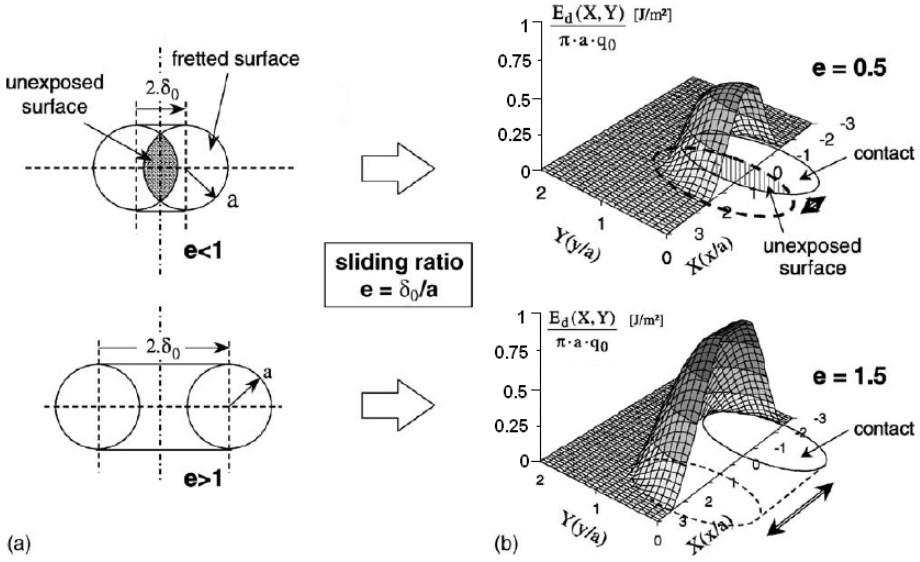

Figure 45: (a) Definition of the sliding ratio, (b) Energy density distributions as a function of the sliding ratio [105].

Figure 45 presented the distribution of dissipated energy density in a fretting cycle of ball-on-flat contact, which is a function of the sliding amplitude. The maximum of the locally dissipated energy Ed_0 locates at the center of the contact, and it depends on the sliding ratio *e*, which is the ratio of actual

sliding amplitude δ_0 to Hertzian contact radius a, $e = \delta_0/a$. For small sliding amplitudes (e≤1), Ed_0 is expressed by Eq.1-20.

$$Ed_0 = Ed(0,0) = 2aq_0[e(1-e^2)^{1/2} + \arcsin(e)] \qquad (1\text{-}20)$$

For large amplitudes (e>1), Ed_0 remains constant (Eq.1-21).

$$Ed_0 = Ed(0,0) = aq_0\pi \qquad (1\text{-}21)$$

So, the cumulated maximal locally dissipated energy is:

$$\sum Ed_0 = \sum_{i=1}^{N} Ed_0(e, q_0, a) \qquad (1\text{-}22)$$

where q_0 is the maximal shear stress, $q_0 = \mu \cdot p_0$ (μ is friction coefficient and p_0 is the maximal Hertzian contact pressure in contact area).

Recently, they introduced another concept ("energy capacity" χ), which was defined as the critical energy density, i.e., the maximal accumulated dissipated energy density which can be dissipated in the interface before coating failure, to predict contact durability under complex industrial loading conditions. The coating endurance (Nc) can be obtained by dividing the energy capacity by the average value of maximal dissipated energy density per cycle [194].

$$\chi = \sum_{(Nc)} Ed_0 = \sum_{i=1}^{Nc} Ed_i(0,0) \qquad \Rightarrow Nc = \frac{\chi}{\overline{Ed}_{0(Nc)}} \qquad (1\text{-}23)$$

where N_c is the durability of the coating, and $Ed_{(i)}(0)$ is the maximal dissipated energy density in the ith cycle, $\overline{Ed}_{(Nc)}(0)$ is the average value of maximal dissipated energy density during N_c cycles. Thus coating durability can be related to a single energy density capacity variable. In their tests, the energy density capacity was independent of the contact geometry and load conditions, as shown in Figure 46.

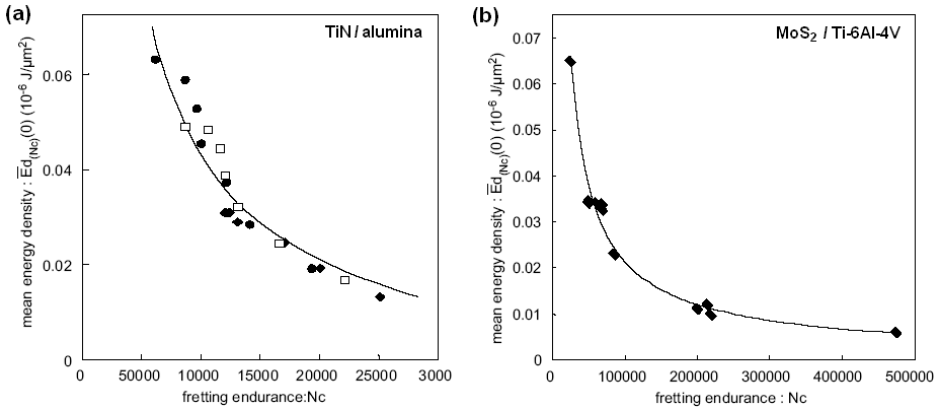

Figure 46: *Ed-N* master curve to quantify the coating durability (under different load conditions): a) $\chi = 0.4\times10^{-3}$J/µm^2, b) $\chi = 2\times10^{-3}$J/µm^2 [194].

▪ Initial maximal dissipated energy density

In fact, it is difficult to obtain the energy capacity of a material couple because the contact area and contact pressure evolve with the test process. In order to get a simple prediction model, Fridrici *et al.* [195] suggested to use the initial maximal dissipated energy density, $Ed_{0\ max\ ini}$, to predict coating lifetime, which means to predict coating lifetime just according to the maximal dissipated energy density of first few cycles.

$$Ed_{0\ \max\ \mathrm{ini}} = 4\mu_{ini} \cdot \delta_{0ini} \cdot p_0 \qquad (1\text{-}24)$$

where μ_{ini} is the initial friction coefficient, $\delta_{0\mathrm{ini}}$ is the actual displacement amplitude of first few cycles. For small displacement amplitudes, the result of this equation is very close to that of Fouvry's formulas. In the fretting tests of bonded MoS_2 under two contact configurations (punch on plane and cylinder on plane), one master curve was obtained for different normal loads, as shown in Figure 47. So, it is a simple and effective method for predicting coating lifetime.

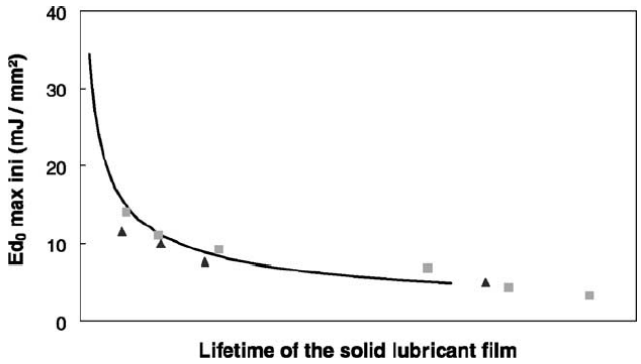

Figure 47: Relation between the lifetime of bonded MoS_2 coating and the initial maximal dissipated energy density for punch on plane contact (■: P = 2000 N; ▲: P = 3000 N) and comparison with the predicted lifetime from the cylinder on plane contact (plain line) [195].

6 Conclusions

Using coatings to reduce friction and palliate wear is a very effective measure to protect contacting surfaces and economize energy; however, it is difficult to find out the optimum coating from numerous available possibilities for a given tribological application. In order to understand the situation, in this chapter, bibliography synthesis was carried out from the following aspects:

- Deposition methods and coating types and structures linked to tribological applications;
- Tribological response of coating systems;
- Important parameters influencing the tribological response of coating systems;
- Coating selection methods;
- Wear prediction of coatings.

The development of coating deposition techniques made a great progress during the last two decades. Each of them is limited to certain situations due to the achievable thickness, deposition rate, maximum substrate temperature, component size and shape, porosity, cost, etc. In order to meet the increasing requirements for tribological performance, many new coatings and coating structures are developed.

The friction reduction of coatings mainly depends on the shear strength at the contact interface and the real contact area. The major difference of wear resistance between coating systems and bulk materials results from the discontinuity of properties between the coating and the substrate.

The tribological response of a coating system is influenced by many parameters from the counterpart, the coating, the interface, the substrate and the running conditions. The effects of parameters for friction reduction and wear resistance under different wear mechanisms are quite different.

The existing selection methods for tribological coatings include general description of the global process, the pre-selection methods, and the selection methods linked to experimental results.

Wear map is a straightforward method for wear prediction, but the process of obtaining the map is time-consuming. Models based on dissipated energy are probably more promising.

According to the literature study, the following 4 aspects are very important, and they will be respectively discussed in the subsequent chapters:

- Appropriate pre-selection strategy and effective pre-selection tool;
- Relationships between tribological response and coating properties and running conditions;
- Simple wear prediction model;
- Approach for evaluating and comparing coatings.

CHAPTER 2

METHODOLOGY OF COATING SELECTION

CHAPTER 2: METHODOLOGY

CHAPTER 2: METHODOLOGY

This chapter analyzes the main problems linked to coating selection, and discusses the general selection process and the research method. Three different cases are studied about how to select suitable coatings for different tribological applications.

1 Main problems linked to coating selection

The research and use of tribological coatings has a long history, but there is not yet a simple general rule to help the selection of tribological coatings. The reasons should be attributed to the problems explained in the following sections.

1.1 Estimation of wear mechanisms

In general, it is believed that the identification of wear mechanism was one of the most important factors in coating selection [196], because before we know which coating we need, the real reason of surface failure should be found. However, in most situations, the wear of a surface is usually related to several wear mechanisms, they transform each other during the rubbing process and even sometimes they occur simultaneously. For example, Farrow [197] put forward that wear mechanisms interact during the evolution of wear process (Figure 48).

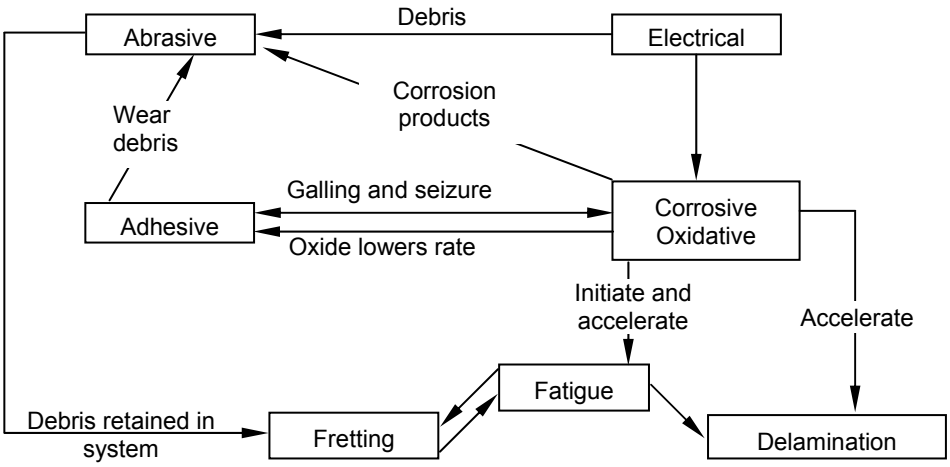

Figure 48: Interaction of wear mechanisms [197].

Under this situation, in order to avoid the identification of wear mechanisms, Matthews *et al.* [171] suggested to select coating according to different contact types. Under each contact type, some wear mechanisms possibly become the dominant ones, so there are common requirements for coating properties under the same contact type (Chapter 1, section 4.1).

1.2 Effect of various parameters on tribological performance

As described in section 1.3 of Chapter 1, the tribological performance is not an intrinsic property of materials, but a function of the whole tribological system. In coating systems, the tribological performance is influenced by many parameters from 5 aspects: the counterpart, the coating (influenced by deposition method and deposition parameters), the substrate, the solicitation and the running environment, as shown in Figure 49. Any change of a parameter possibly results in a great difference of tribological performance, which is a huge obstacle of finding a general rule for coating selection from literature, databases, or bench tests.

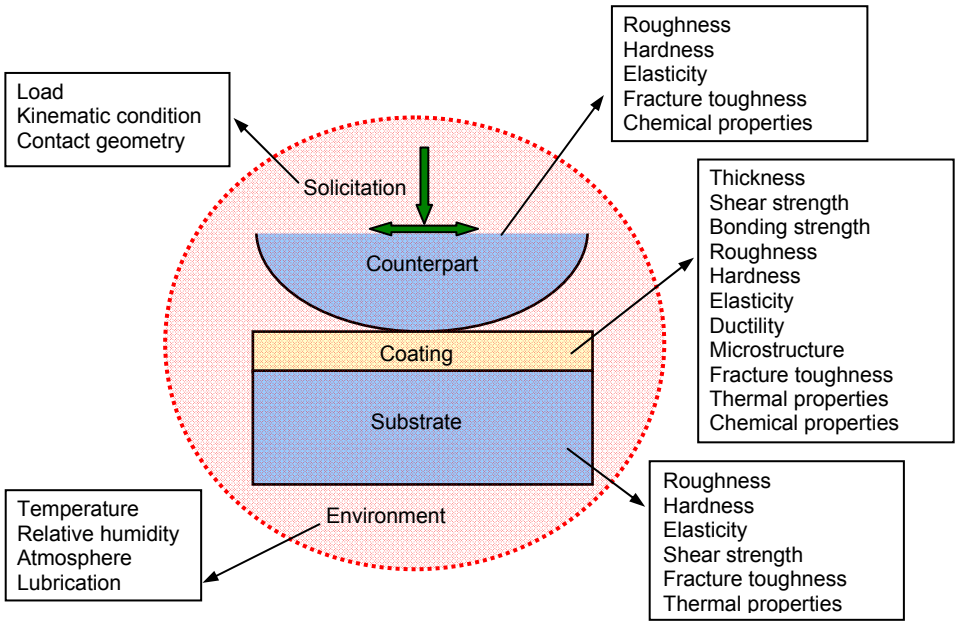

Figure 49: Parameters of a coating system influencing the tribological performance.

1.3 Possibility of using literature

During the last decades, the research on tribological coatings was made a great progress. There are a large number of papers about the deposition method, the characterization of properties, and the investigation of tribological performance for various coatings. Can the coating selection for a given tribological application be achieved just according to the test data in literature?

A coating material can be deposited by different deposition methods, deposition parameters, on different substrates, and the coating was tested under various contact configurations, solicitations, running environments, mating with different counterparts, etc. So, even for the same kind of coating, in different papers, the test results present great difference. For example, Sedlaček *et al.* [60] reviewed DLC coatings in recent years literature and they found 800 DLC coatings, which belong to 25 coating types (a-C:H; a-C; a-C:Cr; Ti–C:H; etc.), 16 deposition methods (a-C⇨7; a-C:H⇨11; W–DLC (a-C:H/WC)⇨2; etc.). The tests were performed under different conditions, relating to 55 counter-surfaces, 9 testing methods (pin on disk, reciprocating sliding, fretting, etc.), the coating's thickness in the span: 0.0035 ~ 10μm; sliding speed: 0.0014 ~ 3 m/s; contact pressure: 0.16 ~ 5.40 GPa; temperature: 20 ~ 400 °C; relative humidity: 0 ~ 100%; etc. So, the test results are far apart from one another, the friction coefficient was in the range from 0.002 to 1.3; the wear rate of the coatings changed from 8.46×10^{-10} to 1.57×10^{-04} mm^3/Nm and the wear of counter-surface from 9×10^{-10} to $1.54x10^{-04}$ mm^3/Nm. So, the test results depend on the specific conditions in the relevant literature, and any change of the situation can make the data in literature unusable. It is difficult to find test

results from literature which were obtained under the exactly same situation with the given application. Hence, from literature, we cannot estimate the specific friction coefficient and wear rate of a coating under a new application, and we can just estimate that this coating may be more or less suitable for an application than another one.

2 General selection processes

According to the three problems previously mentioned, the wear mechanism cannot be accurately estimated, the tribological performance is influenced by many parameters and the test results in literature cannot be completely referred. So, in order to find the optimum coating for a specific application, some simulation tests must be carried out to estimate the tribological performance of coatings. However, we cannot measure all of the available coatings by time-consuming tribological tests. Which coatings can be picked out as the candidates for simulation tests? A systemic pre-selection process will be necessary. Figure 50 shows the general process of coating selection.

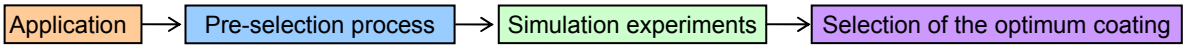

Figure 50: General process of coating selection.

2.1 Pre-selection process

In most situations, the pre-selection process is performed according to the experiences of experts and some successful cases in industries, which is a laborious process and the optimum coating can be omitted. A pre-selection tool based on database system will be more effective.

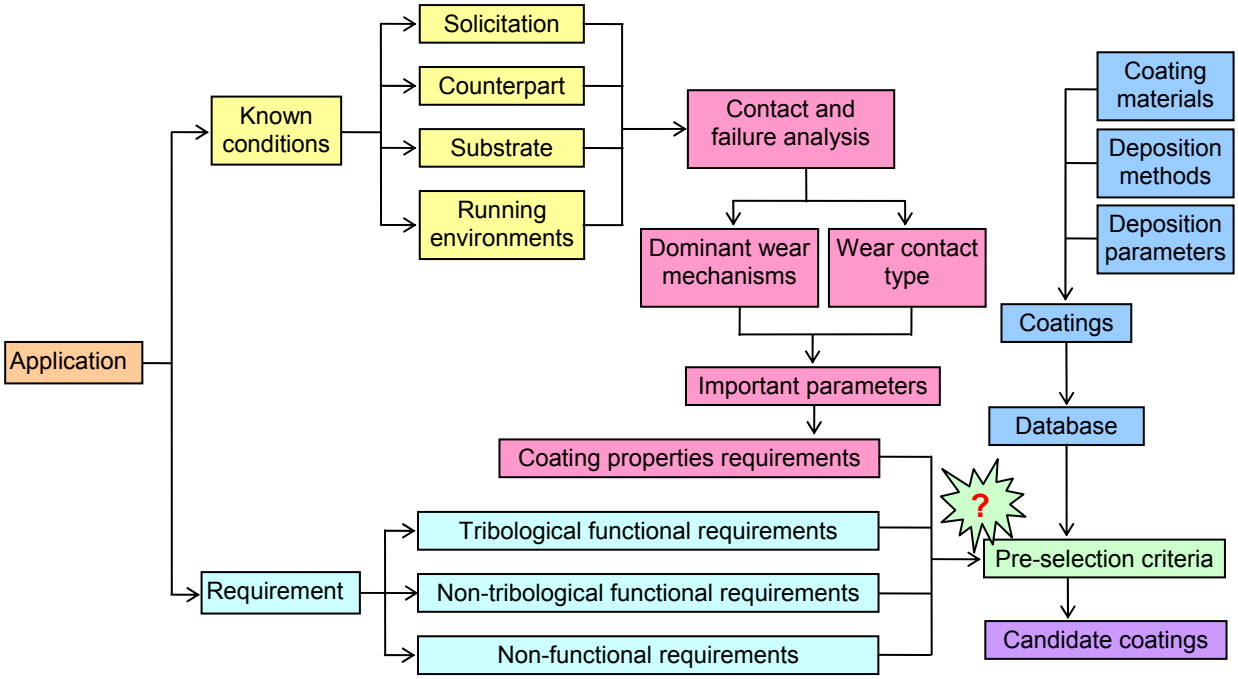

Figure 51: General coating pre-selection process.

Figure 51 shows the frame of pre-selection process. When we select coatings for a specific application, the solicitation (contact configuration, load, kinematic, etc.), counterpart (material, topography, geometry, mechanical and chemical properties, etc.), substrate (material, topography, shape, size, mechanical, thermal and chemical properties, etc.) and running environments (lubrication,

temperature, RH, atmosphere, etc.) should be known. There are also some definite requirements for the coated surface, which include tribological functional requirements (changing or reducing friction, prolonging service lifetime, etc.), non-tribological functional requirements (corrosion resistance, thermal, electrical, magnetic, biocompatible, etc.) and non-functional requirements (cost, productive efficiency, ecological, etc.). According to the known conditions, some analysis about the contact and the possible failure mechanism of the rubbing surface must be performed to investigate the dominant wear mechanisms. From the dominant wear mechanisms or wear contact type (sometimes it is difficult to estimate the dominant wear mechanisms), some important parameters can be confirmed, which induces the requirements of coating mechanical, physical and chemical properties.

On the other hand, there are many available coatings from literature and industries, including the coating materials, deposition methods, deposition parameters, and some test results of tribological performance. The best way of organizing the coatings is to develop a database. The detail of the development of database and pre-selection rules will be discussed in Chapter 3.

2.2 Simulation experiments

Due to the complexity of tribological response in coating systems, candidate coatings from the pre-selection process must be further investigated through simulation experiments to find the optimum one and ensure that it really meets the requirements. Before the tests, the type of simulation experiments must be chosen. After the tests, how to estimate the test results and find out the optimum coating need to be considered, especially when coatings have themselves advantages in different aspects.

According to the similar extent of test conditions with the real application, the simulation experiments can be divided into different levels, from model test, to simplified component test, to component test, to sub-system test, to bench test, to field test [198]. The model test is the simplest and cheapest, but the reliability of test results is also the lowest. The field test is carried out under the real application conditions, so the test result is the most reliable; however, the field test is the most complex, and its cost is also the highest. In a specific application, which kind of test is chosen depends on the importance of the application. In the selection process suggested by Matthews *et al.* [171], both laboratory tests and bench/field tests are included.

As for the test results, in most cases, it is easy to decide which coating is the optimum one. However, in some situations, the tribological performances of coatings are very close, and each of them has its own advantages and disadvantages. A comprehensive approach balancing the coating characteristics and the requirements of the application must be employed. A predictive model of coating lifetime is also necessary to be created from the simulation experiments.

3 Research approach of the thesis

In the research process, at first, literature study must be carried out in order to obtain the research progress in coating types, deposition methods, wear mechanisms and effect of important parameters on tribological response of coating systems. Then, some case studies are necessary to investigate the difference about wear mechanisms, coating requirements and important parameters under different tribological applications. Three cases are selected: cylinder bore / piston rings in internal combustion engines, blade / disk contact of fan in turbofan engines, valve / seat contact in Diesel engines. According to the study of literature and cases, some pre-selection rules will be proposed and a selection tool based on database will be developed, through which several candidate coatings can be picked out for a given application.

On the other side, two kinds of simulation experiments will be performed. The interest of the experiments will be focused on thin solid lubricant coatings. In the first kind of experiment, a pressure sprayed MoS_2 coating will be tested under different conditions (ball-on-flat fretting, cylinder-on-flat fretting and ball-on-disk unidirectional sliding) to investigate the effect of test parameters on tribological performance of the coating. In the other experiment, several commercial bonded solid lubricant coatings will be studied under the same test conditions (cylinder-on-flat fretting) to indentify the relationship between coating properties and tribological performance. According to the experimental results, some approaches of comparing coatings and predicting coating lifetime will be suggested.

Combining the pre-selection tool and the approaches of comparing coatings proposed from the experiments, coating selection for tribological applications will be achieved. Figure 52 is the frame of the research approach proposed in this thesis.

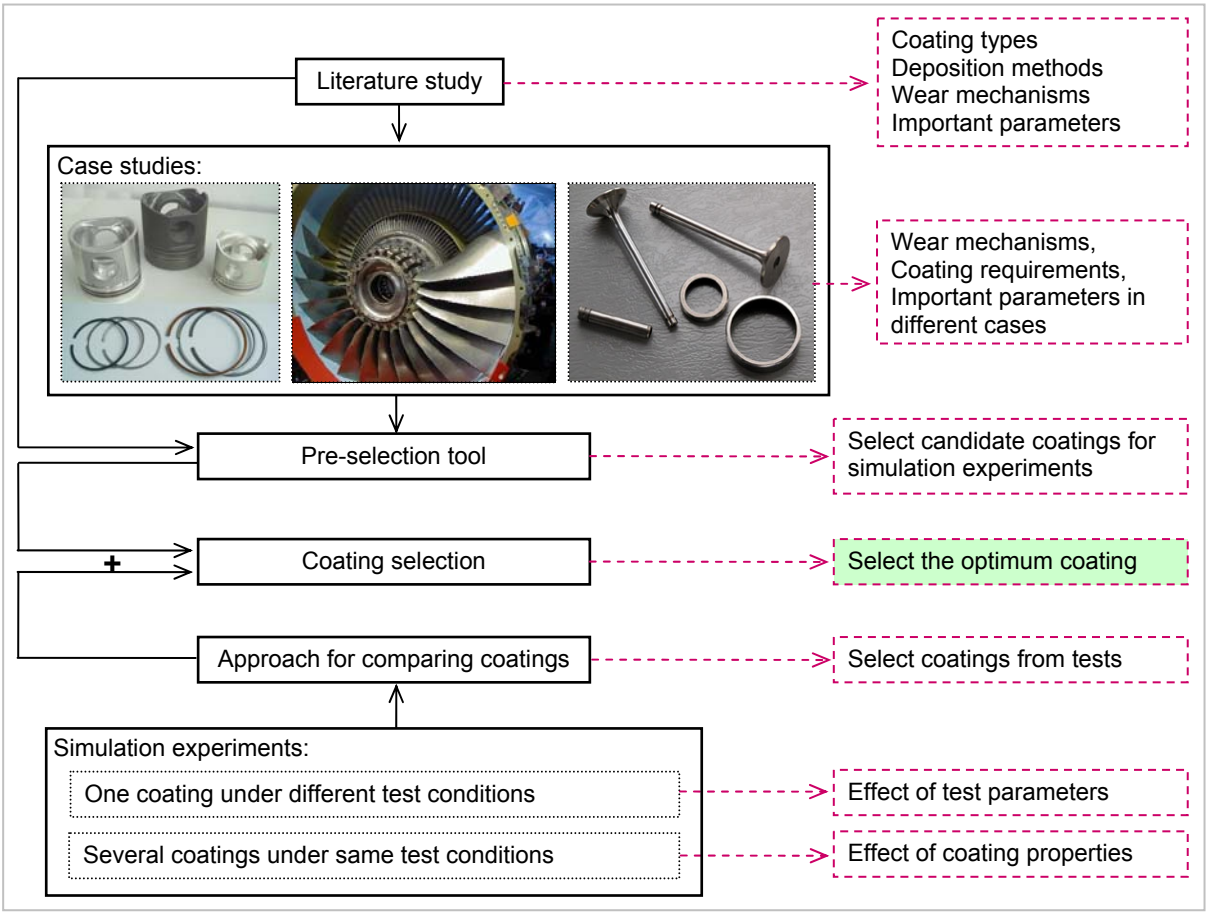

Figure 52: Research approach for coating selection.

4 Case studies

4.1 Cylinder bore / piston rings in internal combustion engines

4.1.1 Introduction

▪ Principle of internal combustion engines

Internal combustion engines include gasoline engines and Diesel engines (divided into 2-stroke and 4-stroke, and the latter is more widely used). The main differences include two aspects: one is that in

gasoline engines, an air/fuel mixture is drawn into cylinders during the intake stroke, while in Diesel engines, only air is aspirated; the other is that in gasoline engines, the air/fuel mixture is ignited by a spark plug at approximately the top of the compression stroke, while in Diesel engines, the fuel is injected into cylinders after the air is compressed to the burning point temperature of the fuel causing it to self-ignite. For a 4-stroke engine, one combustion cycle includes four piston strokes - intake stroke, compression stroke, power stroke and exhaust stroke, as shown in Figure 53.

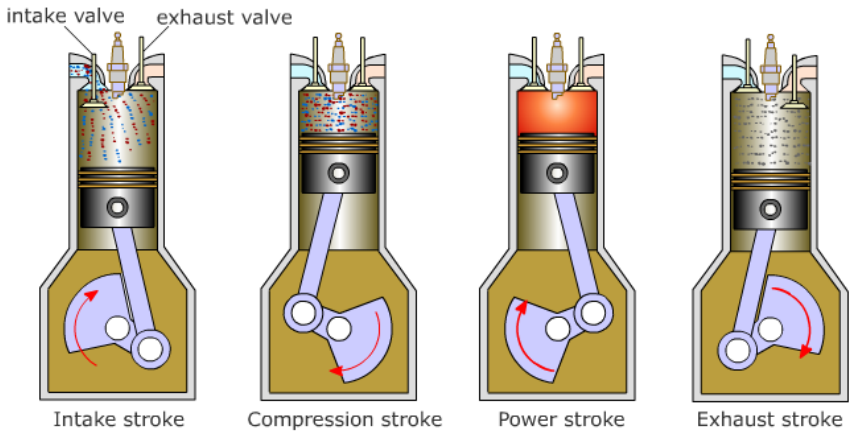

Figure 53: Principle of 4-stroke internal combustion engine.

- *Intake stroke*: The intake valve is opened and the piston moves downwards to create a negative pressure in the combustion chamber so that the air/fuel mixture (or air in Diesel) is sucked into the chamber. When the piston reaches to the bottom place, the intake valve is closed.

- *Compression stroke*: Two valves keep close and the piston moves upwards. The air/fuel mixture (or air) is compressed. The spark plug ignites the air/fuel mixture (or the fuel is injected into the cylinder in Diesel) in a short period before the piston reaches to the top place.

- *Power stroke*: Temperature and pressure in the combustion chamber rapidly increase due to the combustion of the fuel. The high pressure drives the piston downwards, which pushes the crankshaft to rotate.

- *Exhaust stroke*: At the end of the power stroke, the exhaust valve is opened, and the piston moves upwards to dissipate the exhaust gas.

- **Structure and function of cylinder bore / piston rings**

The running of an engine is because the high pressure generated by the combustion of the fuel in a closed chamber pushes the piston and then the crankshaft to rotate, so the piston assembly is the heart of a reciprocating internal combustion engine, which is composed of a piston and a ring pack.

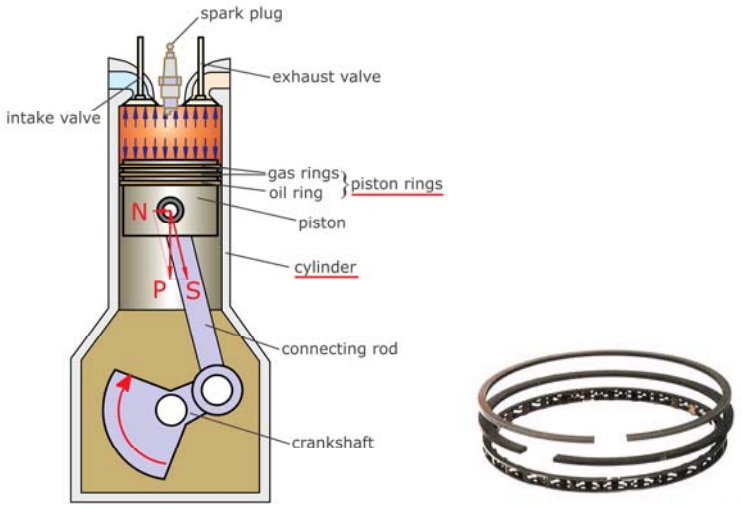

Figure 54: Structure of piston rings and cylinder bore.

The piston rings are generally made up of two gas rings that prevent the air/fuel mixture from leaking into the crankcase and seal the combustion chamber, and an oil ring that prevents excessive lubricant from intruding into the combustion chamber (Figure 54). Once a failure takes place, the mixture will be leaked so that the engine efficiency decreases; on the other hand, the lubricant will be burnt in the combustion chamber and form carbon deposit. Another role of the piston rings is to transfer heat from the piston into the cylinder wall to cool the piston down to acceptable temperatures. These basic functions of the cylinder bore / piston rings pair guarantee the effective running of an engine.

In order to facilitate the maintenance of the cylinder, or to improve the tribological performance of the cylinder (e.g., lightweight aluminum-silicon alloy engines), in most engines, cylinder liners are embedded into the engine blocks. According to the liners contacting the coolant or not, the liners are divided into “wet” liners and “dry” liners (as shown in Figure 55). The former directly contact with the coolant and the heat of the cylinder wall is easily dropped off by the coolant, which are suitable for heavy-duty Diesel engines. The engines without liners are inexpensive to manufacture, but they are only used for light-duty gasoline engines.

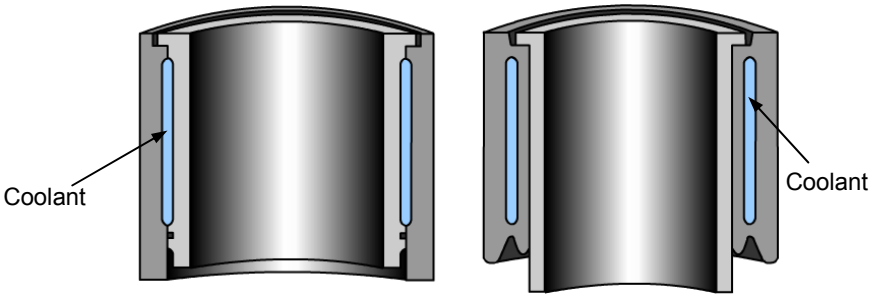

Figure 55: “wet” liner and “dry” liner.

▪ **Materials of cylinder bore / piston rings**

- *Material of engine blocks:* In the past, cast iron with lamellar graphite (GGL) was the preferred material used for engine blocks due to its favorable tribological properties, low costs of production with sand casting technology, good machinability. In heavy-duty Diesel engines, vermicular graphite cast iron (GGV) with higher strength and better toughness can be used to replace GGL, but GGV is more complex to found and it has a lower machinability [199]. In order to reduce the fuel consumption and

CO_2 emissions of vehicles, hypereutectic Al-Si alloys, especially A390, due to its high specific strength (its density is about one third of cast iron), are increasingly used as engine block material during the last decades and, today, more than 60% of the engines for passenger cars are produced in this kind of material. However, inadequate wear resistance and low seizure loads of aluminum alloy have prevented their direct usage as cylinder bore [200], which requires liners of cast iron with lamellar graphite or other surface treatments, such as galvanic coatings and thermal spray coatings [199, 201].

- *Material of piston rings*: An excellent piston ring material should possess the following features: toughness, elasticity, corrosion resistance, light weight, excellent tribological performance, surface treatment ability and long service life [202]. Gray cast iron (GG) is a traditional key piston ring material. However, to meet the increasing performance demands of modern engines, ring sets are working under higher and higher temperatures, and ordinary cast iron compression rings cannot endure the temperature range, so in many modern engines, steel and ductile iron are used as top rings [203]. The steel including gas nitrided stainless steel and tool steel is getting popular as top gas ring material due to its high strength, great toughness, elasticity and fatigue properties [204, 205].

▪ Operating conditions and environments

The exhaust gas of automobiles is still believed to be an important source of air pollution and global warming, so the requirement for the engine exhaust emissions is stricter and stricter. In Europe, from 1993 to now, the emission standards changed from Euro1 to Euro5 for Light Duty Vehicles, and EuroI to EuroV for Heavy Duty ones. Moreover, the shortage of fuel resource requires to decrease the fuel consumption and to improve the fuel efficiency in automotive engines. For solving these problems, some approaches have been brought forward and are being attempted. The main measures are as follows:

- *Low-heat-rejection engine*： engines operate at higher temperature with a low heat removal, where the maximal temperature of top ring can reach 650°C. Some special materials with high thermal stability, low thermal conductivity and low thermal expansion must be employed.
- *Mixed fuels engine*： some substitute fuels are added into the fossil fuel, such as compressed natural gas, methanol and ethanol, liquid petroleum gas, liquefied natural gas, hydrogen, etc [206]. Engines running with mixed fuel may suffer excessive cylinder bore wear because of the corrosion by mixed fuel [207].
- *Lightweight and low-cost aluminum-silicon engine*： for reducing emissions and improving efficiency, lightweight material aluminum-silicon alloy with a density of 2.79 g/cm^3 is used as the substitutor of cast iron with a density of 7.8 g/cm^3. However, inadequate wear resistance and low seizure loads of aluminum alloy have prevented their direct usage as the cylinder bores. Cast iron cylinder liners embedding in a lower silicon cast aluminum block is a popular strategy [200].
- *Reducing frictional losses:* the friction between rings and cylinder bore has been estimated to account for 20% of the total engine mechanical friction [208]. High friction coefficient induces high wear and poor fuel economy. For reducing friction, various coatings are considered: Ni–Mo–MoS_2, Ni–BN, graphite–Ni, etc.
- *Exhaust gas recirculation (EGR) system:* EGR is a technique used in most gasoline and Diesel engines by recirculating a portion of exhaust gas back to engine cylinders, which can reduce the burning temperature and the emission of NO_x because NO_x formation progresses is much faster at high temperatures. However, EGR increases the concentration of soot in the cylinder

that induces a higher demand for wear resistance of piston rings and cylinder bore materials [209].

In general, the running conditions of cylinder bore / piston ring contact are related to:

- *High temperature*: During the power stroke, there is a very high temperature due to the combustion of the fuel. Generally, for conventional engines, the temperature of the top ring is about 200°C, while for low-heat-rejection engines, it is near 650°C [210].
- *Unstable lubrication:* In one single stroke of the piston, the interface between piston ring and cylinder bore may experience boundary, mixed and full fluid film lubrication [211].
- *Corrosion medium*: Corrosion by mixed fuel and some acidic matter may occur (Diesel fuel contains more sulfur than gasoline fuel, which possibly generates sulfuric acid during its combustion and introduces corrosive attack [212]).
- *Cyclic load*: The side force (denoted by "N" in Figure 54) repeats every 4 strokes, which induces friction between cylinder bore and piston rings and piston skirt, and it possibly results in fatigue wear.
- *High pressure*: In the power stroke, the pressure in the combustion chamber can reach 4~5 MPa for gasoline engines, 7~8 MPa for Diesel engines and 12~15 MPa for heavy-duty Diesel engines.

The piston assembly is known as the most complicated tribological component in the internal combustion engines to analyze, because of large variations of load, speed, temperature and lubricant availability [203, 204].

▪ Possible failure of cylinder bore / piston rings contact

According to the engine type, the running conditions, the mated material of the cylinder bore / piston rings contact, the possible failures of the contact surfaces include:

- *Wear*: The rings tightly press on the cylinder bore by their elasticity, high combustion pressure and side force, which induces friction and wear at the interface of the cylinder bore / piston rings contact when the piston moves up and down in the cylinder. According to Sudarshan and Bhaduri [213], the wear mechanisms of cylinder liner include adhesion, scuffing and abrasion. Adhesive wear is influenced by lubricating conditions, the nature of materials and their surface roughness. Scuffing occurs under high temperature when two relatively sliding metallic surfaces directly contact and when the lubrication is inadequate. Abrasive wear arises due to asperities of the hard surface and particles generated by internal or external means.
- *Corrosion:* Corrosion is another failure category caused by the fuel, lubricant or oxidation. Fursund [214] investigated the wear of cylinder liner in large Diesel engines and found sulfur content in the fuel is a key factor for controlling corrosion.
- *Collapse:* Because of the high operating temperature, mechanical properties of the materials decrease so that they cannot carry the load.

Generally, the worst failure occurs on the top dead center (TDC) of the cylinder and the top ring where temperature, pressure and lubrication situation are the most severe. Surface treatment by depositing a coating on piston rings and/or on cylinder bore is an excellent solution to this problem.

4.1.2 Requirements for surface treatments

Besides preventing the failure of the contact surfaces and prolonging the service life of engines, coatings are also used to substitute for a liner in light-duty engines because the using of liners increases the dimensions and weight of the engine due to a specific wall thickness and a relatively large web width between the individual cylinder-bores [200].

- **Feature of the engines**

For selecting the right coatings, the feature of engines must be made clear. According to the power, fuel, structure, material and other factors, engines can be classified as the results in Table 10.

Table 10: Features of different engines.

Power	**Feature**
Light-duty	Low temperature, low pressure, low requirements for the coating
Heavy-duty	High temperature, high pressure, high requirements for the coating
Medium-duty	Intermediate temperature, intermediate pressure, intermediate requirements for the coating
Fuel	**Feature**
Gasoline	Low pressure
Diesel	Higher pressure, higher corrosion than gasoline engine
Mixed fuel	Intermediate pressure, possible high corrosion according to the fuel
Structure	**Feature**
Liner-less	Gasoline engine or light-duty Diesel engine, high requirement for wear resistance
Wet liner	Heat easily dissipates
Dry liner	Heat difficultly dissipates, high requirement for thermal properties
Material of cylinder bore	**Feature**
Cast iron (GG, GGL, GGV)	Good tribological performance, low strength
Alloy cast iron	Good tribological performance and some special performances
Al-Si alloys	Poor tribological performance, low strength
Steel	High strength, suitable for a variety of surface treatments
Material of ring	**Feature**
Cast iron	Good tribological performance
Steel	High strength, great toughness, superior thermal fatigue resistance
Heat rejection	**Feature**
Conventional engine	-
Low-heat-rejection engine	High temperature, special requirement for thermal properties

Diesel engines are more efficient than gasoline engines, which result in lower fuel consumption. Moreover, Diesel engines produce very little carbon monoxide as they burn the fuel in sufficient air. However, in order to let the compressed air reach the burning point temperature of the fuel, Diesel engines have a higher compression ratio, usually from 16:1 to 25:1, than gasoline engines where the compression ratio is rarely greater than 11:1 to avoid preignition. So, the combustion chamber suffers a higher pressure in a Diesel engine than in a gasoline engine.

- **Requirements for coatings**

For cylinder bore / piston rings contact, desired characteristics of the coatings include:

- *Wear resistance*: Improving the wear resistance and scuffing resistance is generally the primary objective of coating applied in cylinder bore / piston rings contact, at least the performance should be as good as the cast iron liner. The desired coatings should possess

high hardness, high temperature strength, high fracture toughness and strain compliance with the substrate.

- *Low friction*: Low friction coefficient leads to high fuel efficiency and low wear. The coatings should have low shear strength or can easily form transfer films on the counterface under the environment of cylinder.
- *Corrosion resistance*: In the combustion chamber of engines, the components suffer a severe corrosive environment with high temperature, thermal shock, oxidizing atmosphere, lubricating oil, fuel and combustion products including particles, sulfuric and formic acid due to the impurity of the fuel. The coatings must be able to resist corrosion in such an environment.
- *Machinability*: Honing is an important process for cylinder bore because the numerous small valleys (as shown in Figure 56) generated by honing can reserve lubricating oil and conceal debris and particles to reduce abrasive wear. Therefore, a good coating material for cylinder bore should have a high machinability, especially suitable for the honing process [200].

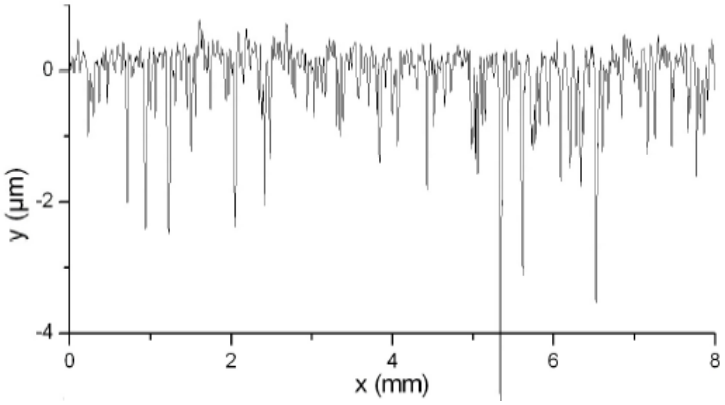

Figure 56: Topography of a cylinder bore after honing process [215].

- *Thermal performance*: A good coating should have a similar thermal expansion coefficient with the substrate so that excessive internal stresses will not be induced under high temperature. For conventional engines, the coating material should have a high thermal conductivity to assure an appropriate temperature in the combustion chamber, while for low-heat-rejection engines, heat transfer to the block should be low because a low heat loss means high fuel efficiency.
- *Strong affinity for oil*: Wetting ability and adsorption affinity of coating material for lubricating oil influence the lubrication regime, and then friction and wear of the contact surfaces.
- *Good adhesion*: Good bonding strength between coating and substrate is the precondition of wear resistance and thermal shock resistance. The bonding strength strongly depends on pretreatment of substrate surface, deposition method, deposition parameters and coating materials. Sometimes, an interlayer will be employed to improve the adhesion of coating.
- *Excellent cost / performance ratio*: In actual applications, besides the functional requirements, the cost / performance ratio is also very important, including the cost of the coating, the deposition efficiency, and the possibility of mass production.

4.1.3 Possible coatings

According to the failure and the running conditions of cylinder bore / piston rings contact, some possible coatings for piston rings and cylinder bore in industries or in literature can be found.

4.1.3.1 Piston rings

- **Chromium plating**

Chromium plating is the most common wear resistant coating for piston rings, because of its high hardness, high melting point, good thermal conductivity, low friction coefficient, excellent corrosion resistance and abrasion resistance. In a gasoline engine, piston rings plated with a hard chromium coating could extend the maintenance interval over 100,000 km [216]. The doping with hard particles in the electroplating process can improve the tribological performance. For example, Federal-Mogul Corporation developed chromium ceramic coating CKS by doping alumina particles in chromium plating, which increased scuff resistance. Recently, the chromium diamond coating GDC, embedding diamond particles in hard chromium, resulted in a considerably higher scuffing resistance and wear resistance than that of chromium ceramic coatings. However, hexavalent chromium contained in the plating bath is a hazardous substance, so its use is suffering a strict limit. Some other coatings are being studied to replace hard chromium coating, such as HVOF coatings [217, 218].

- **Thermal sprayed molybdenum based coatings**

Thermal sprayed molybdenum based coatings are also common wear resistant coatings of piston rings, although its abrasion resistance is not as good as that of chromium plating. Their general characteristics include high thermal conductivity, low thermal expansion, self-bonding to steel substrates and porous structure easily conserving lubricating oil, which contributes to a better scuffing resistance than chromium plating. The maximum service temperature of sprayed molybdenum coatings is about 315°C, or else they will be oxidized.

- **Gas or ion nitriding**

Cast iron or steel rings can be treated by gas or ion nitriding, and for steel rings, gas nitriding is still the most common surface treatment to reduce scuffing and abrasive wear, due to its high hardness (about 1100HV) [205].

- **PVD coatings**

Thick nitrides (ZrN, CrN and TiN) and carbonitrides (ZrSiCN and TiSiCN) coatings deposited on Ti–6Al–4V and 304 stainless steel substrates by a plasma enhanced magnetron sputtering (PEMS) technique presented good erosion resistance, which may be applied to protect piston rings for heavy-duty Diesel engines [219]. Ion plating CrN is an excellent candidate coating of top ring and it profits from its low friction coefficient, high hardness, high adhesion to substrate, and excellent scuffing resistance [202]. Although the friction coefficient of r.f. magnetron sputtering Cr_xN coatings was similar to the chromium plating, Cr_xN coatings effectively reduced wear of piston rings about 94% [220]. PVD DLC coatings present low friction and high wear resistance. Metal-doped hydrogenated DLC (Me-C:H) coatings with some outstanding tribological performances depending on the doped material are more suitable for the crucial environment in engines. The most used and successful Me-C:H coating for wear parts is the coating doped with tungsten carbide (WC) because of its excellent adhesion to steel, high elasticity, chemical inertness, low friction and high wear resistance [209]. Kylefors [200] compared several common piston ring coatings in his thesis, and found PVD WC/C coatings

outperformed all of the other coatings; especially, the wear of liner is hardly detected, as shown in Figure 57.

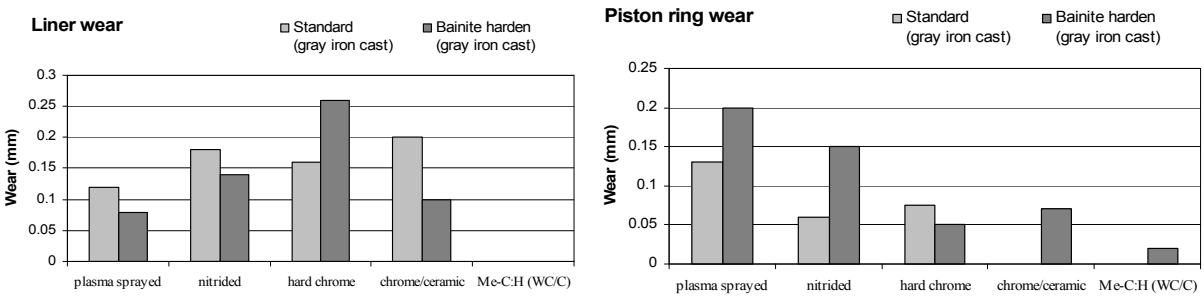

Figure 57: Test results of piston ring coatings from a pin-on-plate set-up simulating a liner/piston ring system (test parameters: load 8 MPa, temperature 80°C, test time 6 h, frequency 6 Hz and oil added with 1 wt.% soot).

- **Plasma sprayed coatings**

Plasma spraying is a widely used technology in the cylinder bore / piston ring contact, profiting from its inexpensive cost and high adaptability for various materials. Plasma sprayed coatings present better scuffing resistance but worse abrasion resistance than chromium plating [218]. Plasma sprayed chromium coating (with a thickness of 200 μm) on a ductile iron substrate of an actual heavy-duty top ring [221], Ni+WC coating on cast substrate [222], Al–Mo–Ni coating (with a thickness of 550~700 μm) on AISI 440C steel [223] were investigated by different researchers as piston ring coating, and the friction reduction and wear resistance of the coatings depended on the coating materials.

- **Refractory cermet coatings**

The cermet coatings present excellent abrasion, erosion, fretting and corrosion resistance, which show great promise as alternatives to chromium plating in many situations. These refractory materials can be deposited by HVOF spraying or detonation spraying. The common thermal sprayed cermet coatings include WC/Co and CrC/NiCr. The former can only be used in applications with operating temperature less than 500°C because some brittle phases are probably formed under higher temperature. Three kinds of CrC/NiCr coatings with different particle size deposited on steel substrate by HVOF were evaluated and compared with hard chromium, the result showed that HVOF CrC/NiCr coatings presented a slightly higher friction coefficient and much better wear resistance than hard chromium [217].

4.1.3.2 Cylinder bore

The use of surface treatments and coatings on cylinder walls is less common than piston rings in industries, but more and more engines are made of cast aluminum silicon alloys that present poor tribological performance and require cylinder liners of cast iron with lamellar graphite or other surface treatments [224].

- **Chromium plating**

Chromium plating is also successfully applied on cylinder bore in industries due to the same reasons described in section 4.1.3.2.

- **Phosphate coating**

Phosphating is a widely used method of reducing wear of iron and steel substrates. The phosphate coating itself can also function as a lubricant and resist mild corrosion [9]. Phosphating is an economical selection for cylinder bore of light-duty engines.

- **Nitriding**

Nitriding of cast iron cylinders has been widely used in industries to resist wear due to the high hardness and fair cost. However, nitriding process cannot be used for aluminum alloy cylinders.

- **Plasma sprayed coating**

Different thermal spraying processes are being used to deposit coatings for cylinder bores, and the plasma spraying process has reached the status of high volume product. Regarding materials, plasma spraying offers a large range of possibilities and optimization potential. Barbezat [199] compared the characteristics of three different thermal spray processes: wire ARC, HVOF and plasma spraying (Table 11), where plasma spraying is the best process for cylinder bores in Al-Si cast alloys. The wear resistance of the plasma sprayed coating is significantly higher than that of cast iron. Ferrous powders blended with lubricant particles or ceramic particles are the common spraying materials for cylinder bores [114, 199, 212, 225]. Uozato *et al.* [212] investigated a 250 μm thick ferrous powder (Fe–C–Ni–Cr–Cu–V–B alloy) coating deposited by plasma spraying on the cylinder bores of a liner-less aluminum cylinder block, and the coating has a potential of wear and corrosion resistance equivalent to current cast iron liner bores. Titanium suboxide coatings deposited on grey cast iron cylinder liners by plasma spraying were also investigated [226], and the results revealed the coatings met or exceeded the wear resistance of the grey cast iron, but they showed no friction reduction effect.

Table 11: Comparison of the thermal spraying processes applied in engine cylinder bores [199].

Criteria	Processes		
	Wire ARC (wire)	HVOF (wire or powder)	Rotating plasma (powder)
Versatility in the choice of material	Metallic alloys. Restricted choice of materials. **Low**	Metallic alloys carbides, composites. Limitation for refractory Materials. **Medium**	Metallic alloys carbides, ceramics, composites. High versatility **High**
Heat transfer into the engine block	**Medium**	**Very high**	**Low**
Reliability of the melting process	Formation of the melted particle is difficult to control. **Medium**	**High (powder) Medium (wire)**	**High**
Coating thickness as sprayed	500 μm	200 μm	200 μm
Coating properties for cylinder bores	**Medium**	**High**	**High**
Process cost	**Low**	**Very high**	**Low**
Industrial status	Start of small basis	Prototypes	In industrial production for 5 years

- **Laser alloyed coating**

Laser alloyed 75Ni25Cr layer on grey cast iron liner demonstrated an excellent corrosion resistance in diluted H_2SO_4 solution and NaOH solution and 4.34 times wear resistance of grey cast iron liner. So,

laser alloying can be a good solution to improve wear and corrosion resistance of the grey cast iron liners in mixed fuel environment, where excessive cylinder bore wear and corrosion could take place [207].

- **Thermal barrier coating**

In adiabatic engines, ceramics are the preferred coating materials of cylinder liner due to their wear resistance, high-temperature resistance and low thermal conductibility. For thermal barrier coatings, the surfaces must have a low friction coefficient and a high wear resistance at high operating temperatures. The piston crown temperature must be raised to over 880°C for uncooled engines, the prime requirement of the cylinder liner / ring system is good resistance to thermal shock and retention of strength to high temperature. Si_3N_4 is a possible coating material because of its low thermal conductivity, relatively high strength at temperatures to about 1100°C. Much interest focuses on zirconia because it is strong even at 1500°C, and has low conductivity and relatively high thermal expansion coefficient, which reduces the detrimental interfacial stresses [227].

4.1.4 Coating Selection

As selecting coatings for the cylinder bore / piston rings contact, besides the consideration of functional tribological requirements, we also need to take into account other aspects, such as the features of the engine, the cost of the coatings, the feasibility and efficiency of the deposition processes, the environment problem, etc. The selected coatings should be appropriate according to the comprehensive evaluation of various aspects.

- **Piston rings**

At first, the functional requirements for coatings should be compared, including friction reduction, scuffing resistance and corrosion resistance. Vetter *et al.* [228] compared wear resistance and scuffing resistance of different piston ring surface treatments applied in industries, including sprayed, galvanized, nitrided, PVD coatings (Figure 58), where PVD CrN and GDC (Cr plated + diamond) coatings are the best ones from the viewpoint of tribology.

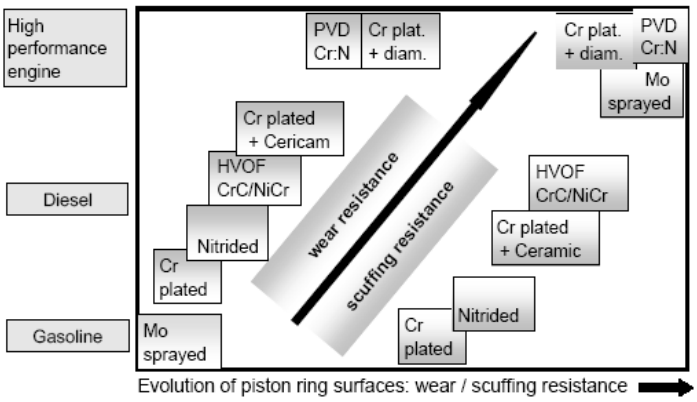

Figure 58: Different piston ring treatments and the trend of the wear and scuffing resistance [228].

The coating characteristics of various aspects are listed in Table 12, where PVD CrN and GDC are not necessarily the optimum coating for any engines. For example, the deposition process of GDC coating can result in high pollution, while PVD coatings have a small thickness and high cost. Under different situations, a coating can also have different performance. For example, Mo sprayed coating has a fair abrasion resistance but it is the best coating for scuffing resistance. Hence, according to the features of different engines, different coatings can be selected, as shown in Table 13.

Table 12: Coatings for piston rings.

Coating name	Substrate temperature (°C)	Friction	Hardness (HV)	Thickness (μm)	Work temperature (°C)	Cost	Deposition efficiency	Pollution
Chromium plating	45~60	low	800~1100	40~500	<500	low	low	high
Mo sprayed	50~150	high	400~800	100~400	<315	low	high	low
Gas/ion nitriding	500~600	high	>1100	50~600	<500	low	high	low
HVOF CrC/NiCr	~500	low	790	100~300	<800~900	high	high	low
HVOF WC/Co	~500	high	1200	100~300	<450~530	high	high	low
CKS	45~60	fair	660	40~500	<500	low	low	high
GDC	45~60	fair	830	40~500	<500	low	low	high
PVD CrN	100~500	low	1500~2000	<40	<850	high	low	low
PVD TiN	100~500	fair	1700~2300	<10	<525	high	low	low
PVD Me-C:H	<250	very low	1000~3500	<5	variable	high	low	low

Table 13: Coatings selection for piston rings.

	Gasoline engine light-duty Diesel engine		Medium-duty Diesel engine		Heavy-duty Diesel engine		Low-heat-rejection engine	
Features	Light duty+ low cost		Low cost		High performance		High temperature shock	
Coating	Top gas ring	Second gas ring and oil ring	Top gas ring	Second gas ring and oil ring	Top gas ring	Second gas ring and oil ring	Top gas ring	Second gas ring and oil ring
	Cr plating; Mo spraying	Cr plating; Mo spraying; Iron ring without coating	Cr plating; Mo spraying; Nitriding; CKS	Cr plating; Mo spraying; Nitriding	PVD CrN; GDC; CKS	Nitriding; CKS; Cr plating; PVD Me-C:H	HVOF CrC-NiCr; PVD CrN	Nitriding; CKS; Cr plating

- **Cylinder bore**

The main difference between the cylinder bore and the piston rings for coating selection is the requirements and limits of deposition process due to the large dimension of the cylinder. Especially for liner-less engines, the whole dimension of engine blocks should be considered, and the processes must be suitable for the deposition on internal surfaces. Generally, PVD and CVD processes are not suitable to the treatment of cylinder bores. Electroplating immerged in a bath is not suitable to liner-less engines. Thermal spraying process can only be used for large-bore engines where there is enough space for the spraying gun. The processes must be able to achieve the deposition of thick coatings because a honing process is necessary on the coating of cylinder bores and engines should work well until a major overhaul.

During the process of coating selection, the cylinder bore should not be isolated from the piston rings, but the coating selection of the cylinder bore / piston rings should be regarded as an integrative treatment. Counterparts give an important effect on the friction and wear performance of a coating. The wear resistance of cylinder bores should be better than that of piston rings because it is easier to replace piston rings.

Table 14: Coatings selection for cylinder bore.

		Characteristics	Coatings
Cast iron block without liner	Gasoline light-duty Diesel	Light-duty, Low cost	Cast iron liner without coating; Phosphating
	Medium-duty Diesel		Nitriding
	Mixed fuel	Corrosion resistance	Laser alloying
Cast iron block or Aluminum alloy block with liner	Gasoline light-duty Diesel	Light-duty, Low cost	Cast iron liner without coating; Phosphating
	Mixed fuel	Corrosion resistance	Laser alloying
	Medium-duty Diesel		Nitriding; Cr plating
	Heavy-duty Diesel	High requirement for performance	Plasma sprayed ferrous powder coating; Cr plating
Aluminum alloy block without liner	Gasoline light-duty Diesel	Light-duty, Low cost	Plasma sprayed ferrous powder coating
	Medium-duty Diesel		Plasma sprayed ferrous powder coating
Low-heat-rejection engine		High thermal shock	Plasma sprayed thermal barrier coating

4.1.5 Summary

The cylinder bore / piston rings contact works under the severe environments with high pressure, high temperature, poor lubrication, corrosive medium and cyclic load, which result in some limits for the selection of coating materials. The high expectation for coating lifetime (large coating thickness) and the geometry size and structure of the surfaces decide the possible deposition processes. Considering other factors, such as cost, efficiency, and pollution, thermal sprayed coatings are becoming the promising ones for cylinder bores.

4.2 Blade / disk of fan in turbofan engines

4.2.1 Introduction

A turbofan engine for civil aircraft includes seven sections: the fan, the low-pressure compressor, the high-pressure compressor, the combustion chamber, the high-pressure turbine, the low-pressure turbine and the nozzle (Figure 59), where the fan is one of the most critical parts in a turbofan engine because all of the airstream passes through it. After the fan, the airstream is separated into two parts: one part passes through the turbojet where it is burnt to power the fan, while the other part just bypasses the turbojet in order to improve the propulsive efficiency and decrease the noise.

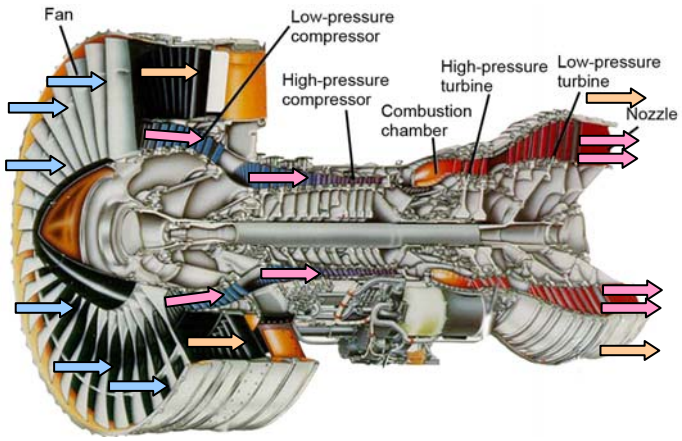

Figure 59: Composition of a turbofan engine.

(a) (b) (c) (d)

Figure 60: Different turbofan engines: (a) CFM56-5A, (b) CFM56-7B, (c) GE90 (d) Trent 900.

Figure 60 shows several civil turbofan engines: (a) CFM56-5A is equipped in Airbus A319 and Airbus A320; (b) CFM56-7B is applied in Boeing 737; (c) GE90 is used in Boeing 777; (d) Trent 900 is mounted in Airbus A380.

The fan is composed of a disk and many blades which connect together through dovetail joint (Figure 61 and **Erreur ! Source du renvoi introuvable.**). During a flight, the blades are submitted to high frequency vibrations and centrifugal force, which result in fretting failure of the contact surfaces. The attachments between the rotating blades and disk often experience mixed-mode fretting with portions of the load history resulting in either partial slip or gross slip fretting depending on the magnitude of the excursions in engine speed and temperature [229]. Fretting fatigue in dovetail joints is one of the most difficult and costliest problems in the US Air Force related to high cycle fatigue [230].

Figure 61: Fan of a turbofan engine [167].

Figure 62: Dovetail joint of blade / disk [231].

The solutions to this degradation problem generally include two aspects [167]:

- A foil or metal sheet with a small thickness can be inserted between the two contact surfaces. The selection of materials and thickness of the inserted part should ensure that the deformation of the inserted part can accommodate to the relative displacement between the foot of the blade and the socket of the disk, thus the solicitation and degradation of the contact surfaces can decrease to a very low extent. The inserted part should be checked during every maintenance of the turbofan engine, even be replaced if it is necessary.
- Surface treatment is applied on the contact surfaces. This solution modifies the nature of the contact surfaces by depositing a coating on one of the surfaces (in general, the surface of the blade foot is chosen because it is easier to deposit a coating on it than on the socket of the disk). This solution has been adopted by Snecma in all of its engines.

4.2.2 Contact and failure analysis

- **Material**

For turbofan engines, the components are usually fabricated from a titanium alloy, Ti–6Al–4V (titanium, 6% aluminum, 4% vanadium) because of its low density, high specific strength and corrosion resistance. The main shortcoming of this material is its poor tribological performance with a high friction coefficient and a low wear resistance. The microstructure of Ti–6Al–4V alloy depends on the applied thermal treatments; for aeronautical applications, the major thermal treatment is water quenching plus air tempering which gives the alloy an alpha/beta phase structure. Its mechanical properties (Table 15) can be slightly different depending on the thermal treatment parameters.

Table 15: Mechanical properties of Ti-6Al-4V [232].

Elastic modulus, E(GPa)	Poisson ratio, v	Yield stress, $\sigma_{Y0.2}$ (MPa)	Rockwell hardness, HRC	Density (g/cm^3)	Alternating bending fatigue limit, σ_d (MPa)	Alternating shear fatigue limit, τ_d (MPa)
119	0.33	970	41	4.4	450	260

- **Contact analysis**

During the running of a turbofan engine, the rotation of the fan will generate a centrifugal force which is put on the blades. This force converts into a normal load between the blade and the disk at the blade root. The vibrations of the blades due to unsteady aerodynamic effects induce small amplitude relative displacement of the contact surfaces (Figure 63).

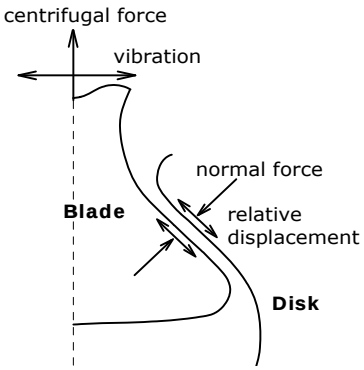

Figure 63: Loads of the blade / disk interface [167].

Some researchers [233-235] used a nominally flat indenter or fretting pad with rounded edges against a flat specimen to simulate the contact at the blade / disk interface in fretting fatigue tests (Figure 64).

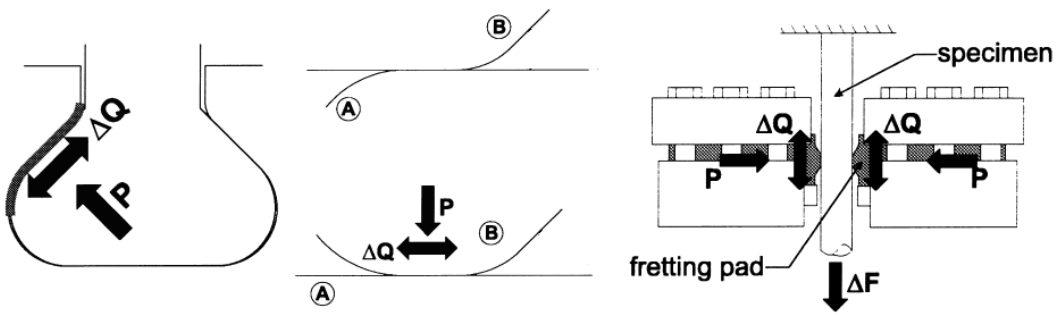

Figure 64: Equivalent contact interface of blade / disk and the fretting fatigue simulation test [234].

According to Nicholas [230], the turbo engine mission spectrum includes high amplitude low frequency cycles due to takeoff, landing, and low amplitude high frequency cycles induced by the vibrations (Figure 65).

- High amplitude low frequency cycles: they correspond to the takeoff and landing of airplanes, and one flight means a cycle. This specification is about 3000~6000 cycles flight without maintenance. According to the results of finite element method, the distribution of the pressure on the contact surfaces is 500 to 800 MPa at the border of the contact and 200 to 300 MPa in the interior. The tangential displacement is about 50 to 100 μm [167].
- Low amplitude high frequency cycles: they correspond to the vibrations which occur during a part of a flight, usually about several percent of the flight (according to the aerodynamic instability). The frequency is about several hundreds Hertz (200 to 400 Hz). The tangential sliding induced by the high frequency vibration is about 5 μm [167].

So, the contact surfaces of blade / disk are submitted to two kinds of fretting spectra (different tangential displacement amplitude and frequency).

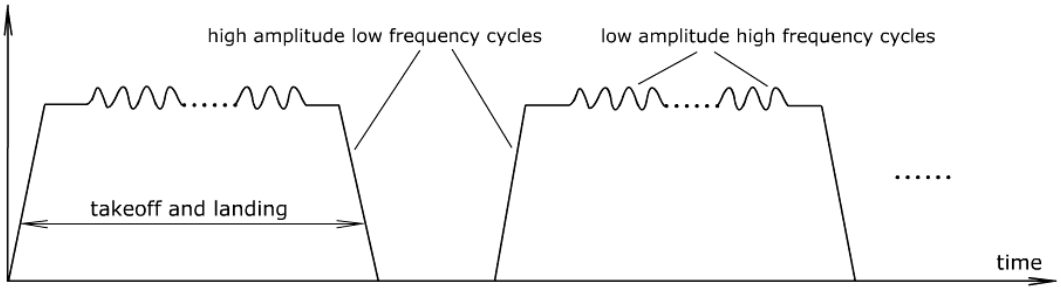

Figure 65: Mission spectrum of turbo engine [167, 230].

- **Failure analysis**

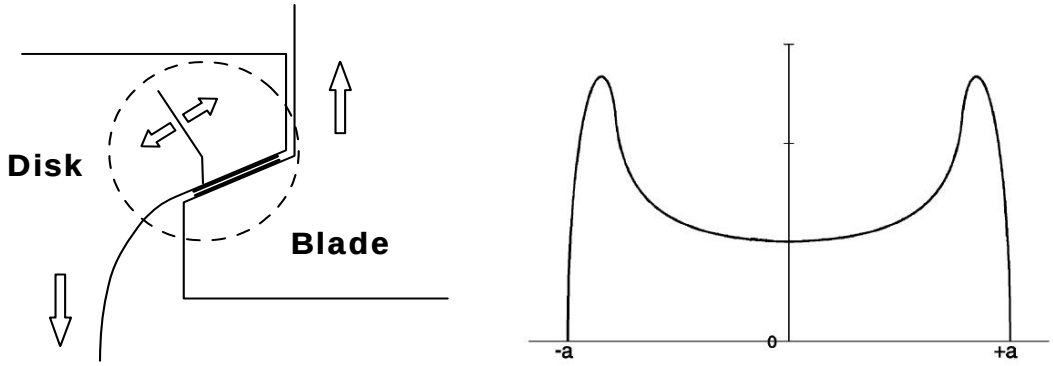

(a) (b)

Figure 66: a) General schematic of the cracks in the disk, b) rough distribution of contract pressure for the contact interface of blade / disk [167].

Under the cyclic mission spectrum, fretting wear [236] and fretting fatigue [233, 234, 237] are the main surface failures due to small amplitude relative sliding at the contact interface of blade / disk. According to the tests of Snecma Moteurs in [167], the principal cracks locate in the disk surface near the border of contact area, as shown in Figure 66a, which is in agreement with the distribution of contact pressure at the contact interface of blade / disk (Figure 66b)). The propagation of the cracks includes two stages: during the first stage, the cracks start along the direction of 75° with the contact

interface until the length of cracks reaches 1.6 mm, which validates the hypothesis of fretting damage. Then the cracks propagate in the perpendicular direction of the contact surfaces, which is not controlled by fretting. Besides the cracks, the wear of bearing surface in the disk is also observed, and the maximum wear depth of the disk surface is about 200 μm.

4.2.3 Coating selection

- **Requirements for surface treatments**

According to the failure and contact conditions of the blade / disk connection, the following requirements for the surface treatments should be met to mitigate the damage of the contact surfaces.

- *Low friction coefficient:* It is well understood that friction coefficient, μ, is an important driver of fretting fatigue performance. A low μ can reduce the shear loading and thus reduce the crack driving force [237].
- *Compressive residual stresses:* under fretting conditions, compressive residual stresses of contact surfaces can reduce the wear rate and the crack propagation rate. Some surface pretreatments and coating deposition processes, such as shot-peening, ion implantation, carburizing, nitriding, and ion beam enhanced deposition, which induce compressive residual stresses in the surface layer, are probably effective for mitigating fretting damage, especially for fretting fatigue [3].
- *High bonding strength:* The main difference of the tribological properties between coatings and bulk materials is the interface failure (cohesive cracking or detachment of coatings) between coatings and substrates, which results from the discontinuity of mechanical properties or poor bonding strength between coatings and substrates; so, a high bonding strength is the precondition of good wear resistance of coatings.
- *High wear resistance*: Wear resistance depends on several aspects. Generally, a high surface hardness will result in a high wear resistance. So, some hard coatings are employed for mitigating fretting damage, for example, PVD TiN coatings [93, 103, 238].
- *Good accommodation:* A soft coating can accommodate to the interfacial strain through its own plastic deformation, namely reduce the fretting contact loadings. Under this situation, the protective capability for the contact surfaces depends on the wear resistance of the soft coating. Once the coating is worn, the tribological behavior is similar to the uncoated situation [103, 236].

- **Selection process**

According to the requirements of the blade / disk connection for the surface treatment methods, some deposition processes can be directly eliminated because they are obviously unable to meet the requirements. For example, some deposition methods, such as chromium plating, laser treatments, etc., are generally not recommended to be used under fretting fatigue conditions, because these treatments often induce tensile residual stresses [3]. Additionally, the deposition chamber must have an enough dimension to mount the large blade (for CFM56-3 engine, the diameter of the fan is about 1.8 m).

For the feasible deposition methods, we should find suitable coating materials for the substrate, considering the capability of being deposited, the bonding strength with the substrate, the adaptability with the counterface and environment, and the possible tribological performance. Several possible

coatings can be picked out according to literature. At last, the coatings will be evaluated and compared from the tribological viewpoint and other non-functional requirements.

- **Possible surface treatments**

✓ **Shot-peening**

Shot-peening is the most common pretreatment process employed to resist fretting damage in tribological applications. Fridrici *et al.* [239] studied the effect of shot-peening on fretting wear of Ti–6Al–4V. The results showed that shot-peening did not obviously influence friction coefficient (Figure 67a) wear volume (Figure 67b). The benefit brought by shot-peening is that it can limit the crack nucleation and propagation in the mixed slip regime (Figure 68). Liu *et al.* [240] investigated the fretting fatigue resistance of Ti–6Al–4V through combining shot-peening process with hard CrN coatings or soft Cu–Ni–In coatings. The results showed that in partial slip contact conditions, shot-peening of coated and uncoated Ti–6Al–4V may improve the fretting fatigue resistance, while in gross slip contact conditions, the improvement from shot-peening was very slight. Fu *et al.* [241] also investigated the influence of shot-peening on fretting wear and fretting fatigue resistance of Ti–6Al–4V, and found that shot-peening can result in a significant improvement in fretting wear resistance, while the effect on fretting fatigue is not very well (Figure 69), because work-hardening (reduction of fracture toughness) and roughening of the surface resulting from shot-peening are probably harmful for the long-term fretting fatigue conditions. So shot-peening is just suitable for some situations of Ti–6Al–4V under fretting contact.

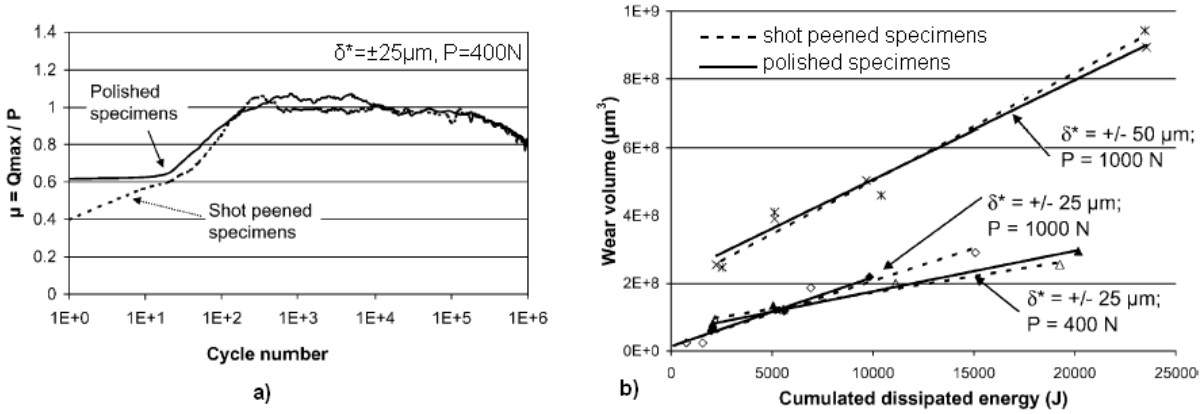

Figure 67: Effect of shot-peening on fretting wear of Ti–6Al–4V, a) friction coefficient evolution, b) wear volume variation with cumulated dissipated energy [239].

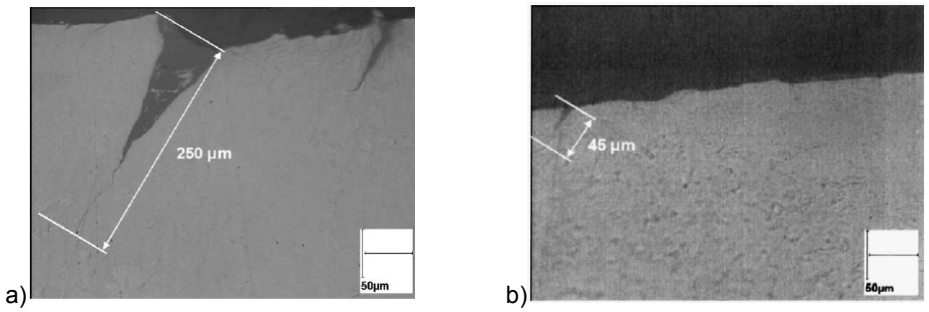

Figure 68: Maximal crack length of the cross-section of a) the polished plane and b) the shot-peened plane for fretting tests with δ* = ±25 µm, P = 1000 N and 5×10^5 cycles [239].

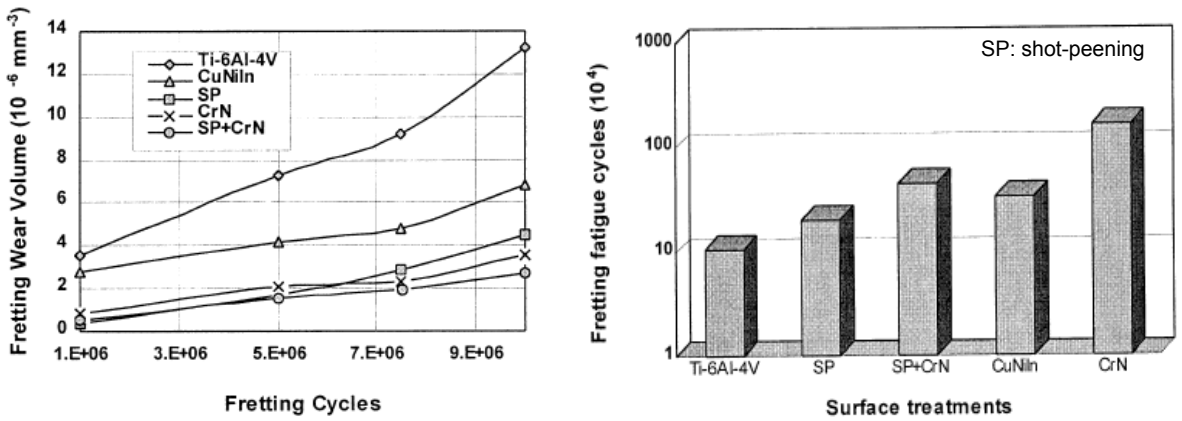

Figure 69: Influence of several surface treatments on a) fretting wear and b) fretting fatigue of Ti-6Al-4V [241].

✓ LSP and LPB

Golden *et al.* [237] investigated the fretting performance of some coatings on Ti–6Al–4V substrate combining with advanced surface treatments such as LSP (Laser Shock Processing) and LPB (Low Plasticity Burnishing) that induce deep compressive residual stress (approximately 1 mm) with low cold work in comparison with shot-peening. The addition of LSP and LPB to the dovetail specimens without coating greatly improved fretting fatigue strength of Ti–6Al–4V.

✓ MoS_2 coating

MoS_2 with lamellar crystal structure is the preferred low friction coefficient coatings, because the attraction between two lamels is very weak, just by van der Waals. It results in a low shear strength and a low friction coefficient. However, inside a lamel, the atoms are bonded by strong covalence which provides excellent load carrying capacity. Wu *et al.* [242] compared the tribological performance of several anti-friction coatings (Cu–Ni–In, DLC, 25%Ti/75%MoS_2, 75%Ti/25%MoS_2) on Ti–6Al–4V substrate by pin-on-disk test and block-on-ring test, and found that low friction coatings (DLC and Ti/MoS_2) presented better wear resistance than plasma-sprayed Cu–Ni–In coating which showed a similar friction coefficient with bare Ti–6Al–4V substrate (Figure 70).

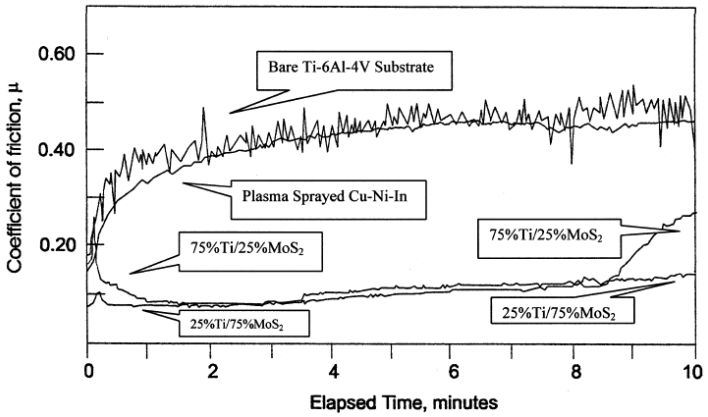

Figure 70: Evolution of friction coefficient of several coatings on Ti-6Al-4V substrate in pin-on-disk tests [242].

✓ Cu–Ni–In coating

Cu–Ni–In coating has been widely investigated in literature for mitigating fretting fatigue of Ti–6Al–4V. Fridrici *et al.* [236] studied the contact between a shot-peened Ti–6Al–4V cylinder coated with a 150~200 μm thick plasma sprayed Cu–Ni–In and a shot-peened Ti–6Al–4V plane under fretting

conditions. The Cu–Ni–In layer did not result in obvious change of the total wear depth in the gross slip regime, and the friction coefficient was almost the same with and without Cu–Ni–In coating (Figure 71a), which was in accordance with the result of Wu *et al.* [242]. However, it reduced the length of the cracks observed on the counterbody and induced a 5 µm shift of mixed and gross slip regimes due to its plastic accommodation and lower tangential contact stiffness (Figure 71b). Hager-Jr *et al.* [243] studied the gross slip fretting wear of Ti–6Al–4V ellipsoid against Ti–6Al–4V disk plasma-sprayed with Cu–Ni–In, Al–bronze, Mo, or Ni coatings. The friction coefficient was very high for all of the coatings, and none of the as-sprayed coatings was able to adequately protect the mated ellipsoids.

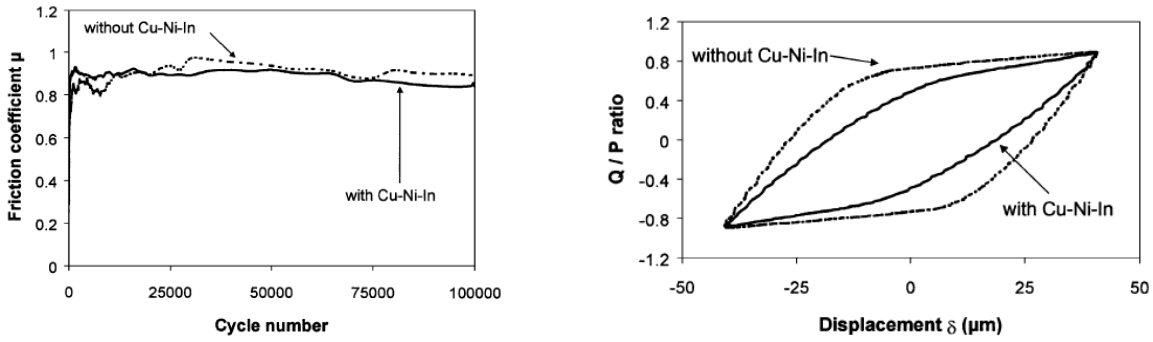

(a) (b)

Figure 71: Effect of Cu-Ni-In coating on the fretting behavior of Ti-6Al-4V, a) friction coefficient (δ=40 µm, P=1000 N); b) comparison of tangential contact stiffness (δ=40 µm, P=1000 N) [236].

Besides plasma spraying process, Cu–Ni–In coatings on Ti–6Al–4V by other processes were also investigated. Rajasekaran *et al.* [244] found the Cu–Ni–In coating on Ti–6Al–4V substrate by detonation gun spraying presented a longer fretting fatigue lifetime than by plasma spraying because of its higher surface hardness and higher compressive residual stresses. According to Liu *et al.* [240], a 3-5 µm thick Cu–Ni–In coating by ion-beam-enhanced deposition (IBED) process slightly extended the fretting fatigue lifetime of Ti–6Al–4V, and the combination of shot-peening and Cu–Ni–In coating did not result in significant improvement of the fretting fatigue resistance (Figure 72).

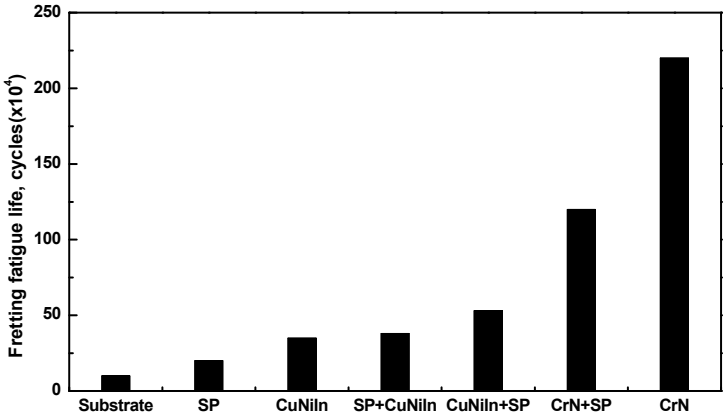

Figure 72: Fretting fatigue lifetime of several surface treatments (40 µm sliding amplitude, against Ti-6Al-4V pads) [240].

✓ PVD TiN coating

Thin hard coatings, especially PVD TiN coatings, are widely employed to improve the tribological performance of conventional engineering materials. They can also be used to palliate fretting wear and fretting fatigue due to their high hardness and compressive residual stresses [93, 238]. Fouvry *et*

al. [103] found that a thin (4 μm) TiN coating can prevent the nucleation of fretting cracks even for the highest loading conditions until the substrate is gradually reached. However, there is little information about the industrial application of TiN coating on Ti–6Al–4V substrate under fretting conditions. Shima *et al.* [245] studied the fretting behavior of TiN coatings on several substrates, including SUJ2, S48C, S25C, Ti–6Al–4V and ASCM20. TiN coatings implied a lower friction coefficient than uncoated Ti-6Al-4V substrate (Figure 73a) and more pronounced effect of wear resistance on Ti–6Al–4V substrate than on other substrates (Figure 73b).

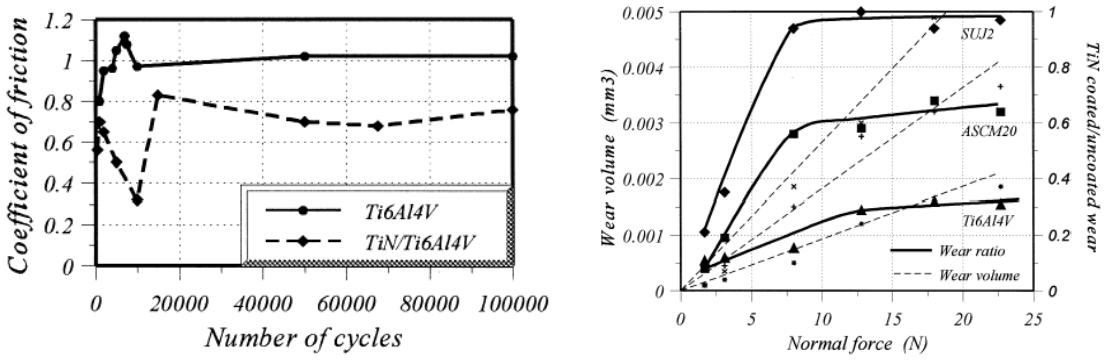

(a) (b)

Figure 73: Effect of TiN coating on tribological performance: (a) friction coefficient, (b) wear resistance [245].

✓ IBED CrN

IBED process can achieve a high bonding strength due to the bombardment of an independently generated flux of ions during the deposition. According to Fu *et al.* [246], a 1 μm thick IBED CrN coating significantly reduced fretting wear volume than PVD CrN coating and uncoated Ti–6Al–4V substrate despite its slightly higher friction coefficient than PVD CrN coating (Figure 74). However, the combination of IBED CrN and shot-peening resulted in a shorter fretting fatigue lifetime than IBED CrN itself [240, 241] (Figure 69 and Figure 72).

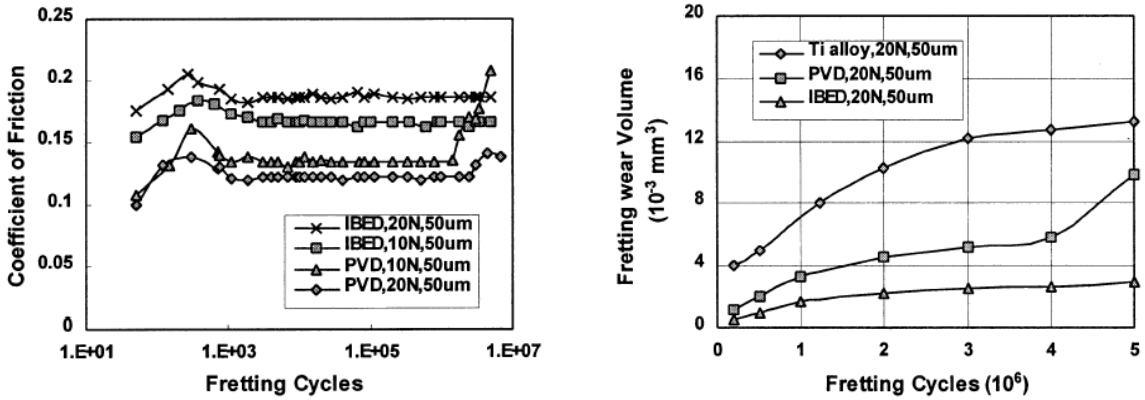

Figure 74: Fretting behavior of IBED CrN coating on Ti–6Al–4V substrate [246].

✓ Cu-Al coating

Jin *et al.* [247] investigated fretting fatigue resistance of a plasma sprayed Cu–Al coating on the alumina-gritted Ti–6Al–4V substrate. The degradation of Cu–Al coating depended on the applied fretting fatigue load: when the fatigue load was small, the coating showed a gradual removal; with the increase of fatigue load, the coating was quickly separated from the substrate surface due to the insufficient bonding strength. The Cu–Al coating cannot reduce friction under fretting fatigue conditions.

Ren *et al.* [248] compared the fretting fatigue resistance of four coatings: TiCN (filtered cathodic arc), CrN (filtered cathodic arc) + MoS_2 (magnetron sputtering), Cu–Al (cathodic arc) and Ag+ (ion irradiation). They found none of the coatings extended the fretting fatigue lifetime of Ti–6Al–4V substrate; Cu–Al coating even led to a shorter fretting fatigue lifetime than the uncoated Ti–6Al–4V despite its better fretting wear resistance than the other three coatings.

✓ **DLC**

DLC is an excellent coating due to its high hardness and very low friction coefficient, but its application under fretting is very few. Golden *et al.* [237] compared several surface treatments (electroless plated Ni–B, plasma sprayed Mo, plasma nitride, LSP, LPB and DLC) on Ti–6Al–4V subjected to fretting fatigue, and found the DLC coatings could extend the fretting fatigue lifetime of Ti–6Al–4V alloy over an order of magnitude due to its low friction coefficient throughout the test, while the specimens coated with Ni–B, Mo and nitride did not bring any obvious improvement for fretting fatigue.

▪ **Coating evaluation and selection**

According to the requirements, the comparison of the possible coatings is carried out from the tribological viewpoint (Table 16). Shot-peening, LSP and LPB can induce high compressive residual stresses, MoS_2 and DLC result in a very low friction, hard coatings show high wear resistance, and soft coatings present good accommodation.

Table 16: Comparison of the possible coatings.

Coatings	Friction reduction	Compressive residual stress	Bonding strength	Accommodation	Wear resistance	Fatigue resistance
Shot-peening	- -	+ +	O	- - -	+	+
LSP and LPB	- -	+ + +	O	- - -	+	+
MoS_2 coating	+ + +	O	D	+	-	+ +
Cu-Ni-In coating	O	O	+ +	+ +	-	+
PVD TiN coating	+	+	+ +	- - -	+ + +	+ +
IBED CrN coating	+ +	+ +	+ + +	- - -	+ + +	+ + +
Cu-Al coating	+ +	O	+	+ +	+	-
DLC	+ + +	+	D	- -	+ + +	+ +

* D: the performance depends on the deposition method; O: the surface treatment cannot obviously influence the performance.

From the Table 16, IBED CrN coating presents the best performance except accommodation, but this coating is just tested in laboratories. The combination of IBED CrN and MoS_2 possibly brings a better effect for friction reduction and fretting fatigue resistance. It needs to be validated through a series of further tests. Another approach is combining several surface treatments: shot-peening + plasma sprayed Cu-Ni-In + bonded MoS_2, which has been adopted by Snecma Moteurs. This approach gives following advantages. Firstly, shot-peening induces compressive residual stresses and roughens the surface, which can improve the bonding of Cu–Ni–In coating. Secondly, the Cu-Ni-In coating has a great capacity of accommodation by plastic deformation which limits nucleation and the propagation of cracks, and another role of the Cu–Ni–In coating is to be a retainer for the solid lubricant, due to its surface roughness. Thirdly, the polymer bonded lubricant containing MoS_2 decreases the friction coefficient.

For the two approaches, IBED CrN + MoS_2 and shot-peening + plasma sprayed Cu–Ni–In + bonded MoS_2, some experiments must be performed to further evaluate their tribological performance. At the

same time, non-functional requirements should be considered, including cost, efficiency of the deposition process and the dimension of the blade.

4.2.4 Summary

The blade / disk connection of fan in turbofan engines are submitted to two kinds of fretting spectra, which usually result in fretting wear and fretting fatigue of the disk. Depositing a coating on the surface of blade foot can mitigate the degradation. Several requirements for the coatings are proposed, and the relevant coatings in literature are investgated. Comparing the requirements and the coatings, two approaches (IBED CrN + MoS_2 and shot-peening + plasma sprayed Cu–Ni–In + bonded MoS_2) are promising.

4.3 Valve / seat in Diesel engines

4.3.1 Introduction

Diesel engines are more and more used in automobiles due to its higher fuel efficiency than gasoline engines. The working principle of four-stroke Diesel engines has been introduced in section 4.2.1.1. Each stroke is realized through the cooperative motion of several parts, such as the piston assembly, the intake valve, the exhaust valve, the valve train, etc. According to the description of the four strokes, the valves have the following functions:

- Accurate opening and closure of the valves guarantee the processes of sucking air and exhausting the gas.
- Correct contacts between the surfaces of valves and their seats ensure the seal of the combustion chamber during the compression stroke and the power stroke.

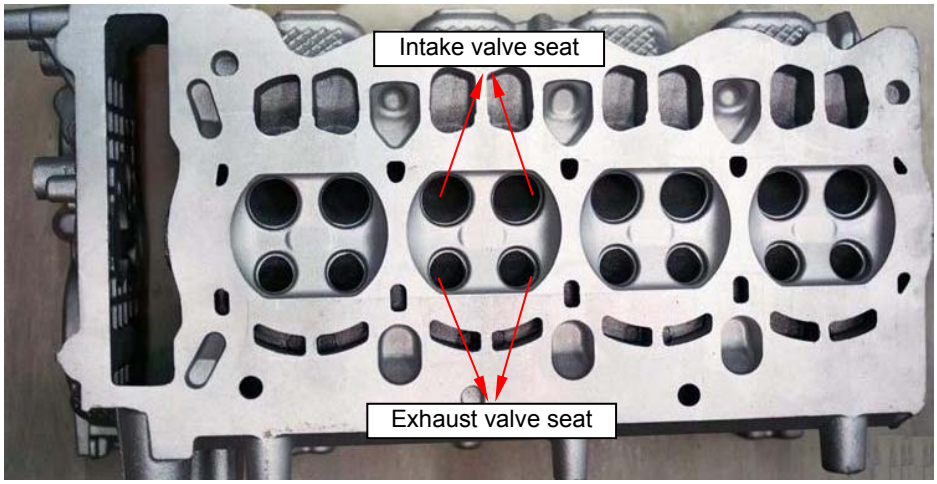

Figure 75: Cylinder head.

In general, intake valve has a larger diameter than exhaust value for sucking sufficient air. The valve seat is the surface against which an intake or an exhaust valve rests during the portion of the engine operating cycle when that valve is closed, and it is often machined on the cylinder head (Figure 75).

4.3.2 Working conditions

- **Contact geometry**

The sketch map of a valve is as shown in Figure 76. The seating faces of the valve and its seat have the same seating face angle, and in general, this angle is 45°. The diameter of the valve is about 20 ~ 40 mm depending on the number of valves and the diameter of the cylinder, and the width of contact area is about 1 ~ 2 mm.

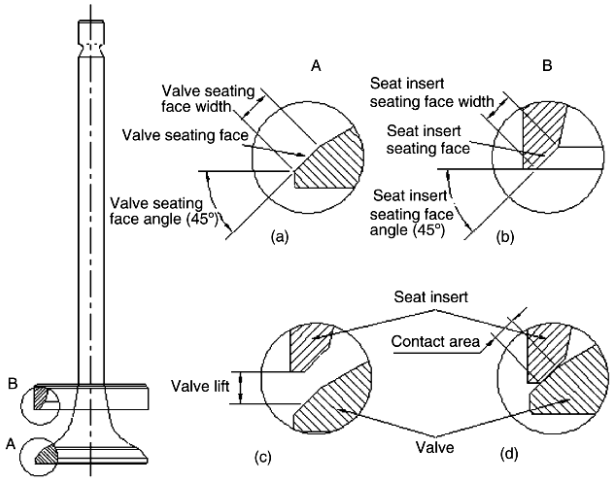

Figure 76: Geometry structure for the seating faces of valve and seat insert. (a) valve; (b) seat insert; (c) valve open; (d) valve closed [249].

- **Temperature**

In a combustion cycle, the valve suffers a large variation of temperature. During the intake and compression strokes, the temperature of gas in the combustion chamber is about 80°C, and during the power and exhaust strokes, it reaches 700°C. Therefore, the valves suffer high temperature. Especially for the exhaust valves of heavy-duty engines, they can be heated by the exhaust gases up to 340 ~ 550°C at full load [250] (the temperature of valves is lower than the maximal value of the gas due to the cooling of cylinder head when the valves seat on their seats).

- **Impact speed**

In a combustion cycle, each valve opens and closes once, and the rotating speed of an engine is generally in the range of 1000 ~ 4000 r/min. So, a valve impacts its seat about 500 ~ 2000 times per minute, i.e., 8 ~ 33 Hz. The variation of contact frequency means different impact speeds, which imposed an important influence on the failure of the valves and the seats [249].

- **Mechanical effect**

For Diesel engines, the combustion pressure can reach 20 MPa. According to PSA, when a Diesel engine runs at the speed of 4000 r/min, the valves impact their seats under a load about 400 ~ 470 N. When the valves are at the closure position, they suffer a force about 250 N from the valve springs. When a valve suffered a load of 470 N, the average pressure of contact surfaces is only about 4 MPa through a theoretical calculation. However, considering the contact deformation of the valve and its seat, the actual contact pressure can be much higher.

- **Other conditions**
  - Corrosion medium, such as the products of combustion, the fuel.

- Poor lubrication: the contact between the valve and its seat may occur under dry conditions.
- Rotation of valves and misalignment including lateral misalignment and angular misalignment.

4.3.3 Failure analysis

- **Wear mechanism**

Operating in a harsh environment, the contact between the surfaces of valves and seats can cause wear, which makes the valves sink or recede into the seats (Figure 77). Excessive recession leads to valves not seating correctly and valve leakage, which will adversely affect the engine compression ratio, the engine efficiency, performance, exhaust emissions, and engine life. Several researchers investigated the wear mechanism of valves and their seats, and the main mechanisms include:

- *Impact wear* [251-253]: Impact of the valves on the seats by the action of the valve springs at high temperature causes plastic deformation of the surfaces and the formation of a series of circumferential ridges and valleys. It also leads to surface cracking and subsequent material loss at high closing velocities.
- *Sliding wear* [249, 252-254]: When a valve head is pressed into its seat by the combustion pressure, the elastic deformation of the valve head will cause micro-sliding at the valve / seat interface. Sliding results in the formation of radial scratches on the contact surfaces due to adhesive wear, abrasive wear and shear strain.
- *Tribochemical wear* [249, 254]: The high temperature and corrosive exhaust gas induce the tribochemical wear (oxidation wear) in exhaust valves, while tribochemical seldom occurs in intake valves because they are cooled by the fresh air.

The dominating wear mechanism of valves and their seats depends on the engine operating parameters: if a high valve mass or closing velocity is used, then impact wear is critical; if high peak combustion loads are in use, then sliding wear could be more severe.

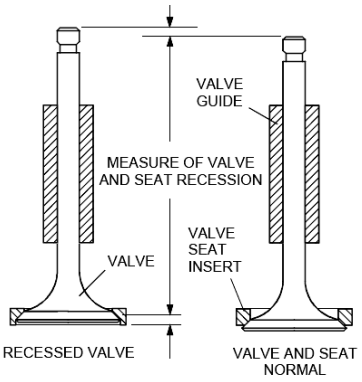

Figure 77: Valve recession [253].

- **Influence of running condition parameters**

The wear of valves and seats are influenced by many running condition parameters. Chun *et al.* [249] pointed out the following factors: combustion pressure, engine rotating speed, temperature, lubrication, seating face angle, valve rotation, misalignment, valve closing velocity, material matching, etc. They studied the influence of the valve closing velocity and the cycle number on the wear of valves and seats. Wang *et al.* [254] believed the most important factors related to valve seat wear include combustion pressure, temperature and cycle number. Ootani *et al.*[251] investigated the influence of temperature and sliding speed.

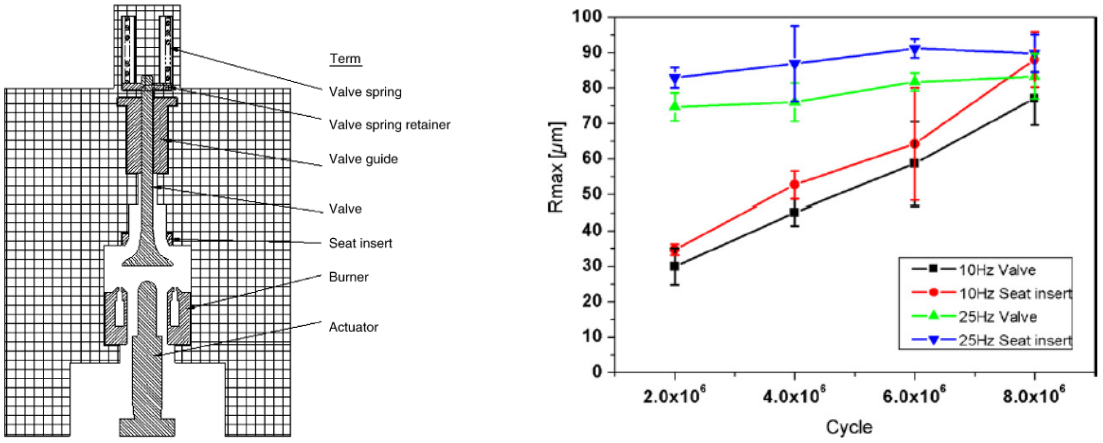

(a) (b)

Figure 78: a) A tester for valves and valve seats, b) R_{max} evolution with cycle number and impact frequency [249]

- *Impact speed*

During the operating process of an automobile, the rotating speed of the engine is often shifted, so the valves impact their seats at different speeds. Chun *et al.* [249] used the tester shown in Figure 78a to investigate the influence of impact frequency (impact speed) and cycle number on the average maximum roughness (R_{max}) of valves and seats. From Figure 78b, a high impact frequency (25 Hz) resulted in a larger R_{max} than low frequency (8 Hz). Lewis et Dwyer-Joyce [253] also found the same results: with the increase of valve closing velocity, valve recession increased (Figure 79), and they proposed a predictive model of the compound impact wear (impact plus sliding), where impact speed is an important parameter (Eq.1-12).

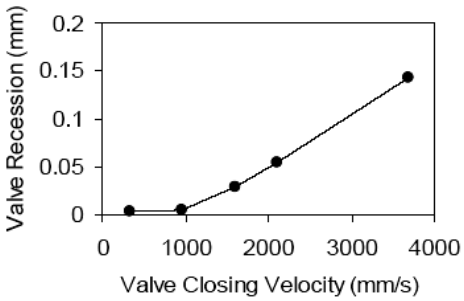

Figure 79: Evolution of valve recession with valve closing velocity (after 100000 cycles) [253].

- *Number of cycles*

In Lewis' model, wear volume *V* is linearly proportional to cycle number *N*. The increase of wear with the number of cycles was also validated by the test results of Chun *et al.* [249] (Figure 78b) and Wang *et al.* [254].

- *Temperature*

During the running of engines, the valves and valve seats suffer a large variation of temperature, which influences the speed of oxidation wear and the interfacial shear strength. Wang *et al.* [254] investigated the wear of Sil 1 valve and Sil XB seat under temperature from 180°C to 650°C under 17640 N for 864000 cycles. The results showed that the depth and width of wear scar decrease with the increase of temperature due to the existence of oxide films. These oxide films prevent the direct metal to metal contact and reduce the friction coefficient, thus reduce adhesive wear and deformation controlled wear.

Ootani *et al.* [251] investigated the influence of temperature on wear of austenitic heat-resistant steel (SUH36) rings and Fe-base sintered alloy disks under plane impact plus rotating sliding condition. At 200°C with a sliding speed over 0.4 m/s, the disks and the rings presented a higher wear rate than that at room temperature due to softening, while at 400°C, oxidation occurred and no acceleration of the wear rate was observed at any sliding speed, as shown in Figure 80.

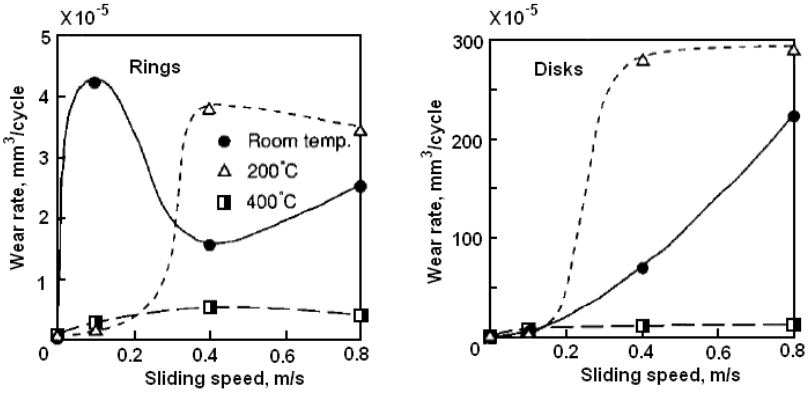

Figure 80: Wear rate as a function of sliding speed for different temperatures [251].

- *Combustion pressure*

Wang *et al.* [254] investigated the effect of combustion pressure on the wear of valve seat in the tests of a simulator (load: from 6610 N to 24255 N, temperature: 510°C, 864 000 cycles). When the load is in the range of 6615 ~ 17640 N, a linear relationship exists between wear scar depth / width and load; from 17640 to 24255 N, a different slope of wear rate suggests the change of wear mechanisms from adhesion to shear strain controlled wear (Figure 81). Under the high load, the shear strain on the seat surface exceeds the plastic limit of the materials, which can be characterized as the radial flow of material on the surface. Lewis and Dwyer-Joyce [253] also got a similar result where valve recession obviously increased for high combustion load (Figure 82).

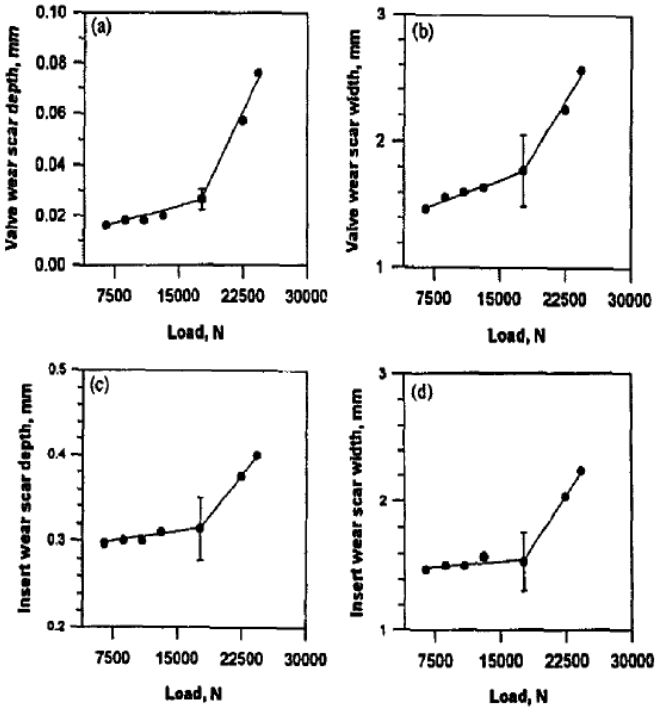

Figure 81: Wear of valve and seat as a function of load: (a) valve wear scar depth; (b) valve wear scar width; (e) seat insert wear scar depth; and (d) seat insert wear scar width [254].

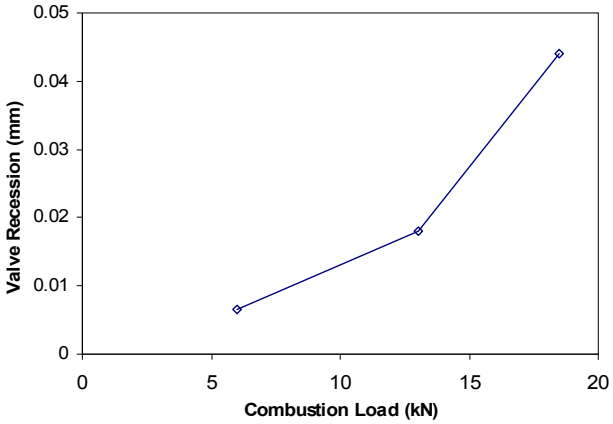

Figure 82: Evolution of valve recession with combustion load (after 25000 cycles) [253].

In conclusion, the wear of valves and seats depends on running parameters, and the important ones include impact speed, temperature, cycle number and combustion pressure. The change of these parameters can result in different wear mechanisms. High temperature induces tribochemical wear and the formation of oxidation film which can protect the contact surface until it breaks. High values of impact speed, cycle number and combustion pressure will accelerate the wear of valves and seats.

4.3.4 Solutions

For reducing the consumption of fuel and the pollution of environment, more and more automobiles are equipped with aluminum alloy engines. If the seating face of a valve seat is directly machined on the cylinder head, it will be worn soon due to the poor tribological performance of aluminum alloys and the replacement of the cylinder head will result in a very high cost. In order to ensure the engine performance and extending the lifetime of the valve and the seat, the solutions are as follows:

- *Using valve seat inserts*: a valve seat insert (Figure 76) is a ring and is embedded in the cylinder head, and this solution has been used by most engine manufacturers. The valve seat insert is made of materials with excellent wear resistance, in general, sintered alloy [251]. The development of sintered seat insert allows the incorporation of solid lubrication into the matrix to reduce sliding wear in “dry” condition. However, in bench tests, Lewis and Dwyer-Joyce [252] found that greater valve recession occurred in a sintered seat insert than in a cast seat insert (two kinds of seat insert material have the same hardness) because the cast insert material has a higher fracture toughness, which is a very important parameter for resisting impact wear.

- *Developing new valve materials*: The exhaust valves are generally made of austenitic heat-resistant alloy steel. According to Gebauer [255], light weight γ-TiAl base alloy (with additions of molybdenum and silicon) exhaust valves, which can contribute to a noticeable fuel saving, are developed in Germany to replace the conventional steel valves. The light weight of a valve also means smaller impact energy when the valve seats on its seat, then results in a low wear.

- *Depositing a wear resistant coating on the surface of the seat*: This solution is just attempted in laboratories. It is not yet employed in actual engines; however, it is a promising solution because depositing a coating is more convenient than using seat insert and there are more and more high performance coatings developed. The aim of this case study is to select coatings for valve seats.

- **Requirements for the coatings**

When wear resistant coatings are used on the seat surface, they must meet the following requirements:

- *High temperature resistance*: in general, the exhaust valve can reach about 400 ~ 500°C or higher temperature depending on the engine performance. On the other hand, the coatings should have a similar thermal expansion coefficient with the aluminum alloy substrate to prevent the detachment of coating due to high internal stresses under the thermal shocks.

- *Wear resistance*: the coatings should have a good durability to ensure that the lifetime of the engine is longer than 300,000 km, i.e., the coatings must have good wear resistance. In the contact of valves and seats, the surfaces suffer two kinematic wear modes: impact and micro-sliding wear. For resisting micro-sliding, the coating should have a high hardness; in order to resist impact, the coatings should have good ductility and fracture toughness.

- *Corrosion resistance*: the exhaust seats work in exhaust gas, so the coatings should resist the corrosion by exhaust gas and oxidation.

- *Pressure resistance*: the coatings must endure the high combustion pressure.

- *High thickness*: for ensuring the longtime operation of engines, thick coatings (about 200 μm) are necessary. On the other hand, thin hard coatings are easily ruptured due to the poor load-carrying capacity of the aluminum substrate under high impact loads.

- *High bonding strength*: the coatings must survive the repeating impact and thermal shock without a detachment problem, so the selected deposition method must be able to deposit thick coatings with high bonding strength.

- *Low porosity*: under impact conditions, the wear resistance of coatings with low porosity (porosity less than 5%) is better than that of coatings with medium and high porosity (porosity higher than 5%).

- *Easy to be deposited*: the deposition process should adapt to the size of cylinder head because the coating is directly deposited on the cylinder head, and the deposition process should be efficient.

- **Properties of the substrate**

Most cylinder heads in engines are made of aluminum alloy, especially the hypoeutectic aluminum silicon cast alloys such as A390 due to their light weight, high specific strength, and low thermal expansion coefficients. Its chemical composition and mechanical properties are respectively shown in Table 17 and Table 18.

Table 17: Chemical composition of die casting A390 alloy (wt. %).

Si	Cu	Fe	Mg	Mn	Ni	Ti	Zn	Other, each	Other, total	Al
16~18	4.0~5.0	≤1.3	0.45~0.65	≤0.5	≤0.1	≤0.2	≤1.5	≤0.1	≤0.2	Bal

Table 18: Mechanical properties of die casting A390 alloy.

Hardness HV (GPa)	Tensile strength, ultimate (MPa)	Tensile strength, yield σ_Y (MPa)	Elongation at Break (%)	Elastic modulus E (GPa)	Fatigue strength (MPa)	Shear strength (MPa)	Melting point (°C)	Coefficient of thermal expansion ($m/m \cdot K \times 10^{-6}$)
137	317	248	≤1.0	81.4	138	191	507~649	21.06

- **Coating selection**

From literature, the coatings used under impact conditions include thermal sprayed coatings [256, 257], PVD coatings [258-260], electroplated coatings, welding coatings and laser clad coatings. However, hard PVD coatings present brittleness and poor bonding strength for a thickness exceeding 10 μm, so multi-layer or multi-component structure must be considered to improve the toughness, which will result in a high cost and complex deposition process. A cylinder head usually has a large size, where the seat just occupies a small area. If electroplating process is used, a large quantity of stop-off need to be applied to prevent the bath from contacting with the substrate. So welding, laser cladding and thermal spraying are the possible deposition methods for valve seats.

Li *et al.* [257] compared the impact wear performances of plasma sprayed (APS--Ar/H_2 and APS--Ar/He) and HVOF sprayed Cr_3C_2-25%NiCr coatings (200 μm thick). They found the wear resistance of HVOF sprayed coatings was the highest of all the coatings under various loads. High velocity spraying processes (such as HVOF and D-gun spraying) can produce coatings with high wear resistance due to high bonding strength and low porosity. The common wear resistant thermal sprayed coatings include carbides (WC/Co, Cr_3C_2-NiCr), oxides (Cr_2O_3, Al_2O_3, TiO_2), cobalt alloys, molybdenum alloys (unsuitable for the situations above 340ºC) and self fluxing alloys (NiCrSiB). However, wear resistant thermal sprayed coatings for sliding wear are hard and brittle (such as carbide and oxide based coatings), which makes them useless under impact loading conditions and sensitive to fatigue. The combination of tungsten carbide-cobalt (WC-Co) and nickel based self-fluxing alloy (NiCrSiB) resulted in optimal properties of hardness and toughness [256].

Welding and laser cladding processes provide strong metallurgical bonding thick coatings. The welding coatings mainly include hardfacing alloy coatings, such as cobalt alloys and nickel alloys. The laser cladding process is used for self fluxing alloys.

Table 19: Possible coatings for valve seats.

No.	Coating Material	Deposition process	Characteristics
1	Cr_3C_2-25%NiCr	Thermal spraying (HVOF)	Hard, dense coatings with excellent oxidation and corrosion resistance, service temperatures up to 850°C.
2	WC-Co	Thermal spraying (HVOF, D-gun)	High erosion (low angle), impact, abrasion, fretting, sliding wear resistance, higher cobalt levels improving coating toughness, service temperatures up to 480°C.
3	Self fluxing alloys (NiCrSiB)	Laser cladding /HVOF	Resistance to wear by abrasive grains, hard surfaces, fretting, cavitation, and erosion at both low and high temperatures to 840 °C, suitable for great impact angles
4	NiCrSiB-(WC-Co)	Thermal spraying (HVOF)	The combination of hardness and toughness, adjusting the coating structure according to the impact angle.
5	Cobalt alloys (Tribaloy® or Stellite®)	Thermal spraying (HVOF, plasma) , Welding	Tribaloy: excellent high temperature sliding wear, corrosion, oxidation and general wear resistance. Stellite: high hardness, wear and oxidation resistance.
6	Oxide ceramics (Al_2O_3, Cr_2O_3)	Thermal spraying (HVOF, plasma)	High hardness, suitable for small impact angles.

Some possible coatings for valve seats are listed in Table 19. However, the evaluation of the coatings must depend on experiments, up to now there is not any reported information about the application of coatings on valve seats. In our laboratory LTDS of ECL, the development of a compound impact tribometer (Figure 83) simulating the contact of valves and seats is being performed. Figure 83a shows the principle of realizing the compound impact. A cylinder or ball moving up and down impacts the inclined flat specimens, and a relative sliding occurs between the cylinder or ball and the flat specimens due to the elastic deformation of the flexible plates under the impact. Figure

83b is the photo of the tribometer, where the motion of the cylinder or ball results from an actuator. In order to simulate the actual temperature of the valve seat, the flat specimens can be heated up to 400ºC (Figure 83c).

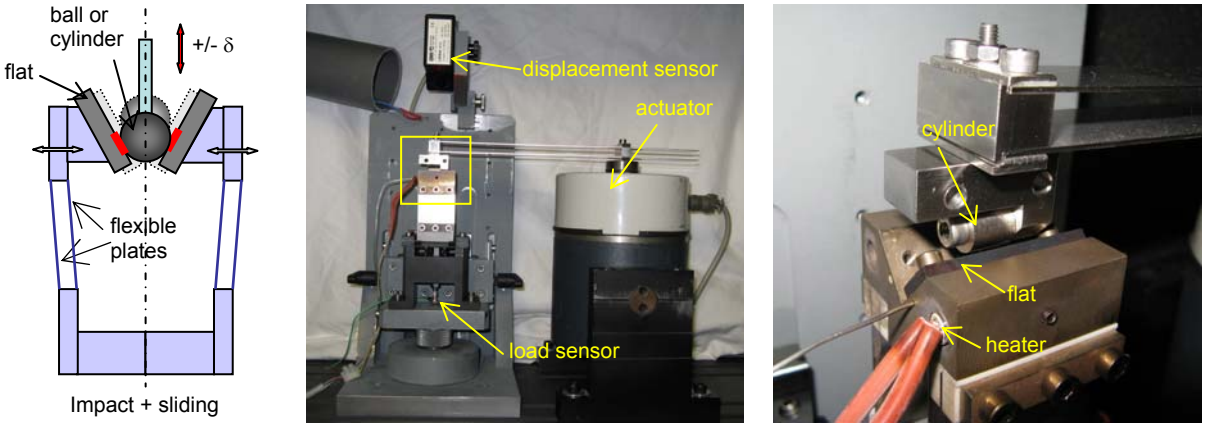

(a) (b) (c)

Figure 83: Compound impact tribometer: (a) the principle; (b) the photo of the tribometer; (c) the contact zone.

4.3.5 Summary

The valve / seat contact in Diesel engines works under complex surroundings: impact loading, high temperature, corrosion medium, etc. The wear of the contact surface due to impact and micro-sliding will decrease the performance of the engines. The harsh environment and the geometry of the substrate limit the use of many coatings. Thermal sprayed, laser clad, or welded thick coatings, combining high hardness and good toughness, are favorable.

4.4 Synthesis of the case studies

Despite the different tribological applications in the above 3 case studies, the coating selection was performed along the same process.

- Investigate the background of the applications like the function of the components, the feature of substrate materials, etc.
- Study the running conditions including motion, loading, operating temperature, environment, etc.
- Analyze the failure.
- Summarize the requirements for coatings.
- Search relevant coatings from literature used in similar applications.
- Evaluate and compare the coatings according to the requirements and limits.

The three case studies are summerized in Table 20.

Table 20: Summary of the three case studies.

	Cylinder bore / Piston ring in internal combustion engines	Blade / Disk of fan in turbofan engines	Valve / Seat in Diesel engines
Background	Seal the combustion chamber, transfer heat	Critical parts in turbofan engines suffered all of the airstream	Ensure the suction of air, exhaust of the gas, and the seal of the combustion chamber
Substrate materials	Aluminum alloy for cylinder, iron or steel for piston rings	Titanium alloy (Ti-6Al-4V)	Aluminum alloy for the cylinder head
Running conditions	High temperature, unstable lubrication, corrosion medium, cyclic load, high pressure	Two kinds of fretting spectra due to centrifuge force, vibration, and takeoff and landing of airplanes	Impact loading, high temperature, corrosion medium, poor lubrication, rotation and misalignment
Main failure	Wear (adhesion, scuffing, abrasion), corrosion and collapse	Fretting wear and fretting fatigue	Impact wear, sliding wear and tribochemical wear
Requirements	1. Adhesive wear resistance 2. Low friction 3. Corrosion resistance 4. Machinability for cylinder coating 5. Thermal performance 6. Strong affinity for oil 7. High bonding strength 8. Low price	1. Low friction 2. Compressive residual stresses 3. High bonding strength 4. Resist fretting wear 5. Good accommodation	1. High temperature resistance 2. Impact wear resistance 3. Corrosion resistance 4. High thickness 5. High bonding strength 6. Low porosity 7. Easy to be deposited
Relevant coatings or surface treatments in literature	*Piston rings:* 1. Chromium plating, CKS, GDC 2. Sprayed Mo- based coatings 3. Nitriding 4. PVD CrN 5. Plasma sprayed coatings 6. Refractory cermet coatings *Cylinder bore:* 1. Chromium plating 2. Phosphate coating 3. Nitriding 4. Plasma sprayed Fe- coatings 5. Laser alloyed coatings 6. Thermal barrier coatings	1. Shot peening 2. LSP, LPB 3. MoS_2 coating 4. Cu-Ni-In coating 5. PVD TiN 6. IBED CrN 7. Cu-Al 8. DLC	1. HVOF Cr_3C_2-25%NiCr 2. HVOF, D-gun sprayed WC-Co 3. Laser clad, HVOF NiCrSiB 4. HVOF NiCrSiB-(WC-Co) 5. Welded, HVOF, plasma sprayed cobalt alloy coatings 6. HVOF, plasma sprayed oxide ceramic coatings
optimum approaches	*Piston rings* PVD CrN, GDC *Cylinder bore:* Plasma sprayed Fe- coatings	Shot peening + Cu-Ni-In+MoS2 IBED CrN + MoS_2	-

5 Conclusions

The selection process of tribological coatings is complex because of the dependence of tribological response of a coating system on many parameters, the dispersion of test results in literature and the difficulty of estimating wear mechanisms. In this chapter, a general process of coating selection and the research approach are given. The selection process includes two phases: pre-selection and simulation experiments. Several candidate coatings will be picked out in pre-selection phase, where some criteria will be employed according to the specific application and a database will be necessary. In actual applications, some simulation experiments must be carried out to investigate and compare the tribological performance of the candidate coatings under similar or real running conditions of the applications.

In this chapter, three case studies have been peformed, including cylinder bore / piston rings in combustion engines, blade / disk connection in fan of turbofan engines and valve / seat contact in

Diesel engines, which represent different tribological situations. In the contact of cylinder bore / piston rings, adhesive wear is the main failure due to the high temperature and unstable lubrication in cylinders. In the blade / disk connection, fretting wear and fretting fatigue result in the damage of contact surfaces due to the vibration and centrifugal force. For the valve / seat contact, impact wear and micro-sliding are the reasons of failure. According to the contact types, the failure analysis, the running conditions and the dimension of the components in the cases, different requirements for coatings can be obtained. After that, a long process of investigating literature was carried out to find candidate coatings, so a pre-selection tool based on database will be expected. From the three cases, the requirements for coatings are quite different in different situations, and the candidate coatings are also different.

CHAPTER 3

PRE-SELECTION OF COATINGS

CHAPTER 3: PRE-SELECTION OF COATINGS

CHAPTER 3: PRE-SELECTION OF COATINGS

This chapter introduces the pre-selection process of coatings, including the pre-selection approach (requirements, limits and selection criteria) and the development of a pre-selection tool based on database. In the pre-selection tool, a strategy combining exclusion, weight point and reliability is used to evaluate and compare the coatings.

As described in Chapter 2, the pre-selection process of coating is complex. Much work must be done to match characteristics of coatings (coating materials and deposition methods) with the requirements and limits of a specific application. Effective approach and selection strategy are very important for the pre-selection process.

1 Pre-selection approach

1.1 Requirements for coating selection

In a specific tribological application, there are many requirements for the coating, including tribological performance, non-tribological performance and non-functional requirements. They come from the direct demand of end users, or from contact characteristics and failure analysis.

1.1.1 Tribological performance requirements

Tribological performance requirements mainly include two aspects: friction reduction and wear resistance (or durability).

In most situations, coatings with friction reduction ability are expected because a low friction can reduce energy consumption and frictional loading, subsequently induce low wear. In general, friction reduction coatings (soft metals, lamellar solids, polymers…) result in a friction coefficient about 0.1~0.2 in ambient air. Under some special conditions, ultra-low friction can be obtained, for example, sputter-deposited MoS_2 coating in ultra-high vacuum [87], highly hydrogenated DLC coating in vacuum [88].

Sometimes, a suitable or even high friction is expected: for example, in the applications of brakes and clutches. Therefore, the requirement for friction coefficient can be qualitatively divided into 5: ultra-low friction (<0.01), very low friction (0.01~0.2), low friction (0.2~0.4), moderate friction (0.4~0.6), stable friction (a given constant value over a large range of conditions).

The wear resistance requirement can be expressed by wear rate, wear volume or expected coating lifetime. However, the values in literature are quite different due to their dependence on running conditions. So, we just use some qualitative description, and add some requirements for relevant coating properties. As the description done in Chapter 1, different coating properties are required under different wear modes. Favorable coating properties and possible coatings for various wear modes are summarized in Table 21 [2, 171, 256].

Table 21: Favorable coating properties and recommended coatings for various wear modes [2, 3, 171, 256].

Wear mode		Dominating phenomena	Favorable coating properties	Recommended coatings
Abrasive wear		Third body particles indentation or two body ploughing	1. High hardness; 2. Low roughness; 3. High microtoughness; 4. High H/E; 5. Sufficient thickness.	Hardfacing coatings, thermal sprayed hard coatings (carbides, ceramics, Co-, Ni- alloys), PVD hard coatings (TiN, TiCN, TiAlN, CrN), hard chromium plating.
Adhesive wear		Scoring, scuffing, galling and seizure	1. Dissimilar metals; 2. Low shear strength at the contact interface; 3. High load carrying capacity; 4. Low relative hardness; 5. Low roughness.	Low friction coatings (MoS_2, PTFE, graphite, DLC, soft metal coatings, electroless NiP-PTFE), thermal sprayed cermets, CVD TiC, PVD TiN.
Fatigue wear		Cyclic surface stresses, cracks, pits	1. High microtoughness; 2. High yield strength.	Tough coatings.
Corrosive wear		Interaction of corrosion and wear	1. Chemical inertness; 2. Low porosity; 3. Sufficient thickness.	Galvanic protection coatings (Zn-, Ni-coatings), inert barrier layers (ceramic, cermet, polymer coatings).
Fretting wear		Wear debris continuously trapped within contact	1. High hardness. 2. Low shear strength at the contact interface; 3. Oxidation resistance.	Low friction coatings (MoS_2, PTFE...), PVD hard coatings, thermal sprayed cermets (HVOF WC-Co).
Fretting fatigue		Nucleation and propagation of cracks	1. Compressive residual stresses; 2. Good elasticity or accommodation;	Shot-peening+ Cu-Ni-In/MoS_2 coating, IBAD hard coatings
Impact wear		High energy impacting stress	1. High hardness; 2. High toughness.	Welded coatings, thermal sprayed coatings (carbides, Co-, Ni-, Mo- based alloys, amorphous FeCr alloys), PVD coatings (TiCN, Me-DLC, TiAlN).
Erosive wear	Low-angle erosion (<45º)	Micromachining	1. High hardness; 2. Low porosity.	Hard coatings (PVD TiN, TiCN, TiAlN, thermal sprayed Co-, Ni- based alloy, carbide, ceramic and self-fluxing alloy coatings, welded coatings...).
	High-angle erosion (>45º)	Platelet mechanism or brittle fracture	1. Optimal hardness; 2. High toughness; 3. Low porosity.	Thermal sprayed two-phase coatings, WC-Co, NiCrSiB - (WC-Co).
Cavitation		Mechanical shock by bubble collapse	1. High toughness; 2. High hardness; 3. Low porosity.	Plasma sprayed coatings (stainless steel, Cu-, Ni- based alloys, carbides), laser clad coatings.

- ***Abrasive wear:*** Abrasive wear is induced by indentation of third body hard particles or ploughing of asperities on hard counterface. To prevent abrasive wear, the coatings must primarily be hard; especially, the hardness of the coatings should exceed that of the abrasive particles. When a hard coating is selected, its roughness should be low, or else the rough hard coating can severely wear the counterface. To avoid forming new abrasive particles from the fracture of asperities, high microtoughness is favorable. For ductile coatings, high H/E ratio is an indicator of abrasive wear resistance. Under high stress abrasion, thick coatings will be

expected. The recommended coatings include weld hardfacing coatings, thermal sprayed hard coatings (carbides, ceramics, Co-, Ni- based alloys), PVD hard coatings (TiN, TiCN, TiAlN, CrN...) and hard chromium plating.

- ***Adhesive wear:*** Adhesive wear results in transfer of material from one surface to the other. According to the wear extend, adhesion is also named as scoring, scuffing, galling and seizure. In order to reduce adhesive wear, low friction is the most important property, so the selected coatings should present a low shear strength at the contact interface. When metals are used as coatings, they should be dissimilar with the material of the counterface. High load carrying capacity, low relative hardness and low roughness are also important. The recommended coatings include low friction coatings (MoS_2, PTFE, graphite, DLC, soft metal coatings), electroless NiP-PTFE, thermal sprayed cermets, CVD TiC, PVD TiN.
- ***Fatigue wear:*** Fatigue wear occurs under repeated loading and unloading cyclic surface stresses, eventually results in the formation of surface or subsurface cracks and leaves pits. The coatings with high microtoughness and high yield strength will be favorable because they can prevent the formation and propagation of cracks. Multilayer or multicomponent tough coatings will be recommended.
- ***Corrosive wear:*** Corrosive wear takes place under corrosive environment, where both corrosion and wear are involved and influence each other, and results in the reinforcement of their effectiveness. In order to mitigate corrosive wear, two kinds of coatings can be considered: one is barrier coatings to separate the protected surface from the corrosive environment, and the other is self-sacrificial galvanic protection coatings. The barrier coatings should be inert in the corrosive environment, dense and thick enough, to assure the separation effect. The self-sacrificial coatings should have more negative electrode potential than the protected surface. The recommended coatings include Zn-, Ni- electrochemical, electroless and hot dipping coatings, welded or thermal sprayed Al-, Ni-, Co-, Cu- based alloys, ceramic, cermet, MCrAlY coatings, and polymer coatings.
- ***Fretting wear:*** Fretting wear is the result of reciprocating small amplitude motion. Wear debris trapped in the contact area plays a very important role in fretting wear, so the coatings that can result in hard wear debris or oxidation particles are hostile. The coatings with low friction at the contact interface can reduce the shear loading. The recommended coatings include low friction coatings (MoS_2, PTFE...), PVD hard coatings, thermal sprayed Co-based alloys, iron-based alloys, self-fluxing alloys, carbide (WC-Co, Cr_3C_2-NiCr) ...
- ***Fretting fatigue:*** Fetting fatigue is due to cyclic stresses under small amplitude motion. Crack nucleation and propagation are influenced by contact pressure, fatigue stresses and displacement amplitude. The coatings with low friction and good elasticity or accommodation can also reduce the fretting contact loading. Compressive residual stresses have a beneficial effect on the crack initiation and propagation. The recommended coatings include shot-peening+Cu-Ni-In/MoS_2, IBAD hard coatings.
- ***Impact wear:*** Impact wear occurs under repeated impact loading. The coatings must have a good combination of high hardness and toughness. The recommended coatings include welded or thermal sprayed coatings (carbides, Co-, Ni-, Mo- based alloys, self-fluxing alloys, amorphous FeCr alloys), PVD coatings (TiCN, Me-DLC, TiAlN) and complex structure coatings (sandwich, graded, duplex, multilayer, nanocrystalline, multicomponent).
- ***Erosive wear:*** Erosive wear is caused by the impact of small solid particles, including low-angle erosion and high-angle erosion. For the former, surface material is removed by cutting

or micromachining, while for the latter, platelet mechanism may be the predominant removal mechanism for metals, and cracks initiated by brittle fracture for ceramics. Therefore, under low-angle erosion, high hardness is the most important coating property; under high-angle erosion, the combination of high hardness and toughness is important. Significant improvements of erosion resistance can be obtained when the ratio of particle hardness to coating hardness is less than 1. Additionally, low porosity is also beneficial to resisting erosion. The recommended coatings include: for low-angle erosion, hard coatings (PVD TiN, TiCN, TiAlN, thermal sprayed Co-, Ni- base alloys, carbides, ceramics and self-fluxing alloys, welded coatings); for high-angle erosion, thermal sprayed two-phase coatings, WC-Co, NiCrSiB - (WC-Co).

- ***Cavitation:*** Cavitation occurs in liquid, and is induced by mechanical shock from bubble collapse. The most effective coating properties are high toughness, high hardness, and low porosity. The recommended coatings include plasma sprayed coatings (stainless steel, Cu-, Ni-based alloys, carbides), laser clad coatings.

In brief, the tribological requirements will be transformed into some requirements for coating properties, such as shear strength, thickness, hardness, roughness, toughness, bonding strength, etc.

1.1.2 Non-tribological performance requirements

When coatings are used, besides the tribological performances, sometimes, they must also meet performance requirements from other aspects, such as corrosion resistance, thermal performance, electrical performance, magnetic performance, nontoxicity and biological performance. The non-tribological performance requirements and some possible coatings are summarized in Table 22.

Table 22: Non-tribological performance requirements and possible coatings [7, 9, 261].

	Requirement	Possible coatings
Corrosion resistance	Corrosion resistance under the corrosion media and maximal operating temperature	Conversion coatings; Ion implantation; Laser surface process; Hot dipping Zn, Al, Zn-Fe, Zn-Al, Al-Si, Pb-Sn alloys; Electroplated Zn, Cr, Cd, Sn; Electroless Ni, Ni-P; Thermal sprayed Ni-, Co- based alloys, MCrAlY alloys.
Thermal performance	1. Maximal service temperature 2. Thermal barrier, thermal conductivity 3. Thermal expansion coefficient	Thermal barrier coating: YSZ; Low thermal conduction and expansion: ceramics; High thermal conduction and expansion: metals and alloys.
Electrical performance	1. Dielectric 2. Semiconductor 3. Conductor 4. Superconductor	Conductor: metals (Ag, Au, Cu, Al), alloys and graphite; Dielectric: polymers and ceramics; Semiconductor: Si, Ge, SiC, GaAs; Superconductor: BSCCO and YBaCuO.
Magnetic performance	1. Diamagnetic 2. Paramagnetic 3. Ferromagnetic	Diamagnetic: Cu, Ag, Au alloys; Paramagnetic: Mg, Mo alloys; Ferromagnetic: Fe, Ni, Co alloys.
Biological performance	1. Bio-inertness 2. Bioactivity 3. Biocompatibility	UHMWPE, titanium, stainless steels, Co-Cr alloys, ceramics (TiN, CrN, TiAlN, Al_2O_3, ZrO_2), hydroxyapatite and DLC.
Nontoxicity	1. No emission of toxic substance; 2. Permission of contacting with food.	Stainless steels, tin, aluminum, ceramics and some polymers.

- **Corrosion resistance requirement**

According to the running environment, corrosion can be divided into aqueous or wet corrosion (water, seawater, acid solution, basic solution, other chemical reagents) and gaseous or dry corrosion (atmospheric corrosion, oxidation, high temperature corrosion). A coating usually presents different resistances for different corrosion types. Therefore, in an application, the information about corrosive media and the maximal operating temperature should be provided.

Some deposition methods can produce excellent corrosion resistance coatings. Phosphating coatings are used to protect iron, steel, aluminum, copper, magnesium and their alloys. Chromating coatings are commonly applied on Al-, Zn-, Mg-, Cd-, Sn- and iron- based alloys to resist atmospheric corrosion. Anodizing is one of the most common surface treatments of aluminum for corrosion protection. Surface modification by ion implantation or laser surface processing can improve the corrosion resistance of titanium alloys and steels. Hot dipping zinc coating, electroplated zinc, cadmium, chromium, tin coatings and electroless nickel coating protect steels from corrosion. Thermal sprayed zinc, aluminum, copper coatings resist atmospheric and immersion corrosion, and thermal sprayed Ni-, Co- based alloys, MCrAlY alloys (M=Ni, Co) resist high temperature corrosion [261].

- **Thermal performance requirement**

The thermal performances of coatings are very important when they are used under high temperature or high frictional loading (high frictional heat) conditions. The thermal performance includes three aspects: thermal resistance (high temperature hardness, resisting thermal creep, thermal fatigue and phase transition), thermal conduction and thermal expansion. The thermal resistance requirement can be simply expressed by the maximal service temperature. The thermal conduction requirement can be qualitatively described by thermal barrier, low, moderate and high thermal conductivity. Ideal thermal expansion requirement is that the thermal expansion coefficient of the coating is close to that of the substrate, in order to reduce residual stresses at the interface between the coating and the substrate.

Yttria stabilized zirconia (YSZ) layer is the most common thermal barrier coating due to its low thermal conductivity and relatively high (compared to many other ceramics) thermal expansion coefficient. YSZ can be deposited by air plasma spraying (APS) or electron beam physical vapor deposition (EB-PVD). MCrAlY (M=Ni, Co) is usually used as the bond coating between nickel superalloy substrates and YSZ coatings. Generally, metals and alloys present higher thermal conductivity and thermal expansion than ceramics and polymers.

- **Electrical performance requirement**

More and more coatings are used in electronic and microelectronic industries. In different applications, electrical performance requirement for the coatings can be dielectric, semiconductor, conductor or superconductor. The main electrical conductor coatings are metals (Ag, Au, Cu, Al...), alloys and graphite. The dielectric coatings include polymers and ceramics. Semiconductor coatings are usually made of Si, Ge, SiC, GaAs, etc. BSCCO and YBaCuO are the research focus of superconductor coatings.

- **Magnetic performance requirement**

As for magnetic performance, coating materials can be grouped into diamagnetic, paramagnetic and ferromagnetic. Most elements, like Cu, Ag, and Au, are diamagnetic. Paramagnetic materials include Mg, Mo, Li, and Ta. The examples of ferromagnetic materials are Fe, Ni, and Co.

- **Biological performance requirement**

In the field of medical implants in the human body (such as hip joint prostheses, artificial heart valve, dental implants...), UHMWPE, stainless steels, Co-Cr alloys and ceramics are the common bearing materials of implants. However, the first three materials can cause osteolysis by wear debris, and ceramics risk a brittle fracture. Coatings are increasingly being used to improve the tribological performance of the implants and prolong their service time. The coatings should meet the following requirements: biocompatibility (bio-inertness or bioactivity), corrosion resistance in the human body environment, without osteolysis caused by wear debris and good strength.

Hydroxyapatite is the main composition of teeth and bones, and it is often coated on hip replacements and dental implants due to its excellent biocompatibility. Titanium is biocompatible and has the inherent property to osseointegrate, so it is widely used in medical applications including surgical implements and implants. Ceramic coatings, such as TiN, CrN, TiAlN, Al_2O_3, ZrO_2, are more and more used as medical coatings due to their bio-inertness and excellent wear resistance. A thin DLC coating with bio-inertness and excellent friction reduction can further improve the performance of medical implants.

- **Nontoxicity requirement**

Nontoxicity can be explained from different levels. When the coated component is used to contact with food, nontoxicity means that the coating should not contaminate the food by wear debris or reactive products. Heavy metal is usually harmful to the human body, such as Cd, Pb, As... Stainless steels, tin, ceramics and some polymers can be used as coating materials contacting food. When the coated components are used for normal objective, the coating should not release any substance that does harm to health. So, nontoxicity requirement can be no emission of toxic substance and permission of contacting with food.

1.1.3 Non-functional requirements

Besides the above functional requirements, some requirements that will not influence the performance of the coatings may be proposed by the end users. These requirements include the following aspects: cost, efficiency of deposition, color, pollution, etc.

- **Cost**

In industrial applications, the cost of a coating is an important factor to be considered. The cost includes the investment of the deposition device, the price of coating materials and the energy consumption during the deposition process. Generally, the investment of gaseous deposition (PVD, CVD and ion implantation) is higher than solution deposition (electroplating and electroless deposition), and molten (thermal spraying) deposition is placed in the middle. For thermal spraying processes, the order of device cost from low to high is: flame spraying, electric arc spraying, plasma spraying, HVOF and detonation spraying.

- **Efficiency of deposition**

Apart from the cost, efficiency of the deposition process, including the deposition rate, operating convenience, the possibility of mass production, is another important factor considered in industrial applications. In all the deposition processes, welding and thermal spraying have the highest efficiency, and PVD presents the lowest deposition rate. A high deposition rate is possible for CVD process. The deposition rate of electroplating and electroless deposition mainly depends on the depositing materials and the plating baths, and electroplating is usually more efficient due to the effect of external electrical

current. Welding, thermal spraying and brush plating show excellent operating convenience, and they can be used for fieldwork and local cover of the substrate surface.

- **Color**

When the coated components are used for decoration or some special industries, their color and luster may be required. In decorative applications, gold, silver and lustrous coatings are favorable. In medical and food industries, white means quiet and cleanness. Table 23 shows the color of some coatings.

Table 23: Color of some coatings.

Coating	Color	Coating	Color
Chromium plating	Blue-white	CrN	Silver-gray
TiN	Gold	TiCN	Blue-gray
ZrN	Bright gold	CrAlTiN	Silver-gray
DLC	Black	AlTiN	Blue-gray or purple-black
MoS_2	Dark gray	Si_3N_4	Dark gray
PTFE	Black	Al_2O_3	White

- **Pollution**

Nowadays, pollution is more and more being concerned. The pollution in deposition processes includes environmental pollution and harm to the health and safety of the operators. For example, the use of chromium plating is being limited more and more strictly due to the toxicity of hexavalent chromium contained in the plating baths; effluent with metallic ions is the main pollution of electroplating and electroless deposition; noise, light radiation, dust and fumes with particles have to be faced in thermal spraying; toxic and corrosive byproducts may be generated in CVD process. The disposal procedures against pollution will induce additional costs. Sometimes, pollution also occurs during the use of coated devices. For example, when cadmium-plated parts are heated or soldered, toxic fume will be released.

1.2 Limits from the tribological applications

In a specific tribological application, the running conditions, the substrate and the counterpart can bring some limits for the coating selection.

1.2.1 Limits from running conditions

The running conditions (like temperature, relative humidity, atmosphere, loading, relative sliding speed...) in the application can prevent the use of some coatings. For example, the maximal operating temperature exceeds the maximal endurable limit of some coatings, or the coatings are unsuitable for the corrosive media of the application. The limits from some special running conditions are summarized in Table 24, where some favorable and unsuitable coatings are also listed.

Table 24: Limits from special running conditions and relevant coatings [6, 93, 171].

Special running conditions	Limits	Favorable coatings	Unsuitable coatings
High temperature	Resisting phase transition, thermal creep, high temperature oxidation	Ni-, Co- based alloys, ceramics, cermets	Low melting point coatings, like polymers, some nonferrous metals
N_2, H_2, Vacuum, inert gases, dry air, low RH,	Formation of transfer film without oxidation and humidity	a-C:H, MoS_2	TiN, a-C, graphite
Oxygen	Resisting oxidation	Inert coatings	Coatings trending to be oxidized
Alternating load	Resisting fatigue cracks	Coatings with high fatigue strength	Tensile residual stress coatings
Impact load	Resisting fracture	Coating with high toughness, like welded coatings, thermal sprayed coatings	Brittle coatings
High load	Resisting plastic deformation	Coating with high hardness, such as Co- based alloys, ceramics, cermets	Soft coatings
Rolling contact	Resisting adhesion, abrasion and fatigue wear	Thin solid lubricant coating or thin hard coating (<1μm)	Thick coatings
High sliding speed	Resisting the effect of flash temperature and frictional heat	Coatings with low friction, high thermal conductivity, good high temperature hardness.	Low melting point coatings

- **Atmosphere**

Atmosphere means the running environment of the coated components. The possible gaseous environment is usually ambient air, vacuum, high vacuum, nitrogen, oxygen, hydrogen and inert gases. Coatings tending to be oxidized, like MoS_2, present better tribological performance in the atmosphere without oxygen. a-C:H coatings have a longer lubricating life in an inert environment due to low friction coefficient and low wear rate, while a-C coatings show lower friction coefficient in ambient air. Coated components can also work in liquid environment, like water, seawater, lubricant and various chemical agent. In liquid environment, corrosion and abrasive wear by suspending particles should be considered.

- **Temperature**

In some applications, the coated components work under high temperature surroundings, such as piston rings in engines, cutting tools for high speed machining or dry machining, turbine blades in the hot sections of gas turbofan engines. Therefore, the coatings with low maximal service temperature cannot suit the applications. The possible coatings must have excellent high temperature hardness and high temperature corrosion resistance. The thermal expansion coefficient of the coatings should be close to that of the substrate. Table 25 shows the maximal service temperature of some coatings that are often used under high temperature, including Co- based alloys, Ni- based alloys, ceramics (carbides, nitrides and oxides) and cermets.

Table 25: The maximal service temperature of some coatings [9, 262-264].

Coating material		Max. service temperature	Coating material		Max. service temperature
Co- based alloys (CoCrNiWC or CoMoCrSi)	Stellite® 1	760 ºC	Nitrides	TiN	500~600 ºC
	Stellite® 6	500 ºC		CrN	650~700 ºC
	Stellite® 12	700 ºC		TiAlN	800~900 ºC
	Stellite® 21	1150 ºC		ZrN	600 ºC
	Tribaloy® T-400, T-800	800 ºC		Si_3N_4	1500 ºC
Ni- based alloys	MCrAlY(M=Co,Ni)	850-980 ºC	Oxides	TiO_2	540 °C
	Ni-5Al	800 ºC		Al_2O_3	800~1700 °C
	Ni-20Cr	980 ºC		YSZ	1350~1430 °C
	Self fluxing NiCrSiB	540-840 ºC	Cermets	WC-Co	480~540 ºC
Carbides	TiC	500 ºC		WC-Ni	480 ºC
	Cr_3C_2	870~900 ºC		Cr_3C_2 -NiCr	540~900 ºC

- **Relative humidity (RH)**

In different applications, the relative humidity conditions may be dry, low RH, high RH and liquid. Relative humidity can influence friction, wear and corrosion performance of the coatings. Therefore, under different relative humidity conditions, different coatings will be expected. For example, MoS_2 and DLC (a-C:H) suit dry or low RH conditions; graphite, PVD TiN and DLC (a-C) are suitable for high RH conditions. Under liquid conditions, the friction and wear of a coating depend on the coating itself and the liquid property (water or oil). For example, DLC (a-C:H) coatings present worse wear resistance under water-lubricated conditions than in air, while their wear rates slightly decrease under oil-lubricated conditions [265]. The excellent friction and wear performances of solid lubricant coatings usually result from transfer tribolayers in dry sliding conditions, while under liquid conditions, the formation of the tribolayers can be hold back.

- **Loading**

Loading, including its type (static, alternating, impact) and value, leads to different requirements for coating properties. For example, under the alternating load, the fatigue strength of the coatings may be important; under impact load, the toughness of the coatings can be crucial; under high load (contact pressure), thick coatings with high hardness will be expected.

- **Relative movement**

Relative movement, including type (sliding, rolling and fretting), speed (low, intermediate, high, ultra high), amplitude and frequency (for reciprocating sliding and fretting), results in different coating requirements from thermal performance, mechanical properties, etc. Under rolling contact, the contact area is usually classified as “point contact” and “line contact”, where there are high contact pressures. The contact area often fails by adhesive wear, abrasive wear and fatigue wear, and a thin soft coating or hard coating can improve the wear resistance, but the coatings must be thin (<1μm) to match the

deformation of the substrate [6]. Under high and ultra high sliding speed, frictional heat and flash temperature should be looked as an important aspect during the coating selection.

1.2.2 Limits from the substrate

The limits from the substrate depend on its material, size and shape. Common engineering materials are shown in Figure 84. For a known substrate material, its properties can limit the use of some deposition method. For example, the substrate materials with a low maximal endurable temperature cannot be covered by high temperature deposition methods, like CVD; the unsolderable substrate materials cannot be used in welding and laser cladding process; the dielectric substrate materials are unsuitable for the electroplating process. The substrate material can also limit the selection of coating material. For example, some coating materials can achieve higher bonding strength on the substrate material than other coating materials; in high temperature applications, the coating material should have a similar thermal expansion coefficient with that of the substrate material.

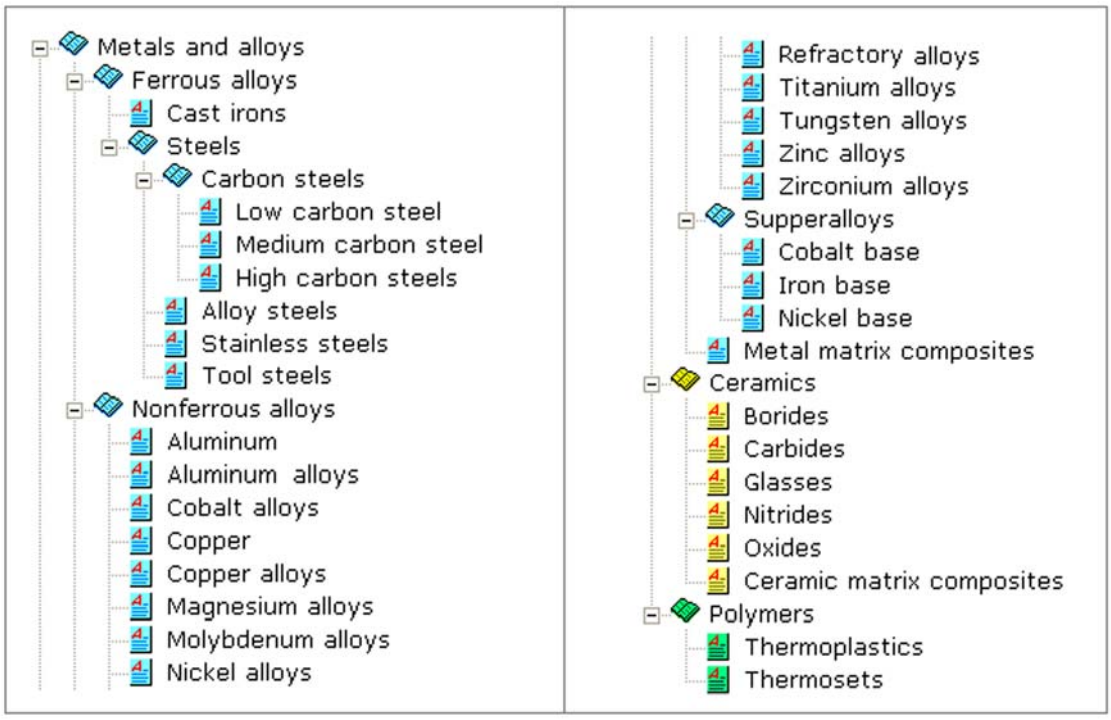

Figure 84: Common substrate materials.

The size and shape of the substrate can also result in some limits to deposition methods. The size of the coated component should be smaller than the chamber or the bath of a deposition method. The deposition methods with a chamber include PVD, CVD and ion implantation. Electroplating, electroless deposition and hot dipping are carried out in a bath. The components with complex shapes (inner surfaces, blind holes, slots…) cannot be coated by line of sight processes, like PVD, ion implantation and thermal spraying. If the component includes sharp edges, like cutting tools, the selected deposition processes must ensure the coating without build-ups and detachments from the substrate at the sharp edges. For selective deposition with a large blank area, the deposition methods where the whole component is immerged in a bath or gaseous circumstance (coating material particles) are unreasonable because a lot of stopoff media need to be used.

1.2.3 Limits from the counterpart

The hardness, roughness and chemical properties of the counterpart can influence the tribological performance of a coating system. When the counterface is hard and rough, hard coatings will be expected, in order to resist abrasive wear.

In adhesive wear and diffusion wear applications, the selected coating material should be chemically stable, in order to reduce adhesion and diffusion with the counterface. Favorable coatings may be chemical inert or dissimilar with the counterpart material, or they can form a protective microfilm at the contact interface.

1.3 Pre-selection criteria

A coating is an integration result of coating material, coating structure and deposition method. Specific deposition parameters, matching between the coating material and the deposition method are not the focus in this chapter. Therefore, the coatings mentioned in the subsequent paragraphs are the common coatings in literature or in industries expressed by deposition method plus coating material.

The pre-selection of coatings is the process of matching the characteristics of coatings (the deposition method and the coating material) with the requirements and limits from the tribological application. The following criteria should be considered in the matching process.

1.3.1 Criteria based on the deposition method

- *Deposition method must suit the substrate material.* The deposition method must be feasible on the substrate material. For example, the deposition temperature should be lower than the maximal endurable temperature of the substrate material (except welding and laser cladding).
- *Deposition method must suit the geometry of the substrate.* The size of the substrate should not exceed the limit of the deposition device. For selective deposition, the deposition method should avoid a lot of stopoff media. The throwing power of the deposition method should suit the shape of the substrate.
- *Achievable coating thickness meets the relevant requirement.* In a specific application, there may be an expected coating thickness. The achievable coating thickness range of the selected methods should cover the expected value. Figure 6 shows the achievable coating thickness of some common methods, which depends on deposition principle, bonding strength and residual stresses. For thin coatings, the deposition method should have good controllability in the accuracy and uniformity of the thickness.
- *Deposition method should impart sufficient bonding strength between coatings and substrates.* Sufficient bonding strength between coatings and substrates is the precondition of good wear resistance. The bonding strength depends on deposition method (the bonding mechanism), and it is also influenced by the materials of the coating and the substrate, coating thickness, deposition parameters (temperature, substrate bias voltage, gas pressure…).
- *Coating should meet the requirements in porosity, residual stresses and topography.* In different applications, a dense or porous coating can be expected. The selected deposition method should ensure that the deposited coatings can meet the required porosity. Different deposition processes can induce different residual stresses at the interface between the coating and the substrate due to high deposition temperature and different thermal expansion of the coating and the substrate.

When a smooth surface is expected, the selected deposition method should be able to produce coatings with low roughness or the deposited coatings can be post-treated.

- *Deposition rate and investment of deposition devices should be acceptable.* The investment and throughput of a deposition method are the most interesting aspects for a company. Therefore, the deposition rate of the selected deposition method must be acceptable for the company, and the investment of deposition devices should not exceed the budget.
- *Pollution should accord with relevant regulations.* Wastes and harmful byproducts produced in a deposition process must be correctly disposed, and the final pollution caused by the deposition should meet the relevant regulations.

1.3.2 Criteria based on coatings

- *The coating materials must suit the substrate material.* There are many aspects that need to be considered about the relationships between the coating material and the substrate material. First, the coating material must be able to be deposited on the substrate material (sometimes with the use of an intermediate layer). Second, for thin hard coatings, their elastic modulus should be close to that of the substrate. Third, in high temperature applications, the thermal performance of the coating material should be in accordance with the substrate.
- *The coating materials must suit the counterpart.* The coating material should be chemically inert and dissimilar with the material of the counterpart to prevent adhesive wear. The coatings that can form a low friction transfer film with the counterface are favorable. The hardness difference between the counterface and the coating should not be too large, in order to prevent abrasive wear.
- *The coating materials must suit the running conditions.* The running conditions include operating temperature, relative humidity, atmosphere, loading type, contact pressure, relative movement, sliding speed, as described in section 1.2.1.
- *The coatings should meet the tribological requirements.* The tribological requirements, including friction and wear resistance, can be transformed into the requirements for coating properties, as described in section 1.1.1.
- *The coatings should meet the non-tribological requirements.* In some special applications, the coating must meet some non-tribological requirements (section 1.1.2).
- *The coatings should meet the non-functional requirements.* When there are some non-functional requirements (such as color, cost, efficiency...), the coatings should be suitable.

In conclusion, there are 13 criteria, but not all of them are necessary in each application, and the extent of requirements can be different for different applications.

2 Development of the pre-selection tool

In order to apply the above criteria to select coatings, the “Pre-selection Tool for Tribological Coatings (PTTC)” similar to the “Surface treatment selector” in [176] is developed. PTTC focuses on the selection of coatings for tribological applications. It includes the common deposition methods used for tribological coatings and the common tribological coatings. To achieve the expected function, the deposition methods and the coatings must be reasonably described, and appropriate selection strategies should be employed.

2.1 Description of deposition methods

In order to apply the pre-selection criteria based on the deposition method, the deposition methods need to be described correctly. The deposition methods are expressed by the characteristics listed in Table 26. Some of them are qualitatively evaluated, because it is impossible to quantitatively describe them (coating uniformity, thickness control) or it is difficult to obtain the reference value from literature. Figure 85 is an example of the description of deposition method.

Table 26: Characteristic description of deposition methods.

Name of characteristic	Note
Name	Name of the deposition method.
Coating materials	Material types that can be deposited by the deposition method.
Substrate materials	Substrate material types for which the deposition method is suitable (the same types listed in Figure 84).
Substrate temperature	Maximal temperature suffered by the substrate during the deposition process (it can be a range expressed by Celsius degrees).
Coating thickness	Achievable coating thickness by the deposition method (it is a range expressed by micrometer).
Thickness control	Controllability of coating thickness, i.e., the possibility of obtaining an accurate thickness (qualitative description by excellent, good, fair, poor, very poor).
Coating uniformity	Coating uniformity in thickness and microstructure (qualitative description by excellent, good, fair, poor, very poor).
Bonding strength	Bonding strength between the coatings and the substrate (qualitative description by excellent, good, fair, poor, very poor).
Bonding mechanism	Bonding mechanism of the coatings on the substrate (including atomic, surface forces, mechanical, chemical, metallurgical, diffusion).
Porosity	Porosity of the coatings deposited by the deposition method (qualitative description by low, moderate, high plus value in percentage).
Deposition rate	Speed of coating growth on the substrate (qualitative description by very low, low, fair, high, very high, plus value in μm/min or kg/hr).
Process cost	Investment of the deposition method (qualitative description by very low, low, fair, high, very high)
Geometry limit	Including size limit and throwing power of the deposition method. Size limit for the substrates is described by no limit, limit by chamber size, limit by bath size. Throwing power can be expressed by versatile (no limit), line in sight, unsuitable for sharp edge, unsuitable for blind hole.
Pretreatment	Pretreatment for the substrate surfaces before the deposition process, such as cleaning, degreasing, roughening.
Post-treatment	Post-treatment for the coating after the deposition process.
Pollution	Pollution caused by the deposition process.
Application	Common application fields of the deposition method.
Process description	Introduction of the deposition process, including principle, advantages, disadvantages and sketch map.

Ion Beam Assisted Deposition (IBAD)

Coating Material	:	Almost any materials
Substrate Material	:	Almost any materials
Substrate Temperature (° C)	:	100
Coating Thickness (μm)	:	0.02~10
Thickness Control	:	Good
Coating Uniformity	:	Fair
Bonding Strength	:	Excellent
Bonding Mechanism	:	Atomic
Porosity	:	Low
Deposition Rate (μm/min)	:	Low (0.01~0.1)
Process Cost	:	Very high
Geometry Limit	:	Line of sight, limited by the chamber size
Pretreatment	:	Mechanically and chemically clean
Post-treatment	:	None
Pollution	:	Low
Application	:	Lubrication, wear resistance, corrosion protection(aqueous corrosion, high-temperature oxidation) and optical film.
Process description	:	

Ion Beam Assisted Deposition (IBAD) refers to the process where evaporated atoms produced by physical vapor deposition (PVD) are simultaneously struck by an independently generated flux of ions. The extra energy imparted to the deposited atoms causes atomic displacements at the surface and in the bulk, as well as enhanced migration of atoms along the surface. These resulting atomic motions are responsible for improved film properties, including better adhesion and cohesion of the film, modified residual stress, and higher density, in comparison with similar films produced by PVD without ion bombardment. When the ion beam or the evaporant is a reactive species, compounds such as refractory silicon nitride can be synthesized at very low temperatures. Furthermore, adjustment of the ratio of reactive ions to atoms arriving at the substrate surface allows adjustment of the stoichiometry of solid solutions. The adhesive strength of these IBAD interfaces is typically 10 to 100 times higher than for the same films deposited at thermal energies with an electron beam or other PVD source without ion assistance. The IBAD process is a hybrid of PVD and ion implantation. It combines the advantages of both techniques, while eliminating most of the disadvantages of each.

■ **Advantages:**

- ☐ Unique coating properties, very high-kinetic energy ion beam may leads to excellent adhesion and high density.
- ☐ Independent control over kinetic energy and current density of ions.
- ☐ Directionally control of ion beams.
- ☐ Low deposition pressure.
- ☐ High deposition rates.
- ☐ No gas atom incorporation.
- ☐ No substrate heating.

■ **Disadvantages:**

- ☐ Needs separate ion source.
- ☐ Moderately higher cost than physical vapor deposition.
- ☐ Line of sight process.
- ☐ Substrate size limited because of small ion beam size(~100mm diameter).

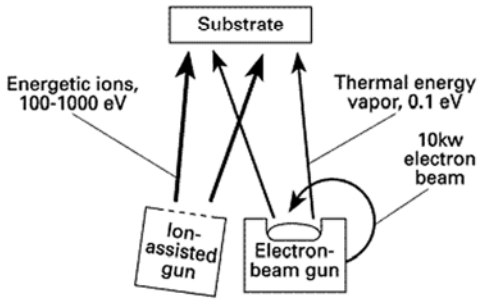

Figure 85: Example of the description of deposition method.

As described in Chapter 1, more and more deposition methods are developed. However, not all of them suit tribological applications. Here, only common deposition methods for tribological coatings are included, as shown in Figure 86 [7, 9, 266].

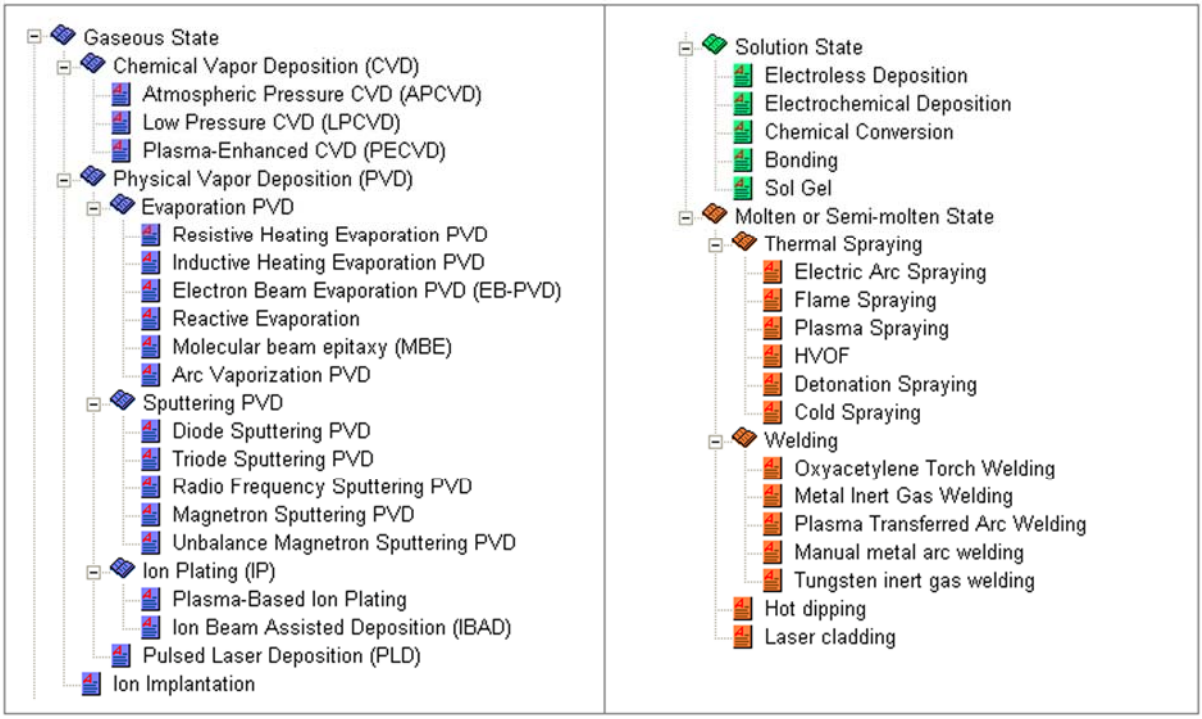

Figure 86: Deposition methods included in the pre-selection tool.

2.2 Description of coatings

According to the pre-selection criteria, the characteristics listed in Table 27 are used to describe a coating. However, it is impossible to obtain all information of coating characteristics for every coating due to the incomplete information in literature. Additionally, most coating characteristics depend on the deposition parameters and running conditions, and the values change in a wide range. Therefore, some characteristics are expressed by qualitative evaluation, quantitative range or qualitative evaluation plus quantitative range, even by blank, which means unobtainable.

Table 27: Characteristics used for coating description.

Name of characteristic	Note
Name	Name of the coating (including brief coating material and deposition method).
Coating material	Detailed name of coating materials.
Coating material type	Type of the coating materials (similar classification with substrate material).
Composition	Composition of the coating material
Deposition method	Deposition method for the coating (Figure 86).
Substrate materials	Typical substrate material types on which the coating can be deposited. Blank means the substrate material types mentioned in the relevant deposition method.
Friction coefficient	The friction coefficient is expressed by qualitative evaluation (ultra-low, very low, low, moderate, high) plus quantitative range rubbing against steels in ambient air, because of the dependence of friction coefficient on test parameters and running conditions.

Wear resistance	Wear resistance of the coating described by wear mode (general, abrasion, adhesion, corrosion, fatigue, fretting, impact, erosion, or cavitation) plus qualitative evaluation (excellent, good, fair, poor or very poor).
Corrosion resistance	Corrosion resistance of the coating described by corrosion type (general, atmospheric, oxidation, high temperature, water, seawater, acid solution, basic solution, other chemical agent) plus qualitative evaluation (excellent, good, fair, poor or very poor).
Thermal conduction	Thermal conductivity of the coating described by quantitative range (W/m·K).
Thermal expansion	Thermal expansion coefficient of the coating described by quantitative range (10^{-6}/K).
Maximal endurable temperature	The maximal service temperature of the coating in oxidation atmosphere (ºC).
Electrical performance	Electrical performance of the coating described by qualitative evaluation (dielectric, semiconductor, conductor, superconductor) plus quantitative range (electrical resistance, μΩ· cm).
Magnetic performance	Magnetic performance of the coating described by qualitative evaluation (diamagnetic, paramagnetic, ferromagnetic).
Biocompatibility	Biocompatibility of the coating described by qualitative evaluation (bioactive, bioinert, nonbiocompatible).
Toxicity	Toxicity of the coating described by qualitative evaluation (toxic, nontoxic, food contact).
Hardness	Hardness of the coating described by qualitative evaluation (very high, high, moderate, low, very low) or quantitative range (GPa).
Elastic modulus	Elastic modulus of the coating described by quantitative range (GPa).
Fracture toughness	Fracture toughness of the coating ($MPa \cdot m^{0.5}$).
Yield strength	Yield strength of the coating (MPa).
Color	Color of the coating.
Favorable environment	Environment where the coating presents low friction or low wear.
Unsuitable environment	Environment where the coating presents high friction or high wear.
Unsuitable counterpart	Counterpart materials that induce high friction or high wear rubbing against the coating.
Applications	Common applications of the coating.
Description	Comments for some special features of the coating and the sources of information.

According to the characteristics listed in Table 27, an example of coating description is shown in Figure 87. In the database, most of the common tribological coatings are included. They are organized by soft coatings, hard coatings and complex structure coatings, as shown in Figure 88 [262-264, 266-272]. Soft coatings include lamellar solids, polymers, soft metals, and composites; hard coatings include nitrides, carbides, oxides, borides, cermets, carbons, metals and alloys. A coating material can be deposited by different methods. For example, MoS_2 coatings are deposited by sputtering PVD, IBAD, bonding and CFUBM (closed field unbalanced magnetron sputtering).

PVD TiN

Coating Material	:	TiN
Material Type	:	Nitride
Material Composition	:	TiN
Deposition Method	:	Physical Vapor Deposition (PVD)
Substrate Material	:	-
Coating Thickness (μm)	:	1~5
Coating Hardness (GPa)	:	20~30
Elastic Modulus (GPa)	:	200~590
Coating Ductibility	:	good
Yield Strength (MPa)	:	-
Fatigue Strength (MPa)	:	-
Fracture Toughness (MPa.$m^{0.5}$)	:	-
Friction Coefficient	:	low (0.35~0.4)
Wear Resistance	:	general (excellent)
Corrosion Resistance	:	general (excellent)
Max. Service Temperature (° C)	:	600
Favorable Environment	:	humid air
Unsuitable Environment	:	-
Unsuitable Counterpart	:	-
Electricity Performance	:	Conductor(30~70μΩ.cm)
Thermal Conduction (W/mK)	:	19.3
Thermal Expansion (10^{-6}/K)	:	9.35~10.1
Magnetron Performance	:	Diamagnetic
Biocompatibility	:	bioinert
Coating Color	:	gold
Toxicity	:	Food contact
Application	:	cutting tools for steels, forming, punching, plastics injection molds, implanted prostheses, decoration
Description	:	Eliminates galling, fretting, microwelding, erosion, seizing and adhesive wear. Coating thickness is in the range of 0.25 to 12 microns. Typical applications are 1 to 5 microns. Highly inert to acids, bases, solvents, caustic, etc. Oerlikon Balzers; BryCoat Inc.Sulzer Metco,IONBOND, Richter Precision Inc.

Figure 87: Example of coating description.

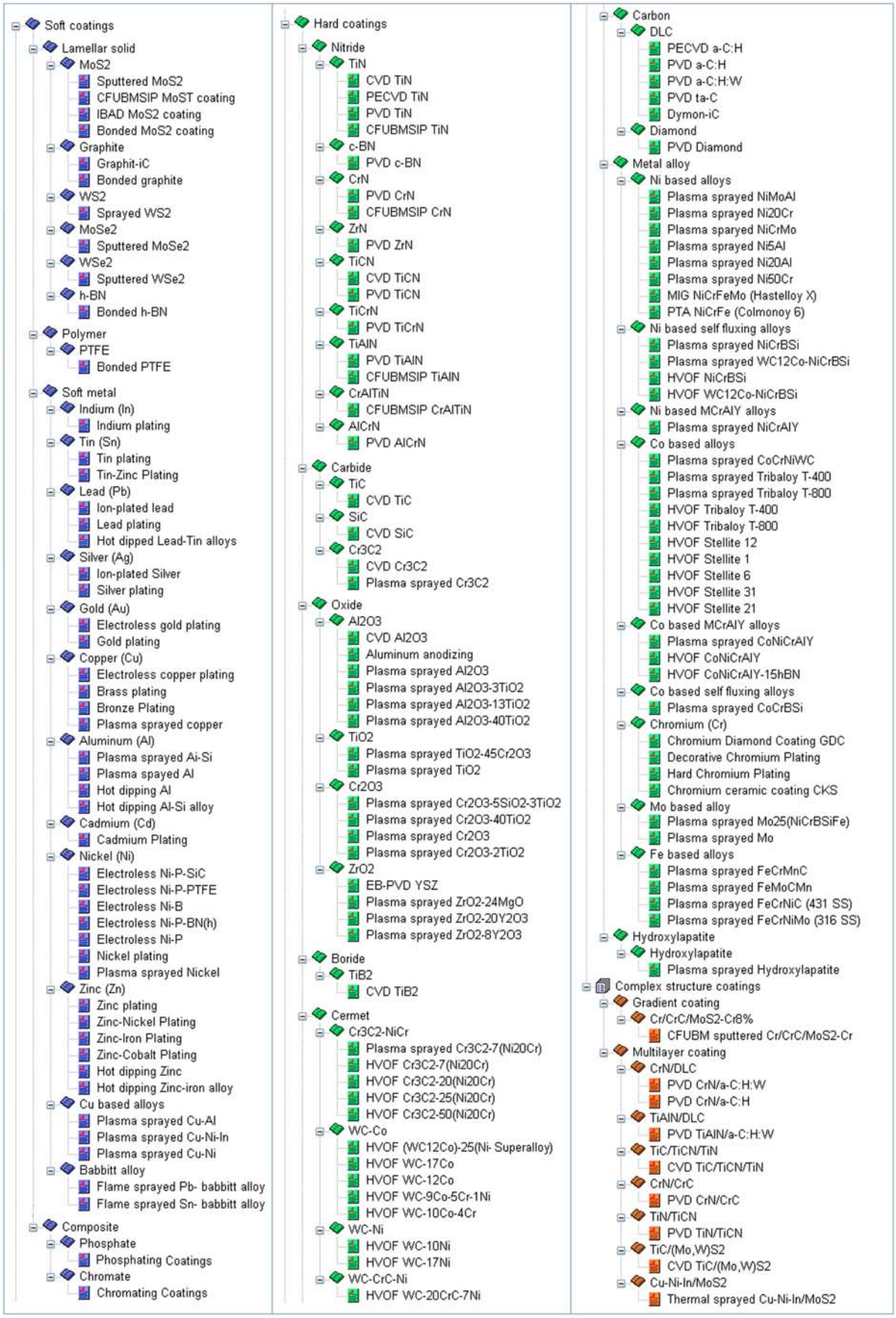

Figure 88: Coatings included in the database.

2.3 Pre-selection strategy

In the pre-selection process, two strategies are used. One is simple and straightforward, i.e., just searching the coatings ever used in similar applications from the database. For example, when we select coatings for a cutting tool, then we can simply find all the coatings that are used for cutting tools in industries and in literature. The other is a complex strategy, i.e., evaluating and comparing coatings comprehensively considering the requirements and limits of an application. The focus of this section is the latter, where an approach combining exclusion and evaluation will be used, i.e., exclude the impossible coatings, and evaluate and compare the remaining coatings by weight point and reliability, as shown in Figure 89.

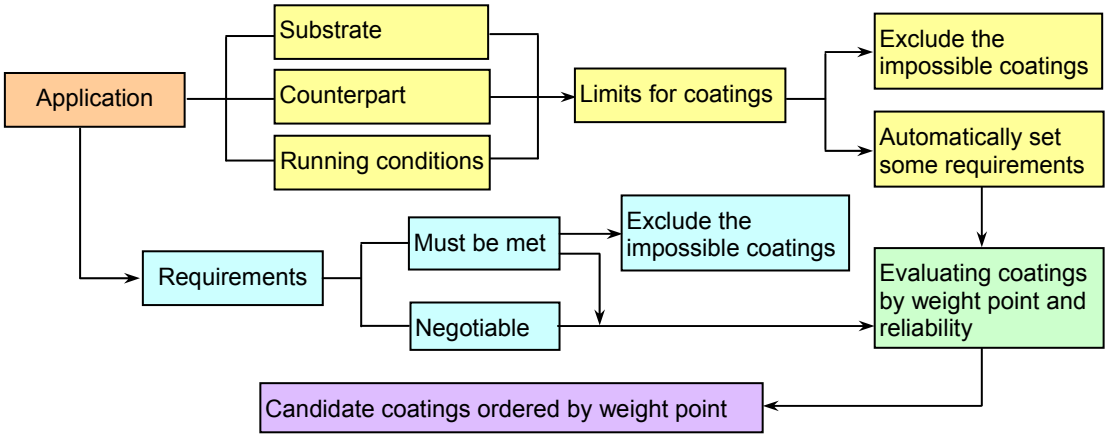

Figure 89: Diagram of the pre-selection strategy.

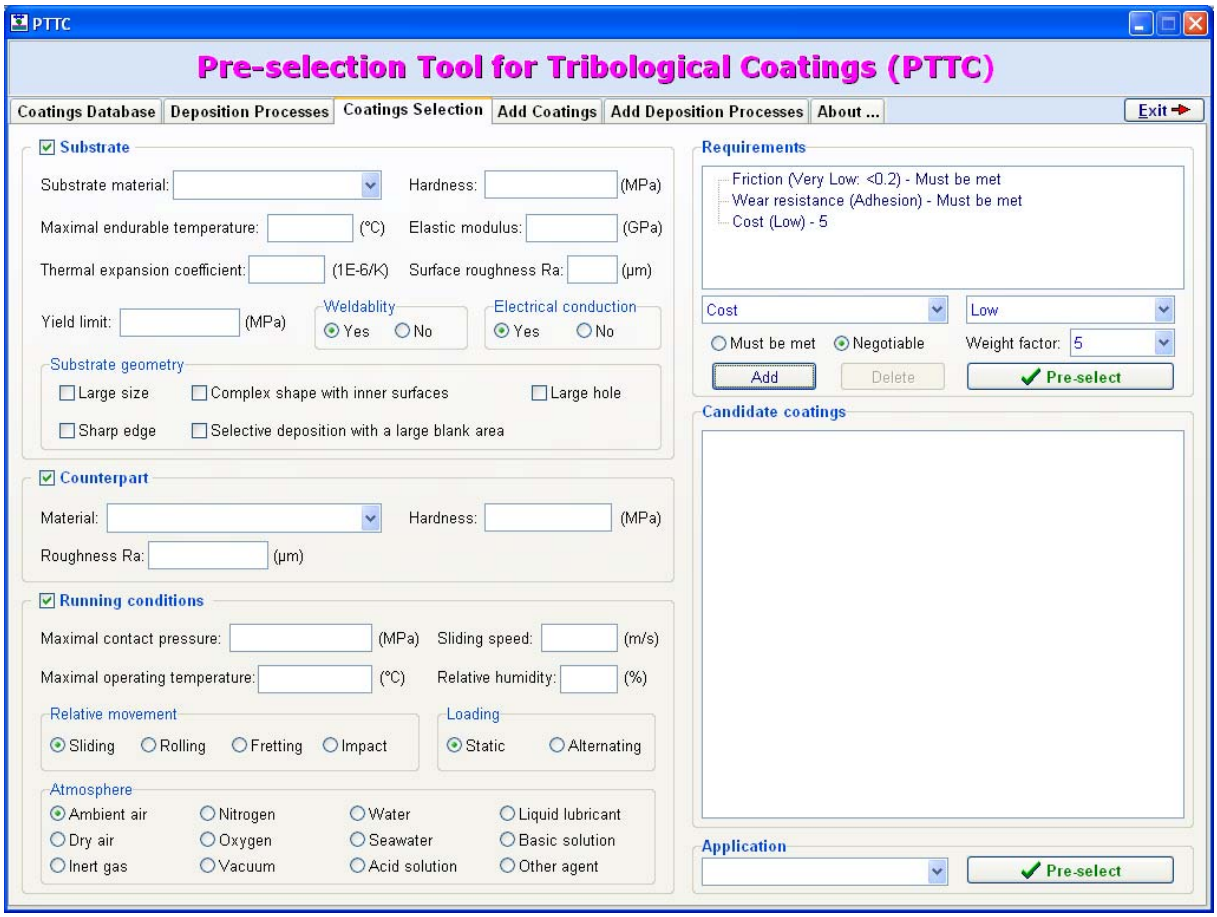

Figure 90: Interface of coating pre-selection.

At first, information about the substrate, the counterpart and the running conditions should be provided (Figure 90). Substrate information includes substrate material, hardness, maximal endurable temperature, elastic modulus, thermal expansion coefficient, surface roughness, yield limit, weldablity, electrical conduction and geometry features. Counterpart information includes counterpart material, hardness and roughness. Running conditions information includes maximal contact pressure, sliding speed, maximal operating temperature, relative humidity, relative movement, loading and atmosphere. In a specific application, the information can be selectively provided. According to the provided information, some coatings cannot be used. Therefore, they will be excluded. On the other hand, the provided information can induce some requirements for coating properties, and these requirements will be automatically set during providing relevant information.

The rules are as following:

- Substrate material: exclude the coatings whose materials or deposition methods are unsuitable for the substrate material.
- Maximal endurable temperature: exclude the coatings whose deposition methods induce a higher substrate temperature than the maximal endurable temperature (except welded and laser clad coatings).
- Weldablity “No”: exclude the coatings deposited by welding and laser cladding.
- Electrical conduction “No”: exclude the coatings deposited by electrochemical deposition.
- High roughness: exclude the coatings with a very thin thickness.
- Substrate geometry “large size”: exclude the coatings deposited by methods with a chamber or a bath, like PVD, CVD, electroless deposition, electrochemical deposition (except brush plating), sol-gel and chemical conversion.
- Substrate geometry “Complex shape with inner surfaces”: exclude the coatings deposited by line of sight methods, like PVD, thermal spraying, welding and ion implantation.
- Substrate geometry “Large holes”: exclude the coatings deposited by line of sight methods, except thermal spraying processes.
- Substrate geometry “Sharp edges”: exclude the coatings deposited by electrochemical deposition.
- Substrate geometry “Selective deposition with a large blank area”: exclude the coatings deposited by immerging methods, like CVD, electrochemical deposition, electroless deposition.
- Counterpart material: exclude the coatings whose unsuitable counterparts include this material.
- Counterpart high hardness and high roughness: set a requirement about the coating hardness — “Harder than xxx MPa”, where “xxx” is the hardness of the counterpart.
- Maximal contact pressure higher than yield limit: set 2 requirements about the coating hardness and thickness — “Harder than xxx MPa” and “Thick coating: >500 μm”.
- Relative movement “Sliding”: set 2 requirements about the wear resistance and friction — “Adhesion” and “Low: <0.4”.
- Relative movement “Rolling”: set a requirement about the wear resistance — “fatigue”.
- Relative movement “Fretting”: set 2 requirements about the wear resistance and friction — “Fretting” and “Low: <0.4”.

- Relative movement “Impact”: set 2 requirements about the wear resistance and toughness — “Impact” and “High toughness”.
- Loading “Alternating”: set a requirement about the wear resistance — “fatigue”.
- Atmosphere and relative humidity: exclude the coatings whose unsuitable environments include this atmosphere; set a requirement about corrosion resistance — resist corrosion in relevant atmosphere.

Then, some requirements need to be set. Requirements from 17 aspects can be considered (Table 28). According to the importance of a requirement for the application, it can be “Must be met” or “Negotiable”. If a requirements is “Must be met”, then the coatings without the relevant properties and without relevant information will be directly excluded.

Table 28: Requirements and their items.

Requirements	Items
Friction	Ultra-low: <0.01, Very low: <0.2, Low:<0.4, Moderate:<0.6, Stable value xxx
Wear resistance	General, Abrasion, Adhesion, Corrosion, Fatigue, Impact, Fretting, Erosion, Cavitation
Corrosion resistance	General, Atmospheric, Oxidation, High Temperature, Water, Seawater, Acid Solution, Basic Solution, Other Chemical Agent
Thermal conduction	Barrier, Low, Moderate xxx W/mK, High
Thermal expansion	Low, Similar to the Substrate, High
Electrical performance	Dielectric, Semiconductor, Conductor, Superconductor
Magnetic Performance	Diamagnetic, Paramagnetic, Ferromagnetic
Biological Performance	Bioinert, Bioactive, Biocompatible
Toxicity	Nontoxic, Food Contact
Thickness	Very Thin: <1 um, Thin: 1~10 um, Moderate: 10~100 um, Thick: 100~500 um, Very Thick: >500 um
Cost	Low
Pollution	No, Low
Color	Gold, Silver, White, Gray, Black, Lustrous
Efficient	High Deposition Rate, Mass Production, Operating Convenience
Hardness	Harder than xxx MPa, Softer than xxx MPa, Little Harder than xxx MPa, Little Softer than xxx MPa
Toughness	High
Porosity	Low, High, Certain value xxx %

xxx means a specific value.

Finally, the remaining coatings will be evaluated and compared by weight point and reliability. Weight point (W) is the sum of product of weight value (k) and weight factor (w) for each requirement (Eq.3-1).

$$W = \sum_{i=1}^{n} (k_i \cdot w_i) \tag{3-1}$$

where n is the number of requirements, k_i is the weight value of requirement *i* and w_i is the weight factor of the requirement *i*.

Weight value *k* can be obtained by the following two rules:

- When the relevant coating property is expressed by a qualitative level, generally, the weight value is set as “excellent”=10, “good”=7.5, “fair”=5, “poor”=2.5, “very poor”=0. For the properties with opposite evolutions, the weight value equals to 10 or 0. For example, when there is a “Diamagnetic” magnetic performance requirement, the weight value of diamagnetic coatings is 10, while that of paramagnetic or ferromagnetic coatings is 0. For the properties with fuzzy evaluation, the weight value will be subjectively set. For example, when “gold” coatings are expected, the weight value can be set as “gold”=10, “yellow”, “bronze” or “copper”=6, “brown”=3, other color=0.
- When the relevant coating property is expressed by a quantitative range, the weight value is the result of Eq.3-2~ Eq.3-4. When a coating with a lower value of the relevant property (like friction reduction requirement) is better, Eq.3-2 will be used. When a coating with a higher value of the relevant property (like high hardness requirement) is better, Eq.3-3 will be used. When a coating with a certain value of the relevant property (like thermal expansion requirement) is expected, Eq.4-4 will be used.

$$k = f(x) = \begin{cases} 10, & x \le x_0 \\ 10 \cdot \dfrac{x_0}{x}, & x > x_0 \end{cases} \tag{3-2}$$

$$k = f(x) = \begin{cases} 10, & x \ge x_0 \\ 10 \cdot \dfrac{x}{x_0}, & x < x_0 \end{cases} \tag{3-3}$$

$$k = f(x) = \begin{cases} 10, & |x - x_0| \le t \\ 10 \cdot \dfrac{t}{|x - x_0|}, & |x - x_0| > t \end{cases} \tag{3-4}$$

where x_0 is the expected value of the relevant property, x is the value of the relevant property for a coating, *t* is a tolerance away from the certain value of the relevant property.

The weight factor reflects the importance of the relevant requirement. It can be chosen from 1 to 10 (1 — least important, 10 — most important). The weight factor of “Must be met” requirements is 10, and it cannot be changed. The weight factor of the requirements being automatically set equals to 5, and is adjustable.

Reliability is used based on some presumption due to the incompletion of coating information. The total reliability (*R*) is the product of the reliability for each requirement (*r*) (Eq.3-5).

$$R = \prod_{i=1}^{n} r_i \tag{3-5}$$

The reliability of each requirement (*r*) can be set as following:

- When the relevant coating property of a requirement is definitely provided, the reliability of the coating equals to 100%.

- When the relevant coating property for a requirement is not provided, but its parents, children or brothers are obtainable, the reliability of the coating will be decreased. For example, for a “abrasion” wear resistance requirement, if a coating has only “general” wear resistance information, then the reliability of the coating equals to 80%; if a coating has wear resistance information about other wear modes (like adhesion, fretting, erosion), the reliability of the coating equals to 50%.
- When the relevant coating property for a requirement is blank, the weight value will be set as a lower middle value, 3, and the reliability will be decreased to 30%.

Finally, all the remaining coatings are ranked according to the weight point considering all of the setting requirements. The first 10 coatings will be selected as candidates, and their reliability will be provided.

2.4 Return to the case study

Now, we return to the case study “piston rings in internal combustion engines” discussed in Chapter 2, and try to use the pre-selection tool to select the candidate coatings. Coatings have been widely used on piston rings in the industry. By appling the simple strategy, the coatings industrially used on piston rings can be rapidly found out, as shown in Figure 91.

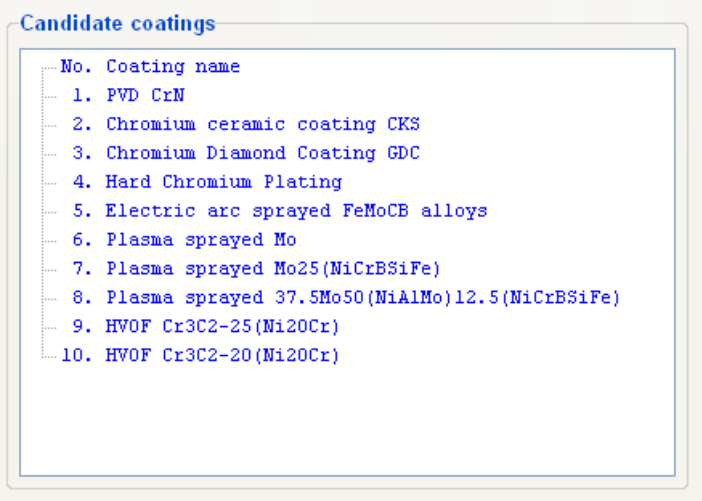

Figure 91: Coatings used for piston rings in the industry.

The candidate coatings can also be selected by the complex strategy. According to the analysis in Chapter 2, the maximal operating temperature of the piston ring is about 200ºC, the coating should have performance of adhesive wear resistance, low friction coefficient, oxidation corrosion resistance and low cost. The adhesive wear resistance is set as “Must be met”, other requirements are negotiable, and their weight factor is 8 or 5. The result of pre-selection is shown in Figure 92.

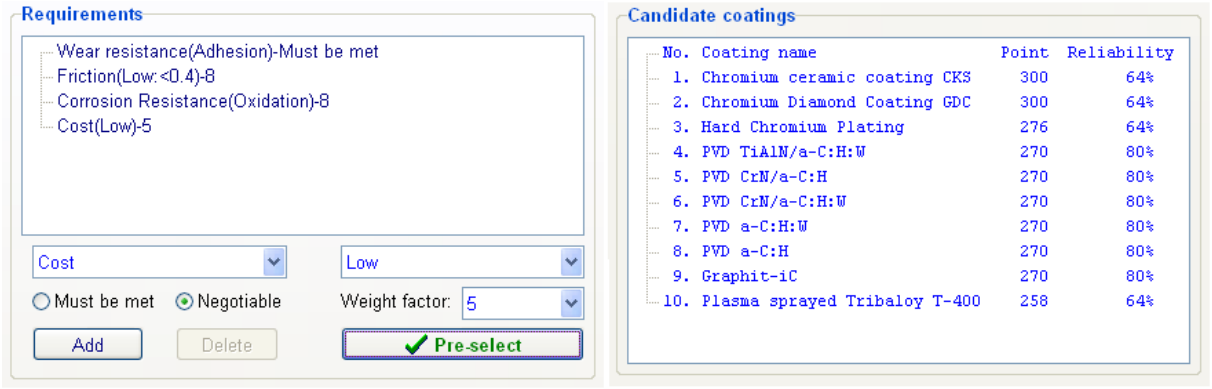

Figure 92: Candidate coatings for piston rings according to the relevant requirements.

In the results of Figure 91 and Figure 92, the search of the former is simple and rapid, and there are some successful examples about the use of the candidate coatings. However, the evaluation and comparison of the candidate coatings are unavailable, so it is unknow which one is better for a given engine. Especially, when the count of the coatings used in similar applications is very large, the situation is more complicated. The latter provides evaluation and comparison for the candidate coatings by weight point and reliability, and for a given engine, the requirements can be appropriately adjusted. Although some of the candidate coatings have never been used in similar applications, they may be able to bring us a pleasant surprise.

3. Conclusions

In this chapter, a pre-selection tool is developed. During the development, the requirements (including the tribological requirements, non-tribological requirements and non-functional requirements) and limits from the application (substrate, counterpart and running conditions) are comprehensively considered. The relationships between the requirements and limits and the characteristics of coatings (the deposition method and the coating material) are also discussed. In order to match the requirements and limits with the characteristics of coatings, 13 criteria are used.

In the database, the properties of coatings and deposition methods are expressed by qualitative evaluation, quantitative range, or qualitative evaluation plus quantitative range due to their dependence on deposition parameters and running conditions and the incompletion of coating information in literature. In the selection process, two strategies are used. One is a rapid search for all the coatings used in similar industrial application, and the other is a complex strategy combining the exclusion of the impossible coatings and the evaluation of the remaining coatings by weight point and reliability. The requirements are divided into “Must be met” and “Negotiable”, and the importance of each requirement is expressed by a weight factor. The candidate coatings are the first 10 ranked by their weight point.

Finally, the pre-selection tool is used to select candidate coatings for the case study “piston rings” discussed in Chapter 2.

CHAPTER 4

EXPERIMENTS AND MATERIALS UNDER INVESTIGATION

CHAPTER 4: EXPERIMENTS AND MATERIALS UNDER INVESTIGATION

CHAPTER 4: EXPERIMENTS AND MATERIALS UNDER INVESTIGATION

This chapter introduces the materials under investigation, including the coatings, substrates and counterparts, and the experiments performed to evaluate the mechanical properties of the coatings and their tribological performance.

For a specific tribological application, several candidate coatings can be selected through the pre-selection tool. However, it is difficult to determine which coating is the optimum one, because the situations can be different between the application and the tests in literature. So, some experimental data are necessary to help to evaluate the candidate coatings. On the other side, some approaches with a view to comparing the candidate coatings or predicting their endurance need to be found from experimental investigations. Two kinds of experiments will be performed. One is that one coating is tested under different conditions to investigate the effect of running conditions on tribological performance of the coating. The other is that several coatings are tested under same given conditions to identify the relationship between the coating properties and the tribological performance.

1 Materials

In the experiments, two kinds of coatings will be used. One is a MoS_2 coating deposited by pressure spraying process, and it will be tested under three contact configurations to investigate the effect of running conditions on the tribological performance. The other kind of coatings is 5 commercial bonded solid lubricant coatings principally based on PTFE or MoS_2, and they will be investigated under given test conditions to identify the influence of coating properties on tribological performance.

1.1 Pressure sprayed MoS_2 coating

The pressure sprayed MoS_2 coating was deposited by the tribology group of AIST (Advanced Industrial Science and Technology) Tsukuba East in Japan, in collaboration with Dr. Takashi MURAKAMI.

1.1.1 Substrate material and pretreatment

For pressure sprayed MoS_2 coating, the substrates were made of SUS 316 (austenitic) stainless steel whose chemical composition and mechanical properties are respectively shown in

Table 29 and Table 30. The substrates were machined as two forms: one is a block with a dimension of 17 mm × 9 mm × 6 mm, and the other is a disk with a dimension of 100 mm × 100 mm × 5 mm, as shown in Figure 93. Before the deposition of MoS_2 coating, the surfaces of the substrates were polished with abrasive papers (grade 1000, 2400 and 4000) and then were cleaned in an ultra-sonic bath of acetone / benzene (50/50 mixture) (twice 10 minutes).

Table 29: Chemical composition of the materials.

Material	C	Cr	Ni	Mo	Si	Mn	P	S	Fe
SUS 316	0.06	18	12	2.5	-	-	-	-	Balance
30NiCrMo16	0.27-0.33	1.30-1.50	3.80-4.20	0.40-0.50	0.15-0.35	0.40-0.60	≤ 0.035	≤ 0.035	Balance
AISI 52100	1	1.5	-	-	-	-	-	-	Balance

Table 30: Mechanical properties of the materials.

Material	Elastic modulus (GPa)	Hardness (GPa)	Poisson's Ratio	Density (g/cm^3)
SUS 316	193	1.8	0.30	7.85
30NiCrMo16	183	3.3	0.29	-
AISI 52100	210	4.0	0.30	7.81

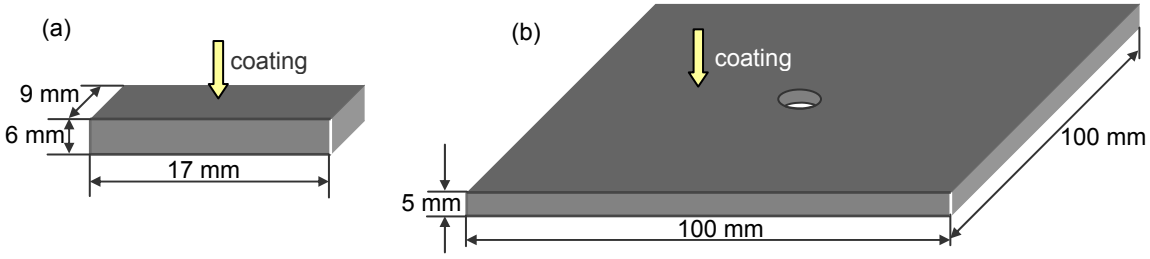

Figure 93: Substrates of pressure sprayed MoS_2 coating: (a) block, (b) disk.

1.1.2 Deposition process

The purity of MoS_2 powder used to spray is better than 98.5%, and the distribution of particle size is shown in Table 31. MoS_2 coating was deposited using a pressure spraying device, and the spraying process is shown in Figure 94. MoS_2 powder was put into the pipe and sprayed to the specimen surface under high pressure air (the air pressure was 0.8 MPa). The distance between the spray nozzle and the specimen surface was 10 mm and the deposition speed was about 10 mm²/s. During the spraying process, the specimen was horizontally moved in order to ensure a constant coating thickness on the whole specimen surface. The SEM micrograph of the coating is shown in Figure 95.

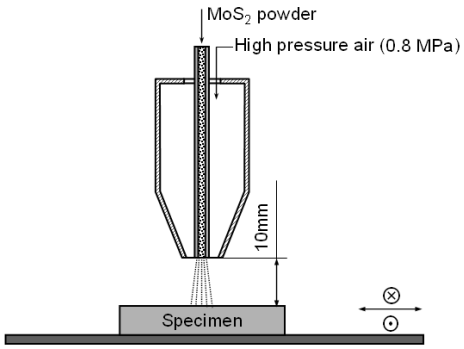

Figure 94: Pressure spraying process.

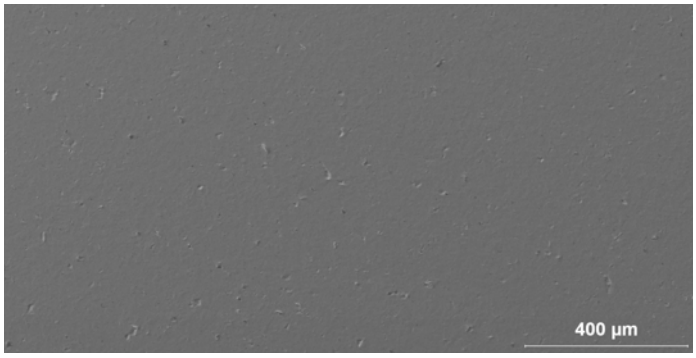

Figure 95: SEM micrograph of pressure sprayed MoS_2 coating.

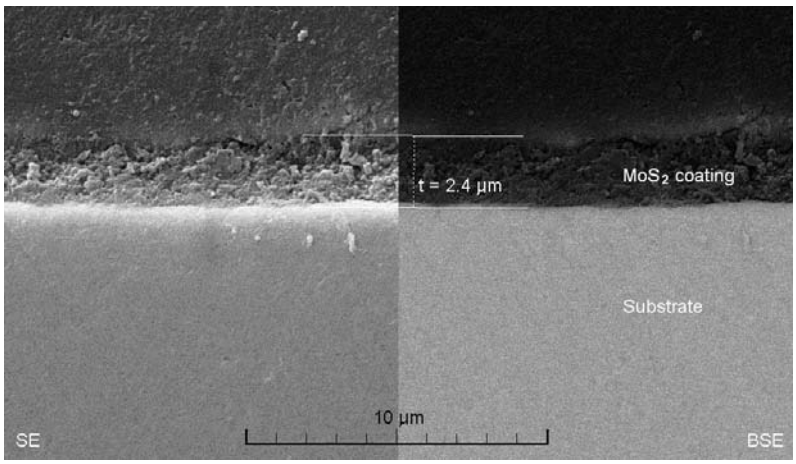

Figure 96: Cross-section of a coated specimen (SEM micrograph).

Table 31: Particle size distribution of MoS_2 powder.

Diameter of MoS_2 particle	<0.002μm	0.002 ~ 10.12 μm	>10.12 μm
Distribution of MoS_2 particle	17.2%	31.1%	51.1%

The thickness of the coating is about 2.4 μm according to the SEM micrograph of a polished cross-section, as shown in Figure 96. The topography of the coating was measured by a stylus profilometer, as shown in Figure 97, from which the roughness of the coated surface was obtained: arithmetic average roughness R_a = 0.08 μm, root mean squared roughness R_q = 0.14 μm and maximum height of the profile R_t = 2.93 μm.

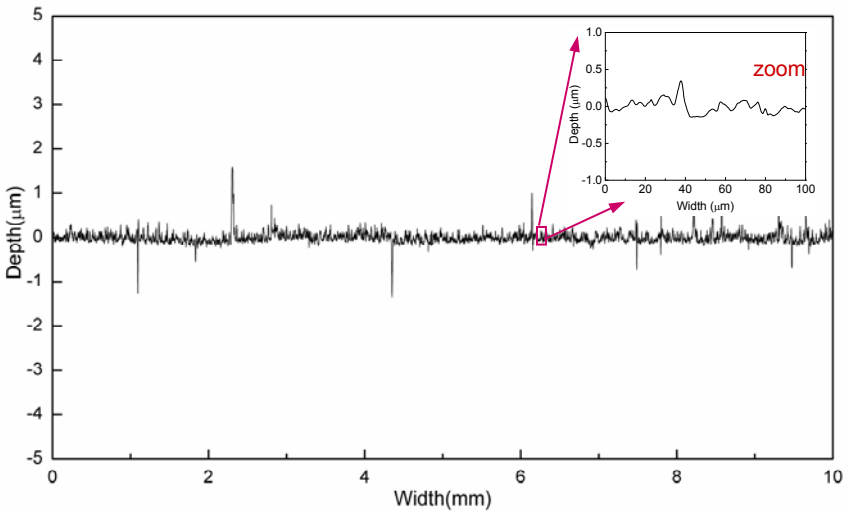

Figure 97: Topography measurement of MoS_2 coated specimen.

1.2 Bonded coatings

The experiments of several coatings under given test conditions were carried out on five commercial bonded solid lubricant coatings, which are principally based on PTFE or MoS_2 and organic or inorganic binding agent.

1.2.1 Substrate and pretreatment

The substrate, machined as blocks with a dimension of 20 mm × 12 mm × 10 mm, was made of 30NiCrMo16 steel, whose chemical composition and mechanical properties are shown in

Table 29 and Table 30. Before applying the bonded coatings, the substrate surfaces were thoroughly degreased, cleaned and roughened, in order to improve the adhesion of the bonded coatings.

1.2.2 Coatings preparation

Before being applied on substrate surfaces, the mixtures of the solid lubricants and the binding agents are in a liquid state. They were sprayed on the clean substrate surfaces by a sprayer from a distance of approximately 20 cm. The nozzle diameter was 0.8 mm and the feed pressure was 0.2 MPa. Then, thermosetting or air hardening was executed according to the type of binding agents. Some basic characteristics of the coatings are summarized in Table 32.

A stylus profilometer was employed to evaluate the roughness of the coatings. Each specimen was measured three times (the length of the surface profile is 1.5 mm), and the mean values of arithmetic

average roughness R_a of the 5 coatings is about 1~2 µm. The micrographs and EDX analysis of the 5 coatings are shown in Figure 98. The EDX spectra presented quite different composition even for the coatings including the same solid lubricant.

Table 32: Basic characteristics of the 5 bonded coatings.

Coating reference		K39	K15	K03	K06	U22
Based solid lubricant		PTFE	PTFE	PTFE	MoS_2	MoS_2
Binding agent		organic	organic	organic	organic	inorganic
Roughness	Ra (µm)	0.75±0.10	1.40±0.14	1.46±0.27	0.91±0.11	1.40±0.24
	Rt (µm)	4.11±0.33	8.65±0.29	7.71±0.54	5.21±0.46	8.40±1.47
	Rq (µm)	0.89±0.11	1.70±0.16	1.69±0.27	1.10±0.12	1.72±0.29
Color		black	black	black	gray-black	gray
Hardening process		thermosetting 15min. 230°C	air hardening 24 hours in air	thermosetting 60min. 160°C	thermosetting >30min. 180°C	air hardening 30min. in air
Recommended thickness (µm)		5~25	7~15	7~15	7~20	5~15
Service temperature (°C)		-40~230	-40~80	-40~180	-40~220	-180~450
Resistance to chemical agents	0,1 n hydrochloric acid	>1000 h	>24 h	>400 h	>100 h a, >200 h for b *	<24 h for a, <150 h for b *
	0.1 n caustic soda	>800 h	>500 h	>400 h	>400 h	<24 h for a, <150 h for b *
Anti-corrosion protection (with a 15 µm thick coating)	Salt Spray test	surface: Ri 0	>24 h for a, >120 h for b *	>400 h	>240 h	<12 h
	Resistance to distilled water	-	>300 h	>500 h	>500 h	<30 h

* a. bright steel, b. zinc-phosphated steel.

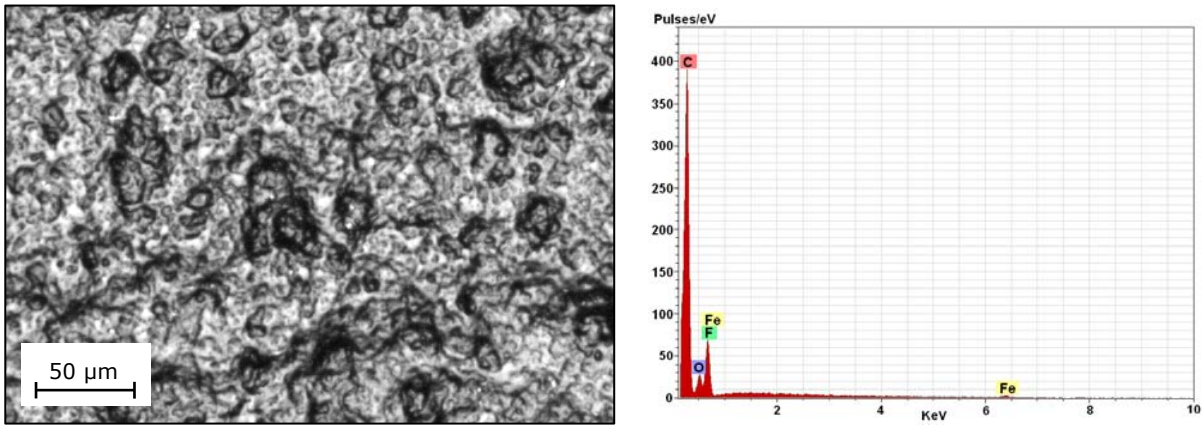

(a) K39

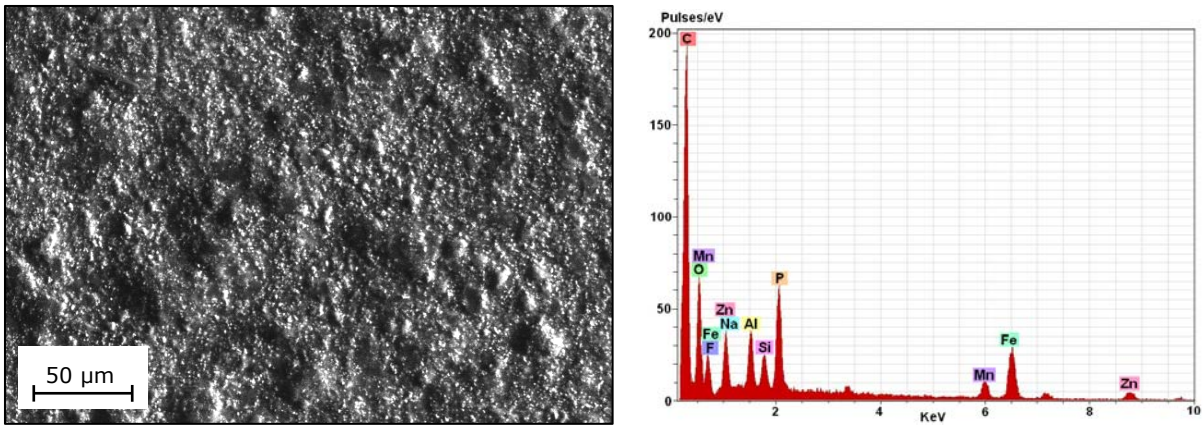

(b) K15

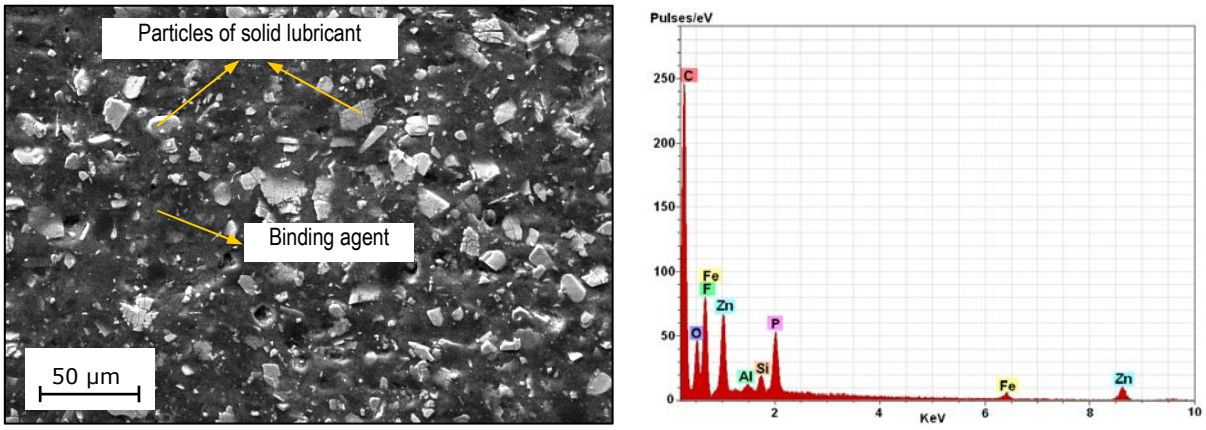

(c) K03

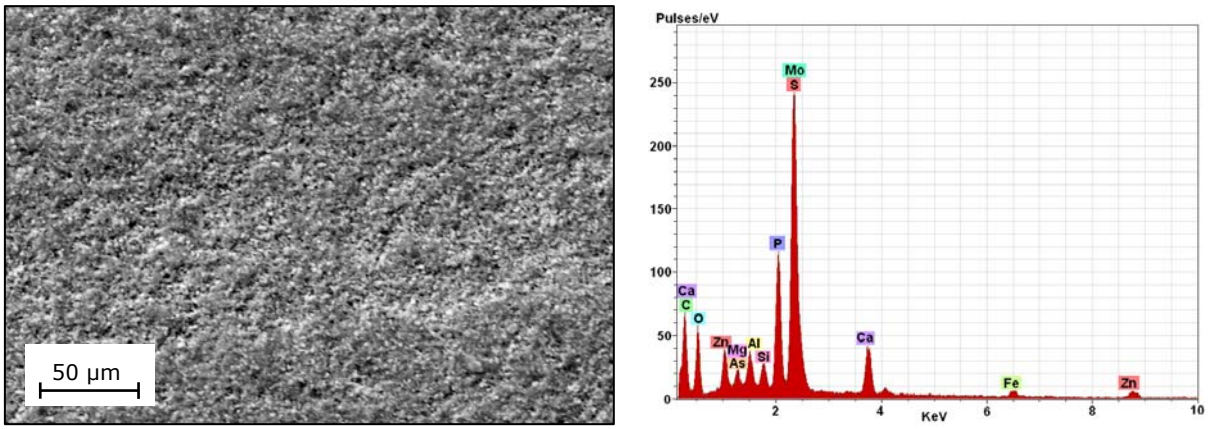

(d) K06

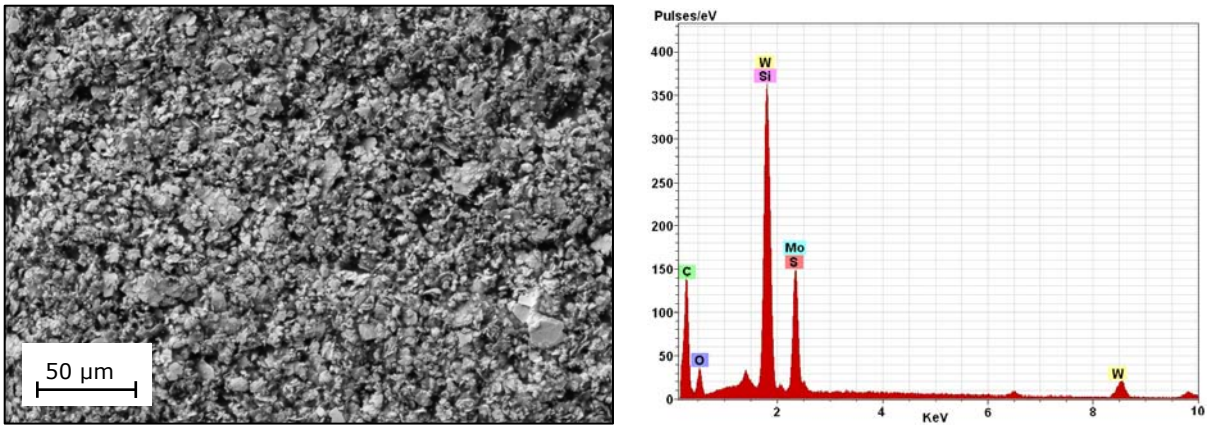

(e) U22

Figure 98: Micrographs and EDX spectra of the coatings.

1.3 Counterparts

In the experiments, 4 kinds of counterparts in different shapes or sizes (Figure 99) were used, and all of them were made of the same material, AISI 52100. Its high hardness leads to the fact that its wear is neglectable when it rubs against solid lubricant coatings. The chemical composition and mechanical properties of AISI 52100 are respectively shown in

Table 29 and Table 30.

The cylinder in Figure 99a will be used for the fretting test of the pressure sprayed MoS_2 coating. The cylinder in Figure 99b will be used for the fretting test of the 5 commercial bonded coatings. The ball in Figure 99c will be used for the fretting test of the pressure sprayed MoS_2 coating and the ball cratering tests of the 5 commercial bonded coatings. The ball in Figure 99d will be used for the unidirectional rotating sliding test of the pressure sprayed MoS_2 coating.

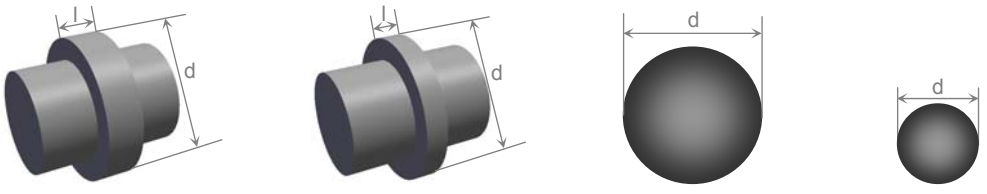

(a) (b) (c) (d)

Figure 99: Counterparts: (a) cylinder (d=20 mm, l=5 mm), (b) cylinder (d=20 mm, l=3 mm), (c) ball (d=25.4 mm), (d) ball (d=10mm).

2 Experiments

2.1 Fretting tests

2.1.1 Fretting rig

The fretting tests were carried out on a tension-compression hydraulic machine MTS®. The schematic outline of the contact on the machine is shown in Figure 100a, where the coated block specimen is mounted on a main shaft and moved up and down by a given small displacement amplitude δ^*, and rubbed against the stationary counterpart (ball or cylinder) under a normal load P. In the test process, displacement δ (measured by an extensometer), normal load P and tangential force Q are recorded, according to which the evolution of friction coefficient μ (the ratio of maximum tangential force to normal load in each cycle) with the cycles, the fretting loop Q-δ (Figure 101) and the fretting logs can be obtained. Because of the elastic deformation of the system and of the specimens, the actual displacement amplitude δ_0 is always smaller than the imposed displacement amplitude δ^*. The area of the quadrangle in Figure 101 is the frictional energy dissipated in the cycle, Ed.

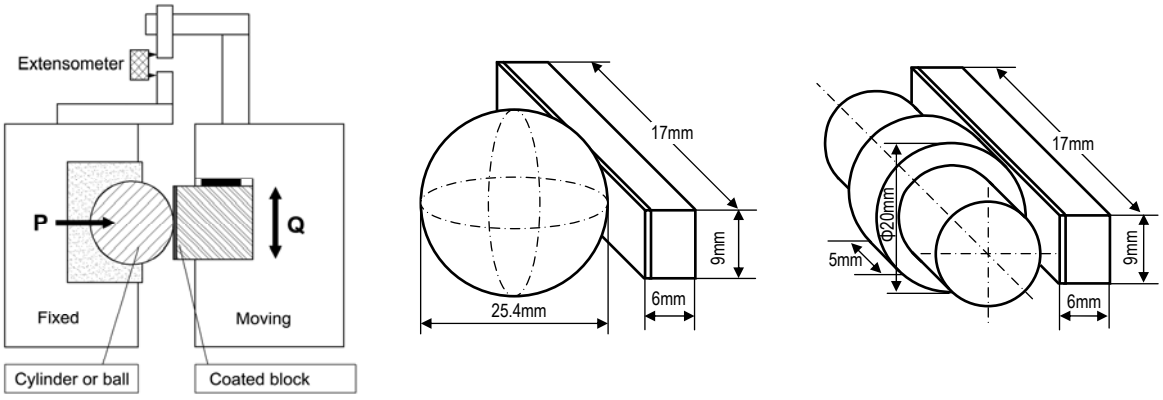

(a) Fretting rig (b) ball-on-flat (c) cylinder-on-flat

Figure 100: Fretting rig and contact configurations.

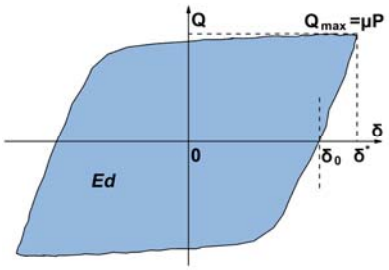

Figure 101: Fretting loop Q-δ curve.

2.1.2 Test conditions

➢ **Pressure sprayed MoS_2 coating**

The fretting tests of the pressure sprayed MoS_2 coating were carried out under two contact configuration: one is ball-on-flat (Figure 100b), and the other is cylinder-on-flat (cylinder: l=5 mm) (Figure 100c). All of the tests were performed in the laboratory atmosphere, and different normal loads *P* (from 100 N to 400 N for ball-on-flat and from 400 N to 1000 N for cylinder-on-flat) and displacement amplitudes (from ±5 μm to ±75 μm) were used. In order to investigate the friction reduction of pressure sprayed MoS_2 coating, the cylinder-on-flat fretting tests of uncoated substrate were also carried out. The main test conditions are shown in Table 33. Before tests, the surfaces of cylinders and balls were ultrasonically cleaned by acetone and ethanol, and the MoS_2 coated specimens were just wiped by napkins.

Table 33: Fretting test conditions for the pressure sprayed MoS_2 coating.

Contact type	Normal load P (N)	Displacement amplitude δ^* (μm)	Frequency (Hz)	Test duration (cycles)	Temperature (°C)	Relative humidity (%)
Cylinder-on-flat	400, 700, 1000	±5, ±25, ±40	5	25000	25 ± 5	35 ± 10
Ball-on-flat	100, 200, 400	±5, ±25, ±40, ±75	5	25000	25 ± 5	35 ± 10

Table 34: Hertzian contact pressures and contact size under cylinder-on-flat configuration.

Normal load P (N)	Maximum pressure p_0 (MPa)	Mean pressure p (MPa)	Contact semi-width a (μm)
400	528	415	96.4
700	699	549	127.5
1000	835	656	152.4

Table 35: Contact pressures and contact size under ball-on-flat configuration.

Normal load (N)	Hertzian theory			Press marks		
	Contact radius *a* (μm)	Mean pressure *p* (MPa)	Maximum pressure p_0 (MPa)	Contact radius *a* (μm)	Mean pressure *p* (MPa)	Maximum pressure p_0 (MPa)
100	205.6	753	1130	264	457.8	960
200	259.0	949	1423	312	654.6	960
400	326.4	1195	1793	407	768.1	960

For the cylinder-on-flat configuration, the contact pressure and contact size were calculated by Hertzian theory ignoring the influence of the coating due to its small thickness in comparison to the contact size, as shown in Table 34. Due to the loading system of the test rig and the counterpart's

geometry size, the ball-on-flat configuration resulted in high contact pressure. The contact pressure by Hertzian theory exceeded the critical stress of plastic deformation of the substrate (σ = 1.6Y = 1.6H/3 =960 MPa), so the result of Hertzian theory cannot be used. In order to get the actual contact area, the surfaces were contacted under the normal load without relative movement for half an hour, and then the size of the press mark was measured through an optical microscope. The mean contact pressure can be obtained by dividing the normal load by the contact area, and the critical stress of plastic deformation is looked as the maximal contact pressure, as shown in Table 35.

- **Five bonded coatings**

The five bonded coatings were tested under the same fretting conditions and contact configuration: cylinder-on-flat (the cylinder with a width of 3 mm is shown in Figure 99b). All the 5 coatings were tested with displacement amplitude of ±10 μm under four normal loads, and the coatings K03, K06 and K39, which presented good endurance, were also tested with displacement amplitude of ±18 μm and ±25 μm under 2 normal loads (300 N and 600 N). The detailed conditions are listed in Table 36. Before the tests, the cylinder was ultrasonically cleaned in an acetone bath. The Hertzian contact pressure and contact size were also calculated ignoring the influence of the coatings, as shown in Table 37.

Table 36: Fretting test conditions for the five bonded coatings.

Coating	Normal load P (N)	Displacement amplitude δ^* (μm)	Frequency (Hz)	Test duration (cycles)	Temperature (°C)	Relative humidity (%)
K03, K06, K15, K39, U22	300, 450, 600, 750	±10	5	500000 or until coating worn through	20 ± 5	30 ± 10
K03, K06, K39	300, 600	±18, ±25	5	500000 or until coating worn through	20 ± 5	30 ± 10

Table 37: Hertzian contact pressures and contact radius.

Normal load, P (N)	Maximum pressure, p_0 (MPa)	Mean pressure, p (MPa)	Contact radius, a (μm)
300	598	469	106.5
450	732	575	130.5
600	845	664	150.7
750	945	742	168.4

2.2 Unidirectional rotating sliding tests

2.2.1 Tribometer

The unidirectional rotating sliding tests were carried out under a ball-on-disk contact configuration (the diameter of the ball is 10 mm, Figure 102a), and the tribometer is schematically shown in Figure 102b. The coated disk specimen was mounted on a shaft, which rotated at the speed n during a test. The ball specimen was fixed in a holder and contacted the disk under a normal load P. The distance between the ball and the center of the disk R can be changed. Then, the combination of rotating speed n and distance R can result in different relative sliding speed. During the tests, the tangential force was recorded.

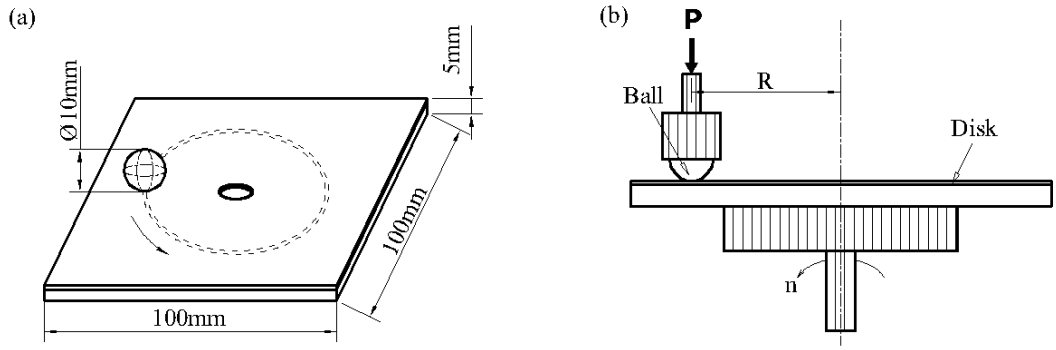

Figure 102: (a) Ball-on-disk contact; (b) unidirectional rotating sliding tribometer.

2.2.2 Test conditions

The sliding tests were also performed under the laboratory atmosphere, and the detailed conditions are listed in Table 38. The used normal loads were very low and the corresponding Hertzian contact pressure is shown in Table 39. In the tests, the rotating speed of the shaft was kept constant (60 rpm), and the distance *R* was changed from 15 mm to 45 mm. The cleaning of specimens and the analysis of wear scars were the same as in the fretting tests.

Table 38: Sliding test conditions.

Normal load *P* (N)	Rotating speed *n* (rpm)	Track radius *R* (mm)	Sliding speed (m/s)	Test duration (cycles)	Temperature (°C)	Relative humidity (%)
0.52,1.03,3.63, 4.64, 6.22	60	15,20,25,30, 35,40,45	0.09,0.13,0.16,0.19, 0.22,0.25,0.28	Until the failure of coatings	25 ± 5	35 ± 10

Table 39: Hertzian contact pressures and contact radius.

Normal load *P* (N)	Maximum pressure p_0 (MPa)	Mean pressure *p* (MPa)	Contact radius *a* (μm)
0.52	364	242	26.1
1.03	458	305	32.8
3.63	696	464	49.9
4.64	756	504	54.2
6.22	833	555	59.7

2.3 Ball cratering tests

Ball cratering test is a simple technique to estimate the abrasion resistance and the thickness of coatings. Its basic principle is shown in Figure 103a, where the ball is rotated against the coated specimen under a normal load, and during the test, abrasive slurry can be fed into the wearing contact. A crater will be formed on the specimen, and the abrasion resistance of coatings can be assessed by comparing the size of the craters. Additionally, once a coating is worn through, its thickness can be easily obtained by Eq.4-1.

$$thickness = \frac{x \cdot y}{\phi_{ball}} \qquad (4\text{-}1)$$

The test rig was Plint TE 66 Micro-Scale Abrasion Tester, as shown in Figure 103b. The ball is clamped between two coaxial shafts, one of which is driven by a variable speed dc geared motor. The rotating speed can be changed from 30 rpm to 150 rpm, and the load is in the range of 0.05 N ~ 5 N.

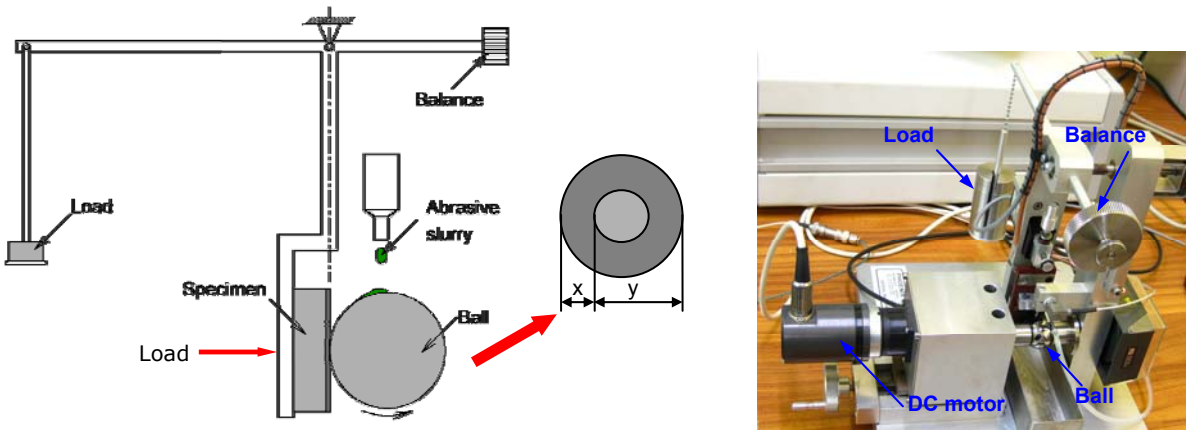

(a) (b)

Figure 103: (a) Principle of ball cratering test, (b) Plint TE 66 Micro-Scale Abrasion Tester.

In the tests, AISI 52100 balls with a diameter of 25.4 mm were used as counterparts (Figure 99c). Due to different objectives, two groups of test parameters were used (Table 40). In order to accelerate the worn through process, water based slurry with 3 μm diamond particles was used in the tests of the coating K39, which has excellent wear resistance.

Table 40: Test conditions of ball cratering.

Aim of the test	Load	Speed	Time	Abrasive slurry
Comparing wear resistance	1 N	60 rpm	1, 2, 5, 10, 30 minutes	Dry friction
Estimating coating thickness	5 N	150 rpm	Until coatings were worn through	Water based slurry with 3 μm diamond particles for K39, dry friction for the other coatings

2.4 Scratch tests

The ductility, cohesion and bonding strength of the coatings were investigated by a scratcher (developed by LTDS), whose platform can be inclined of a small angle with the horizontal direction, in order to simulate a gradually increasing normal load. In the tests, the coated specimens were fixed on the platform, which was slightly inclined of an angle, α, and an indenter was adjusted to contact with the specimens, then the platform horizontally moved 3 mm at a speed of 0.1 mm/s towards the indenter. During the movement of the platform, the depth of the indenter penetrating into the coated specimens gradually increased, and scratch tracks were formed on the coating surfaces (Figure 104). According to the features of the tracks and the correlative normal loads, the ductility, cohesion and bonding strength of the coatings can be assessed.

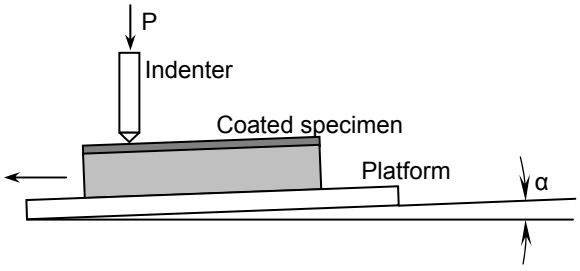

Figure 104: Sketch of scratch tests.

2.5 Nanoindentation tests

In order to determine the mechanical properties of the coatings, nanoindentation tests were performed using the continuous stiffness measurement method with a Nanoindenter XP® equipped with a Berkovich diamond tip (three-side pyramid with an angle of 115.12° between edges). This method consists in superimposing a small displacement oscillation (3 nm, small enough to generate only an elastic strain) at a given frequency during the indentation test (32 Hz). So, the sample endures small loading–unloading cycles. Mechanical properties (hardness, H, and reduced elastic modulus, E^*) are obtained continuously along the whole indentation period by simultaneous measurement of the normal force and the contact stiffness [273]. The maximal applied load was 450 mN, at a constant strain rate, $F'/F = 3\times10^{-2}$ s^{-1}. Seven indentations were performed on each coating with two load/unload cycles for each indentation. Figure 105 shows a typical load-displacement indentation curve.

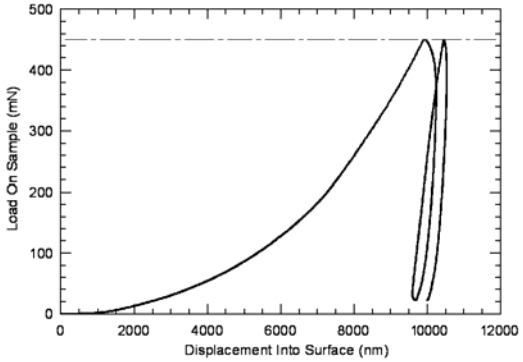

Figure 105: Typical load-displacement indentation curve.

CHAPTER 5

EFFECT OF TEST CONDITIONS ON TRIBOLOGICAL PERFORMANCE OF COATINGS: EXTENSION OF THE DISSIPATED ENERGY APPROACH

CHAPTER 5: EFFECT OF TEST CONDITIONS ON TRIBOLOGICAL PERFORMANCE OF COATINGS: EXTENSION OF THE DISSIPATED ENERGY APPROACH

CHAPTER 5: EFFECT OF TEST CONDITIONS ON TRIBOLOGICAL PERFORMANCE OF COATINGS: EXTENSION OF THE DISSIPATED ENERGY APPROACH

This chapter investigates the effect of test conditions on tribological performance of pressure sprayed MoS_2 coatings. The experiments include ball-on-flat fretting, cylinder-on-flat fretting and ball-on-disk sliding contacts. The effects of contact geometry, kinematics, normal load, displacement amplitude and sliding speed on tribological behavior are discussed. At last, a dissipated energy approach is used to predict the coating lifetime.

1 Tribological behavior

1.1 Evolution of friction coefficient

1.1.1 Fretting tests of uncoated substrate

In order to compare the friction reduction effect of MoS_2 coating, fretting behavior of uncoated substrate under cylinder-on-flat contact has been tested. The evolution of friction coefficient with the number of cycles presented three typical models depending on the test parameters.

For the small displacement amplitude of ±5 µm, the fretting loops of first cycles were quadrangle shapes, and the friction coefficient was low due to the adsorption film or contamination on the surface. Then, the fretting loops gradually transformed to close linear in 50 cycles, and this shape was kept to the end of the test. At the same time, the friction force kept a stable value, depending on the normal load, as shown in Figure 106.

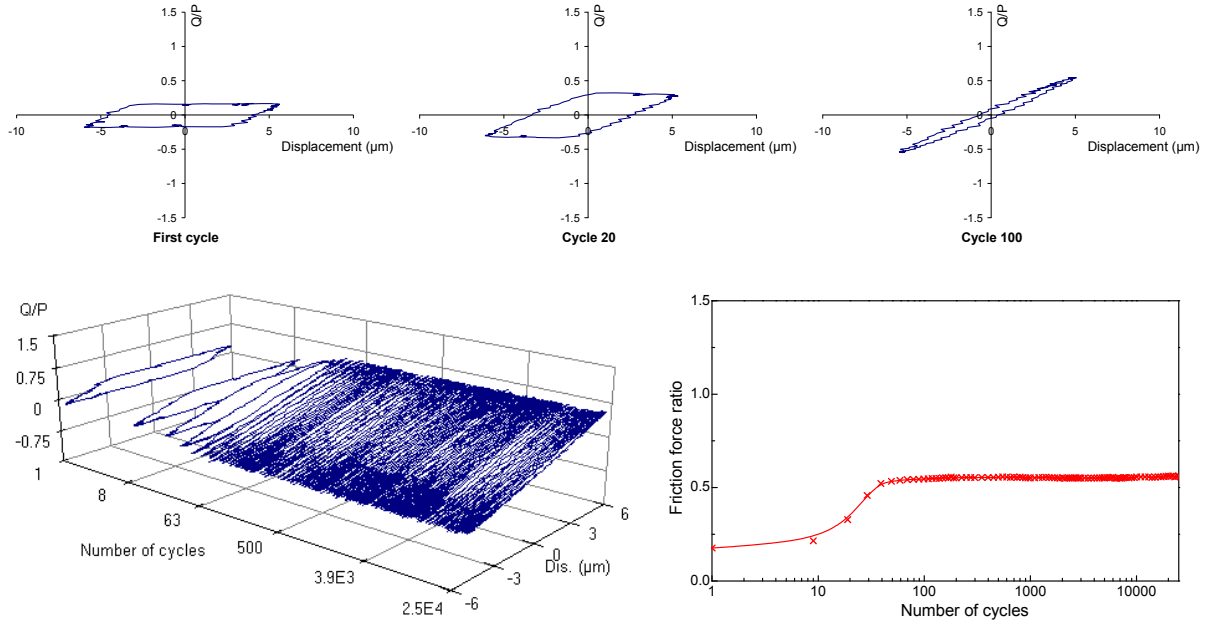

Figure 106: Fretting loops and the evolution of friction force ratio under ±5 µm, 700 N.

For the moderate displacement amplitude of ±25 μm and high normal loads (*P*=700 N, 1000 N), the evolution of fretting loops presented large fluctuation, from quadrangle to ellipse, to quadrangle, and the friction coefficient was also unstable, which is the typical characteristic of the mixed slip regime, as shown in Figure 107.

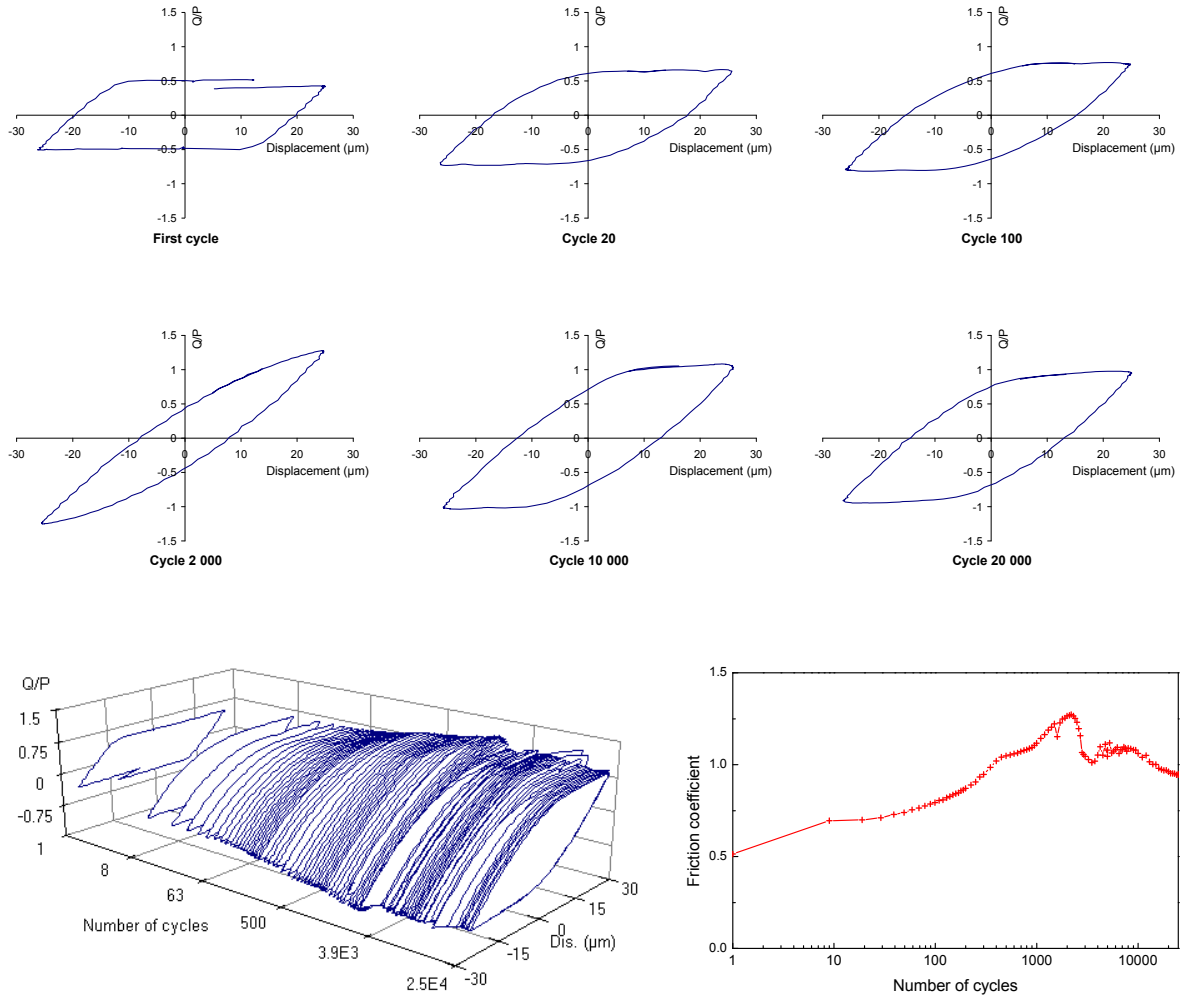

Figure 107: Fretting loops and the evolution of friction coefficient under ±25 μm, 1000 N.

When displacement amplitude continued increasing to ±40 μm, fretting loops kept quadrangle shapes during the whole test duration, as shown in Figure 108. In the first cycles, the friction coefficient had a low value, then it rapidly increased to the largest value in 20 cycles, and in 100 cycles it decreased to a stable value, about 0.8~1.0.

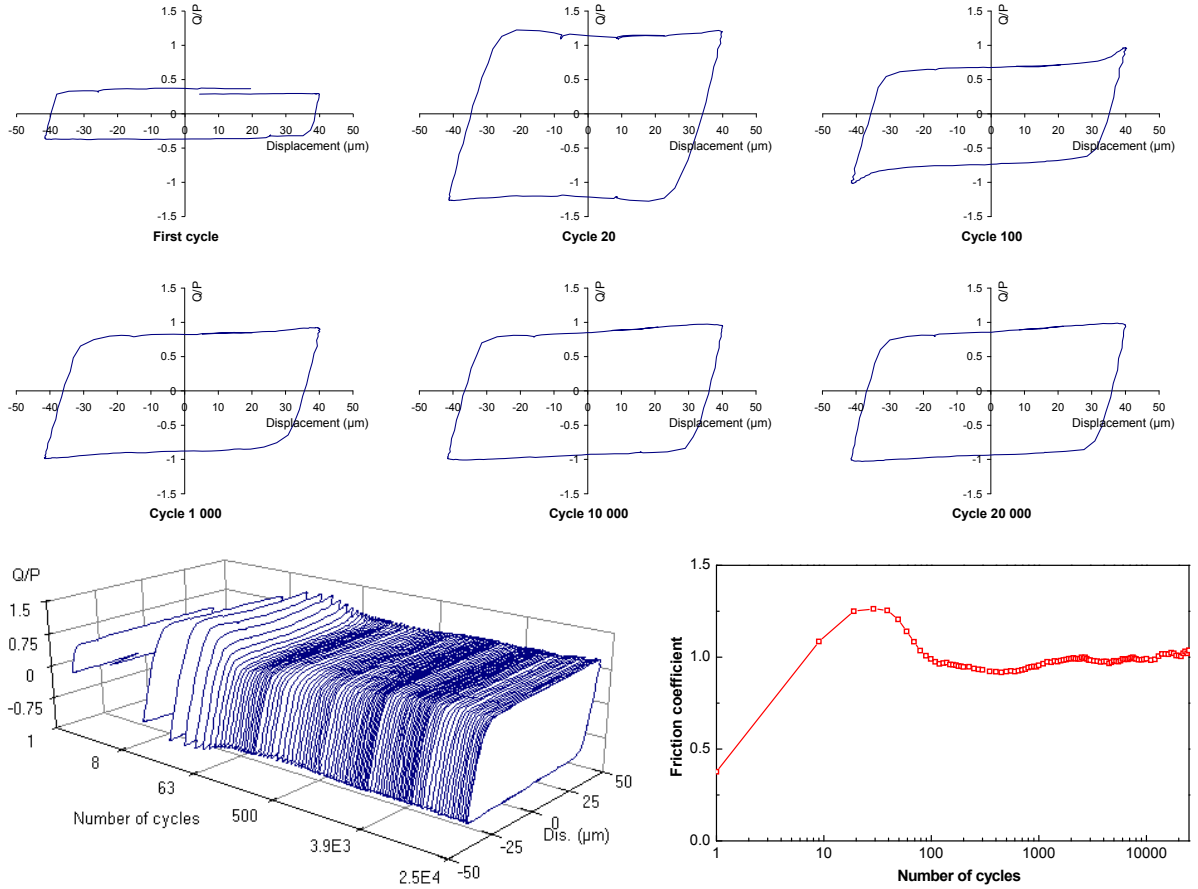

Figure 108: Fretting loops and the evolution of friction coefficient under ±40 µm, 400 N.

The three models respectively exhibited the characteristics of different fretting regimes, so we can obtain the running condition fretting map of uncoated substrate, as shown in Figure 109. The change of fretting regimes mainly depended on the displacement amplitude.

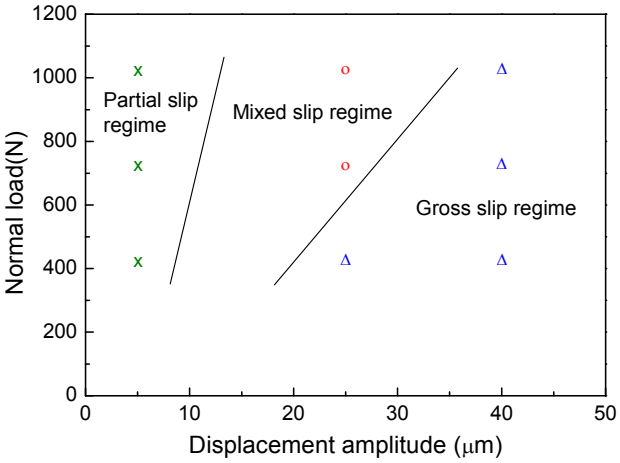

Figure 109: Running condition fretting map for the tests of uncoated substrate.

1.1.2 Fretting tests of MoS_2 coating

■ **Cylinder-on-flat contact**

Under cylinder-on-flat contact, the fretting tests of MoS_2 coating were carried out with the same test parameters as those of uncoated substrate, the evolution of friction coefficient presented two typical models.

For the low displacement amplitude of ±5 μm and the high normal load of 1000 N, the fretting loops changed from quadrangles to ellipses, to close linear, as shown in Figure 110. The friction force ratio was low, about 0.1 to 0.2, in the quadrangle loops, and it slowly increased in ellipse loops, then in linear loops it kept relatively stable values, which were close to the values of uncoated substrate.

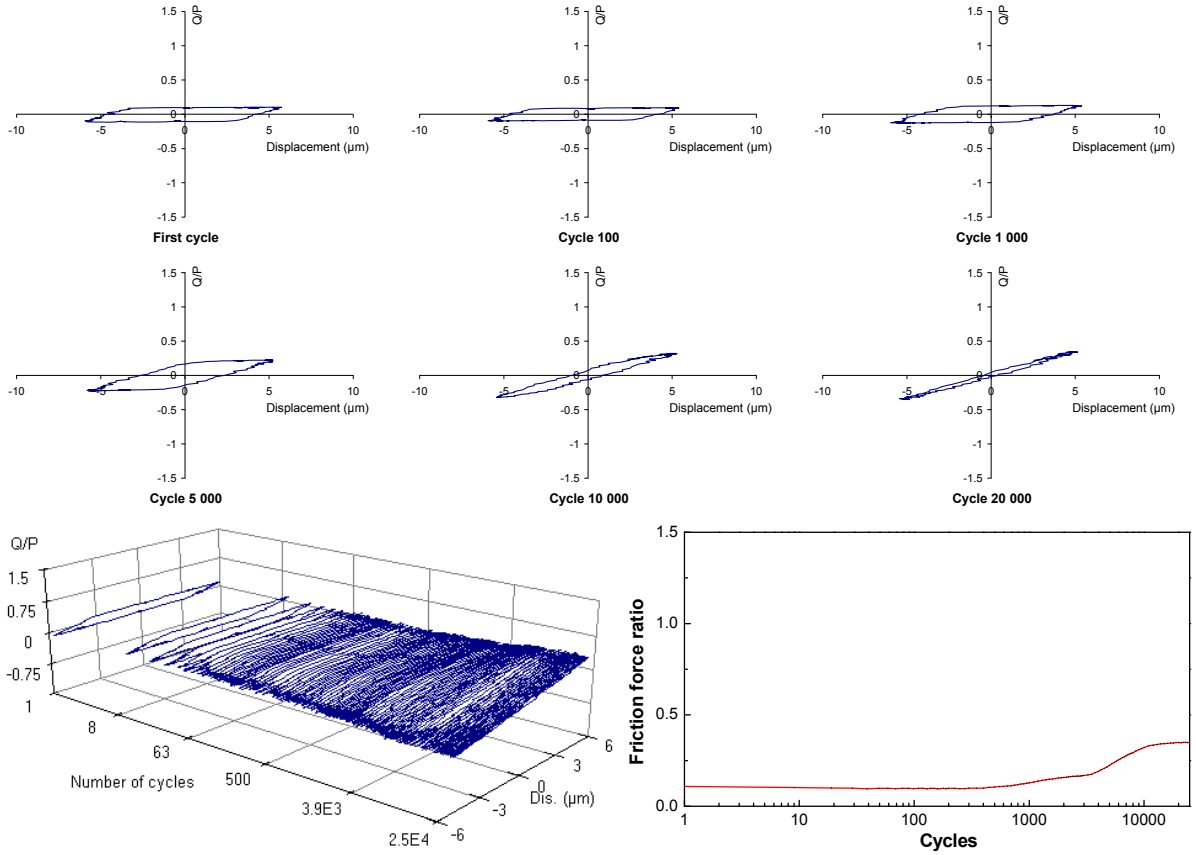

Figure 110: Fretting loops and the evolution of friction force ratio under ±5 μm, 1000 N.

With the increase of displacement amplitude, all of the fretting loops kept quadrangles, and the evolution of friction coefficient included three obvious phases, as shown in Figure 111. In phase I, the MoS_2 coating separated the direct contact of two metal surfaces and formed a low shear strength transfer film on the counterface, which reduced friction coefficient to a very low value, about 0.1 to 0.2. With the degradation of MoS_2 coating, in phase II, friction coefficient rapidly increased. After the coating was completely removed, friction coefficient remained at a high level, as shown in phase III, the values were very close to those of the uncoated substrate under same test parameters.

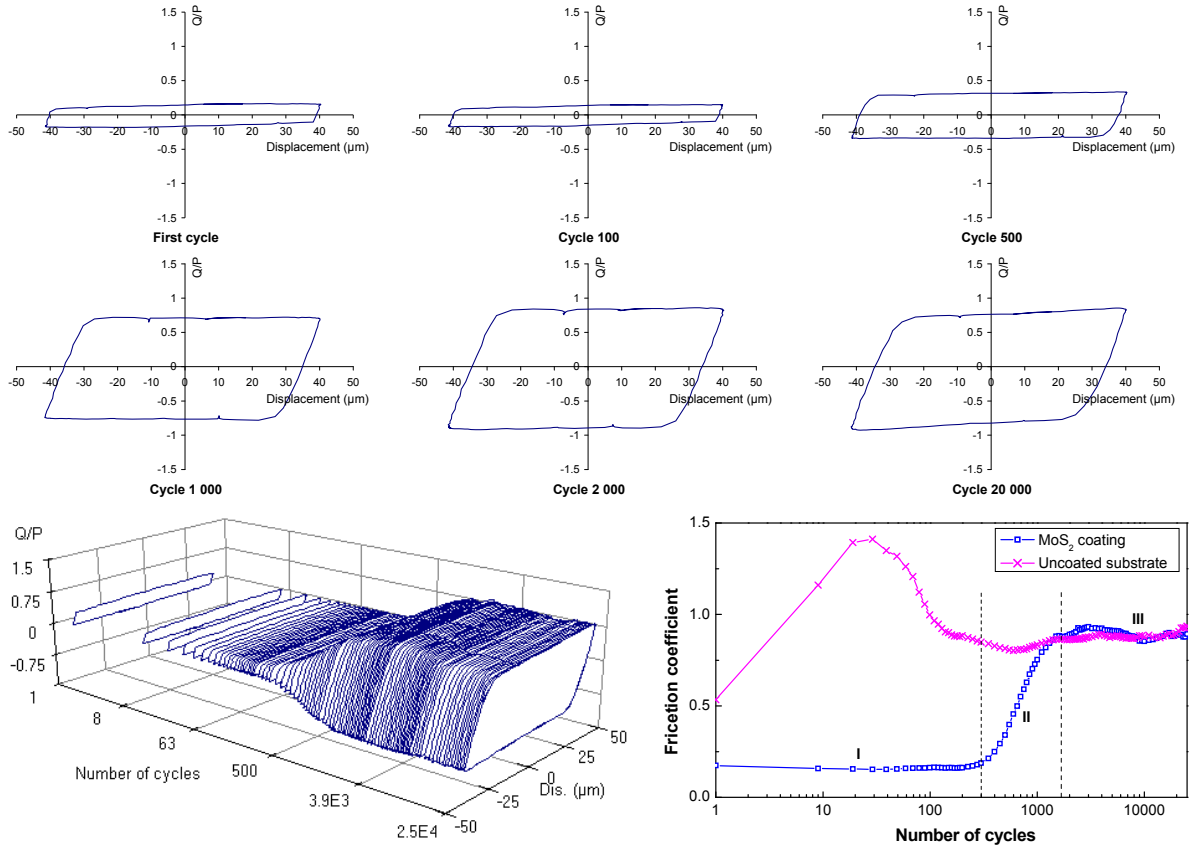

Figure 111: Fretting loops and evolution of friction coefficient under ±40 μm, 700 N.

For the MoS_2 coating, there were only two fretting regimes in the running condition fretting map Figure 112: mixed slip regime and gross slip regime, the partial slip regime disappeared under our test conditions because the low friction of MoS_2 coating promoted the relative slip. Figure 113 shows the change of running condition fretting map caused by the MoS_2 coating.

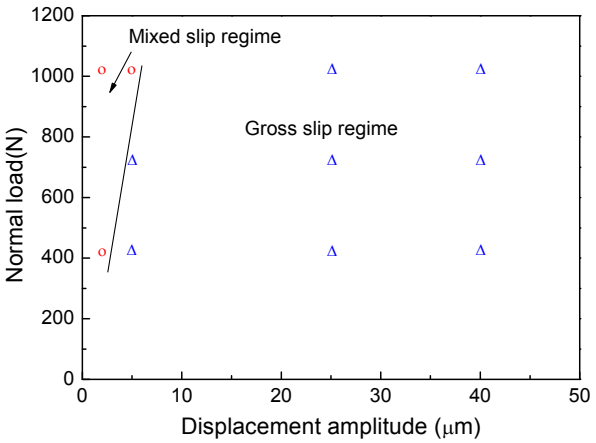

Figure 112: Running condition fretting map for the tests of MoS_2 coating.

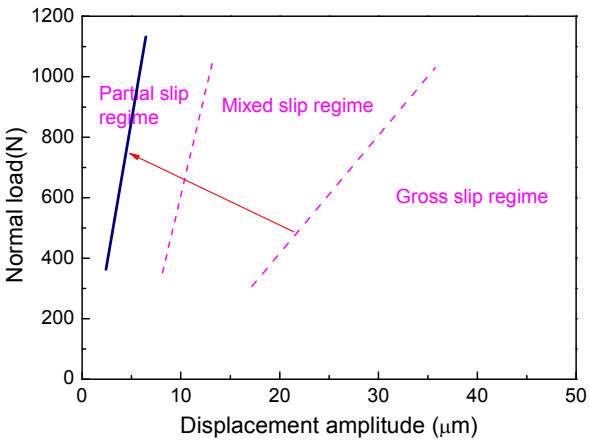

Figure 113: Comparison of running condition fretting maps for the tests with and without the MoS_2 coating.

■ Ball-on-flat contact

Under the contact of ball-on-flat, the evolutions of friction coefficient were similar to that under the cylinder-on-flat contact. The evolution process of friction coefficient also included three phases: low friction phase, rapidly increasing phase and stable high friction phase.

On the other hand, there were some differences in the evolution of friction coefficient between the two configurations. For the tests with same displacement amplitude, the initial friction coefficient was higher and the number of cycles with low friction was larger under the ball-on-flat contact (Figure 114).

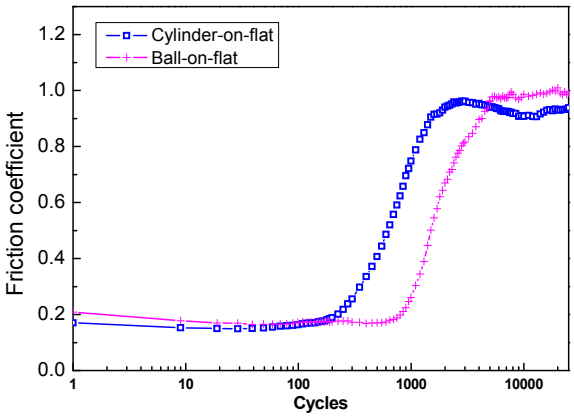

Figure 114: Comparison of friction coefficient under two contact configurations (the values of friction coefficient are the mean of the tests with a displacement amplitude of ±40 µm).

1.1.3 Ball-on-disk sliding tests of MoS_2 coating

Figure 115a shows the typical evolutions of friction coefficient under ball-on-disk sliding tests, which also include three phases:

• In phase I, there was a low friction coefficient due to the low shear strength of the transfer film. When the normal load was low, at first the friction coefficient slowly increased (phase I_A), then it reached a steady plateau (phase I_B), where the formation of transfer film and debris was probably in a balanced state. When the normal load was high, the phase I was very short because of the rapid wear of the coating.

• With the degradation process of MoS_2 coating, in phase II, friction coefficient rapidly increased. Comparing Figure 115a and Figure 115b, the climbing slope of friction coefficient was steeper in sliding test because the centrifugal force facilitated the ejection of debris, while, in fretting tests, debris stayed in the contact area as “third body” playing an important role for the evolution of friction.

• At last, the coating was completely removed, and the friction coefficient reached a high value, as shown in phase III.

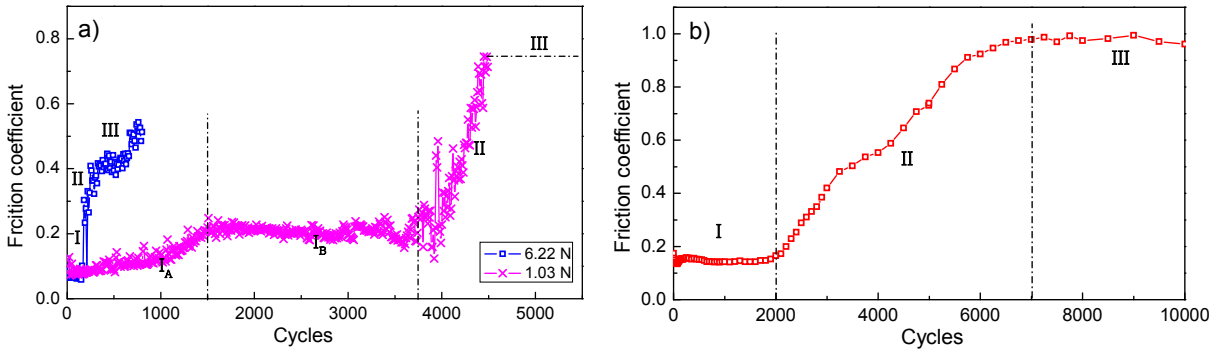

Figure 115: Evolutions of friction coefficient: a) ball-on-disk sliding tests (v=0.19 m/s), b) ball-on-flat fretting test (200 N, ±25 µm).

In fact, for the MoS_2 coating under any contact configuration, the evolutions of friction coefficient included three phases: the friction reduction of MoS_2 coating, the degradation process of the coating

and direct contact of two metal surfaces. However, the detail of each phase, including the value of friction coefficient and the number of cycles in each phase, depended on the specific contact configuration and test parameters.

1.2 Effect of test parameters on friction coefficient

1.2.1 Contact pressure

No matter what is the contact configuration, for the pressure sprayed MoS_2 coating, the friction coefficient always decreased with the increase of normal load, as shown in Figure 116. In fact, for thin soft films, this relationship has been validated and explained by several researchers [70, 71, 75], as the description in Eq.1-7.

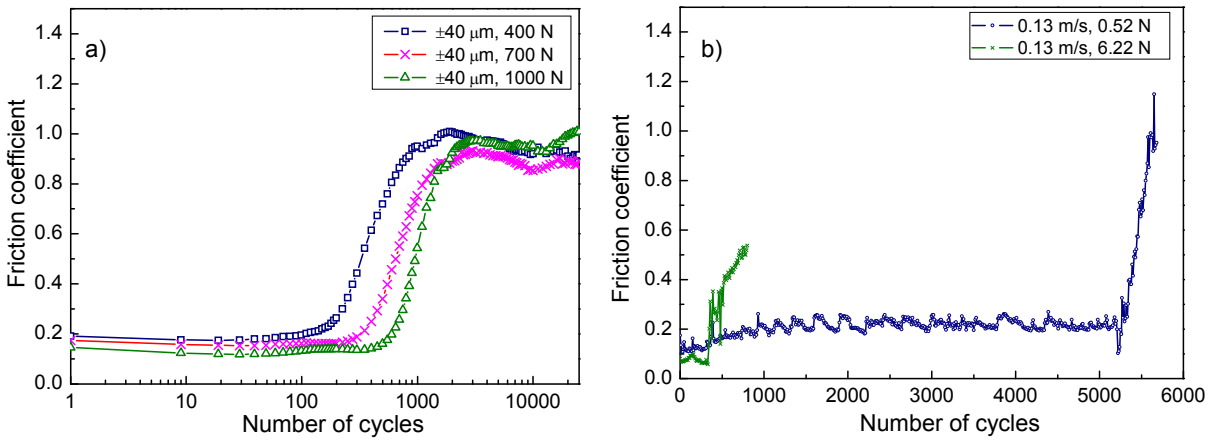

Figure 116: Effect of normal load on friction coefficient: a) cylinder-on-flat fretting, b) ball-on-disk sliding.

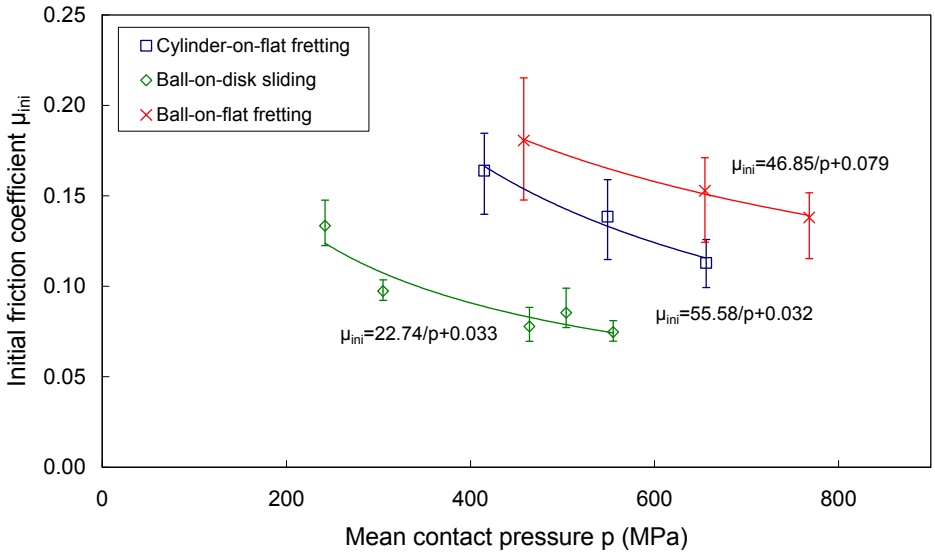

Figure 117: Evolution of initial friction coefficient with mean Hertzian contact pressure.

For the three test configurations, the evolution of initial friction coefficient (the mean value under all displacement amplitudes or sliding speeds for a same normal load) with the mean contact pressure is shown in Figure 117. The values of α in cylinder-on-flat fretting tests and ball-on-disk sliding tests are close, about 0.032~0.033, which is the limit value of friction coefficient under high contact pressure. However, in ball-on-flat fretting tests, it is about 0.079. The values of s_0 are different in three tests: 22.7 for ball-on-disk sliding tests, 55.6 for cylinder-on-flat fretting tests and 46.9 for ball-on-flat fretting

tests. This result is incompatible with the viewpoint that s_0 and α are material constants, which can be attributed to the following reasons.

In ball-on-disk sliding tests, the higher sliding speed than in fretting tests could promote faster formation of transfer film on the counterface, which induced the lowest initial friction coefficient in the three test configurations. Figure 118a shows the wear track on the ball surface, and MoS_2 was found in the EDX analysis of the circle area (Figure 118b), i.e., there is an obvious transfer film.

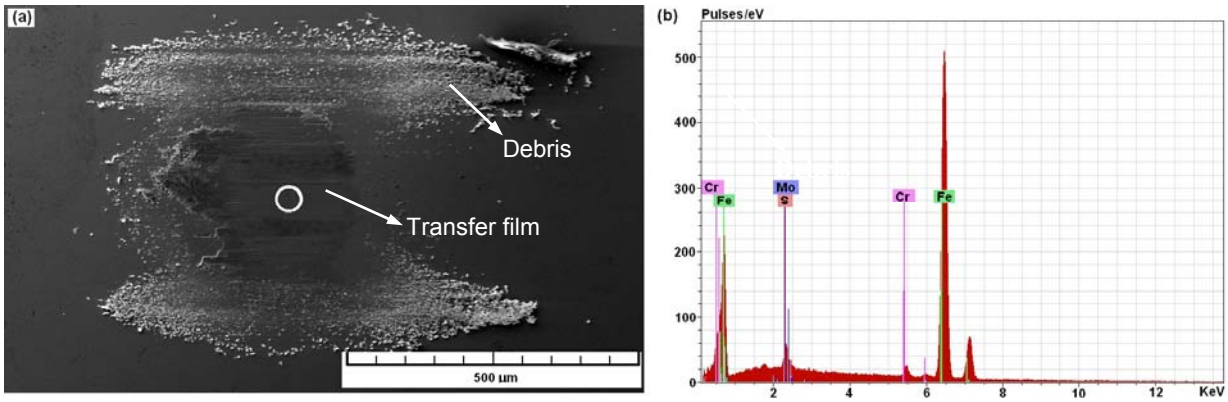

Figure 118: (a) SEM micrograph of wear track of the ball under conditions: 1.03 N, 0.14 m/s (stopped at 2000 cycles); (b) EDX spectrum of wear track (the area in the circle).

Figure 119 shows the wear track of MoS_2 coating and its profile under cylinder-on-flat contact with δ^*=±5 µm and P=1000 N, where there are only some pressurized marks, and the substrate was not reached. From the wear scar under ball-on-flat contact with small displacement amplitude (Figure 120), there is a stick region unworn through in the center part. However, according to the profile, the depth of wear scar in the center part exceeds the coating thickness, which indicates an obvious plastic deformation in the substrate under the high contact pressures. So, the increase of contact area due to plastic deformation of the substrate may be the reason why there are high s_0, α and friction coefficient in ball-on-flat tests.

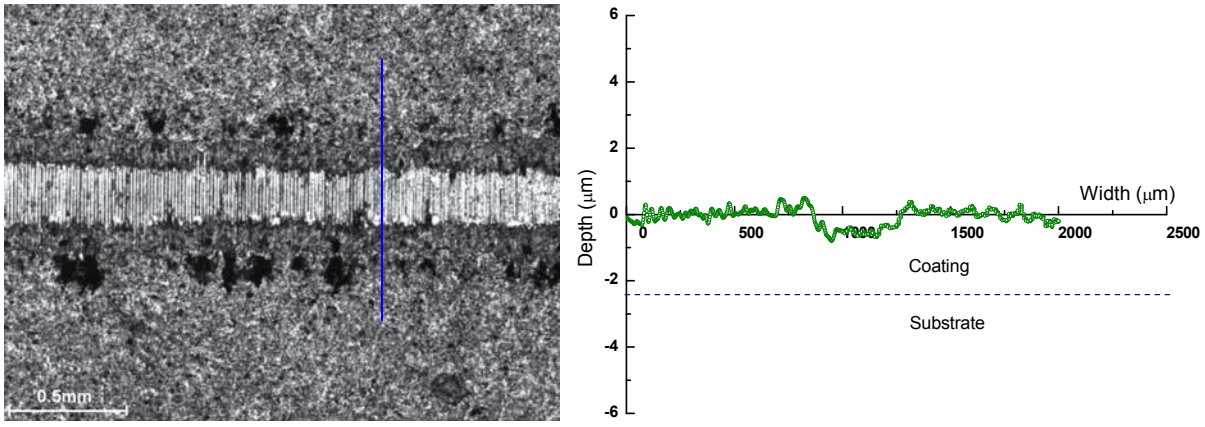

Figure 119: Wear scar of MoS_2 coating and its profile under cylinder-on-flat contact (±5 µm, 1000 N).

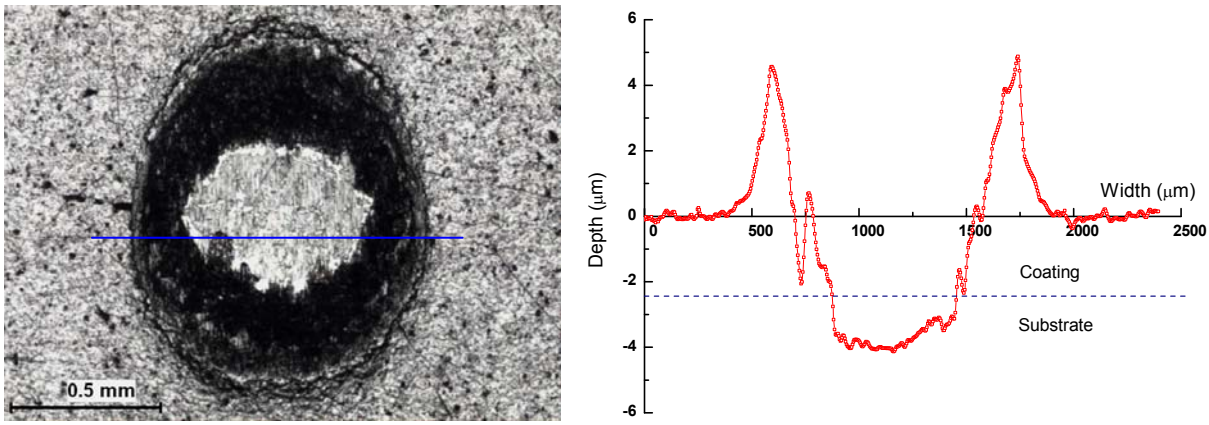

Figure 120: Wear scar of MoS_2 coating and its profile under ball-on-flat contact (±5 μm, 400 N).

1.2.2 Displacement amplitude in fretting test

In the fretting tests of two contact configurations, the initial friction coefficients increased with the increase of displacement amplitude, as shown in Figure 121. For the low displacement amplitudes, the climbing slopes of friction coefficient under two contact configurations and all loads were similar. The increase of initial friction coefficient probably resulted from two reasons. Firstly, the increase of displacement amplitude induced a change of fretting regimes and an extension of sliding area. When displacement amplitude was ±5 μm, there was an obvious stick area at the centre part of wear scar (Figure 122c), and the tests worked in the mixed slip regime (Figure 122a). As displacement amplitude increased to ±25 μm, the stick area disappeared (Figure 122d), the fretting logs presented the characteristic of gross slip regime (Figure 122b). Secondly, large displacement amplitude enlarged the contact area exposed to humid air where MoS_2 coating tended to be oxidized. With the continuous increase of displacement amplitude in the gross slip regime, the climbing slope of friction coefficient dropped off (Figure 121).

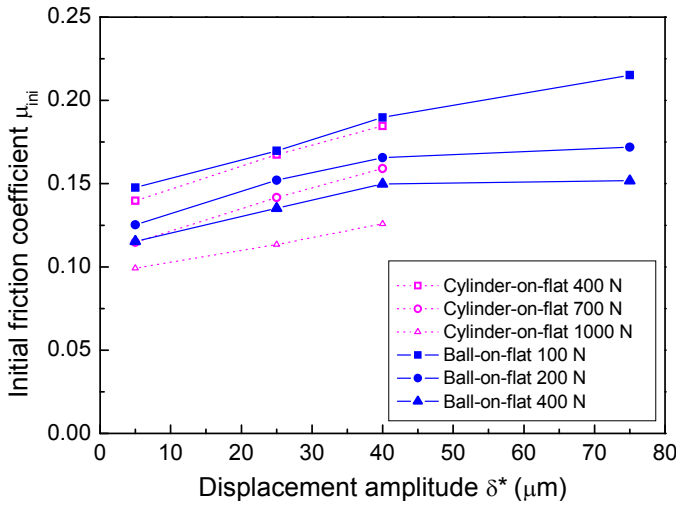

Figure 121: Effect of displacement amplitude δ^* on initial friction coefficient μ_{ini} in fretting tests.

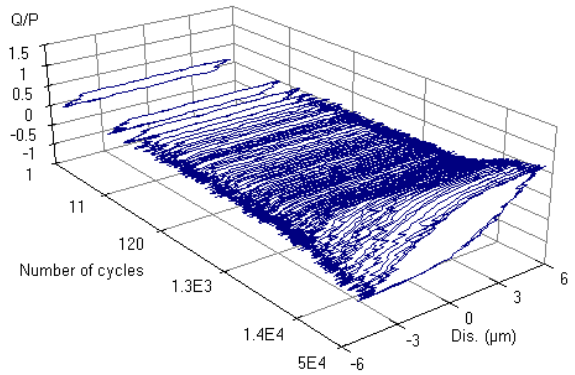

a) Displacement amplitude: ±5µm, normal load: 200N

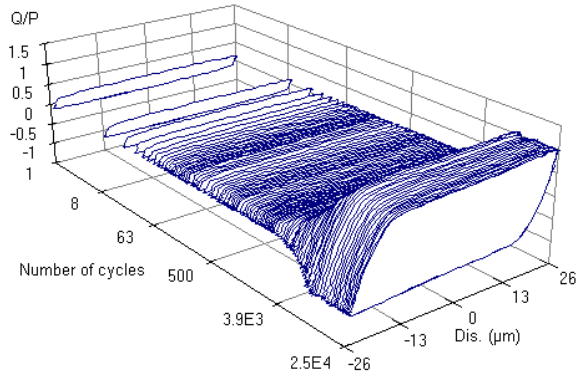

b) Displacement amplitude: ±25µm, normal load: 200N

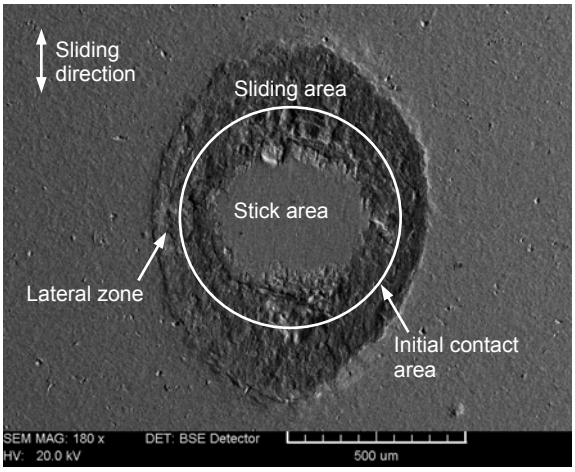

c) SEM micrograph of wear scar (±5µm, 200N)

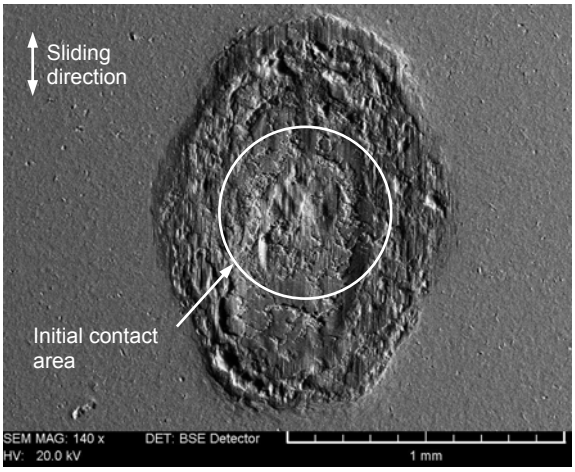

d) SEM micrograph of wear scar (±25µm, 200N)

Figure 122: Fretting logs and SEM micrographs of wear scars under the ball-on-flat configuration.

1.2.3 Sliding speed in sliding test

Figure 123 shows the effect of sliding speed on initial friction coefficient in ball-on-disk sliding tests, where the average initial friction coefficient under all of the applied normal loads is almost independent of the sliding speed, which means there is not an obvious effect of frictional heating. This result is probably attributed to the narrow changing range of the sliding speed and the neglectable frictional heating at the initial stage.

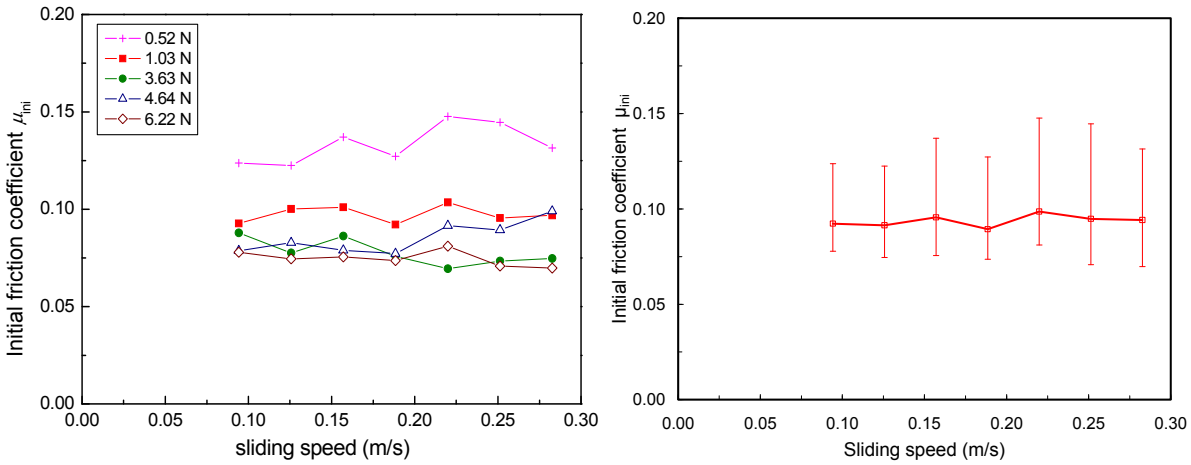

(a) Under different normal loads (b) mean value under all the normal loads

Figure 123: Effect of sliding speed on initial friction coefficient.

1.2.4 Contact configuration

In fretting tests, for the two contact configurations, the major difference is the geometry of counterparts, which results in a more “open” contact in ball-on-flat configuration and differences of contact pressure distribution. According to Hertz, in ball-on-flat contact, the maximal contact pressure is $p_0=3p/2$, while in cylinder-on-flat contact, $p_0=4p/\pi$. Under a same mean contact pressure p, the contact centre of ball-on-flat suffers a larger local deformation. Actually, for our test conditions, plastic deformation of the substrate took place due to the high contact pressure under the ball-on-flat configuration. Additionally, in the more “open” contact of ball-on-flat, the flow of debris in lateral zones increases the width of the contact track beyond the Hertzian radius (Figure 124a), while in cylinder-on-flat configuration, there is no lateral flow of debris (Figure 124b). The larger deformation and the change of contact radius influence the contact area and the distribution of contact pressure under the ball-on-flat configuration, which can result in the difference of friction coefficient in Figure 117.

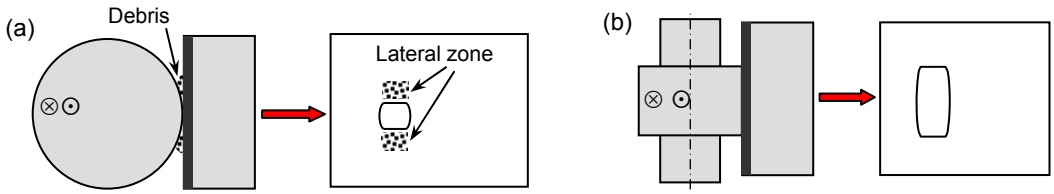

Figure 124: Lateral flow of debris in (a) ball-on-flat and (b) cylinder-on-flat configurations.

1.3 Summary

The pressure sprayed MoS_2 coating decreased the friction coefficient of the contact surfaces from 0.8-1.0 to 0.1-0.2. In fretting tests, the use of MoS_2 coatings made the partial slip regime disappear in the running condition fretting map. The friction coefficient was influenced by test parameters and contact configurations. For the three contact configurations, high contact pressure resulted in a decrease of friction coefficient. In fretting tests, friction coefficient increased with the displacement amplitude. In sliding tests, friction coefficient was almost independent of the sliding speed. The effect of contact configurations on friction coefficient was attributed to the contact area, the distribution of contact pressure and the flow of debris.

2 Coating lifetime

2.1 Coating lifetime definition

Lifetime of a solid lubrication coating (N_c) signifies the service time when the interface remains at a low friction coefficient, i.e., the number of cycles before a sharp increase of friction coefficient occurs. In practice, we can consider a fixed limit value of friction coefficient as the criterion of coating lifetime (for example, the limit value was 0.2 in [71] and 0.25 in [8]). This opinion does not take into account the difference of initial friction coefficient μ_{ini} under different test conditions, that is why some people used a relative ratio of friction coefficient to its initial value as the criterion (for example, 3 was used in [178]). In the present study, we choose this approach and the coating lifetime is defined as the number of cycles when the friction coefficient reaches three times of the initial value ($\mu=3\mu_{ini}$), as shown in Figure 125.

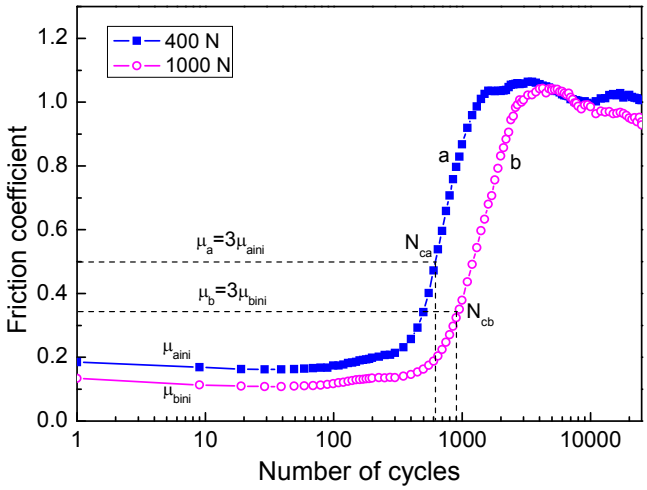

Figure 125: Coating lifetime definition $\mu=3\mu_{ini}$ (cylinder-on-flat fretting, δ*=±25 µm).

2.2 Effect of test parameters on coating lifetime

2.2.1 Contact pressure

In literature, wear rate of coatings generally increases with the increase of contact pressure. Ball-on-disk sliding tests presented similar results that with the increase of contact pressure, coating lifetime monotonously decreased, as shown in Figure 126, which was probably attributed to the difficulty of maintaining MoS_2 transfer film under high contact pressure. The wear of MoS_2 is the process of the formation of transfer film, break and re-formation, and under high pressure, the transfer layer is easier to break and then the debris will be easily ejected by centrifugal force.

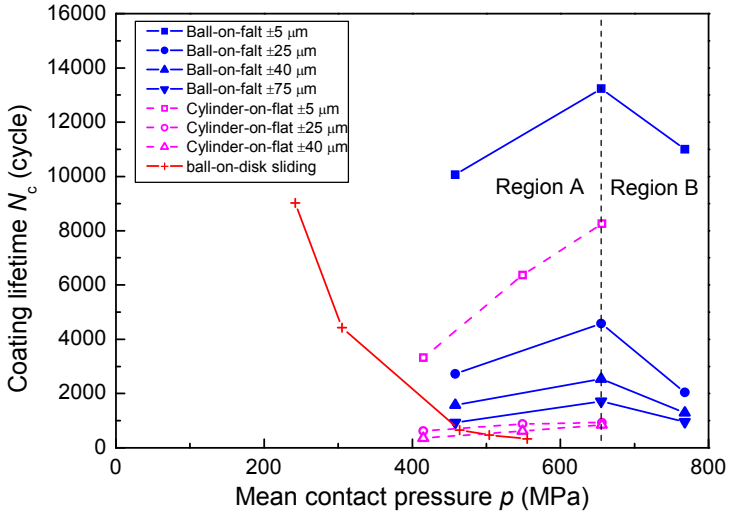

Figure 126: Effect of mean Hertzian contact pressure on coating lifetime.

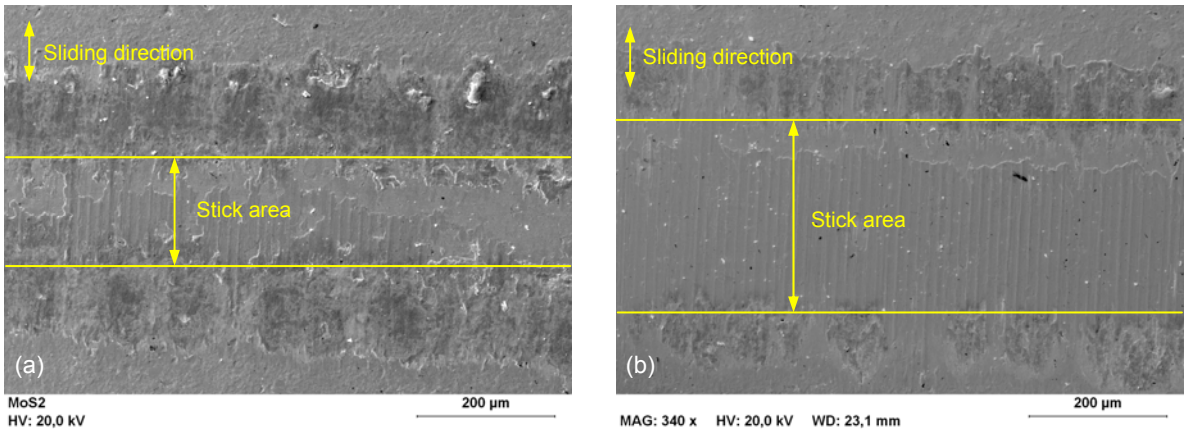

Figure 127: SEM micrographs of wear scars in cylinder-on-flat fretting tests under different contact pressures: (a) δ^* = ± 5 µm, p = 549 MPa, (b) δ^* = ± 5 µm, p = 656 MPa.

The influence of normal load on coating lifetime in fretting tests was completely different from that in sliding tests. In fretting tests, effect of contact pressure presented two different results in two regions as shown in Figure 126. In “Region A”, the coating lifetime increased with the increase of contact pressure. In cylinder-on-flat configuration, contact pressures were relatively low, and the coating lifetime always increased with contact pressure, which can be attributed to two reasons. Firstly, for the small displacement amplitude of ±5 µm, the obvious increase of lifetime with the contact pressure was due to the extension of stick area with the increase of normal load (high normal load increased the contact stiffness). For example, when the mean contact pressure increased from 549 MPa to 656 MPa, the width of stick area in the wear scar obviously increased, about from 160 µm to 280 µm, as shown in Figure 127. Secondly, under fretting friction conditions, the increase of contact pressure can promote the MoS_2 coating to form a transfer film on the counterface [274]. In the ball-on-flat fretting contact, for the relative low contact pressures, the coating lifetime also increased with the increase of contact pressure. In “Region B”, when mean contact pressure increased from 655 MPa to 768 MPa, coating lifetime decreased whatever the displacement amplitude was, because the contact pressure exceeded a critical value and obvious plastic deformation of the substrate took place.

2.2.2 Displacement amplitude in fretting test

Displacement amplitude imposes an important effect on coating lifetime under fretting conditions. When displacement amplitude increased from ±5 µm to ±25 µm, coating lifetime abruptly decreased for both configurations (Figure 128) because the fretting regimes changed from mixed slip to gross slip. Figure 122a shows the fretting logs in mixed slip regime for the test: δ^*=±5 µm, P=200 N in ball-on-flat contact, which is confirmed by the stick area of wear scar (Figure 122c). When displacement amplitude increased to ±25 µm, fretting cycles kept quadrangle shape during the whole test (Figure 122b) and the stick region disappeared (Figure 122d). In the gross slip regime (δ^*>±25 µm), coating lifetime slightly fell with the displacement amplitude (Figure 128), which can be attributed to two reasons. Firstly, the increase of displacement amplitude induced an easier ejection of debris, which means a small chance of recycling MoS_2 debris. Secondly, large displacement amplitude enlarged the contact area exposed to humid air where MoS_2 coating trended to be oxidized.

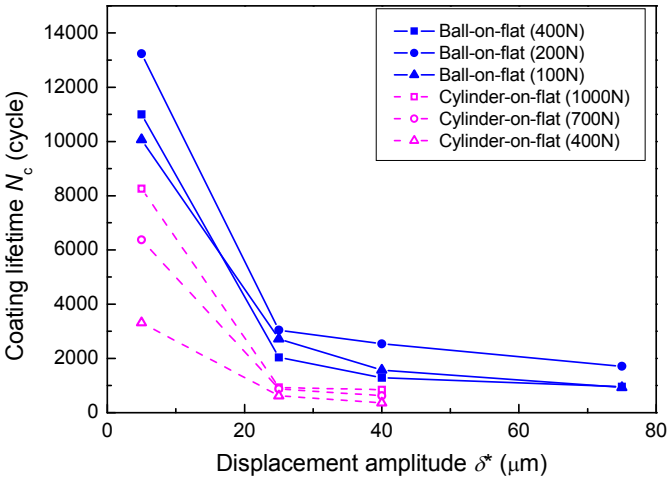

Figure 128: Effect of displacement amplitude on coating lifetime.

2.2.3 Sliding speed in sliding test

According to Figure 129, coating lifetime slightly decreased with the increase of sliding speed because high sliding speed induced more friction heating, which accelerated the oxidation of MoS_2 coating. Additionally, a high sliding speed induced a high centrifugal, which promoted the ejection of debris.

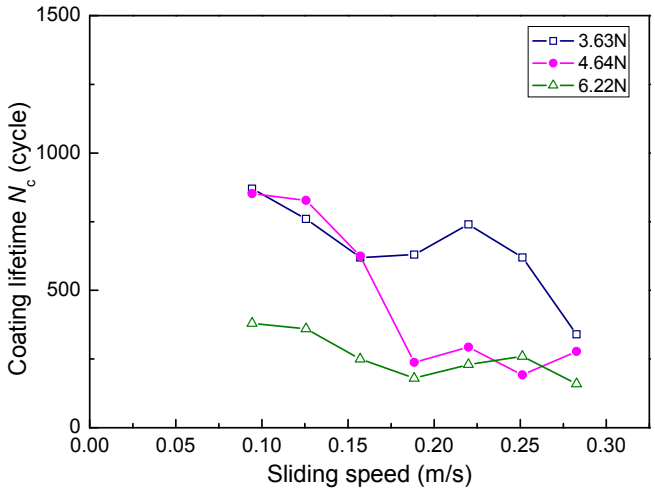

Figure 129: Effect of sliding speed on coating lifetime.

2.2.4 Contact configuration

In fretting tests, two contact configurations were used. From Figure 128, the MoS_2 coating had a longer lifetime in ball-on-flat configuration. For solid lubricant coatings, the lifetime depends on two aspects: one is the wear process, and the other is the rheology and flow of transfer film and debris [275]. The wear mechanism of MoS_2 coating consists of the formation of a transfer film (with low shear strength) on counterface and its break (particle detachment due to the oxidation of MoS_2) and reformation. The ball-on-flat configuration is a more “open” contact, which can result in a lateral flow of debris. According to Figure 122, the width of wear scar is larger than the initial contact size. The longer lifetime probably profited from the increase of contact area in the lateral zone, which progressively contributed to the transmission of the normal load. In cylinder-on-flat configuration the increase of contact area only occurred in the sliding direction.

2.2.5 Kinematic condition

Kinematic condition, including the type of relative motion, speed, amplitude and frequency, will influence not only the wear process (formation and break of transfer film), but also the ejection of debris, which are important factors of coating endurance. In ball-on-disk sliding tests, relatively higher sliding speed than in fretting tests can promote the formation of transfer film, but on the other hand higher sliding speed induced more friction heating and in ball-on-disk configuration there is a longer interval of contact area exposed in air, which facilitate the oxidation process of MoS_2 coatings. Once the detachment of transfer film takes place, centrifugal force from the rotation of the disk can easily eject the debris. In fretting tests, the ejection of debris is relatively difficult. The debris staying in the contact area is repeatedly squeezed to form transfer film on the counterface, so debris plays a more important role in fretting tests for coating lifetime.

2.3 Summary

The lifetime of MoS_2 coating depended on test conditions, which influenced the formation of transfer films and the ejection of debris. In ball-on-disk tests, coating lifetime decreased with the increase of contact pressure, and was slightly influenced by the sliding speed. In fretting tests, the coating lifetime decreased with the increase of displacement amplitude, especially in the mixed slip regime, and increased with the increase of contact pressure until a critical contact pressure.

3 Coating lifetime prediction

According to the Archard model in Eq.1-8, wear volume is related to the product of the normal load P and the sliding distance L. For fretting tests, if in i^{th} cycle, the actual displacement amplitude is δ_{0i} and the actual normal load is P_i, then the wear volume can be expressed as:

$$V \propto \sum_{i=1}^{N} 4P_i\delta_{0i} \qquad (5\text{-}1)$$

In our tests, the focus is not the wear volume, but the coating lifetime. Figure 130 presents the evolution of coating lifetime with Archard factor $P{\cdot}L$ ($\sum_{i=1}^{N_c} 4P_i\delta_{0i}$, where N_c is the coating lifetime in cycles). In the Archard model, wear volume generally linearly increases with the factor $P{\cdot}L$, so a large $P{\cdot}L$ should not be beneficial for the wear volume. However, in Figure 130, the coating lifetime increases with the $P{\cdot}L$ value of lifetime whatever the contact configuration is. And the increase slope is different for different displacement amplitudes, i.e., a low displacement amplitude induces a high increasing slope.

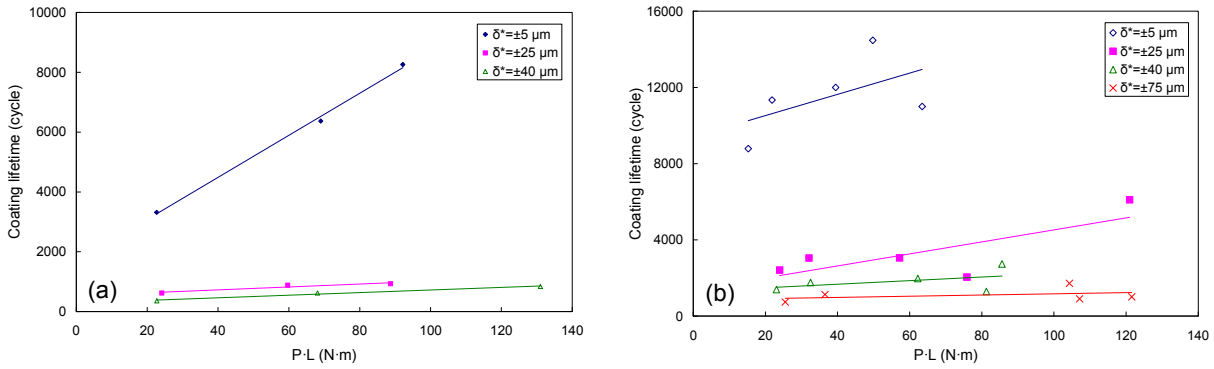

Figure 130: Evolution of coating lifetime with Archard factor P·L, (a) cylinder-on-flat, (b) ball-on-flat.

Dissipated energy is more used in resent researches than Archard factor, because the latter (the product of the normal load and the tangential sliding distance) has not any physical meaning. The Archard factor multiplied by the friction coefficient is the cumulated dissipated energy of the coating in its lifetime, as shown in Eq. 5-2.

$$\sum Ed = \sum_{i=1}^{N_c} 4\mu_i P_i \delta_{0i} \qquad (5\text{-}2)$$

The evolution of coating lifetime with the cumulated dissipated energy also shows linear relationships, and different displacement amplitudes result in different slopes (Figure 131). Therefore, it is not easy to predict coating lifetime by the different linear relationships.

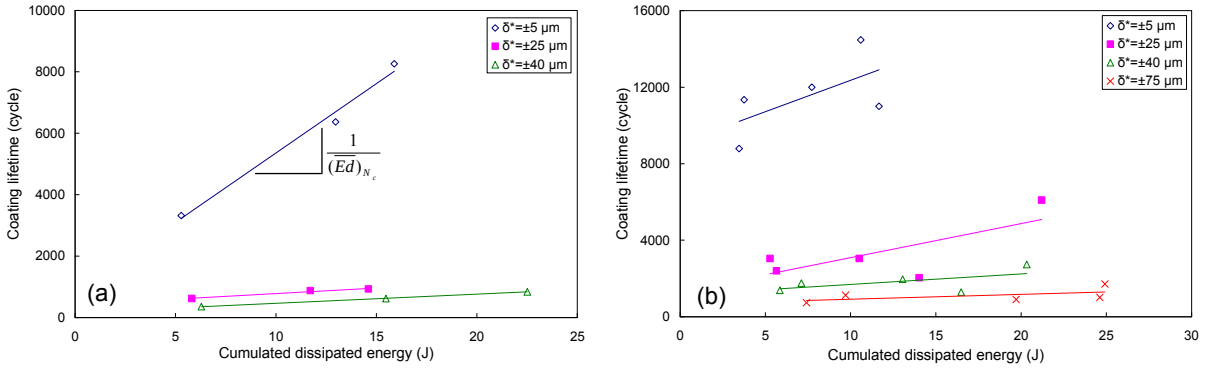

Figure 131: Evolution of coating lifetime with the cumulated dissipated energy: (a) cylinder-on-flat, (b) ball-on-flat.

A higher cumulated dissipated energy relates to a longer lifetime, which is difficult to understand, because a high cumulated dissipated energy generally results in a large wear volume. Actually, Eq.5-2 can be expressed as Eq.5-3, i.e., the cumulated dissipated energy is the product of the coating lifetime and the average dissipated energy of each cycle during the coating lifetime, and the lifetime conceals the effect of the average dissipated energy. So a longer lifetime results in a higher cumulated dissipated energy.

$$\sum Ed = \sum_{i=1}^{N_c} 4\mu_i P_i \delta_{0i} = N_c \cdot \frac{1}{N_c} \sum_{i=1}^{N_c} 4\mu_i P_i \delta_{0i} = N_c \cdot (\overline{Ed})_{N_c} \qquad (5\text{-}3)$$

$$\frac{1}{(\overline{Ed})_{N_c}} = \frac{N_c}{\sum Ed} \qquad (5\text{-}4)$$

Eq.5-3 can be transformed to Eq.5-4, i.e., the reverse of the average dissipated energy is the slope of the curves in Figure 131. A high displacement amplitude induces a high average dissipated energy and a short coating lifetime. The average dissipated energy of each cycle is probably more important than the cumulated value for finding the relationship between the lifetime and dissipated energy. Here, we will use the average dissipated energy of each cycle during the stable low friction stage (Eq. 5-5).

$$(\overline{Ed})_{N_0} = \frac{1}{N_0} \sum_{i=1}^{N_0} Ed_i = \frac{1}{N_0} \sum_{i=1}^{N_0} 4\mu_i P_i \delta_{0i} \qquad (5\text{-}5)$$

where N_0 is the number of cycles with low stable friction. In Figure 132, the relationship between average dissipated energy per cycle and the coating lifetime can be fitted by one master curve whatever the contact configuration and the test parameters under fretting conditions. This master curve is very helpful for predicting the coating lifetime under other test parameters.

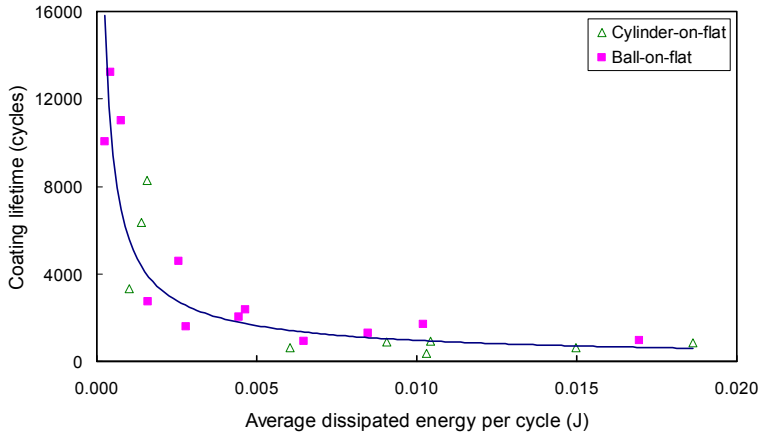

Figure 132: Average dissipated energy - coating lifetime master curve for the two contact configurations.

However, this approach is unsuitable for the ball-on-disk tests because a large radius (the distance between the ball and the center of the disk) leads to a high dissipated energy Ed_i, which has little relationship with the coating lifetime. On the other hand, although there is a master curve between the coating lifetime and the average dissipated energy per cycle, the more accurate relative parameter is the wear volume, not the coating lifetime. According to Fouvry *et al.*[102], the wear depth is more important than the wear volume for the coating lifetime, and the relative energy parameter is local dissipated energy (or dissipated energy density). The maximal dissipated energy density is related to the maximal wear depth, then the coating lifetime. The approach (initial maximal dissipated energy density) put forward by Fridrici *et al.*[195] is easier to use for predicting coating lifetime because the initial value of maximal dissipated energy density is easy to obtain just by running a new test for several cycles under the wanted conditions.

Under the ball-on-flat fretting and ball-on-disk sliding contact configurations, the maximal dissipated energy took place at the center point of the contact area where the contact pressure presents the highest value (Figure 133a and c). In the same way, under the cylinder-on-flat fretting contact configuration, the maximal dissipated energy took place at the center line of the contact area (Figure 133b). Fouvry *et al*. [102] obtained the equation of maximal dissipated density under ball-on-flat and cylinder-on-flat fretting contacts, as shown in Eq.1-21, and Fridrici *et al*. [195] put forward another approximate equation, as shown in Eq.1-24, which is simpler. For small displacement amplitudes, the results of the two equations are very close, so we use the latter. Under the ball-on-disk sliding contact, the contact pressure distribution in the centre section of the contact area can be expressed as Eq.5-6 according to Hertzian theory. Multiplied by the friction coefficient, the relative shear stress distribution is Eq.5-7. In the ball-on-disk unidirectional sliding, the ball passes a point of the disk once per cycle, so the maximal local dissipated energy of the disk occurs at the circle (the dashed one in Figure 133c) formed by the center points of the contact areas, and the value is equal to the integration of the shear stress distribution in the central section. Using the initial friction coefficient to replace the friction coefficient, the initial maximal dissipated energy density under ball-on-disk contact is shown in Eq.5-8.

$$p(x) = p_{\max}\sqrt{1-\frac{x^2}{a^2}} \quad (-a \le x \le +a) \tag{5-6}$$

$$q(x) = \mu \cdot p(x) = \mu \cdot p_{\max}\sqrt{1-\frac{x^2}{a^2}} \quad (-a \le x \le +a) \tag{5-7}$$

$$Ed_{0\,\max\,ini} = \int_{-a}^{+a} \mu_{ini}\, p(x)dx = \int_{-a}^{+a} \mu_{ini}\, p_{\max} \sqrt{1-\frac{x^2}{a^2}}dx = \frac{1}{2}\mu_{ini}\, p_{\max}\, a\pi \qquad (5\text{-}8)$$

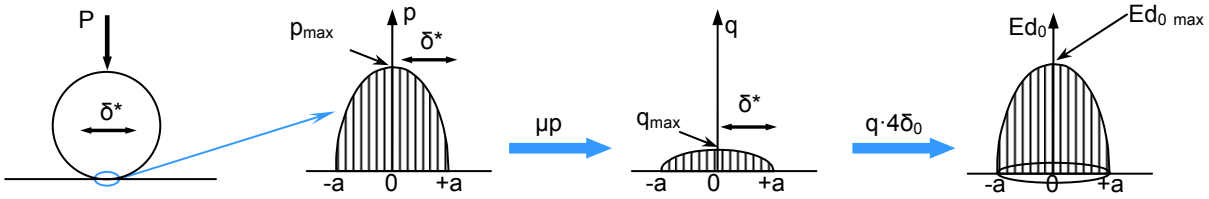

(a) ball-on-flat fretting contact

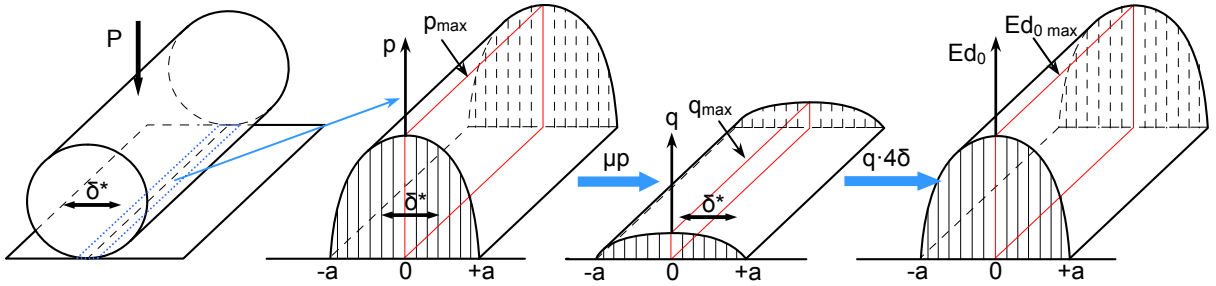

(b) cylinder-on-flat fretting contact

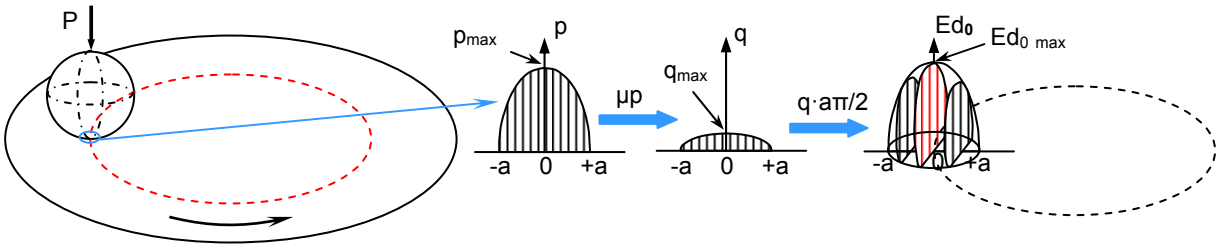

(c) ball-on-disk sliding contact

Figure 133: the distribution of contact pressure and dissipated energy density in the contact area.

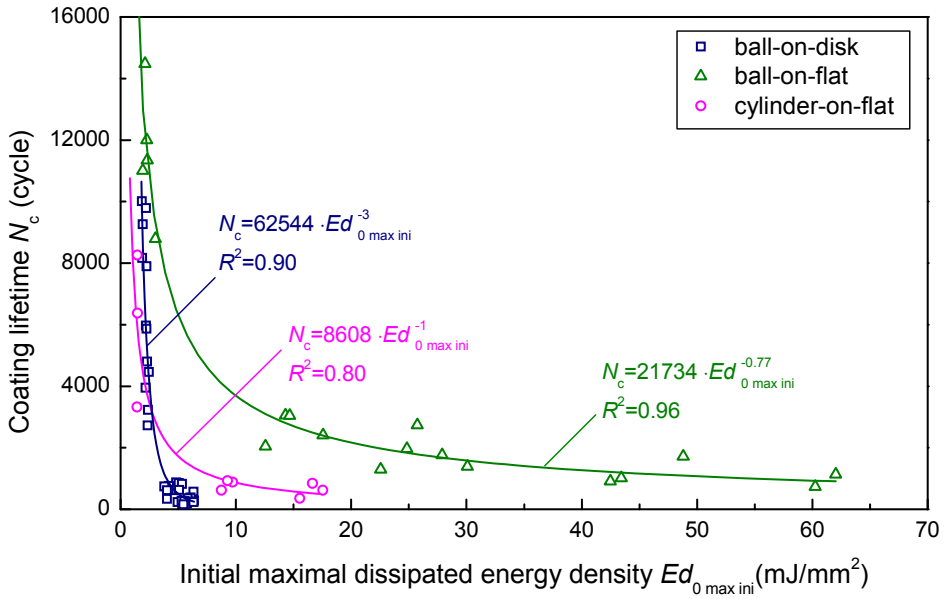

Figure 134: Coating lifetime – initial maximal dissipated energy density master curves.

According to Eq.1-24 and Eq.5-7, under each contact configuration, the relationship between the coating lifetime and the initial maximal dissipated energy density can be fitted by one master curve whatever the test parameters, as shown in Figure 134.

After getting these master curves, it is easy to predict coating lifetime under other test parameters by the only variable — the initial maximal dissipated energy density $Ed_{0\ max\ ini}$. According to Eq.1-24, under fretting contacts, $Ed_{0\ max\ ini}$ depends on the initial friction coefficient (μ_{ini}), the initial actual displacement amplitude (δ_{0ini}) and the maximal contact pressure (p_0). Under the ball-on-disk sliding contact, $Ed_{0\ max\ ini}$ depends on the initial friction coefficient (μ_{ini}), the maximal contact pressure (p_0) and the contact radius (a) from Eq.5-8. The maximal contact pressure and contact radius can be calculated by Hertzian theory, and the initial friction coefficient and displacement amplitude can be obtained just by running new tests under the relative contact configuration and test parameters for several cycles.

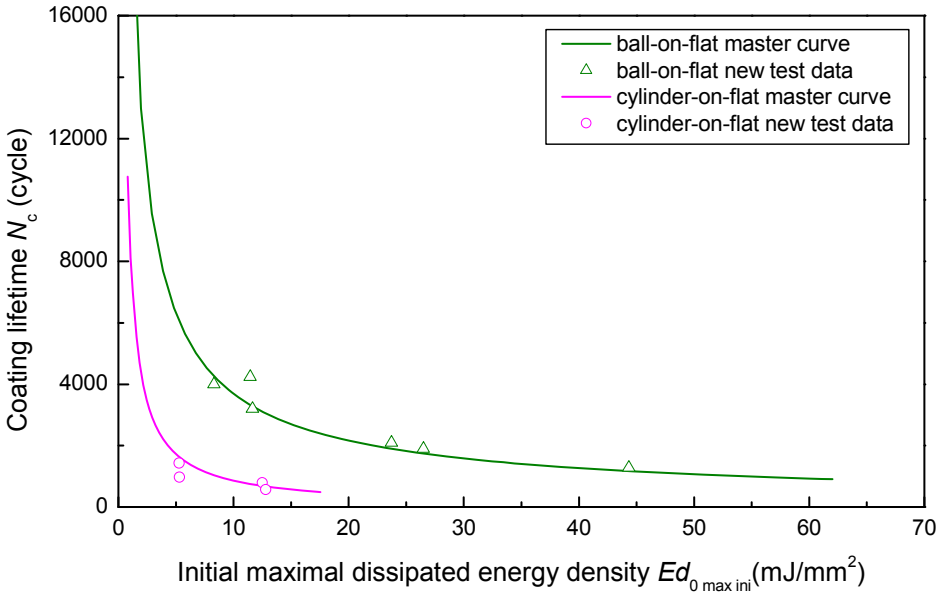

Figure 135: Master curves and new test data under the fretting contacts.

In order to validate this prediction method, some tests were performed. For the cylinder-on-flat fretting contact, the new tests were carried out under 550 N and 850 N with displacement amplitude of ±15 μm and ±32 μm. Under the ball-on-flat fretting contact, the tests with displacement amplitude of ±15 μm, ±32 μm and ±55 μm under 150 N and 300 N were performed. The results are shown in Figure 135, where the master curves mean the predict lifetimes and the data by marks are the actually lifetimes. From Figure 135, we find that this prediction approach is feasible.

In fact, the objective of new tests is just for obtaining δ_{0ini} and μ_{ini}. Under some inconvenient situations, it is also possible to approximately predict the coating lifetime without performing new tests. For the fretting tests in the gross slip regime, the initial actual displacement amplitude (δ_{0ini}) is close to the imposed value (δ^*). The initial friction coefficient can be approximately extrapolated according to the tests that have been carried out. According to the relationships between the initial friction coefficient and the test parameters in Figure 121 and Figure 123, the range of initial friction coefficient under the relative test parameters can be estimated, and then the range of the coating lifetime can be predicted.

4. Conclusions

In this chapter, based on the investigation of pressure sprayed MoS_2 coating under three different contact configurations (cylinder-on-flat fretting, ball-on-flat fretting and ball-on-disk unidirectional sliding), the following conclusions can be drawn:

- Pressure sprayed MoS_2 coating can reduce the friction coefficient from 0.8~1.0 to 0.1~0.2 under fretting conditions, and make the partial slip regime disappear under our test conditions. The specific value of friction coefficient depends on test parameters. Under ball-on-disk, the pressure sprayed MoS_2 coating can result in low friction coefficient, about 0.07~0.15.
- Friction coefficient decreased with the increase of contact pressure whatever the contact configurations, but it evolves along different curves due to the distribution of contact pressure, the change of contact area, etc. Friction coefficient increased with the increase of displacement amplitude under fretting tests. The sliding speed hardly influenced the friction coefficient under ball-on-disk tests under our test conditions.
- Under ball-on-disk contact, the lifetime of pressure sprayed MoS_2 coating decreased monotonously with the increase of contact pressure, while under fretting conditions the lifetime first increased with the increase of contact pressure, and then decreased after the contact pressure passed a critical value. Under unidirectional sliding conditions, the coating lifetime was slightly influenced by sliding speed. Under fretting conditions, the increase of displacement amplitude induced a decrease of coating lifetime, especially in the mixed slip regime.
- Effect of contact configuration on friction coefficient and lifetime focused on the role of debris and the change of contact area and contact pressure.
- Under each contact configuration, the relationship between coating lifetime and dissipated energy density can be fitted by one master curve whatever the test parameters, which can be easily used to predict coating lifetime with other test parameters under the relevant contact configuration.

CHAPTER 6

EFFECT OF COATING PROPERTIES ON TRIBOLOGICAL PERFORMANCE: COATING SELECTION PROCESS

CHAPTER 6: EFFECT OF COATING PROPERTIES ON TRIBOLOGICAL PERFORMANCE: COATING SELECTION PROCESS

CHAPTER 6: EFFECT OF COATING PROPERTIES ON TRIBOLOGICAL PERFORMANCE: COATING SELECTION PROCESS

This chapter investigates several bonded solid lubricant coatings by fretting tests and different evaluation techniques. The relationships between the fretting behaviors and the coating properties are discussed, and a systemic approach is put forward to comprehensively compare the coatings and help the coating selection.

1 Behaviors in the evaluation techniques

1.1 Nanoindentation tests

Seven nanoindentation tests were performed on each coating. The results obtained on K39 are shown in Figure 136a. The scattering observed in Figure 136b may be due to coating heterogeneity or to thickness variation of the coating. The hardness H is the contact pressure, i.e., the ratio of applied load F to the projected contact area A_p, as shown in Eq.6-1, where A_p is a function of the actual contact depth h_r'. The evolution of hardness of K39 versus h_r' is shown in Figure 136c. The scattering observed at low penetration depth is due to the high roughness of the coating. The reduced elastic modulus E^* is related to the contact stiffness S (S=dF/dh) and to the equivalent contact diameter ($2\sqrt{A_p}/\sqrt{\pi}$), as shown in Eq.6-2, where β is a constant, which depends on the geometry of the indenter (β=1.034 for the Berkovich tip) [161]. The elastic modulus of the diamond indenter E^*_i (about 1150 GPa) is taken into account in the calculation of the sample modulus, E^*_{mat} (Eq.6-3). Figure 136d shows the evolution of the reduced elastic modulus E^*_{mat} versus h_r' for coating K39. The reduced modulus E^*_{mat} includes coating and substrate elastic properties. The reduced modulus of the coating E^*_c can be estimated by extrapolating the modulus curve to low contact depths. The values of H and E^*_c for the five coatings are listed in Table 41. The hardness of the coatings ranges between 105 and 180 MPa and the elastic modulus between 4.0 and 7.0 GPa.

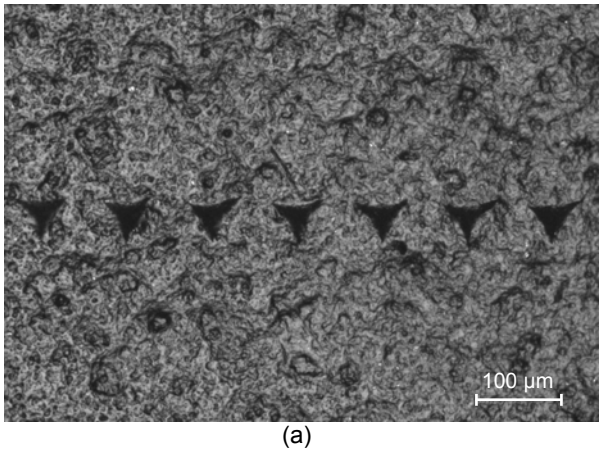

(a)

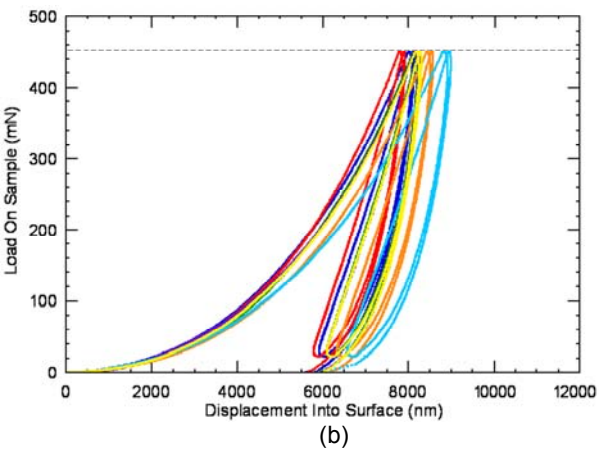

(b)

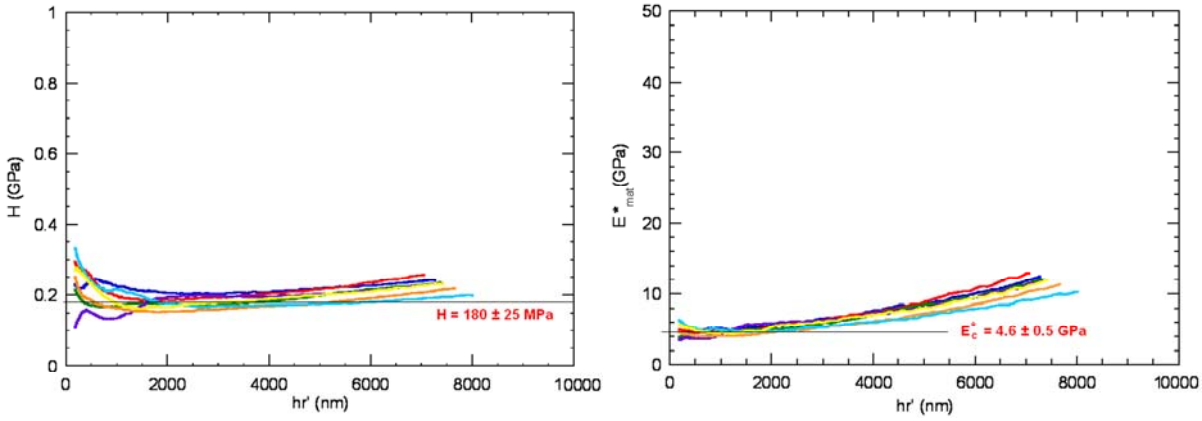

(c) (d)

Figure 136: Results of nanoindentation tests for the coating K39: (a) micrograph of the indentations; (b) load / unload – displacement curves; (c) evolution of hardness versus h_r'; (d) evolution of reduced elastic modulus versus h_r'.

$$H = \frac{F}{A_p} = \frac{F}{f(h_r')} \qquad (6\text{-}1)$$

$$E^* = \frac{\sqrt{\pi} \cdot S}{2\beta\sqrt{A_p}} \qquad (6\text{-}2)$$

$$\frac{1}{E^*_{mat}} = \frac{1}{E^*} - \frac{1}{E^*_i} \qquad (6\text{-}3)$$

Table 41: Results of nanoindentation tests.

Coating	K39	K15	K03	K06	U22
Hardness H (MPa)	180±25	105±25	150±20	110±30	170±30
Reduced elastic modulus E^*_c (GPa)	4.6 ±0.5	4.9±0.8	4.0±0.5	7.0±1.5	5.8±0.5
Ratio of H/E^*_c	0.039	0.021	0.038	0.016	0.029
Ratio of H^2/E^*_c	0.0070	0.0023	0.0056	0.0017	0.0050

1.2 Scratch tests

The coatings presented quite different results in scratch tests, including the critical loads related to cohesion failure (chipping, cracks) and the contact on the substrate, the feature of the tracks, the size and shape of the debris. The cohesion strength of the coatings can be estimated by the critical loads, and their ductility can be qualitatively analyzed according to the feature of the debris and the tracks.

K06 and U22 had low critical loads, and the small particle debris around the tracks reveal their poor ductility (Figure 137a and b). The coating K03 also had a low critical load, but its debris in the form of large particles mean higher cohesion strength and better ductility (Figure 137c). K15 with a higher critical load deformed more plastically, but the detachment of flake debris reveals its poor bonding strength (Figure 137d). Plastic deformation around the scratch track reflected excellent ductility of K39 and the highest critical load signified its best cohesion strength among the 5 coatings (Figure 137e). The critical loads and the evaluation about the ductility of the coatings are listed in Table 42.

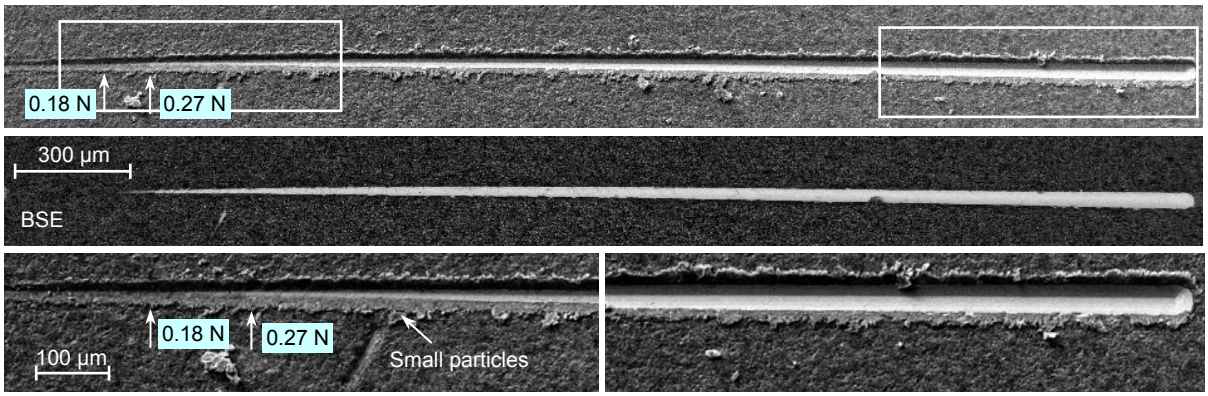

(a) K06

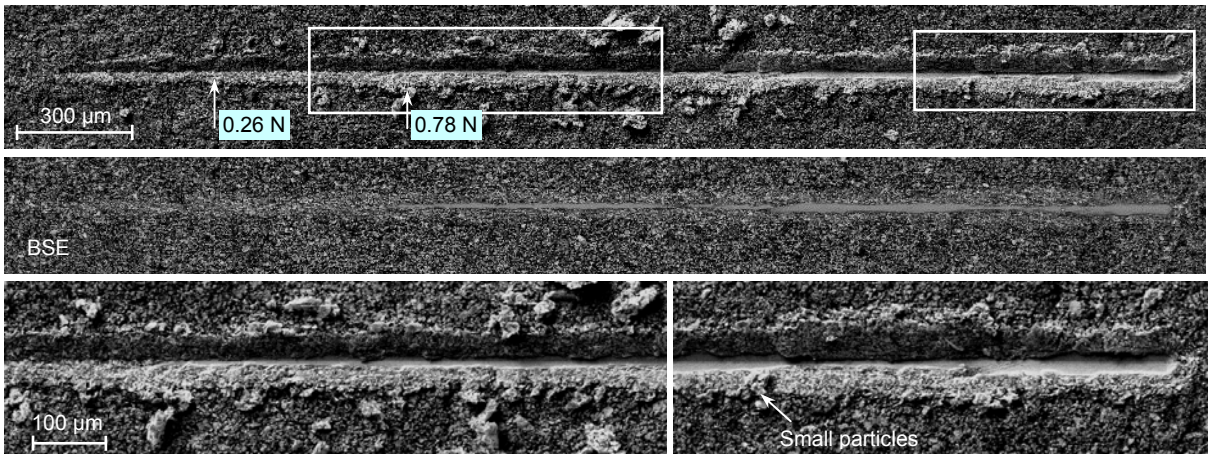

(b) U22

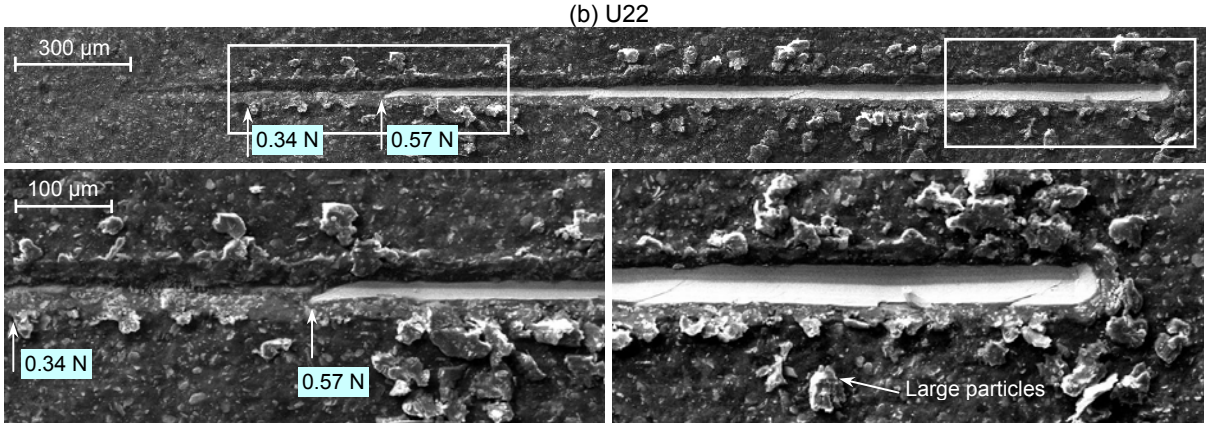

(c) K03

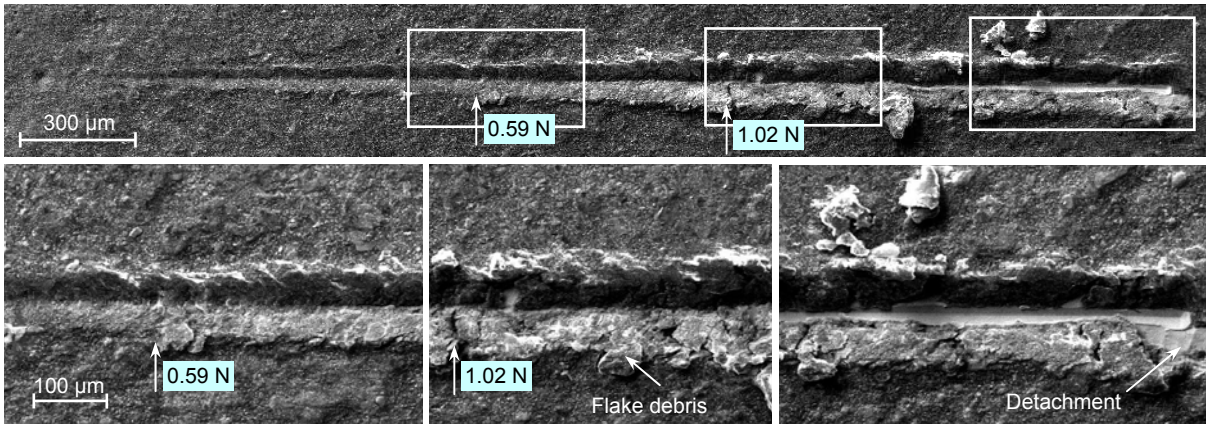

(d) K15

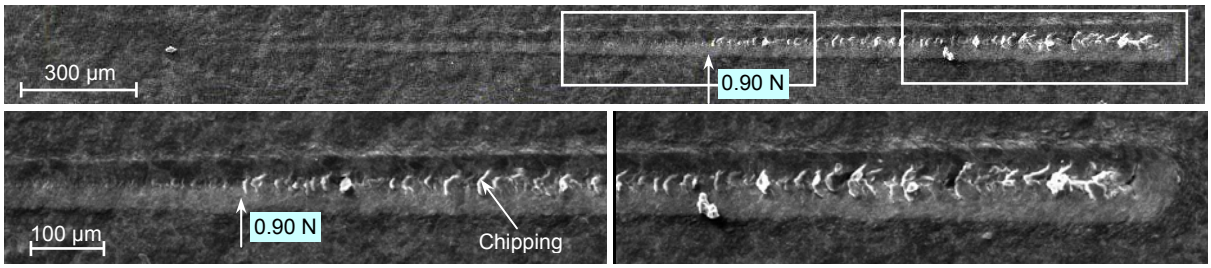

(e) K39

Figure 137: Micrographs of scratches on the coatings.

Table 42: Scratch results of the coatings.

Coating	K39	K15	K03	K06	U22
Critical load (N)	0.90	0.54	0.34	0.18	0.26
Normal force when the substrate is reached (N)	2.36	1.02	0.57	0.27	0.78
Ductility	excellent	good	fair	poor	poor

1.3 Ball cratering tests

In the ball cratering tests under the conditions of 1 N and 60 rpm, K03, K15 and K39 survived 30 minutes, while K06 and U22 were worn through. Figure 138 shows the craters of the 5 coatings after 5 minutes test, where some of the craters were not real circles due to the important surface roughness. The evolution of crater diameter *d* with test time of the 5 coatings is shown in Figure 139a, where the coatings based on PTFE (K03, K15 and K39) presented similar trends, while the crater diameters of K06 and U22 rapidly increased.

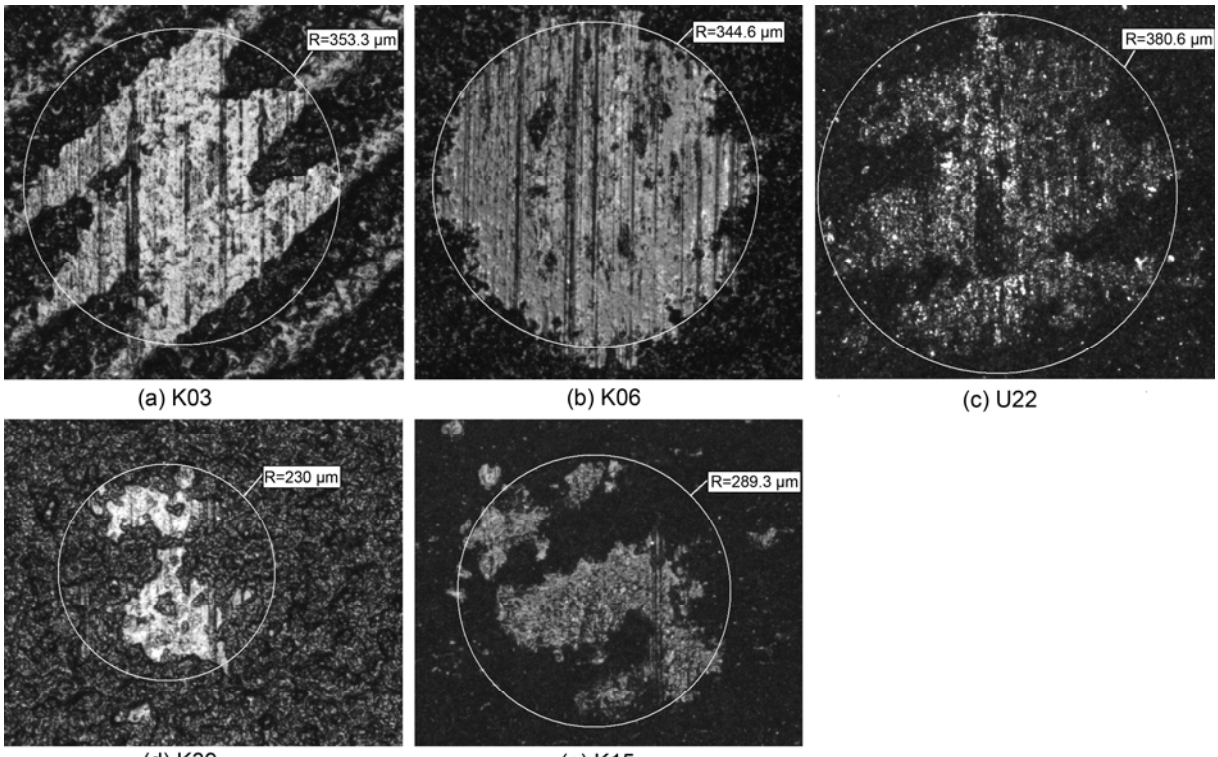

(a) K03 (b) K06 (c) U22

(d) K39 (e) K15

Figure 138: Micrographs of craters under 1 N and 60 rpm in 5 minutes.

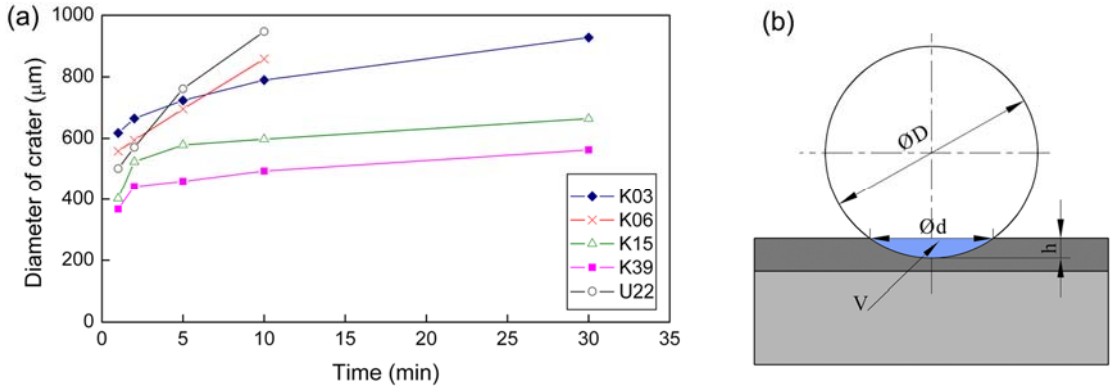

Figure 139: (a) Evolution of crater diameter with test time under 1 N and 60 rpm; (b) sketch map of crater size.

According to the crater diameter *d* and the ball diameter *D*, the wear depth *h* of the coating can be figured out (Figure 139b), and then wear volume *V* of the crater can be obtained by the Eq.6-4. The wear resistance of the coatings can be described by the wear rate of Archard model [94], which is the ratio of wear volume *V* to the product of normal load *P* and sliding distance *L*, as shown in Eq.6-5, where *t* is test duration and *n* is the rotating speed of the ball.

$$V = \pi \cdot h^2 \cdot \left(\frac{D}{2} - \frac{h}{3} \right) \quad (\text{mm}^3) \qquad (6\text{-}4)$$

$$K = \frac{V}{PL} = \frac{V}{P \cdot \pi \cdot D \cdot t \cdot n} \quad (\text{mm}^3/\text{Nm}) \qquad (6\text{-}5)$$

The wear volume of the coatings is almost proportional to the test time except for the first few minutes due to the influence of the large surface roughness of the coatings on the crater size in the initial test stage (Figure 140a). The evolution trends of wear volume for K15 and K39 were similar, while the wear volume of K06 and U22 increased very rapidly. The wear rate of K03, K15 and K39 gradually decreased with test duration, while K06 and U22 had a contrary trend (Figure 140b), i.e., the coatings based on PTFE exhibited better wear resistance than those based on MoS_2. Hence, the evolution of Archard's wear rate in ball cratering tests can be used to determine the coatings with good abrasion resistance (K03, K15 and K39) and the coatings with bad abrasion resistance (K06 and U22). An increase of wear rate is the distinguishing mark of the complete disappearance of the coating in the near future.

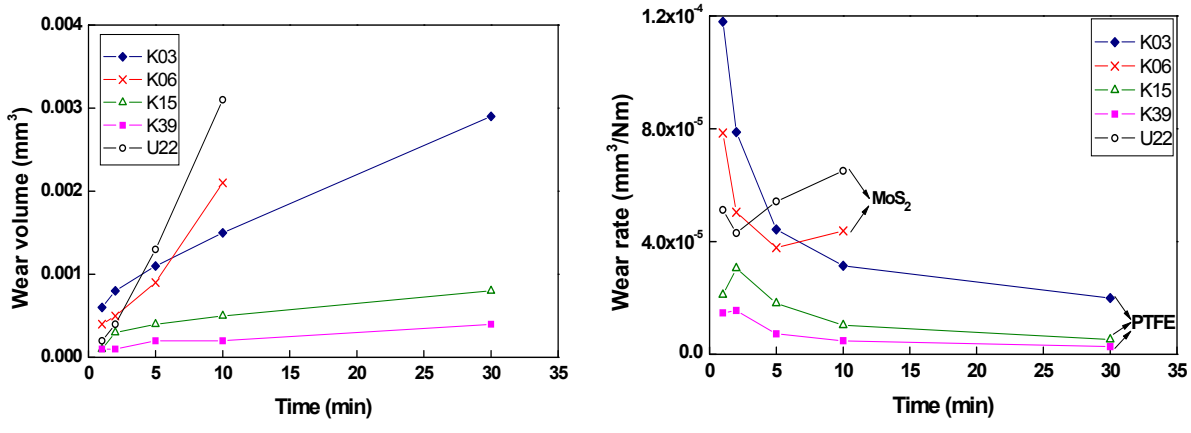

Figure 140: Evolution of (a) wear volume and (b) wear rate with test time in ball cratering: 1N, 60 rpm.

Under the more severe conditions (5 N and 150 rpm), coating K03 was worn through after 5 minutes; detachment of K15 took place after 70 minutes and severe detachment was found after 120 minutes; coating K39 was not worn through after 3 hours, but the substrate was reached after 30 minutes with the addition of diamond slurry. According to the outer and inner diameters of the circular annulus craters, the thickness of the coatings can be obtained by Eq.3-1 (Table 43). Figure 141 shows the micrographs of the craters after the substrate was reached, where coating K03 and K39 were gradually worn, while coating K06 and U22 locally detached and coating K15 severely detached.

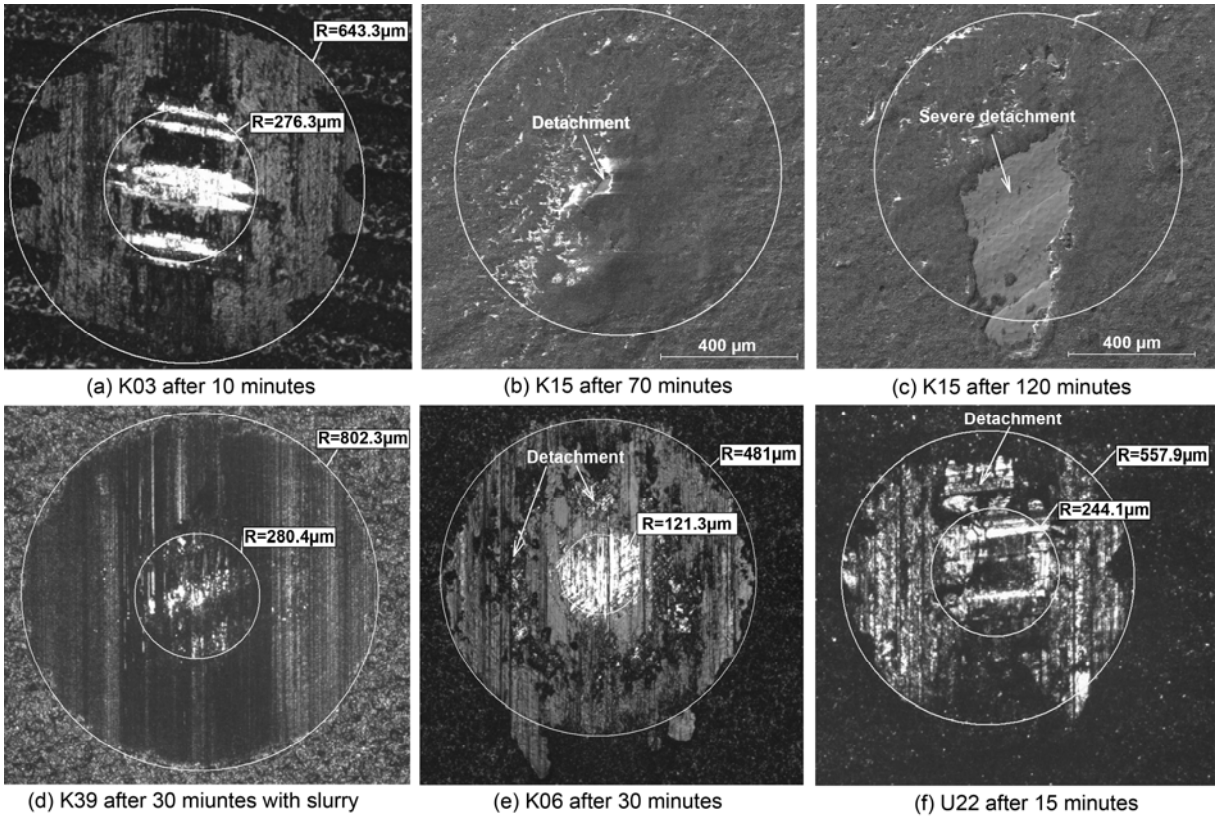

Figure 141: Micrographs of craters for coatings worn through: (a)(b)(c)(d) under 5N and 150rpm, (e)(f) under 1N and 60rpm.

Table 43: Coating thickness determined by ball crater.

Coating	K39	K15	K03	K06	U22
Thickness (μm)	20 ± 2	18 ± 1	11 ± 2	10 ± 1	11 ± 2

The relationships between the ball cratering resistance and coating properties are summarized in Table 44, where the numbers signify the places of the coatings in relevant ranks (1 for the best and 5 for the worst). Ball cratering resistance of the coatings was closely related to the based solid lubricant, cohesion strength and ductility. The coatings based on PTFE with high cohesion strength and good ductility showed better ball cratering resistance than those based on MoS_2. Although the hardest coating, K39, presented the best ball cratering resistance, there was no obvious relationship between the ball cratering resistance and the mechanical properties (hardness and elastic modulus) from the other coatings. However, the ratio of hardness to reduced elastic modulus related to different wear modes. The coatings with high H/E^*_c and H^2/E^*_c were worn by abrasion, while detachment took place for the other coatings. If the bonding strength is enough high, the thicker a coating is, the better its endurance in ball cratering, like K39. However, the bonding strength is usually influenced by the

coating thickness, i.e., a thick coating may induce a decrease of bonding strength due to high residual stress.

Table 44: Relationships between ball cratering resistance and coating properties.

Coating	K39	K15	K03	K06	U22
Ball cratering resistance	1	2	3	4	5
Wear mode	abrasion	severe detachment	abrasion	detachment	detachment
Based solid lubricant	PTFE	PTFE	PTFE	MoS_2	MoS_2
Critical load	1	2	3	5	4
Ductility	1	2	3	4	4
Hardness H	1	5	3	4	2
Reduced elastic modulus E^*_c	4	3	5	1	2
H/E^*_c	1	4	2	5	3
H^2/E^*_c	1	4	2	5	3
Thickness	1	2	3	3	3

2 Tribological behaviors

2.1 Friction coefficient

2.1.1 Evolution of friction coefficient

According to the fretting logs in Figure 142, the coatings K03 and K06 worked in the gross slip regime even under the low displacement amplitude of ±10 µm. Actually, in the fretting tests under our test conditions, all the 5 coatings worked in gross slip regime before their failure.

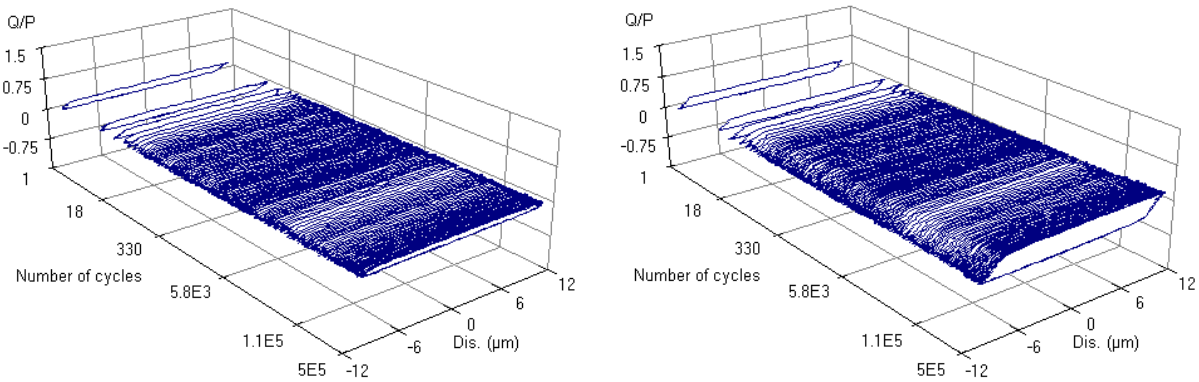

Figure 142: Fretting logs under 300 N and ±10 µm: a) K03, b) K06.

Figure 143 shows the evolution of friction coefficient with the number of cycles for the 5 coatings. Coating K03 induced low friction coefficient, about 0.08~0.1, and the values were slightly influenced by tests parameters. The low friction can be remained in 500 000 cycles at least under ±10 µm and low normal load (300 N and 450 N) (Figure 143a). With the increase of normal load or displacement amplitude, the number of cycles with low friction rapidly decreased (Figure 143b).

Coating K06 could provide a low friction in the test duration of 500 000 cycles under the low displacement amplitude of ±10 µm whatever the normal load, while the value of friction coefficient depended on normal load and increased with the test process, from the initial value about 0.11~0.17 to the stable value about 0.15~0.35 (Figure 143c). The value of friction coefficient was hardly

influenced by the displacement amplitude, but it rapidly increased at about 200 000 cycles for the larger displacement amplitudes of ±18 µm and ±25 µm under 300 N (Figure 143d).

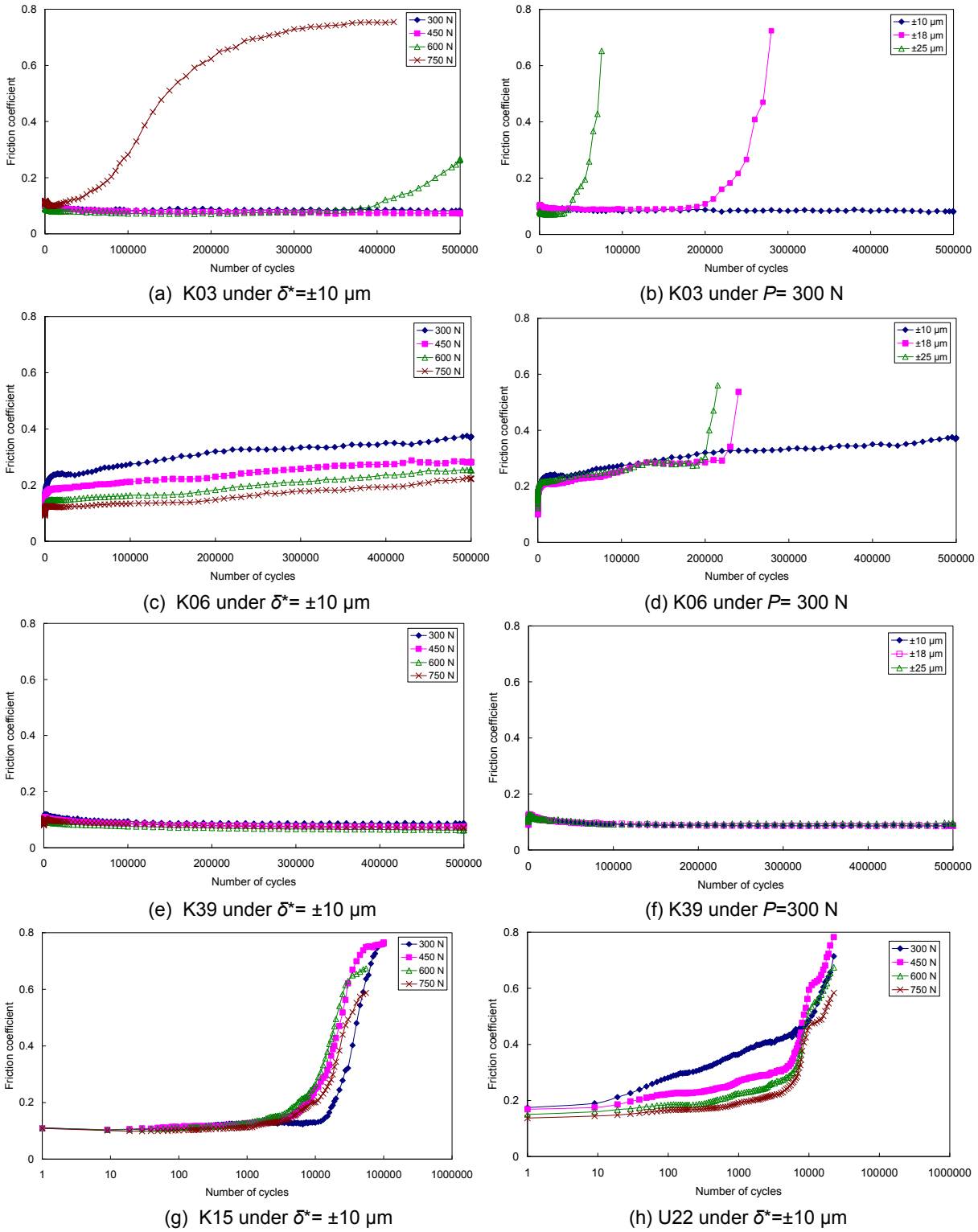

(a) K03 under δ^*=±10 µm

(b) K03 under P= 300 N

(c) K06 under δ^*= ±10 µm

(d) K06 under P= 300 N

(e) K39 under δ^*= ±10 µm

(f) K39 under P=300 N

(g) K15 under δ^*= ±10 µm

(h) U22 under δ^*=±10 µm

Figure 143: evolution of friction coefficient with number of cycles.

Coating K39 kept a low friction during the whole test duration whatever the displacement amplitude and the normal load. In the initial stage, the friction coefficient was about 0.09~0.12, then it gradually decreased to a stable value about 0.06~0.1 (Figure 143e and f).

Coating K15 resulted in low initial friction coefficient (about 0.08~0.11), which was almost independent of the normal load. The friction coefficient of U22 in the initial test stage was about 0.16~0.24, which decreased with increasing the normal load. Both K15 and U22 could only sustain a short test duration even under the low displacement amplitude of ±10 μm, and their friction coefficients started to rapidly increase at about 10000 cycles.

2.1.2 Effect of test parameters on friction coefficient

In Chapter 5, the initial friction coefficient of pressure sprayed MoS_2 coating depended on the test parameters. We also use the initial friction coefficient to analyze the effects of test parameters for the bonded solid lubricant coatings. Figure 144a, b and c respectively present the evolution of initial friction coefficient with the normal load for the coatings K03, K06 and K39, where there was no obvious influence of displacement amplitude on the initial friction coefficient. The initial friction coefficient of K06 decreased with the increase of normal load, while for K03 and K39, the initial friction coefficients were almost independent of the normal load. K15 and U22 were just tested under ±10 μm, the friction coefficient of U22 decreased with the increase of normal load, while that of K15 almost kept constant.

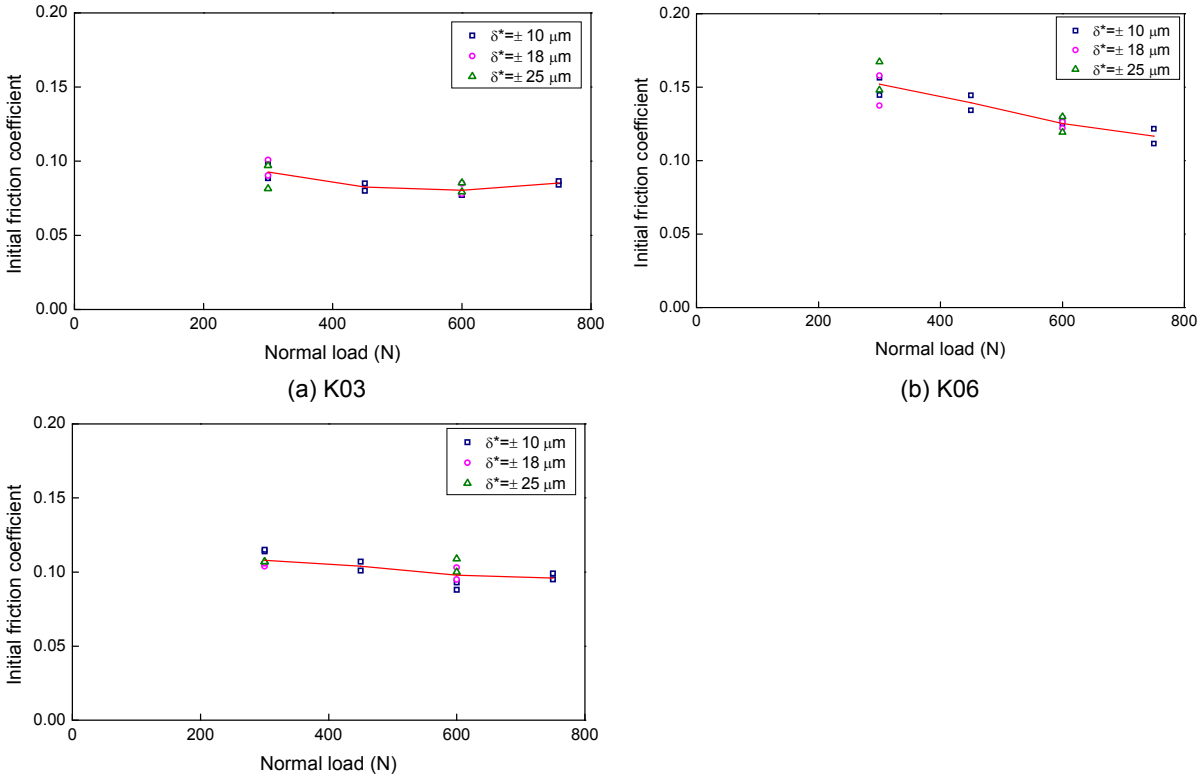

(a) K03

(b) K06

(c) K39

Figure 144: Evolution of initial friction coefficient with normal load.

2.1.3 Effect of coating properties on friction coefficient

Figure 145 shows the comparison of friction coefficients for the coatings under the same test parameters (δ^*=±10 μm, P=300 N). The coatings based on PTFE (K03, K15 and K39) presented low friction coefficient, about 0.08~0.12, and the value slightly decreased with the friction process, while for the coatings based on MoS_2 (K06 and U22), the friction coefficients were higher, about 0.12~0.22, and gradually increased with the number of cycles, which is likely related to the gradual oxidation of MoS_2 [167].

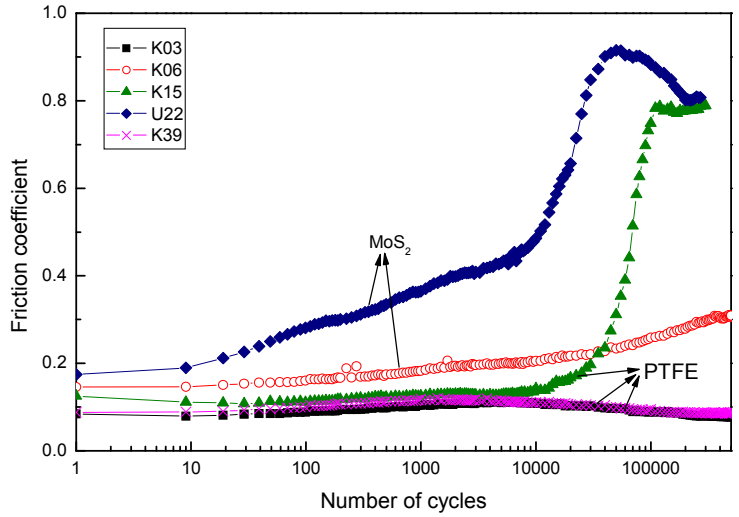

Figure 145: Comparison of evolution of friction coefficient for the coatings under δ*=±10 µm, P=300 N.

In Figure 146, under δ*= ±10 µm, the initial friction coefficients of the coatings based on MoS_2 (U22 and K06) obviously decreased with normal load, which was in accordance with the results of pressure sprayed MoS_2 coating (Chapter 5) because high contact pressure can promote the formation of a transfer film on the counterface [274]. For the coatings based on PTFE (K03, K15 and K39), the values of initial friction coefficient were lower and they almost remained constant with increasing the normal load. Therefore, the friction reduction of the coatings mainly depended on the material of solid lubricant.

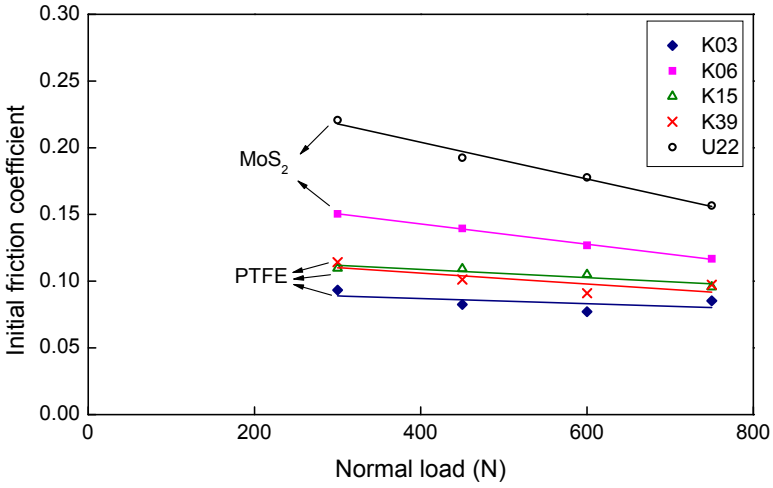

Figure 146: Initial friction coefficient of the coatings under δ*=±10 µm.

Multiplying the initial friction coefficient by normal load, we can get a relevant tangential force. The relationship of this tangential force with normal load can be fitted by a linear equation (Figure 147).

$$Q = \alpha \cdot P + Q_0$$

$$\Rightarrow \frac{Q}{P} = \alpha + \frac{Q_0}{P} \Rightarrow \mu = \frac{Q_0}{P} + \alpha \qquad (6\text{-}6)$$

The Eq.6-6 is same as Eq.5-1, so α is the limit value of initial friction coefficient under very high contact pressure. The values of α and Q_0 for the coatings are listed in Table 45, where the coatings based on PTFE have close values.

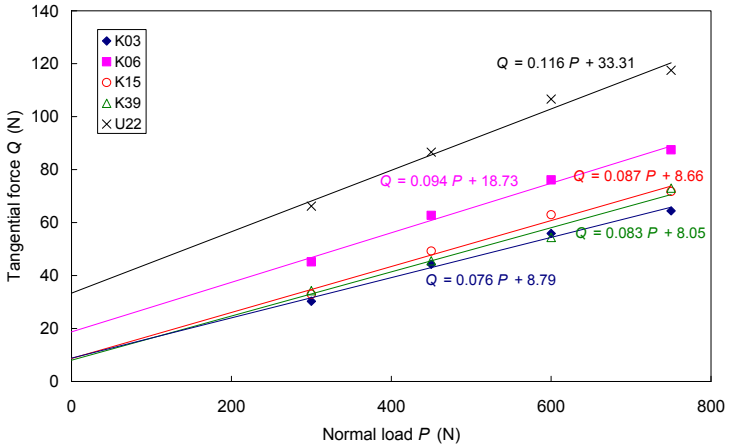

Figure 147: Evolution of initial tangential force with normal load.

Table 45: Limit initial friction coefficient of the coatings.

Coating	K39	K15	K03	K06	U22
Limit initial friction coefficient α	0.083	0.087	0.076	0.094	0.116
Q_0	8.05	8.66	8.79	18.73	33.31

In brief, the friction reduction of the coatings was closely related to the material of solid lubricant. The coatings based on the same solid lubricant presented the similar trend in the evolution of friction coefficient with the test process and with the normal load. The different binding agents cannot change the evolution trend of the friction coefficient, but slightly influenced their values, because the principle of friction reduction and wear mechanism mainly depend on the solid lubricant in the coatings. No obvious relationship was found between the friction coefficient and the mechanical properties (H and E^*_c).

2.2 Wear mechanism

During the friction process, coating K03 was gradually worn being scraped to the two sides of the contact area due to its low cohesion strength, and formed cumulus (Figure 148a). After the coating became enough thin, it detached from the convex ridges of the substrate, and the coating in the grooves of the substrate continued working there (Figure 148b). No crack was found in the contact area, so the good ductility brought the coating a good endurance.

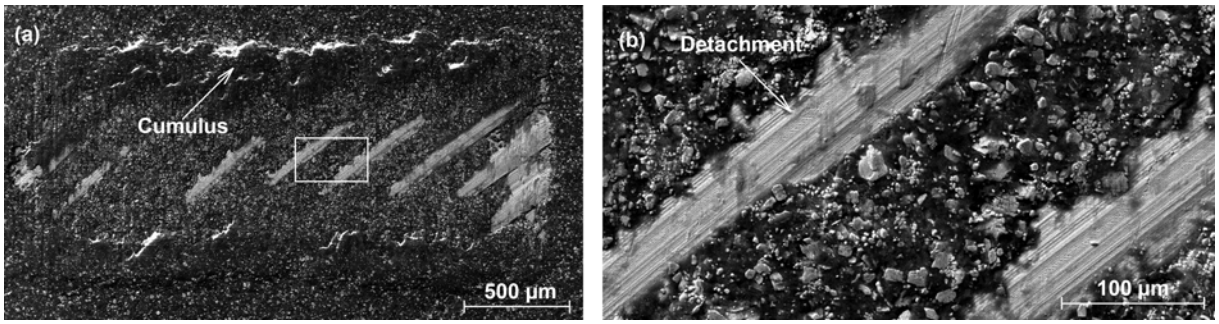

Figure 148: (a) SEM micrographs of wear scar for K03 under 600 N, ±10 µm and 500000 cycles, (b) local magnification.

Coating K39 presented the best wear resistance among the five coatings. In all the tests, neither crack nor detachment was found in the wear scars. Figure 149a, b, c respectively show the wear scar of the counterpart after 3 000, 30 000 and 300 000 cycles under ±10 μm and 600 N, where a transfer film gradually formed and thickened, which is the reason why the friction coefficient decreased with the test process (Figure 145). After 300 000 cycles, there was some strip debris on both sides of the wear scars of the counterpart (Figure 149c) and the coating (Figure 149d), which reflected the excellent ductility of the coating material. Even for the largest displacement amplitude (±25 μm), there were only some small detachments of solid lubricant particles from the binding agent after 500 000 cycles. So, the coating properties, including its excellent ductility, cohesion and bonding strength, and the ability of forming transfer film on the counterface, resulted in the outstanding wear resistance of K39.

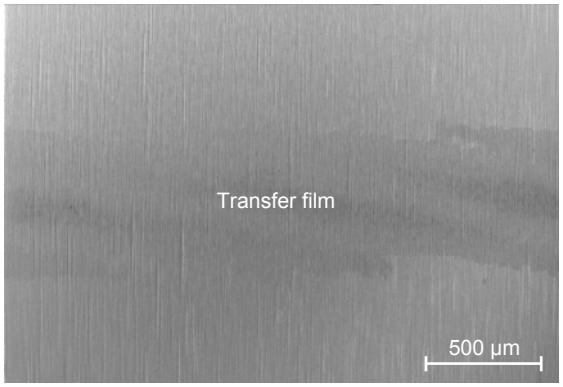

(a) Wear scar of the counterpart, 3 000 cycles

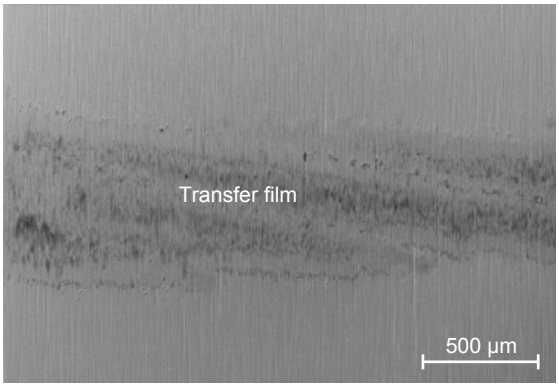

(b) wear scar of the counterpart, 30 000 cycles

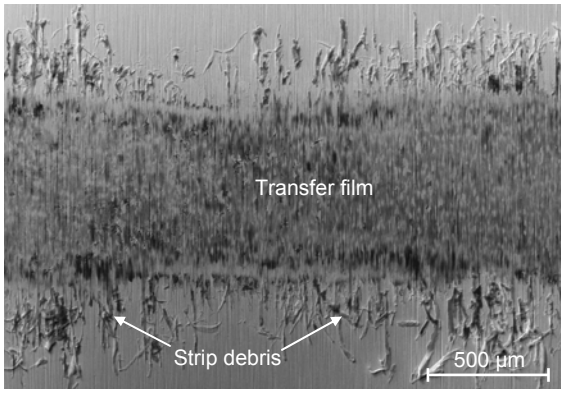

(c) Wear scar of the counterpart, 300 000 cycles

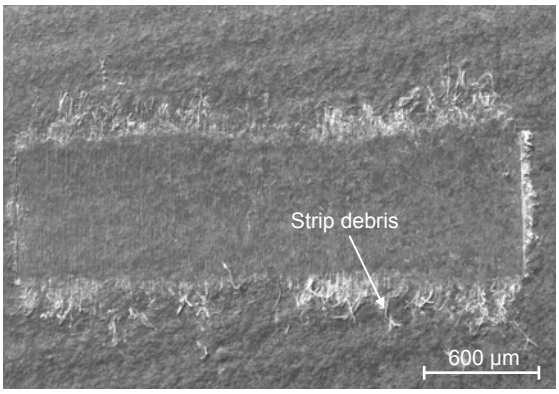

(d) wear scar of K39, 300 000 cycles

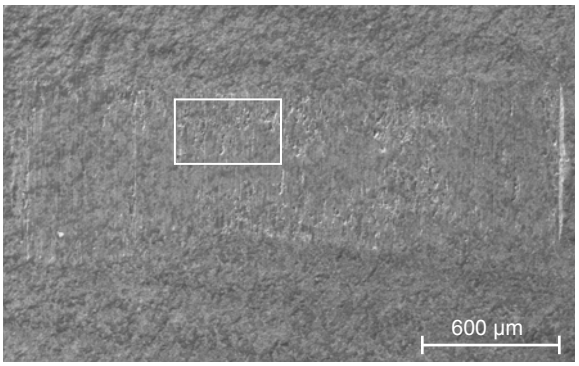

(e) Wear scar of K39

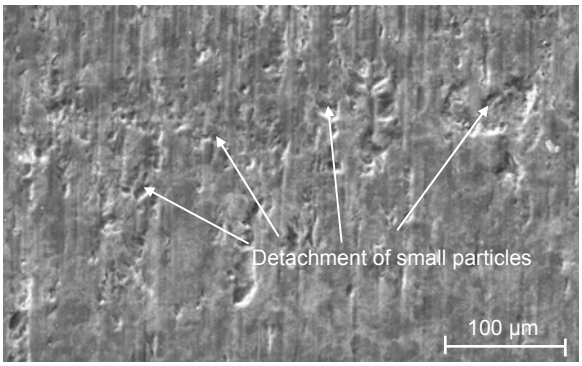

(f) local magnification

Figure 149: SEM micrographs of wear scar for coating K39 and the counterpart under:
(a) (b) (c) (d) ±10 μm, 600N, (e) (f) ±25 μm, 300N, 500 000 cycles.

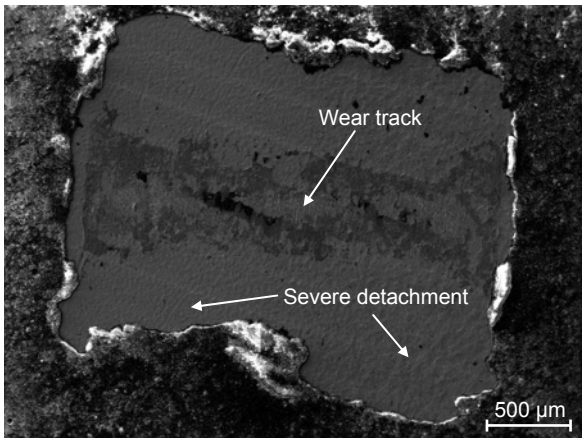

Figure 150: SEM micrographs of wear scar for K15 under ±10 µm, 600 N, 55 000 cycles.

K15 failed in a short test duration even under the low displacement amplitude of ±10 µm. The reason of failure can be easily found from Figure 150, where the coating severely detached from the substrate around the wear track, which is in accordance with the severe detachment in ball cratering tests (Figure 141c). So, the short lifetime of K15 was caused by the insufficient bonding strength, and the lifetime cannot reveal the real wear resistance of the coating itself.

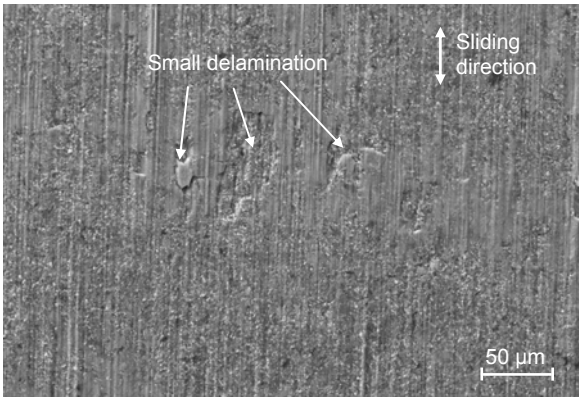

(a) Wear scar of K06

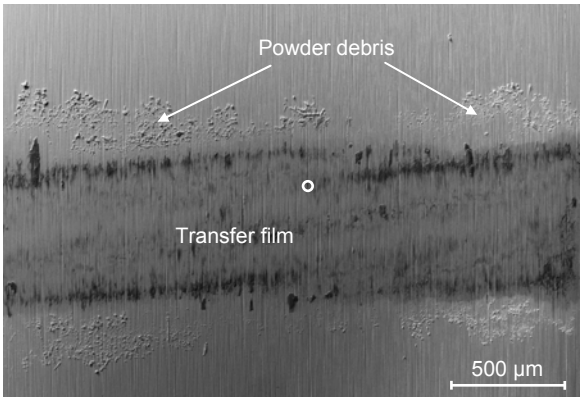

(b) wear scar of the counterpart

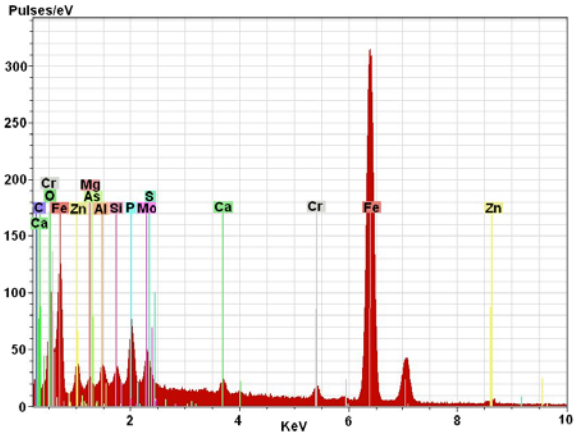

(c) EDX analysis of the small circle area in (b)

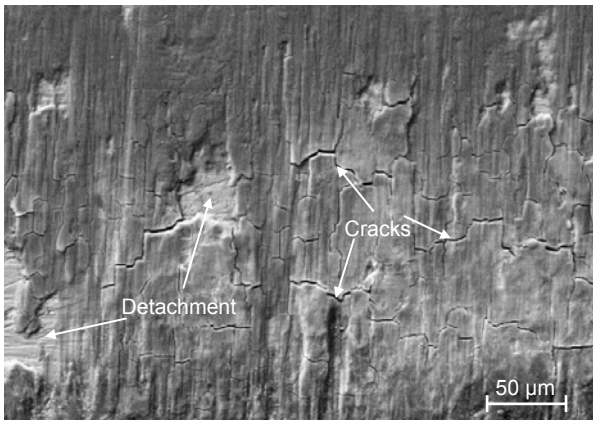

(d) wear scar of K06

Figure 151: SEM micrographs and EDX analysis of wear scar for coating K06:
(a) (b) ±10 µm, 600N, 30 000 cycles, (d) ±10 µm, 600N, 500 000 cycles.

After 30 000 cycles under ±10 µm and 600 N, some small delamination occurred in coating K06, as shown in Figure 151a. For the small displacement amplitude, most of the sheet particles detached

from the coating stayed in the contact area and were repeatedly squeezed to form transfer film on the counterface (Figure 151b). Figure 151c shows the EDX analysis of the small circle area in the wear scar of the counterpart, where the spectra of K06 can be found. The gradual oxidization process of MoS_2 made the transfer film and the coating become brittle, which induced powder debris around the wear scar (Figure 151b) and numerous cracks and detachment of the coating (Figure 151d). The delamination, powder debris and cracks also resulted from poor ductility and insufficient cohesion strength of K06. With the increase of displacement amplitude, the debris can be more easily ejected from the contact area, and the possibility of forming transfer film on the counterface decreased, which resulted in the decrease of lifetime under larger displacement amplitude, as shown in Figure 153c.

Coating U22 was scraped in the center part of the contact area and piled on both sides during the fretting process, then the thickening area broke and detached from the substrate due to high intrinsic stress (Figure 152a). After 10 000 cycles under ±10 µm and 600 N, there were a great quantity of powder debris around the wear scar and local detachments and cracks (Figure 152b). At the same time, no uniform transfer film was formed on the counterface. According to the wear scar in Figure 152c and the transverse EDX line scan analysis in Figure 152d, there were only some island transfers. The bad ductility, low cohesion and bonding strength, and the poor ability of forming transfer film resulted in the short lifetime of this coating.

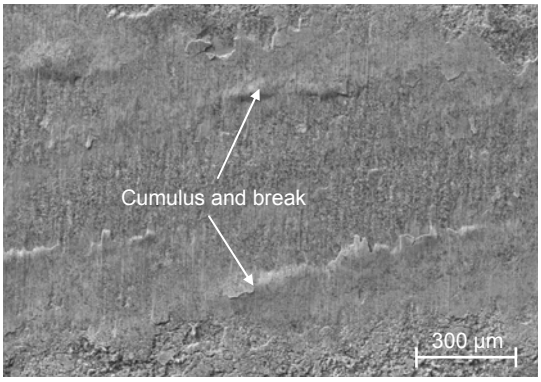

(a) Wear scar of U22, 3 000 cycles

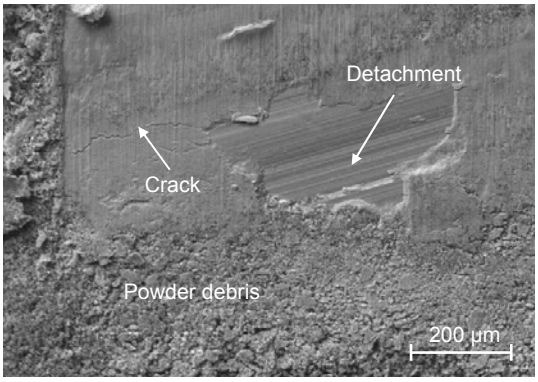

(b) Wear scar of U22, 10 000 cycles

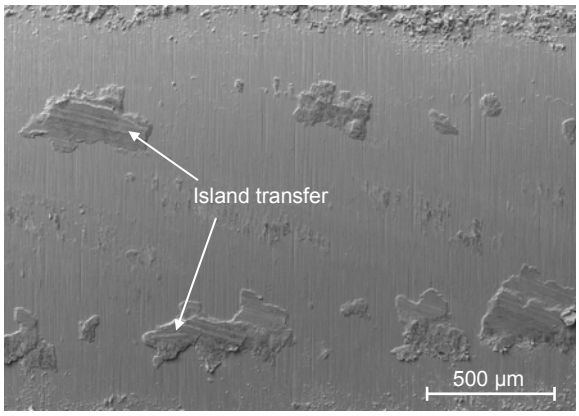

(c) Wear scar of the counterpart, 10 000 cycles

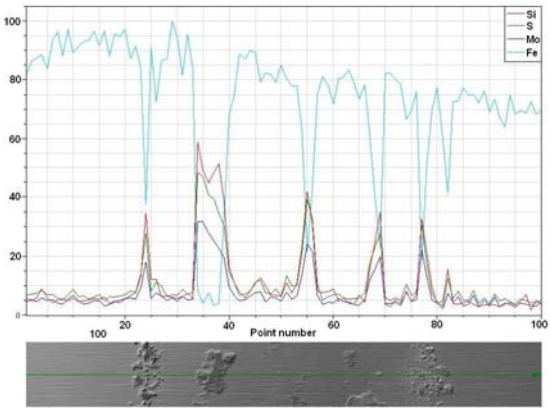

(d) EDX line scan of wear scar on the counterpart

Figure 152: SEM micrographs of wear scar for coating U22 and the counterpart: ±10 µm, 600 N.

2.3 Coating lifetime

2.3.1 Definition of coating lifetime

As described in Chapter 5, if the coating is worn through during the test duration, the number of cycles when the friction coefficient reaches three times its initial value will be defined as the coating

lifetime, N_c. On the other hand, if the substrate is not reached during the test duration of 500 000 cycles, the coating lifetime will be extrapolated according to the maximal wear depth and the coating thickness, i.e., the coating lifetime is the product of the test duration and the ratio of the coating thickness to the maximal wear depth.

According to this definition, the lifetime of the coatings is shown in Figure 153. K39 showed the best endurance, and it could survive the test duration of 500 000 cycles whatever the test parameters (Figure 153a). The coatings K06 and K03 had an equivalent endurance, under low normal loads, K03 was better, while K06 was better under high normal loads (Figure 153b and c). Both K15 and U22 were worn through in a short duration even under the low displacement amplitude (Figure 153d).

2.3.2 Effect of test parameters on coating lifetime

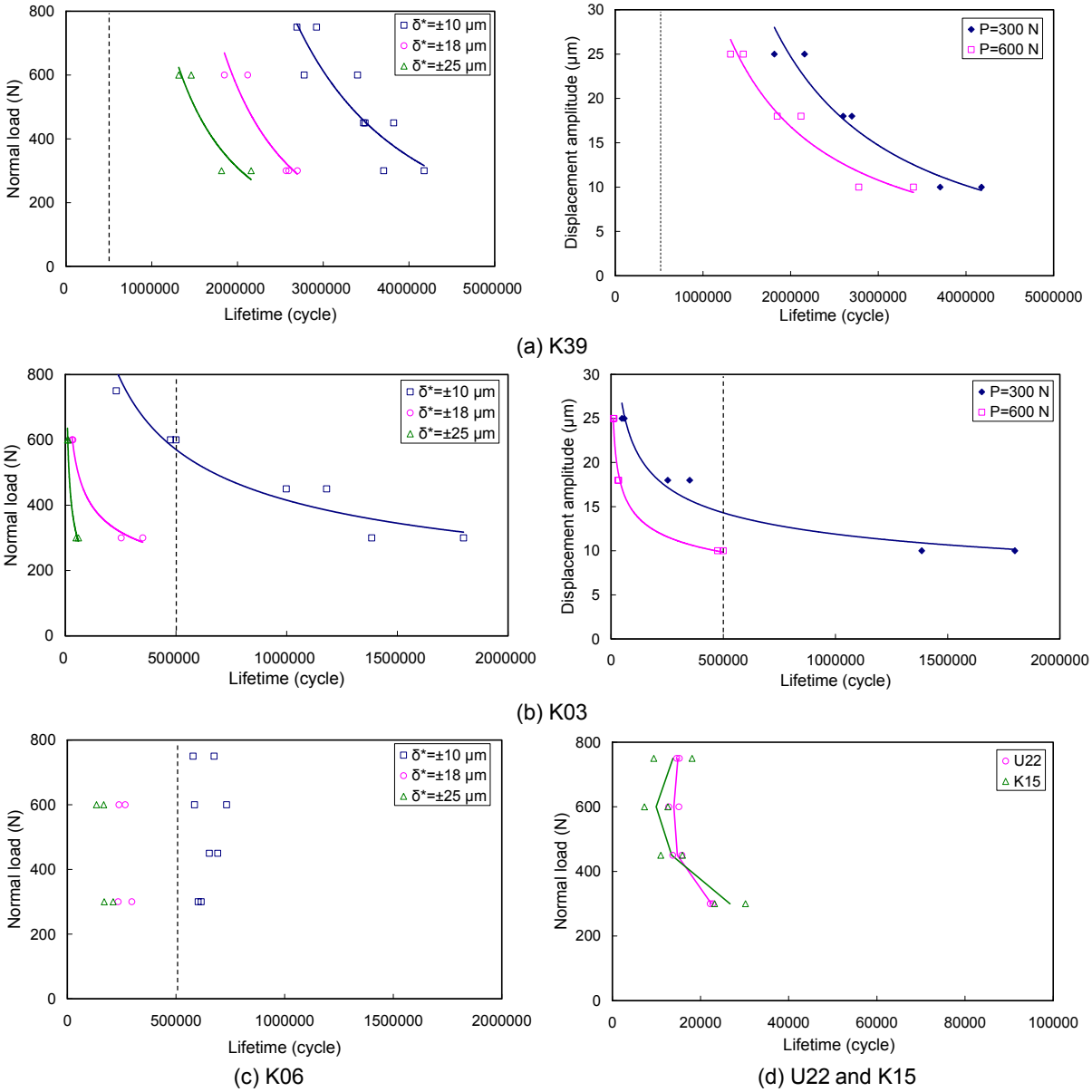

(a) K39

(b) K03

(c) K06

(d) U22 and K15

Figure 153: Effect of test parameters on coating lifetime.

The endurance of the coatings was strongly influenced by test parameters. For all the coatings tested under different displacement amplitudes, the lifetime decreased with the increase of displacement amplitude (Figure 153a, b, c and d). With the increase of normal load, the lifetime of

K03 and K39 rapidly decreased (Figure 153a and c), while the lifetime of K06 was almost independent of the normal load under our test conditions (Figure 153c). As for the coatings K15 and U22, they were just tested under ±10 μm, where the lifetime decreased when the normal load increased from 300 N to 450 N, and then it maintained a stable value with the continuous increase of the normal load (Figure 153d).

2.3.3 Effect of coating properties on coating lifetime

2.3.3.1 Material of solid lubricant

The material of solid lubricant in bonding coatings is very important, which decides the friction reduction, wear mechanism, and mechanical properties.

The coatings based on PTFE (K03, K15 and K39) have lower friction coefficients, which mean lower frictional loads and are beneficial to the lifetimes of the coatings.

The lifetimes of the coatings depend on their wear mechanism. The wear mechanism of the coatings based on PTFE is the forming, thickening and breaking process of the transfer film, while the wear of the coatings based on MoS_2 will be influenced by the oxidation of MoS_2, which make the frictional load gradually increase and the transfer film becomes brittle.

From the features of the scratch tracks in Figure 137, the coatings based on PTFE presented better ductility and cohesion strength, so they have better wear resistance.

2.3.3.2 Cohesion strength

Cohesion strength is an important property for the wear resistance of a coating, and it can directly influence the forming of cracks and chippings. In ball cratering tests, the coating with higher cohesion strength resulted in better ball cratering resistance. However, under fretting conditions, the third body plays a very important role for the endurance of a solid lubricant coating, and the lifetime of the coating not only depends on the cohesion strength but also depends on the rheology and flow of transfer film and debris. So, despite its low cohesion strength, K06 presented a long lifetime in fretting tests.

2.3.3.3. Bonding strength

High bonding strength between the coating and the substrate is the precondition of good wear resistance. The bonding strength depends on the preparation process of the coating. In general, proper pretreatments of the substrate surface (cleaning and roughening) and a high hardening temperature can improve the bonding strength. However, the hardening temperature is decided by the materials of solid lubricant and bonding agent. The thickness of a coating is another factor influencing its bonding strength. Every coating has a suitable range of thickness according to the deposition technique and the coating material. Once the thickness exceeds this range, high internal stress at the interface can weaken the bonding strength. Inadequate bonding strength can result in severe detachment of the coating from the substrate, and the large detached piece cannot stay in the contact area, so the coating has a short lifetime. For example, the short lifetime of K15 is caused by the severe detachment (Figure 150).

2.3.3.4 Transfer film

The formation and maintenance of transfer film is the most important factor for the lifetime of solid lubricant. Solid lubricant coatings usually have low shear strength at the interface, so the top layer can be easily removed. If the top layer removed from the coating cannot form transfer film on the counterface, then it will be ejected out of the contact area as debris. If the transfer film can sustain long time to break, then the coating has a long lifetime.

In the tests, the transfer film of K39 was gradually formed and thickened, and due to its excellent ductility, the transfer film can sustain long time. Although K06 presented a poor ball cratering resistance due to the low cohesion strength and poor ductility, it had a good endurance under fretting conditions because of the formation of a transfer film on the counterface. However, the transfer film can easily break due to its poor ductility and the oxidation of MoS_2, so the lifetime of K06 was shorter than that of K39. U22 could not form any uniform transfer film on the counterface until fractures and detachments of the coating from the substrate took place, which induced a short lifetime.

2.3.3.5 Hardness and elastic modulus

Mechanical properties (hardness and elastic modulus), especially the hardness, are very important for the wear resistance of hard coatings, and the ratio of H to E^*_c is also an important reference for the abrasion resistance of hard coatings [115]. However, we cannot find any obvious effect of the hardness on the coating lifetime. Although the hardest coating, K39, presented the best endurance, the other coatings with similar hardness, like K03 and U22, K06 and K15, exhibited very different lifetimes. The coatings with low E^*_c and high ratio H/E^*_c, H^2/E^*_c were gradually worn, while detachements took place for the coatings with high E^*_c and low ratio H/E^*_c, H^2/E^*_c.

Table 46: Relationships between fretting behaviors and coating properties.

Coating	K39	K15	K03	K06	U22
Fretting lifetime	1	4	3	2	4
Friction coefficient	2	3	1	4	5
Wear mechanism	adhesion	severe detachment	adhesion	delamination, adhesion, oxidation	detachment, oxidation
Based solid lubricant	PTFE	PTFE	PTFE	MoS_2	MoS_2
Critical load	1	2	3	5	4
Ductility	1	2	3	4	4
Hardness H	1	5	3	4	2
Reduced elastic modulus E^*_c	4	3	5	1	2
H/E^*_c	1	4	2	5	3
H^2/E^*_c	1	4	2	5	3
Thickness	1	2	3	3	3

In brief, the relationships between fretting behaviors and coating properties are listed in Table 46. Among the coating properties, high H may be inessential for the lifetime of a soft solid lubricant coating, while low E^*_c and high ratio H/E^*_c, H^2/E^*_c can benefit the wear resistance. The bonding strength with the substrate is the precondition of good endurance. The material of solid lubricant can influence the friction reduction, wear mechanism and some coating properties. The important properties for the lifetime of solid lubricant coatings under fretting conditions are the cohesion strength, ductility and the ability of forming and maintaining a transfer film on the counterface.

3. Coating selection

3.1 Requirements

For solid lubricant coatings, there are two main requirements from the tribological viewpoint: low friction coefficient and good endurance. In fact, we must also consider the requirements from other aspects, such as the service temperature, the corrosion protection, the relative humidity, the ambience and the load carrying capacity, etc. These requirements may be considered as prior conditions in the

pre-selection tool, and according to the characteristics of the coatings suggested by providers, some coatings meeting these requirements can be picked up (Chapter 3).

3.2 Selection criteria

3.2.1 Friction coefficient

Reducing friction is the main objective of using solid lubricant coatings, and the low friction can also reduce the frictional load and mitigate wear of the surface. This criterion is the actual friction coefficient between the contacting surfaces should be smaller than the expected value of the end users.

$$\mu_{act} < \mu_{\exp} \tag{6-7}$$

where μ_{act} is the actual friction coefficient, and $\mu_{\exp}$ is the expected value.

In Chapter 4, the friction coefficient was defined as the ratio of the maximal tangential force to the normal load in a cycle, so this friction coefficient is the maximal value of the cycle. In Figure 101, the area of the quadrangle represents the dissipated energy *Ed* in the cycle, according to which an energy friction coefficient μ_e reveals the mean value of friction coefficient in the cycle [104]. So, the mean value of μ_e during the low friction stage of a test reflects the friction reduction of a coating.

$$\mu_e = \frac{Ed}{4 \cdot P \cdot \delta_0} \tag{6-8}$$

$$\overline{\mu}_e = \frac{\sum_{i=1}^{N_0} \frac{Ed_i}{4 \cdot P_i \cdot \delta_{0i}}}{N_0} = \frac{\sum_{i=1}^{N_0} \mu_{ei}}{N_0} \tag{6-9}$$

where N_0 is the number of cycles in the low friction stage, as shown in Figure 154, in which N_c is the coating lifetime.

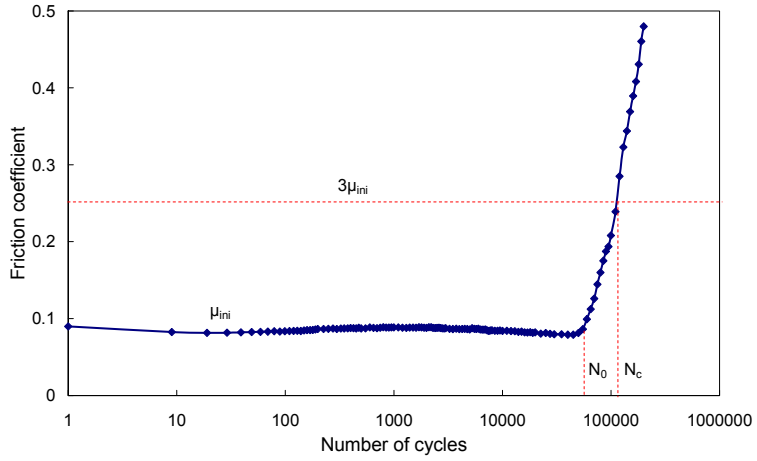

Figure 154: Difference between N_0 and N_c.

According to the definition in Eq.6-9, the mean energy friction coefficients of the coatings are presented in Figure 155. The values of μ_e are lower than the friction coefficients in section 2.1. The mean values $\overline{\mu}_e$ depend on the evolution of friction coefficient in the rubbing process. For the coatings based on PTFE, the friction coefficient decreased with the thickening of the transfer film, and

a good endurance resulted in a large number of cycles with low friction, then a low $\overline{\mu}_e$. For example, $\overline{\mu}_e$ of K03 was in the range of 0.045 ~ 0.075 (Figure 155a), and $\overline{\mu}_e$ of K39 changed between 0.06 and 0.08 (Figure 155b). K15 had a poor endurance and there was not an obvious thickening process of transfer film, so the value of $\overline{\mu}_e$ (Figure 155d) was close to the μ_{ini} in Figure 146. For the coating based on MoS_2, the friction coefficient gradually increased with the test process due to the oxidation of MoS_2, so the value of $\overline{\mu}_e$ was larger than μ_{ini}. For K06, $\overline{\mu}_e$ was in the range of 0.12 to 0.23 (Figure 155c), and $\overline{\mu}_e$ of U22 in the range of 0.18 to 0.36 (Figure 155d).

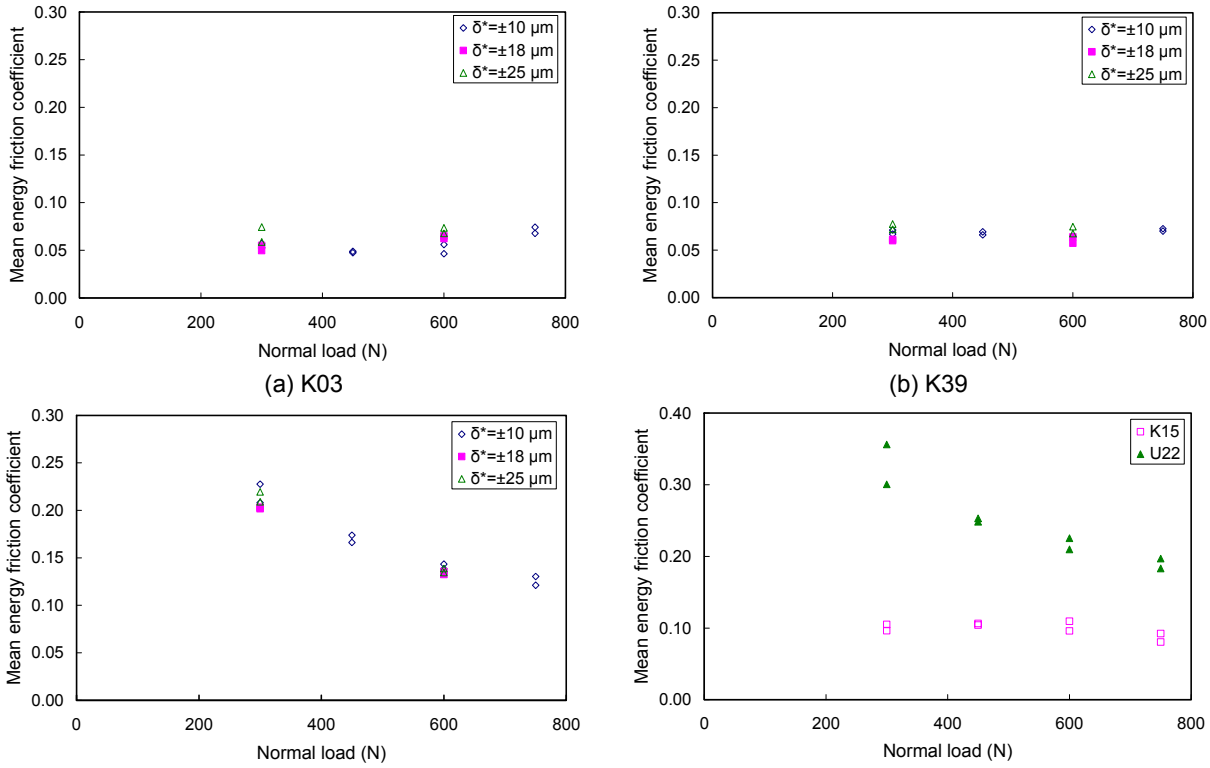

(a) K03 (b) K39

(c) K06 (d) K15 and U22

Figure 155: Mean energy friction coefficient of the coatings.

Table 47: Summary of the friction reduction for the coatings

	μ_{ini}	α	$\overline{\mu}_e$	Effect of P	Effect of δ*	rank
K39	0.09~0.12	0.083	0.06~0.08	→	→	2
K15	0.08~0.11	0.087	0.09~0.11	→	-	3
K03	0.08~0.10	0.076	0.05~0.07	→	→	1
K06	0.11~0.17	0.094	0.12~0.23	↘	→	4
U22	0.16~0.24	0.116	0.18~0.36	↘	-	5

The friction reduction of the coatings is summarized in Table 47. Just from the criterion of friction reduction, the coatings based on PTFE are better than the coatings based on MoS_2 because they have lower and more stable friction coefficient with the change of test parameters. The order from the best to the worst is: K03 ⇒K39 ⇒K15 ⇒K06 ⇒U22. Besides the friction coefficient under common conditions, the effect of running conditions and environment should also be taken into account if the coated component will work in environment with large fluctuation of temperature, RH, load, etc.

3.2.2 Endurance

Endurance is the other important criterion, i.e., the coating should survive a longer lifetime than the expected value.

$$N_c > N_{exp} \quad (6\text{-}10)$$

where N_c is the coating lifetime, and N_{exp} is the expected value of end users.

The endurance test is a time-consuming process, and there are numerous available friction reduction coatings, whose endurances depend on the deposition process and parameters. Therefore, it is better to use some simple techniques to further screen out the poor ones from the candidate coatings obtained by pre-selection tools (databases or expert-systems). Ball cratering and scratch tests are popular techniques for evaluating coatings.

3.2.2.1 Relationships between scratch test and fretting endurance

Scratch tests can be used to estimate the ductility, critical loads for cohesion failure and bonding failure of coatings, which are important factors influencing the fretting endurance. From Table 42, except K15, the coatings with a high critical load and good ductility exhibited good endurance.

The ductility can only be qualitatively assessed through the features of debris and scratch tracks. For soft solid lubricant coatings, the evaluation of cohesion strength and bonding strength is inaccurate because it is relatively difficult to accurately identify the cohesion failure, especially for the coatings with poor ductility, like K06 and U22 (Figure 137a and b). The insufficient bonding strength of K15 was not thoroughly exposed in Figure 137d. In addition, at the beginning of a scratch test, due to the low hardness of the coating, it is difficult to estimate whether the indenter has contacted with the coating or not. Therefore, the results of scratch tests can be used as references for fretting endurance of solid lubricant coatings, but they are not very reliable.

3.2.2.2 Relationships between ball cratering and fretting endurance

From Figure 140 and Figure 153, the coatings presented similar characteristics of wear resistance in both the ball cratering and the fretting tests. In the two tests, K03 and K39 were gradually worn and there was no crack in the contact area, while cracks and local detachments from the substrate were found for K06 and U22. K15 severely detached from the substrate in the two tests, i.e., both tests revealed the poor bonding strength of K15. The endurance of the coatings was also similar in the two tests. In ball cratering, K39 was the best coating, K15 and K03 followed, and K06 and U22 were the worst. In fretting tests, K39 had the best endurance, K06 and K03 followed, and K15 and U22 were the worst (Table 48). Figure 156 shows the relationships more straightforwardly, where only K15 and K06 presented quite different endurance in the two tests.

Table 48: Relationships between ball catering resistance and fretting behaviors of the coatings.

Coating	K39	K15	K03	K06	U22
Ball cratering resistance	1	2	3	4	5
Wear mode in ball cratering	abrasion	severe detachment	abrasion	detachment	detachment
Fretting lifetime	1	4	3	2	5
Friction coefficient	2	3	1	4	5
Wear mechanisms in fretting tests	adhesion	severe detachment	adhesion	adhesion, oxidation, delamination	detachment, oxidation

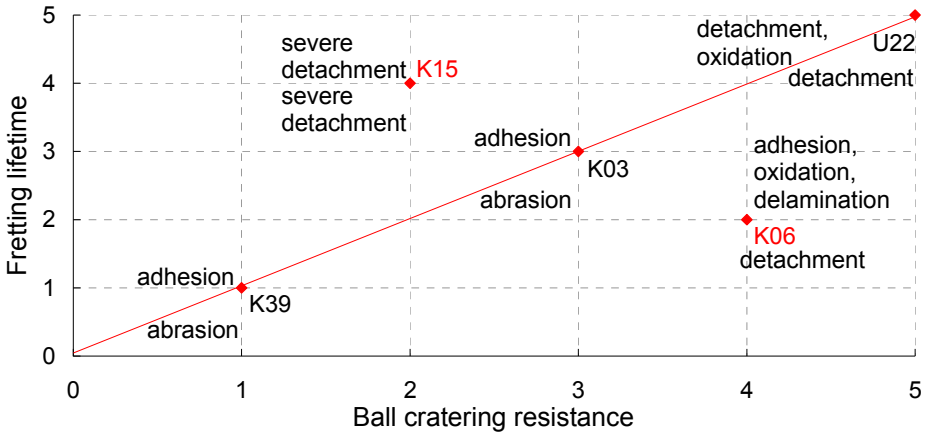

Figure 156: Relationships between ball catering resistance and fretting behaviors of the coatings.

In fact, the behaviors of K15 in two tests are essentially consistent. Excellent wear resistance of K15 in ball cratering tests should be attributed to the low contact pressures (240 MPa ~ 410 MPa), under the low contact pressures, good cohesion strength of K15 led to a long duration before the nucleation of cracks. Once cracks took place, a severe detachment followed, as shown in Figure 141c. In fretting tests, the high contact pressures (584 MPa ~ 923 MPa) induced the fracture of the coating in a short period, and then rapidly detached from the substrate due to the poor bonding strength (Figure 150). Both tests revealed the insufficient bonding strength of K15, so it cannot be looked as a candidate coating despite its good endurance in ball cratering.

The poor wear resistance of K06 in ball cratering is because its low cohesion strength rapidly resulted in cracks and detachment in 5 minutes under 60 rpm and 1 N, as shown in Figure 157a. Meanwhile, the debris detached from the coating could not stay in the contact area under the relative movement of the ball cratering test, so the formation of a transfer film was very difficult on the counterface. Figure 157b shows the wear scar of the ball after 5 minutes under 60 rpm and 1 N, where only few island transfers were found. The EDX analysis of the small circle area in Figure 157b showed that MoS_2 did not exist (Figure 157c), i.e., no transfer film was formed on the counterface. This result is in agreement with the rapid decrease of coating lifetime with the increase of displacement amplitude in fretting tests, because the formation of transfer film is more difficult under larger displacement amplitudes due to the ejection of debris. So, the difference in the aspect of forming transfer film resulted in the different endurances of K06 in two tests, and the ability of forming transfer film in fretting contact cannot be assessed by ball cratering tests.

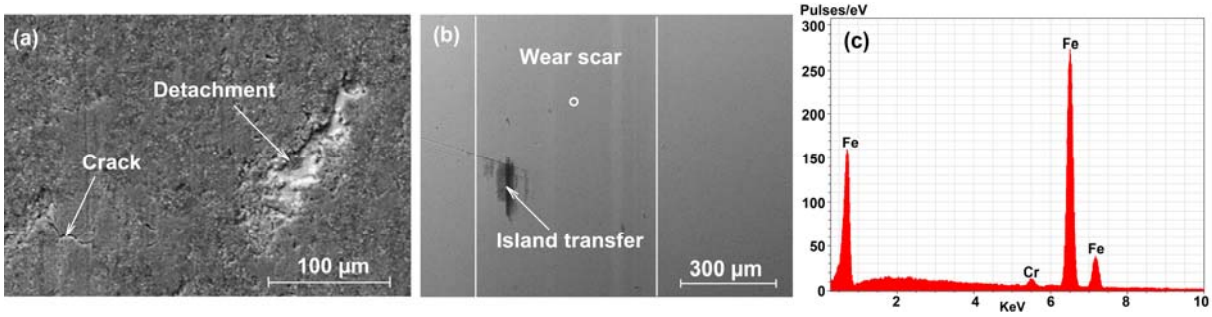

Figure 157: SEM micrographs of wear scars for (a) K06 and (b) the ball in ball cratering tests under 60 rpm, 1 N, 5 min, (c) EDX analysis of the small circle area in (b).

The wear resistance evaluation of the coatings in ball cratering tests was in agreement with the results of fretting tests. The coatings with good ball cratering resistance, K39 and K03, exhibited a long lifetime in fretting tests except for K15 due to its insufficient bonding strength with the substrate. If

ball cratering is used to pre-select coatings for fretting applications, some poor coatings can be quickly removed, and the number of candidate coatings for further tribological tests will be largely cut down. In the present study, coatings K06, K15 and U22 will be removed by the pre-selection process of ball cratering; only K39 and K03 need to be further assessed by fretting tests. The best coating, K39, was included in the candidate ones, and much time can be saved in fretting tests. However, some coatings with good fretting performance may be missed in the pre-selection process of ball cratering, like K06, because the ability of forming transfer film of a coating under fretting conditions cannot be estimated by ball cratering tests.

For the coatings passing the evaluation techniques, their endurance need to be further compared by fretting tests, the wear volume is often used as an endurance indication of materials under friction contacts.

3.2.2.3 Wear volume

The transverse profiles of the wear scars were measured by a stylus profilometer. In order to compare the wear resistance of the coatings themselves, we just measured the wear scars where the substrates were not yet reached after the test duration. Each wear scar was measured 5 times, and the mean values of the depth and area of the cross sections were used. The area of a cross section, S, was calculated by the area of the crater, S^-, minus the area of the cumulus, S^+ (Figure 158). The wear volume is the product of the mean area of the cross sections and the length of the wear scar.

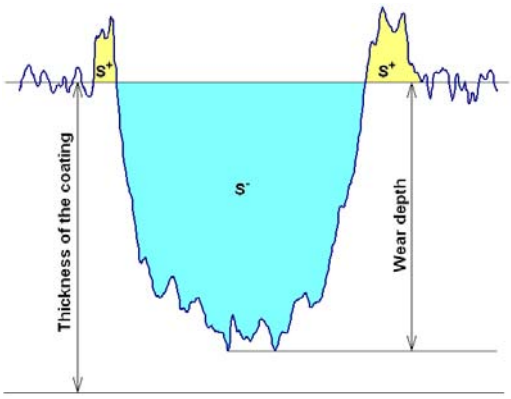

Figure 158: transverse profile of a wear scar.

The wear of a coating is the result of frictional energy dissipation, and there is a direct relationship between the wear volume, V, and the cumulated dissipated energy, $\sum Ed$. $\sum Ed$ can be figured out by the Eq. 6-11. Figure 159 shows the evolution of wear volume V with cumulated dissipated energy $\sum Ed$, which can be expressed by Eq. 6-12, where K_e is an energy wear rate, and $-\alpha/K_e$ is the lowest energy to initiate wear.

$$\sum Ed = \sum_{i=1}^{N} 4 \cdot \mu_i \cdot P_i \cdot \delta_{0i} \qquad (6\text{-}11)$$

$$V = K_e \cdot \sum Ed + \alpha \qquad (6\text{-}12)$$

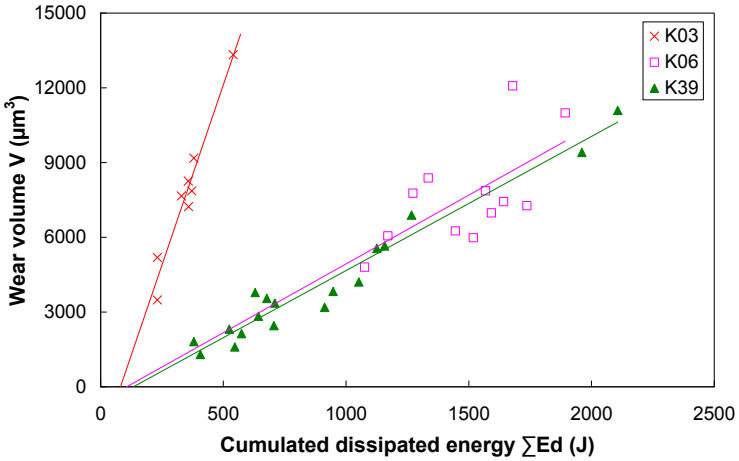

Figure 159: Evolution of wear volume *V* with cumulated dissipated energy ∑*Ed*.

In Figure 159, K_e of K03 is 29.9 µm^3/J, which is larger than that of K06 (5.5 µm^3/J) and K39 (5.4 µm^3/J). The energy wear rate points out that K06 and K39 have similar wear resistances, which are better than K03. However, the energy wear rate cannot denote the real endurance of the coatings because K06 and K39 presented quite different endurance both in ball cratering and in fretting tests. From the data points around the curves, due to the higher friction coefficient of K06, the cumulated dissipated energy of K06 is larger than that of K39 under same test parameters and duration, which induced the larger wear volume and the shorter lifetime of K06. The data of K06 is more discrete because of its special wear mechanisms, where the coating easily delaminated and the particles can be transferred to the counterface or be ejected out of the contact area, which induced the fluctuation of wear volume. It is impossible to accurately assess the endurance of the coatings just through comparing the energy wear rate of the coatings because the different frictional energy is dissipated under same test parameters and the different thickness of the coatings can caused a difference of endurance even though a same volume is worn. The wear rate can only reflect the increase rate of wear volume with the cumulated dissipated energy.

3.2.2.4 Coating lifetime

Coating lifetime is the most direct indication of endurance. However, the lifetime of coatings depends on test parameters. The change of normal load or displacement amplitude resulted in different lifetime curves for the coatings K03, K39 and K06, as shown in Figure 153. So, it is not easy to compare the coating lifetime facing the changing lifetime curves.

3.3 Energy approach

In fact, the change of normal load and displacement amplitude can be expressed by one variable—the dissipated energy, which can probably eliminate the effect of test parameters on the lifetime curve, so we try to use the energy approach to describe and compare the endurance of the coatings.

3.3.1 Initial maximal dissipated energy density

Initial maximal dissipated energy density, $Ed_{0\,max\,ini}$, signifies the maximal local dissipated energy in the contact area during the initial cycles of a test, which is related to initial friction coefficient, maximal contact pressure, contact area size and actual displacement amplitude. For cylinder-on-flat configuration, the maximal dissipated energy density always takes place at the center line of contact

area, where contact pressure presents the maximal value. In gross slip fretting regime with low displacement amplitude, $Ed_{0\ max\ ini}$ is approximately expressed as:

$$Ed_{0\ max\ ini} = 4\mu_{ini} \cdot \delta_{0ini} \cdot p_0 \qquad (6\text{-}13)$$

where p_0 is the maximal contact pressure (Table 37), μ_{ini} and δ_{0ini} are respectively initial friction coefficient and initial actual displacement amplitude.

$Ed_{0\ max\ ini}$ - N_c curves of the coatings are shown in Figure 160, where the tribological performance of each coating can be expressed by one master curve whatever the normal load and the displacement amplitude. The master curves include comprehensive information of tribological performance and comparing the master curves of different coatings can help the coating selection.

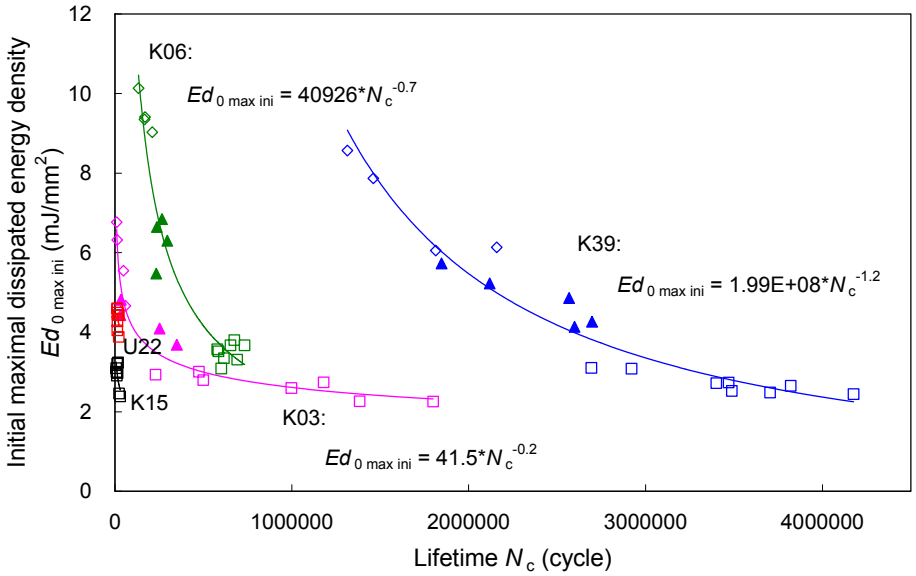

Figure 160: $Ed_{0\ max\ ini}$ - N_c master curves for the coatings (□: δ*=±10 μm, ▲: δ*=±18 μm, ◇: δ*=±25 μm).

- Firstly, the endurance of the coatings can be straightforwardly identified from the curves. K39 presents the best endurance; U22 and K15 are the worst; K03 and K06 occupy the middle places, where K06 is better than K03 except under small displacement amplitude and low normal load.

- Secondly, the friction reduction of the coatings can also be compared through the master curves. According to Eq.6-13, $Ed_{0\ max\ ini}$ depends on maximal contact pressure, initial actual displacement amplitude and initial friction coefficient. For given test parameters, the maximal pressure is the same for all of the coatings because the thin coating may be ignored in the calculation of contact pressure. In gross slip regime, the initial actual displacement amplitude should be close for the coatings under a given displacement amplitude. So, the values of $Ed_{0\ max\ ini}$ under given test parameters mainly depend on initial friction coefficient. Comparing the ranges of the $Ed_{0\ max\ ini}$ values under a given displacement amplitude, we can rank the friction reduction of the coatings. For example, according to the data signified by "□" in Figure 160, K03, K15 and K39 present similar and low friction coefficient, the friction reduction of U22 is the worst among the coatings.

- Finally, the points around the master curves also reveal the effect of test parameters on coating lifetime. From Figure 160, the lifetimes of K03 and K39 depend on displacement amplitude and normal load, while for K06, the data under same displacement amplitude are close, i.e., its lifetime is almost independent of the normal load.

Comparing the curves, K39 is the best coating from both endurance and friction reduction. If friction reduction is prior in the requirements, K03 can rank the second. If the load is unstable, or coating

endurance is prior, then K06 is the second. So, a comprehensive comparison for the coatings can be done in this dissipated energy approach.

3.3.2 Local Archard factor

In Figure 160, just comparing the lifetime of the coatings under a value of $Ed_{0\ \max\ ini}$ cannot reveal the real endurance of the coatings under a certain condition, especially for the situation where a superposition of lifetime takes place for several coatings. Due to the difference in friction reduction of the coatings, the same test parameters can result in different $Ed_{0\ \max\ ini}$ values. A local Archard factor in initial cycles, K_{A0}, can be obtained by removing the friction coefficient, μ_{ini}, from Eq.6-13, which is almost the same for the coatings under same test parameters.

$$K_{A0} = \frac{Ed_{0\max ini}}{\mu_{ini}} = 4 \cdot \delta_{0ini} \cdot p_0 \qquad (6\text{-}14)$$

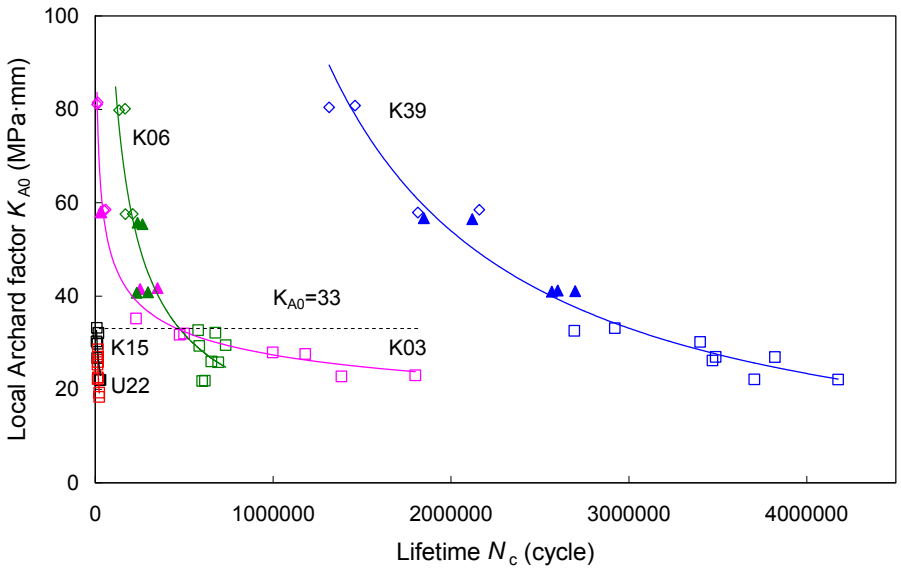

Figure 161: K_{A0} - N_c master curves for the coatings (□: δ*=±10 μm, ▲: δ*=±18 μm, ◇: δ*=±25 μm).

The relationship between K_{A0} and N_c of one coating can also be fitted by one master curve, as shown in Figure 161, where K_{A0} of the coatings presented similar values under same test parameters. Therefore, comparing the lifetime of the coatings under a value of K_{A0} can reveal the endurance of the coating under the relevant running conditions. According to the curves in Figure 161, when K_{A0} is smaller than 33, the order of endurance from the best to the worst is: K39 ⇒K03 ⇒K06 ⇒ K15, U22, or else the order is: K39 ⇒K06 ⇒K03 ⇒ K15, U22.

3.4 Synthetic selection

In an actual coating selection process, coating performances should be comprehensively taken into account, including the friction reduction, the endurance, the effect of running conditions on the friction coefficient and endurance, and some important non-tribological characteristics. In addition, the experiments in laboratory are simulating tests, and the results may be not completely in accordance with the actual applications, so the test results of coatings in other evaluation techniques can be used as references. The polar diagram put forward by Carton *et al*. [39] is a wonderful approach, which can be used to synthetically and straightforwardly compare the coatings. In order to get a comprehensive

evaluation for the performances of the solid lubricant coatings, a similar polar diagram is designed, and the following four aspects will be considered: friction reduction, endurance, behaviors in evaluation techniques and non-tribological performance.

3.4.1 Friction reduction

In order to accurately describe the friction reduction of the coatings, besides the friction coefficient itself, the effect of test conditions should also be taken into account. According to our tests, three parameters will be used: mean friction coefficient, $\overline{\mu}_{ref}$, effect of normal load on friction coefficient, μ_P, and effect of displacement amplitude on friction coefficient, μ_δ.

Mean friction coefficient $\overline{\mu}_{ref}$

The mean value of friction coefficients in all the tests of a coating, $\overline{\mu}$, describes the general friction reduction of the coating, and $\overline{\mu}_{ref}$ is the ratio of $\overline{\mu}$ to a reference friction coefficient (here, 0.1 will be used because it is the common value of friction coefficients for bonded solid lubricant coatings).

$$\overline{\mu} = \frac{1}{n}\sum_{i=1}^{n}\mu_i \qquad (6\text{-}15)$$

$$\overline{\mu}_{ref} = \overline{\mu}/0.1 \qquad (6\text{-}16)$$

Effect of normal load on friction coefficient μ_P

The fluctuation of friction coefficient under different normal loads represents the friction reduction of a coating under unstable loads. The maximal relative fluctuation of average values of μ under different normal loads can be expressed as Eq.6-17, where $\overline{\mu}_{Pi}$ and $\overline{\mu}_{Pj}$ respectively signify the mean values of friction coefficients under the given normal loads P_i and P_j.

$$\mu_P = \frac{Max\left|\overline{\mu}_{Pi} - \overline{\mu}_{Pj}\right|}{\overline{\mu}} \qquad (6\text{-}17)$$

Effect of displacement amplitude on friction coefficient μ_δ

The fluctuation of friction coefficient under different displacement amplitudes represents the effect of displacement amplitude on friction reduction of a coating. The maximal relative fluctuation of average values of μ under different normal loads can be expressed as Eq.6-18, where $\overline{\mu}_{\delta i}$ and $\overline{\mu}_{\delta j}$ respectively signify the mean values of friction coefficients under the given displacement amplitudes δ_i and δ_j.

$$\mu_\delta = \frac{Max\left|\overline{\mu}_{\delta i} - \overline{\mu}_{\delta j}\right|}{\overline{\mu}} \qquad (6\text{-}18)$$

3.4.2 Endurance

In order to accurately describe the endurance of the coatings, there are also three parameters be used: mean coating lifetime, $\overline{N}_{cref}$, effect of normal load and displacement amplitude on coating lifetime, N_{cP} and $N_{c\delta}$.

Mean coating lifetime $\overline{N}_{cref}$

The mean value of coating lifetimes in all the tests of a coating, N_c, describes the general endurance of the coating, and $\overline{N}_{cref}$ is the ratio of $\overline{N}_c$ to a reference coating lifetime (here, 500 000 cycles will be used because it is supposed to be the expected coating lifetime by the end user).

$$\overline{N}_c = \frac{1}{n}\sum_{i=1}^{n} N_{ci} \qquad (6\text{-}19)$$

$$\overline{N}_{cref} = \frac{500\,000}{\overline{N}_c} \qquad (6\text{-}20)$$

Effect of normal load on coating lifetime N_{cP}

The fluctuation of coating lifetime under different normal loads represents the endurance of a coating under unstable loads. The maximal relative fluctuation of average values of N_c under different normal loads can be expressed as Eq.6-21, where $\overline{N}_{cPi}$ and $\overline{N}_{cPj}$ respectively signify the mean values of coating lifetimes under the given normal loads, P_i and P_j.

$$N_{cP} = \frac{Max\left|\overline{N}_{cPi} - \overline{N}_{cPj}\right|}{\overline{N}_c} \qquad (6\text{-}21)$$

Effect of displacement amplitude on coating lifetime $N_{c\delta}$

The fluctuation of coating lifetime under different normal loads represents the endurance of a coating under unstable loads. The maximal relative fluctuation of average values of N_c under different displacement amplitudes can be expressed as Eq.6-22, where $\overline{N}_{c\delta i}$ and $\overline{N}_{c\delta j}$ respectively signify the mean values of coating lifetimes under the given displacement amplitudes, δ_i and δ_j.

$$N_{c\delta} = \frac{Max\left|\overline{N}_{c\delta i} - \overline{N}_{c\delta j}\right|}{\overline{N}_c} \qquad (6\text{-}22)$$

3.4.3 Behaviors in evaluation techniques

The behaviors of the coatings in ball cratering and scratch tests are relative to their fretting performance, so they can be used as references of the coating selection, including ductility (D), critical load (L_c) and ball cratering resistance (K_b). Hardness and reduced elastic modulus are not used because of the ambiguous relationship between them and the coating tribological performance. Due to the qualitative evaluation of ductility in scratch tests, the places in the ranks will be used as the values of the relevant parameters.

3.4.4 Non-tribological features

Some non-tribological features are also important for the coating selection. According to the information provided by the end-user of the coatings, three parameters are selected, including the recommended thickness range (h), corrosion resistance (K_c) and service temperature (T). The recommended thickness ranges of the coatings are 5~25 μm for K39, 7~15 μm for K03 and 5~20 μm for K06. The service temperature ranges are shown in Table 32 (Chapter 4). In salt spray tests, the coatings with a thickness of 15 μm can protect the substrate surface more than 400 hours, while the protecting times of the coatings are different in 0.1 N hydrochloric acid: > 1,000 hours for K39, >400

hours for K03 and >100 hours for K06, or in 0.1 N caustic soda: > 800 hours for K39, >400 hours for K03 and K06. For these parameters, the places of the coatings in the ranks are also used.

According to Eq.6-15 ~ Eq.6-22 and the relevant ranks of the coatings, the values of the parameters are shown in Table 49, where a lower value means a better performance in the term of the relevant parameter. In the polar diagram, only the three coatings with good fretting endurance, K39, K03 and K06, are considered.

Table 49: The values of the parameters for the polar diagram

	Friction reduction			Fretting endurance			Behaviors in evaluation techniques			Non-tribological features		
Coating	$\overline{\mu}_{ref}$	μ_P	μ_δ	$\overline{N}_{cref}$	N_{cP}	$N_{c\delta}$	D	L_c	K_b	h	K_c	T
K39	1.02	0.10	0.01	0.19	0.26	0.63	1	1	1	1	1	1
K03	0.86	0.14	0.05	1.07	0.99	1.72	2	2	2	3	2	2
K06	1.36	0.22	0.03	1.17	0.00	1.10	3	3	3	2	2	1

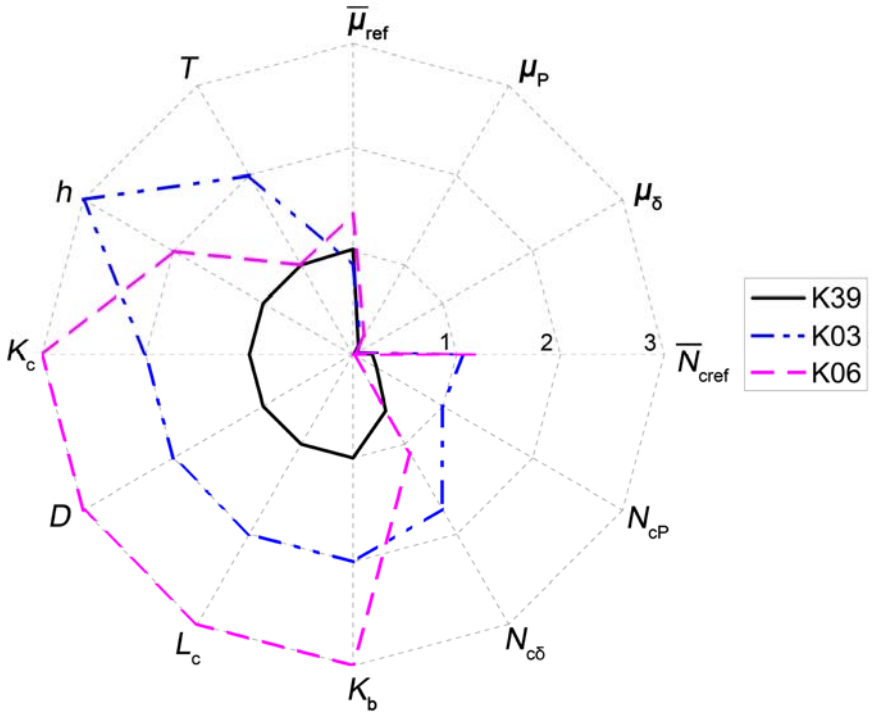

Figure 162: Polar diagram of the coatings.

The polar diagram of the coatings (K39, K03 and K06) is shown in Figure 162, where the coating with a curve close to the center point has a good performance. From Figure 162, we can get straightforward evaluations for the coatings about friction reduction, fretting endurance, behaviors in evaluation techniques and non-tribological features. K39 is the best coating almost from every aspect, while K06 and K03 respectively have their own advantages and disadvantages. K03 behaves better than K06 in friction reduction, ball cratering and scratch tests, and corrosion resistance, while K06 is better in fretting endurance and it can be used in wider ranges of thickness and service temperature. In order to obtain a definite conclusion about the comparison of K03 and K06, the approach “weight point” described by Eq.4-1 (Chapter 3) can be used again. The only difference is that the coating with a lower weight point is better. The weight factors should be set according to the importance of the parameters in the application (10 — most important, 1 — least important). For example, friction reduction or fretting endurance is respectively hypothesized as very important performance, and the

setting of weight factors and the results of the coatings are shown in Table 50. When friction reduction is very important, K03 is better than K06; when fretting endurance is very important, K06 is better than K03. Therefore, by appropriately setting the weight factors according to a given application, definite comparison results of the coatings can be obtained.

Table 50: Evaluate the coatings by weight point.

	Friction reduction			Fretting endurance			Behaviors in evaluation techniques			Non-tribological features			Weight point		
Parameters	$\overline{\mu}_{ref}$	μ_P	μ_δ	$\overline{N}_{cref}$	N_{cP}	$N_{c\delta}$	D	L_c	K_b	h	K_c	T	K39	K03	K06
Weight factors 1	10	10	10	5	5	5	3	3	3	3	3	3	34.7	68.4	72.4
Weight factors 2	5	5	5	10	10	10	3	3	3	3	3	3	34.1	82.1	75.7

In this approach, the polar diagram should be flexible, i.e., the parameters used in the polar diagram are changeable according to the applications. For example, in an application with a wide range of operating temperature, effects of temperature on friction coefficient (μ_T) and on coating lifetime (N_{cT}) should be considered in the polar diagram.

4. Conclusions

In this chapter, several commercial bonded solid lubricant coatings were investigated by fretting tests and different evaluation techniques. Based on the analysis of coating behaviors in the evaluation techniques, the fretting behaviors, the relationships between coating properties and fretting performance, a systemic approach has been put forward to help the coating selection for fretting conditions.

The fretting endurance of the coatings is closely related to their properties, such as abrasion resistance, ductility, cohesion strength and bonding strength. Some simple techniques (ball cratering and scratch tests) can be employed to assess these properties and screen out some poor coatings.

A dissipated energy approach was suggested to compare the fretting performance of the coatings, where the fretting lifetime of each coating can be fitted by one master curve whatever the contact loadings. Comparing the master curves of different coatings can help the coating selection. A local Archard factor is also helpful for comparing the fretting endurance of the coatings under same test conditions.

A polar diagram was designed to comprehensively compare the coatings from several aspects (friction reduction, endurance, behaviors in evaluation techniques and non-tribological performance), where a straightforward evaluation for a coating can be easily obtained. The selection of parameters in the polar diagram should be flexible.

GENERAL CONCLUSIONS

Coatings are more and more widely used in tribological applications. However, the selection of the optimum tribological coating for a specific application is still a difficult task because of the difficulty of estimating wear mechanisms, the dependence of tribological performance on coating properties and running conditions, and the dispersion of test results in literature. Furthermore, there is no general rule to help the selection of coatings for various tribological applications. The objectives of the thesis are to develop a pre-selection tool and propose some approaches to evaluate and compare coatings, sequentially, to help the coating selection. The following research approach was used (Figure 1).

At first, three cases (cylinder bore/piston rings in internal combustion engines, blade/disk of fan in turbofan engines, valve/seat in Diesel engines) were studied. In the applications, different wear modes (adhesion, fretting and impact), running conditions resulted in different requirements for coating properties, and different coatings were selected.

According to the literature and case studies, a pre-selection tool based on database was developed. In the tool, the requirements (tribological, non-tribological, non-functional) and limits (substrate, counterpart and running conditions) of an application were comprehensively considered. 13 criteria were used for matching the requirements and limits with the characteristics of coatings (coating materials and deposition methods). The candidate coatings were selected by combining the exclusion of the impossible coatings and the evaluation and comparison of the remaining coatings by weight point and reliability. The candidate coatings need to be further tested by simulation experiments.

In order to investigate the tribological behaviors of some coatings (that is necessary to finally select the appropriate coating for a given application), two complementary studies were performed: one with the objective to understand the effect of running conditions on the tribological performance of a given coating and the other with the objective to compare different coatings under the same running conditions.

In order to understand the effect of test conditions on tribological performance, pressure sprayed MoS_2 coatings were tested under three different contact configurations: ball-on-disk sliding, ball-on-flat fretting and cylinder-on-flat fretting.

- Pressure sprayed MoS_2 coatings respectively reduced the friction coefficient to 0.07~0.15 and 0.1~0.2 under sliding and fretting conditions, and the specific value of friction coefficient depended on test parameters. In fretting tests, MoS_2 coatings made the partial slip regime disappear under our test conditions due to its low friction.
- Friction coefficient decreased with the increase of contact pressure whatever the contact configurations, but it evolved along different curves due to the difference of contact pressure distribution, debris ejection and contact area evolution. In fretting tests, friction coefficient increased with the increase of displacement amplitude. In ball-on-disk tests, the sliding speed hardly influenced the friction coefficient probably due to its small changing range.
- In sliding tests, the lifetime of MoS_2 coating decreased monotonously with the increase of contact pressure, and was slightly influenced by sliding speed. In fretting tests, the lifetime first increased with the increase of contact pressure, and then decreased after the contact pressure exceeded a critical value. The increase of displacement amplitude made coating lifetime decrease, especially in the mixed slip regime.

- Under each contact configuration, the relationship between coating lifetime and dissipated energy density can be fitted by one master curve whatever the test parameters, which can be easily used to predict coating lifetime with other test parameters under the relevant contact configuration.

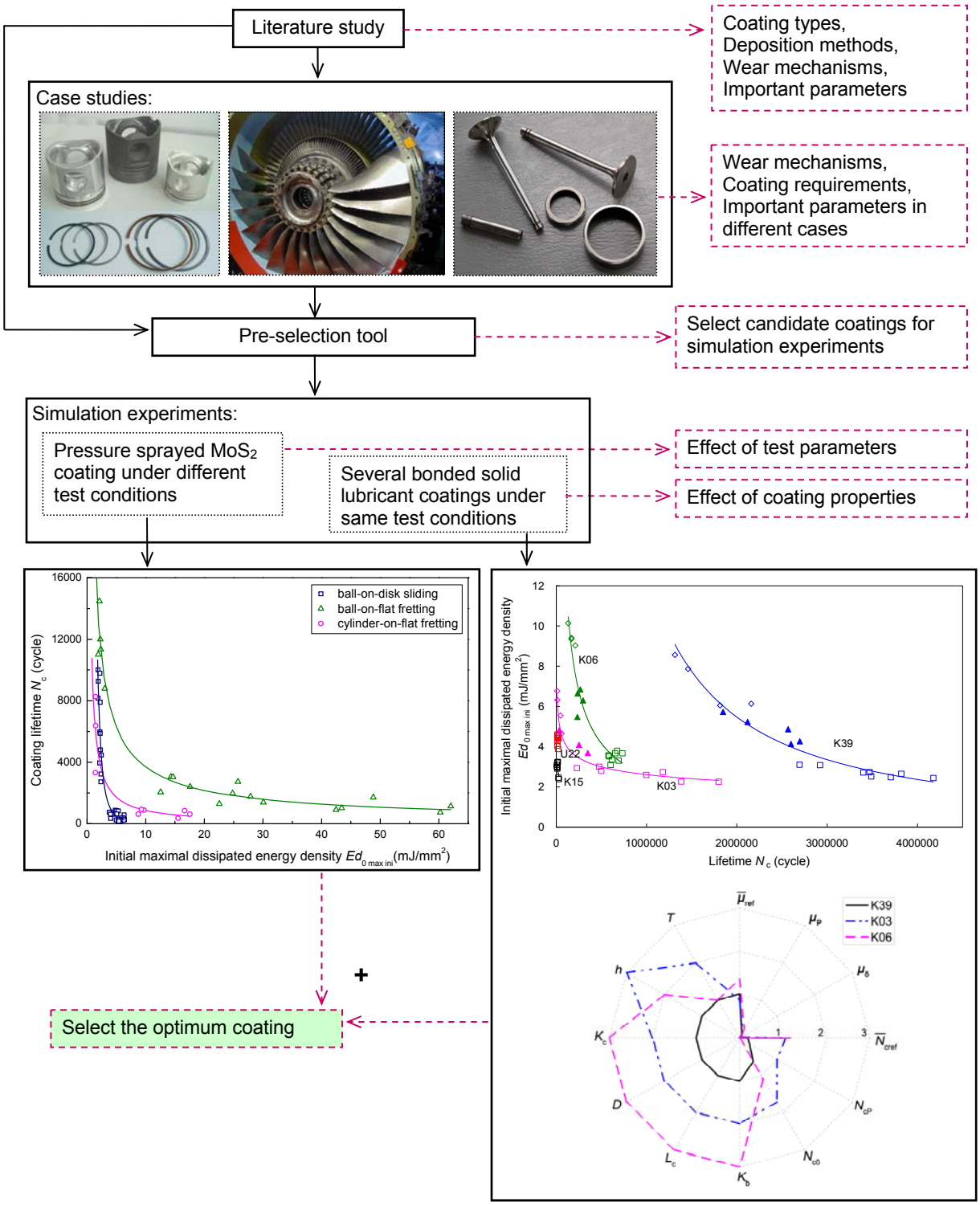

Figure 1: Synthesis of the research approach in the thesis.

In order to identify the relationship between coating properties and tribological performance, 5 bonded solid lubricant coatings principally based on PTFE or MoS_2 were also investigated by several evaluation techniques (nanoindentation, scratch and ball cratering) and fretting tests.

- The relationships between tribological performance of the coatings and their behaviors in evaluation techniques were discussed. The simple techniques (ball cratering and scratch tests) can be employed to evaluate the coatings and screen out the poor ones.
- The fretting behaviors of the coatings were closely related to their properties, such as the solid lubricant, abrasion resistance, ductility, cohesion strength and bonding strength. Coatings based on PTFE presented lower friction than the MoS_2 based coatings, and the evolution of friction coefficient with test time was also different. The fretting endurance of the coatings mainly depended on bonding strength, cohesion strength, ductility and the ability of forming and maintaining a transfer film on the counterface.
- A dissipated energy approach was suggested to compare the fretting performance of the coatings, where the fretting lifetime of each coating can be fitted by one master curve whatever the contact loadings. Comparing the master curves of different coatings can help the coating selection. A local Archard factor is also helpful for comparing the fretting endurance of the coatings under same test conditions.
- A polar diagram was designed to comprehensively compare the coatings from several aspects (friction reduction, endurance, behaviors in evaluation techniques and non-tribological performances), where a straightforward evaluation for a coating can be easily obtained.

In brief, the selection of tribological coatings can be systematically performed by the approaches proposed in the thesis:

- Analyze the tribological application, find out the requirements and limits for the coatings.
- According to the requirements and limits, apply the pre-selection tool to search candidate coatings.
- Use simple evaluation techniques to assess the coating properties and screen out the poor ones.
- Test the remaining coatings under relevant tribological conditions to investigate the influence of test parameters on tribological performance, and to obtain the dissipated energy -- lifetime master curves.
- Evaluate the tribological performance of the coatings by comparing their master curves.
- Comprehensively compare the coatings by the polar diagram approach to determine the optimum coating.

REFERENCES

[1] B. Bhushan, Principles and applications of tribology, John Wiley & Sons, New York, 1999.

[2] ASM, ASM Handbook. vol.18. Friction, lubrication, and wear technology, ASM International, USA, 1992.

[3] Y. Fu, J. Wei, A. W. Batchelor, Some considerations on the mitigation of fretting damage by the application of surface-modification technologies, Journal of Materials Processing Technology 99 (2000) 231-245.

[4] W. Kern, K. K. Schuegraf, Handbook of thin film deposition processes and techniques: principles, methods, equipment and applications, Noyes Publications / William Andrew Publishing, Norwich, 2002.

[5] B. N. Chapman, J. C. Anderson, Science and technology of surface coating, Academic Press, 1974.

[6] K. Holmberg, A. Matthews, Coatings tribology: properties, techniques and applications in surface engineering, Elsevier, Amsterdam, 1994.

[7] R. F. Bunshah, Handbook of deposition technologies for films and coatings: Science, Technology and Applications, Noyes publications, Park Ridge, 1994.

[8] J. Xu, M. H. Zhu, Z. R. Zhou, P. Kapsa, L. Vincent, An investigation on fretting wear life of bonded MoS_2 solid lubricant coatings in complex conditions, Wear 255 (2003) 253-258.

[9] ASM, ASM Handbook. vol.5. Surface engineering, ASM International, USA, 1994.

[10] R. Zenker, G. Sacher, A. Buchwalder, J. Liebich, A. Reiter, R. Häßler, Hybrid technology hard coating - Electron beam surface hardening, Surface and Coatings Technology 202 (2007) 804-808.

[11] Y. Wang, C. G. Li, W. Tian, Y. Yang, Laser surface remelting of plasma sprayed nanostructured Al2O3-13wt%TiO2 coatings on titanium alloy, Applied Surface Science 255 (2009) 8603-8610.

[12] M. C. Joseph, C. Tsotsos, M. A. Baker, P. J. Kench, C. Rebholz, A. Matthews, A. Leyland, Characterisation and tribological evaluation of nitrogen-containing molybdenum–copper PVD metallic nanocomposite films, Surface and Coatings Technology 190 (2005) 345-356.

[13] J. A. Thornton, Influence of apparatus geometry and deposition conditions on the structure and topography of thick sputtered coatings, Journal of Vacuum Science and Technology 11 (1974) 666-670.

[14] C. Donnet, A. Erdemir, Historical developments and new trends in tribological and solid lubricant coatings, Surface and Coatings Technology 180-181 (2004) 76-84.

[15] S. Hogmark, S. Jacobson, L. Mats, Design and evaluation of tribological coatings, Wear 246 (2000) 20-33.

[16] K. Holmberg, A. Matthews, H. Ronkainen, Coatings tribology — contact mechanisms and surface design, Tribology International 31 (1998) 107-120.

[17] D. H. Jeong, F. Gonzalez, G. Palumbo, K. T. Austa, U. Erb, The effect of grain size on the wear properties of electrodeposited nanocrystalline nickel coatings, Scripta Materialia 44 (2001) 493-499.

[18] A. A. Voevodin, M. A. Capano, S. J. P. Laube, M. S. Donley, J. S. Zabinski, Design of a Ti/TiC/DLC functionally gradient coating based on studies of structural transitions in Ti-C thin films, Thin Solid Films 298 (1997) 107-115.

[19] A. A. Voevodin, J. M. Schneider, C. Rebholz, A. Matthews, Multilayer composite ceramic-metal-DLC coatings for sliding wear applications, Tribology International 29 (1996) 559-570.

[20] P. E. Hovsepian, D. B. Lewis, W.-D. Munz, Recent progress in large scale manufacturing of multilayer/superlattice hard coatings, Surface and Coatings Technology 133-134 (2000) 166-175.

[21] Q. Yang, L. R. Zhao, Dry sliding wear of magnetron sputtered TiN/CrN superlattice coatings, Surface and Coatings Technology 173 (2003) 58-66.

[22] S. D. Walck, J. S. Zabinski, N. T. McDevitt, J. E. Bultman, Characterization of air-annealed, pulsed laser deposited ZnO-WS_2 solid film lubricants by transmission electron microscopy, Thin Solid Films 305 (1997) 130-143.

[23] J. S. Zabinski, M. S. Donley, V. J. Dyhouse, N. T. McDevitt, Chemical and tribological characterization of PbO-MoS_2 films grown by pulsed laser deposition, Thin Solid Films 214 (1992) 156-163.

[24] A. A. Voevodin, J. S. Zabinski, Supertough wear-resistant coatings with 'chameleon' surface adaptation, Thin Solid Films 370 (2000) 223-231.

[25] F. P. Bowden, D. Tabor, The friction and lubrication of solids, Clarendon Press, Oxford, 1950.

[26] F. P. Bowden, A. J. W. Moore, D.Tabor, The ploughing and adhesion of sliding metals, Applied Physics 14 (1941) 80-91.

[27] F. P. Bowden, D. Tabor, Friction, lubrication and wear: a survey of work during the last decade, Journal of Applied Physics 17 (1966) 1521-1544.

[28] B. Bhushan, Modern tribology handbook, CRC Press, London, New York, Washington D C, 2001.

[29] N. P. Suh, The delamination theory of wear, Wear 25 (1973).

[30] Y. Ding, N. F. Rieger, Spalling formation mechanism for gears, Wear 254 (2003) 1307-1317.

[31] M. Braunovic, V. V. Konchits, N. K. Myshkin, Electrical contacts: fundamentals, applications and technology, CRC Press, London, New York, 2006.

[32] J. T. Burwell, Survey of possible wear mechanisms, Wear 1 (1957) 119-141.

[33] J. T. Burwell, C. D. Strang, On the empirical law of adhesive wear, Journal of Applied Physics 23 (1952) 18-28.

[34] S. Hogmark, P. Hedenqvist, S. Jacobson, Tribological properties of thin hard coatings: demands and evaluation, Surface and Coatings Technology 90 (1997) 247-257.

[35] B. Podgornik, S. Hogmark, O. Sandberg, Proper coating selection for improved galling performance of forming tool steel, Wear 261 (2006) 15-21.

[36] K. Holmberg, H. Ronkainen, A. Matthews, Tribology of thin coatings, Ceramics International 26 (2000) 787-795.

[37] K. N. Strafford, Tribological properties of coatings-expectations, performance and the design dilemma, Surface and Coatings Technology 81 (1996) 106-117.

[38] C. Subramanian, K. N. Stratford, T. P. Wilks, L. P. Ward, On the design of coating systems: metallurgical and other considerations, Journal of Materials Processing Technology 56 (1996) 385-397.

[39] J.-F. Carton, A.-B. Vannes, L. Vincent, Basis of a coating choice methodology in fretting, Wear 185 (1995) 47-57.

[40] E. Rabinowicz, Friction and Wear of Materials, John Wiley & Sons, New York, London, Sydney, 1965.

[41] J. F. Archard, Elastic deformation and the laws of friction, Proceedings of the Royal Society of London. Series A, Mathematical and Physical Sciences 243 (1957) 190-205.

[42] J. A. Greenwood, J. B. P. Williamson, Contact of nominally flat surfaces, Proceedings of the Royal Society of London. Series A, Mathematical and Physical Sciences 295 (1966) 300-319.

[43] N. P. Suh, H.-C. Sin, The genesis of friction, Wear 69 (1981) 91-114.

[44] B. C. Na, A. Tanaka, Tribological characteristics of diamond-like carbon films based on hardness of mating materials, Thin Solid Films 478 (2005) 176-182.

[45] J. L. Grosseau-Poussard, P. Moine, M. Brendle, Shear strength measurements of parallel MoS_x thin films, Thin Solid Films 307 (1997) 163-168.

[46] L. Vandenbulcke, M. I. D. Barros, Deposition, structure, mechanical properties and tribological behavior of polycrystalline to smooth fine-grained diamond coatings, Surface and Coatings Technology 146-147 (2001) 417-424.

[47] X. Zhu, W. Lauwerens, P. Cosemans, M. V. Stappen, J. P. Celis, L. M. Stals, J. He, Different tribological behavior of MoS_2 coatings under fretting and pin-on-disk conditions, Surface and Coatings Technology 163-164 (2003) 422-428.

[48] Y. L. Su, W. H. Kao, Effect of thickness and carbon content on tribological behaviour and mechanical properties of Ti-C:H coatings, Wear 236 (1999) 221-234.

[49] S. Jahanmir, E. P. Abrahamson, N. P. Suh, Sliding wear resistance of metallic coated surfaces, Wear 40 (1976) 75-84.

[50] J. Takadoum, H. H. Bennani, Influence of substrate roughness and coating thickness on adhesion, friction and wear of TiN films, Surface and Coatings Technology 96 (1997) 272-282.

[51] D. Sheeja, B. K. Tay, K. W. Leong, C. H. Lee, Effect of film thickness on the stress and adhesion of diamond-like carbon coatings, Diamond and Related Materials 11 (2002) 1643-1647.

[52] J. Qi, C. Y. Chan, I. Bello, C. S. Lee, S. T. Lee, J. B. Luo, S. Z. Wen, Film thickness effects on mechanical and tribological properties of nitrogenated diamond-like carbon films, Surface and Coatings Technology 145 (2001) 38-43.

[53] Y. Y. Guu, J. F. Lin, C.-F. Ai, The tribological characteristics of titanium nitride coatings. Part I. Coating thickness effects, Wear 194 (1996) 12-21.

[54] J. H. W. Siu, L. K. Y. Li, An investigation of the effect of surface roughness and coating thickness on the friction and wear behaviour of a commercial MoS_2 – metal coating on AISI 400C steel, Wear 237 (2000) 283-287.

[55] N. Fujisawa, M. V. Swain, N. L. James, J. C. Woodard, R. N. Tarrant, D. R. McKenzie, Carbon coating of Ti-6Al-4V for reduced wear in combined impact and sliding applications, Tribology International 36 (2003) 873-882.

[56] B. Podgornik, S. Hogmark, O. Sandberg, Influence of surface roughness and coating type on the galling properties of coated forming tool steel, Surface and Coatings Technology 184 (2004).

[57] A. Tanaka, T. Nishibori, M. Suzuki, K. Maekawa, Tribological properties of DLC films deposited using various precursors under different humidity conditions, Diamond and Related Materials 12 (2003) 2066-2071.

[58] N. M. Renevier, V. C. Fox, D. G. Teer, J. Hampshire, Coating characteristics and tribological properties of sputter-deposited MoS_2/metal composite coatings deposited by closed field unbalanced magnetron sputter ion plating, Surface and Coatings Technology 127 (2000) 24-37.

[59] W. H. Kao, Y. L. Su, Optimum MoS_2–Cr coating for sliding against copper, steel and ceramic balls, Materials Science and Engineering A 368 (2004) 239-248.

[60] M. Sedlaček, B. Podgornik, J. Vižintin, Tribological properties of DLC coatings and comparison with test results: Development of a database, Materials Characterization 59 (2008) 151-161.

[61] M. Shima, J. Okado, I. R. McColl, R. B. Waterhouse, T. Hasegawa, M. Kasaya, The influence of substrate material and hardness on the fretting behaviour of TiN, Wear 225-229 (1999) 38-45.

[62] F. Svahn, Å. Kassman-Rudolphi, E. Wallén, The influence of surface roughness on friction and wear of machine element coatings, Wear 254 (2003) 1092-1098.

[63] E. W. Roberts, B. J. Williams, J. A. Ogilvy, The effect of substrate surface roughness on the friction and wear of sputtered MoS_2 films, Journal of Physics D: Applied Physics 25 (1992) 65-70.

[64] P. Harlin, P. Carlsson, U. Bexell, M. Olsson, Influence of surface roughness of PVD coatings on tribological performance in sliding contacts, Surface and Coatings Technology 201 (2006) 4253-4259.

[65] E. W. Roberts, W. B. Price, In-vacuo, tribological properties of "high-rate" sputtered MoS_2 applied to metal and ceramic substrates, in: MRS Symp. Proc., 1989.

[66] D. G. Teer, J. Hampshire, V. Fox, V. Bellido-Gonzalez, The tribological properties of MoS_2/metal composite coatings deposited by closed field magnetron sputtering, Surface and Coatings Technology 94-95 (1997) 572-577.

[67] J. Jiang, R. D. Arnell, G. Dixit, The influence of ball size on tribological behaviour of MoS_2 coating tested on a ball-on-disk wear rig, Wear 243 (2000) 1-5.

[68] M. Roy, A. Pauschitz, R. Polak, F. Franek, Comparative evaluation of ambient temperature friction behaviour of thermal sprayed Cr_3C_2-25(Ni20Cr) coatings with conventional and nano-crystalline grains, Tribology International 39 (2006) 29-38.

[69] L. C. Betancourt-Dougherty, R. W. Smith, Effects of load and sliding speed on the wear behaviour of plasma sprayed TiC–NiCrBSi coatings, Wear 217 (1998) 147-154.

[70] I. L. Singer, R. N. Bolster, J. Wegand, S. Fayeulle, Hertzian stress contribution to low friction behavior of thin MoS_2 coatings, Applied Physics Letters 57 (1990) 995-997.

[71] L. E. Seitzman, R. N. Bolster, I. L. Singer, IBAD MoS_2 lubrication of titanium alloys, Surface and Coatings Technology 78 (1996) 10-13.

[72] S. Wilson, A. T. Alpas, TiN coating wear mechanisms in dry sliding contact against high speed steel, Surface and Coatings Technology 108-109 (1998) 369-376.

[73] W. Feng, D. Yan, J. He, X. Li, Y. Dong, Reactive plasma sprayed TiN coating and its tribological properties, Wear 258 (2005) 806-811.

[74] H. Ronkainen, J. Likonen, J. Koskinen, S. Varjus, Effect of tribofilm formation on the tribological performance of hydrogenated carbon coatings, Surface and Coatings Technology 79 (1996) 87-94.

[75] L. C. Towle, Shear-strength and friction measurement on thin layers under high pressure, Journal of Applied Physics 42 (1971) 2368-2376.

[76] N. M. Renevier, J. Hamphire, V. C. Fox, J. Witts, T. Allen, D. G. Teer, Advantages of using self-lubricating, hard, wear-resistant MoS_2-based coatings, Surface and Coatings Technology 142-144 (2001) 67-77.

[77] J. Xu, M. H. Zhu, Z. R. Zhou, Fretting wear behavior of PTFE-based bonded solid lubrication coatings, Thin Solid Films 457 (2004) 320-325.

[78] M. Hua, H. Y. Tam, H. Y. Ma, C. K. Mok, Patterned PVD TiN spot coatings on M2 steel: Tribological behaviors under different sliding speeds, Wear 260 (2006) 1153-1165.

[79] J. L. He, Y. H. Lin, K. C. Chen, Wear performance of CAP-titanium nitride-coated high-speed steel in different dry sliding conditions, Wear 208 (1997) 36-41.

[80] T. L. Huu, D. Paulmier, A. Grabchenko, M. Horvath, I. Mészaros, A. G. Mamalis, Autolubrication of diamond coatings at high sliding speed, Surface and Coatings Technology 108-109 (1998) 431-436.

[81] J. E. Fernández, Y. Wang, R. Tucho, M. A. Martin-Luengo, R. Gancedo, A. Rincón, Friction and wear behaviour of plasma-sprayed Cr_2O_3 coatings against steel in a wide range of sliding velocities and normal loads, Tribology International 29 (1996) 333-343.

[82] W. Ni, Y.-T. Cheng, A. M. Weiner, T. A. Perry, Tribological behavior of diamond-like-carbon (DLC) coatings against aluminum alloys at elevated temperatures, Surface and Coatings Technology 201 (2006) 3229-3234.

[83] T. Kubart, T. Polcar, L. Kopecký, R. Novák, D. Nováková, Temperature dependence of tribological properties of MoS_2 and $MoSe_2$ coatings, Surface and Coatings Technology 193 (2005) 230-233.

[84] E. Liu, Y. F. Ding, L. Li, B. Blanpain, J.-P. Celis, Influence of humidity on the friction of diamond and diamond-like carbon materials, Tribology International 40 (2007) 216-219.

[85] J. Robertson, Diamond-like amorphous carbon, Materials Science and Engineering 37 (2002) 129-281.

[86] M. Z. Huq, J.-P. Celis, Expressing wear rate in sliding contacts based on dissipated energy, Wear 252 (2002) 375-383.

[87] C. Donnet, J. M. Martin, T. LeMogne, M. Belin, Super-low friction of MoS_2 coatings in various environments, Tribology International 29 (1996) 123-128.

[88] A. Vanhulsel, F. Velasco, R. Jacobs, L. Eersels, D. Havermans, E. W. Roberts, I. Sherrington, M. J. Anderson, L. Gaillard, DLC solid lubricant coatings on ball bearings for space applications, Tribology International 40 (2007) 1186-1194.

[89] J. Jiang, R. D. Arnell, The effect of substrate surface roughness on the wear of DLC coatings, Wear 239 (2000) 1-9.

[90] E. W. Roberts, N. B. Price, In vacuum tribological properties of high rate sputtered MoS_2 applied to metal and ceramic substrate, Mater. Res. Soc. Symp. Proc. 140 (1989) 251-264.

[91] E. W. Roberts, Ultralow friction films of MoS_2 for space applications, Thin Solid Films 181 (1989) 461-473.

[92] T. Spalvins, Lubrication with sputtered MoS_2 films: Principles,operation, and limitations, Journal of Materials Engineering and Performance 1 (1992) 347-351.

[93] H. Mohrbacher, B. Blanpain, J.-P. Celis, J. R. Roos, The influence of humidity on the fretting behaviour of PVD TiN coatings, Wear 180 (1995) 43-52.

[94] J. F. Archard, Contact and rubbing of flat surface, Journal of Applied Physics 24 (1953) 981-988.

[95] A. G. Evans, D. B. Marshall, Wear mechanism in ceramics, in: D. A. Rigney (Ed.) Fundamentals of Friction and Wear of Materials, vol 439, ASM, 1981.

[96] Y. S. Wang, S. M. Hsu, Wear and wear transition modeling of ceramics, Wear 195 (1996) 35-46.

[97] S. M. Hsu, M. Shen, Wear prediction of ceramics, Wear 256 (2004) 867-878.

[98] R. Lewis, A modelling technique for predicting compound impact wear, Wear 262 (2007) 1516-1521.

[99] H. Mohrbacher, J.-P. Celis, J. R. Roos, Laboratory testing of displacement and load induced fretting, Tribology International 28 (1995) 269.

[100] A. Ramalho, J. C. Miranda, The relationship between wear and dissipated energy in sliding systems, Wear 260 (2006) 361-367.

[101] A. B. C. Larbi, A. Cherif, M. A. Tarres, Improvement of the adhesive wear resistance of steel by nitriding quantified by the energy dissipated in friction, Wear 258 (2005) 712-718.

[102] S. Fouvry, P. Kapsa, L. Vincent, Quantification of fretting damage, Wear 200 (1996) 186-205.

[103] S. Fouvry, V. Fridrici, C. Langlade, P. Kapsa, L. Vincent, Palliatives in fretting: A dynamical approach, Tribology International 39 (2006) 1005-1015.

[104] S. Fouvry, P. Kapsa, An energy description of hard coating wear mechanisms, Surface and Coatings Technology 138 (2001) 141-148.

[105] S. Fouvry, T. Liskiewicz, P. Kapsa, S. Hannel, E. Sauger, An energy description of wear mechanisms and its applications to oscillating sliding contacts, Wear 255 (2003) 287-298.

[106] J. C. A. Batista, C. Godoy, G. Pintaude, A. Sinator, A. Matthews, An approach to elucidate the different response of PVD coatings in different tribological tests, Surface and Coatings Technology 174 -175 (2003) 891-898.

[107] Z. Zeng, L. Wang, L. Chen, J. Zhang, The correlation between the hardness and tribological behaviour of electroplated chromium coatings sliding against ceramic and steel counterparts, Surface and Coatings Technology 201 (2006) 2282-2288.

[108] D. H. Jeong, U. Erb, K. T. Aust, G. Palumbo, The relationship between hardness and abrasive wear resistance of electrodeposited nanocrystalline Ni–P coatings, Scripta Materialia 48 (2003) 1067-1072.

[109] H.-E. Cheng, M.-H. Hon, Influence of TiN coating thickness on the wear of Si_3N_4-based cutting tools, Surface and Coatings Technology 81 (1996) 256-261.

[110] K.-D. Bouzakis, S. Hadjiyiannis, G. Skordaris, I. Mirisidis, N. Michailidis, K. Efstathiou, E. Pavlidou, G. Erkens, R. Cremer, S. Rambadt, I. Wirth, The effect of coating thickness, mechanical strength and hardness properties on the milling performance of PVD coated cemented carbides inserts, Surface and Coatings Technology 177-178 (2004) 657-664.

[111] A. A. Voevodin, J. G. Jones, T. C. Back, J. S. Zabinski, V. E. Strel'nitzkib, I. I. Aksenov, Comparative study of wear-resistant DLC and fullerene-like CN_x coatings produced by pulsed laser and filtered cathodic arc depositions, Surface and Coatings Technology 197 (2005) 116-125.

[112] E. P. Song, J. Ahn, S. Lee, N. J. Kim, Microstructure and wear resistance of nanostructured Al_2O_3–8wt.%TiO_2 coatings plasma-sprayed with nanopowders, Surface and Coatings Technology 201 (2006) 1309-1315.

[113] M. F. Morks, A. Kobayashi, N. F. Fahim, Abrasive wear behavior of sprayed hydroxyapitite coatings by gas tunnel type plasma spraying, Wear 262 (2007) 204-209.

[114] E. P. Song, B. Hwang, S. Lee, N. J. Kim, J. Ahn, Correlation of microstructure with hardness and wear resistance of stainless steel blend coatings fabricated by atmospheric plasma spraying, Materials Science and Engineering 429 (2006) 189-195.

[115] A. Leyland, A. Matthews, On the significance of the H/E ratio in wear control: a nanocomposite coating approach to optimised tribological behaviour, Wear 246 (2000) 1-11.

[116] K. Yamamoto, K. Matsukado, Effect of hydrogenated DLC coating hardness on the tribological properties under water lubrication, Tribology International 39 (2006) 1609-1614.

[117] T. Roth, K. H. Kloos, E. Broszeit, Structure, internal stresses, adhesion and wear resistance of sputtered alumina coatings, Thin Solid Films 153 (1987) 123-133.

[118] A. Dorner, C. Schürer, G. Reisel, G. Irmer, O. Seidel, E. Müller, Diamond-like carbon-coated Ti6Al4V: influence of the coating thickness on the structure and the abrasive wear resistance, Wear 249 (2001) 489-497.

[119] E. Post, I. Nieminen, Influence of coating thickness on the life of TiN-coated high speed steel cutting tools, Wear 129 (1989) 273-283.

[120] K. Tuffy, G. Byrne, D. Dowling, Determination of the optimum TiN coating thickness on WC inserts for machining carbon steels, Journal of Materials Processing Technology 155-156 (2004) 1861-1866.

[121] X. Nie, A. Leyland, H. W. Song, A. L. Yerokhin, S. J. Dowey, A. Matthews, Thickness effects on the mechanical properties of micro-arc discharge oxide coatings on aluminium alloys, Surface and Coatings Technology 116-119 (1999) 1055-1060.

[122] K.-D. Bouzakis, S. Hadjiyiannis, G. Skordaris, J. Anastopoulos, I. Mirisidis, N. Michailidis, K. Efstathiou, O. Knotek, G. Erkens, R. Cremer, S. Rambadt, I. Wirth, The influence of the coating thickness on its strength properties and on the milling performance of PVD coated inserts, Surface and Coatings Technology 174-175 (2003) 393-401.

[123] K. Holmberg, A. Laukkanen, H. Ronkainen, K. Wallin, S. Varjus, J. Koskinen, Tribological contact analysis of a rigid ball sliding on a hard coated surface Part II: Material deformations, influence of coating thickness and Young's modulus, Surface and Coatings Technology 200 (2006) 3810-3823.

[124] S. Jahanmir, E. P. Abrahamson, N. P. Suh, Sliding wear resistance of metallic coated surfaces, Wear 40 (1976) 75-84.

[125] M. Olsson, P. Hedenqvist, B. Stridh, S. Söderberg, Solid particle erosion of hard chemically vapour- deposited coatings, Surface and Coatings Technology 37 (1989) 321-337.

[126] K. Sato, N. Ichimiy, A. Kondo, Y. Tanaka, Microstructure and mechanical properties of cathodic arc ion-plated (Al,Ti)N coatings, Surface and Coatings Technology 163-164 (2003) 135-143.

[127] J. Xu, Z. R. Zhou, C. H. Zhang, M. H. Zhu, J. B. Luob, An investigation of fretting wear behaviors of bonded solid lubricant coatings, Journal of Materials Processing Technology 182 (2007) 146-151.

[128] N. Fujisawa, D. R. McKenzie, N. L. James, J. C. Woodard, M. V. Swain, Combined influences of mechanical properties and surface roughness on the tribological properties of amorphous carbon coatings, Wear 260 (2006) 62-74.

[129] M. M. Lima, C. Godoy, P. J. Modenesi, J. C. Avelar-Batista, A. Davison, A. Matthews, Coating fracture toughness determined by Vickers indentation: an important parameter in cavitation erosion

resistance of WC–Co thermally sprayed coatings, Surface and Coatings Technology 177-178 (2004) 489-496.

[130] T. L. Oberle, Properties influencing wear of metals, J. Metals 3 (1951) 438.

[131] C. Rebholz, A. Leyland, J. M. Schneider, A. A. Voevodin, A. Matthews, Structure, hardness and mechanical properties of magnetronsputtered titanium–aluminium boride films, Surface and Coatings Technology 120-121 (1999) 412-417.

[132] A. Leyland, A. Matthews, Design criteria for wear-resistant nanostructured and glassy-metal coatings, Surface and Coatings Technology 177-178 (2004) 317-324.

[133] W. Ni, Y.-T. Cheng, M. J. Lukitsch, A. M. Weiner, L. C. Lev, Effects of the ratio of hardness to Young's modulus on the friction and wear behavior of bilayer coatings, Applied Physics Letters 85 (2004) 4028-4030.

[134] Y. Cheng, Y. F. Zheng, Deposition of TiN coatings on shape memory NiTi alloy by plasma immersion ion implantation and deposition, Thin Solid Films 515 (2006) 1358-1363.

[135] S. K. Ghosh, P. K. Limaye, B. P. Swain, N. L. Soni, R. G. Agrawal, R. O. Dusane, A. K. Grover, Tribological behaviour and residual stress of electrodeposited Ni/Cu multilayer films on stainless steel substrate, Surface and Coatings Technology 201 (2007) 4609-4618.

[136] P. Zhang, L. Wang, X. Nie, Tribological properties of a-C/Cr(N) coatings in micro-and nano-scales, Surface and Coatings Technology 201 (2007) 5176-5181.

[137] G. S. Fox-Rabinovich, S. C. Veldhuis, V. N. Scvortsov, L. S. Shuster, G. K. Dosbaeva, M. S. Migranov, Elastic and plastic work of indentation as a characteristic of wear behavior for cutting tools with nitride PVD coatings, Thin Solid Films 469-470 (2004) 505-512.

[138] G. S. Fox-Rabinovich, B. D. Beake, J. L. Endrino, S. C. Veldhuis, R. Parkinson, L. S. Shuster, M. S. Migranov, Effect of mechanical properties measured at room and elevated temperatures on the wear resistance of cutting tools with TiAlN and AlCrN coatings, Surface and Coatings Technology 200 (2006) 5738-5742.

[139] A. Matthews, Developments in PVD tribological coatings (IUVSTA highlights seminar-vacuum metallurgy division), Vacuum 65 (2002) 237-238.

[140] C. Tsotsos, K. Kanakis, A. Davison, M. A. Baker, A. Matthews, A. Leyland, Mechanical and tribological properties of CrTiCu(B,N) glassy-metal coatings deposited by reactive magnetron sputtering, Surface and Coatings Technology 200 (2006) 4601-4611.

[141] B. D. Beake, J. F. Smith, A. Gray, G. S. Fox-Rabinovich, S. C. Veldhuis, J. L. Endrino, Investigating the correlation between nano-impact fracture resistance and hardness/modulus ratio from nanoindentation at 25-500°C and the fracture resistance and lifetime of cutting tools with $Ti_{1-x}Al_xN$ (x = 0.5 and 0.67) PVD coatings in milling operations, Surface and Coatings Technology 201 (2007) 4585-4593.

[142] G.-C. Ji, C.-J. Li, Y.-Y. Wang, W.-Y. Li, Microstructural characterization and abrasive wear performance of HVOF sprayed Cr_3C_2–NiCr coating, Surface and Coatings Technology 200 (2006) 6749-6757.

[143] G. C. A. M. Janssen, R.Hoy, J.-D.Kamminga, Hardness and modulus of CrN_x coatings, Mat. Res. Soc. Symp. Proc. 750 (2003) Y1.2.1-Y1.2.6.

[144] M. Bin-Sudin, A. Leyland, A. S. James, A. Matthews, j. Housden, B. Garside, Substrate surface finish effects in duplex coatings of PAPVD TiN and CrN with electroless nickel-phosphorus interlayers, Surface and Coatings Technology 81 (1996) 215-224.

[145] J. Jiang, R. D. Arnell, J. Tong, An investigation into the tribological behaviour of DLC coatings deposited on sintered ferrous alloy substrate, Wear 214 (1998) 14-22.

[146] G. Z. Xu, Z. R. Zhou, J. J. Liu, A comparative study on fretting wear-resistant properties of ion-plated TiN and magnetron-sputtered MoS_2 coatings, Wear 224 (1999) 211-215.

[147] S. Wilson, A.T.Alpas, Effect of temperature and sliding velocity on TIN coating wear, Surface and Coatings Technology 91-95 (1997) 53-59.

[148] E. Konca, Y.-T. Cheng, A. M. Weiner, J. M. Dasch, A. Erdemir, A. T. Alpas, Transfer of 319 Al alloy to titanium diboride and titanium nitride based (TiAlN, TiCN, TiN) coatings: effects of sliding speed, temperature and environment, Surface and Coatings Technology 200 (2005) 2260-2270.

[149] G. Zhang, H. Liao, H. Li, C. Mateus, J.-M. Bordes, C. Coddet, On dry sliding friction and wear behaviour of PEEK and PEEK/SiC-composite coatings, Wear 260 (2006) 594-600.

[150] J. Jiang, R. D. Arnell, The effect of sliding speed on wear of diamond-like carbon coatings, Wear 218 (1998) 223-231.

[151] J. Jiang, S. Zhang, R. D. Arnell, The effect of relative humidity on wear of a diamond-like carbon coating, Surface and Coatings Technology 167 (2003) 221-225.

[152] I. L. Singer, S. Fayeulle, P. D. Ehni, Wear behavior of triode-sputtered MoS_2 coatings in dry sliding contact with steel and ceramics, Wear 195 (1996) 7-20.

[153] K. L. Johnson, Contact mechanics, Cambridge University Press, Cambridge, New York, Oakleigh, 1985.

[154] D. Galvan, Y. T. Pei, J. T. M. D. Hosson, Influence of deposition parameters on the structure and mechanical properties of nanocomposite coatings, Surface and Coatings Technology 201 (2006) 590-598.

[155] C. Rebholz, M. A. Monclus, M. A. Baker, P. H. Mayrhofer, P. N. Gibson, A. Leyland, A. Matthews, Hard and superhard TiAlBN coatings deposited by twin electron-beam evaporation, Surface and Coatings Technology 201 (2007) 6078-6083.

[156] L. Brabec, P. Bohac, M. Stranyanek, R. Ctvrtlik, M. Kocirik, Hardness and elastic modulus of silicalite-1 crystal twins, Microporous and Mesoporous Materials 94 (2006) 226-233.

[157] Y.-T. Cheng, C.-M. Cheng, Scaling, dimensional analysis, and indentation measurements, Materials Science and Engineering 44 (2004) 91-149.

[158] E. Bemporad, M. Sebastiani, C. Pecchio, S. D. Rossi, High thickness Ti/TiN multilayer thin coatings for wear resistant applications, Surface and Coatings Technology 201 (2006) 2155-2165.

[159] S. Zhang, D. Sun, Y. Fu, H. Du, Effect of sputtering target power on microstructure and mechanical properties of nanocomposite nc-TiN/a-SiN_x thin films, Thin Solid Films 447-448 (2004) 462-467.

[160] B. R. Lawn, A. G. Evans, D. B. Marshall, Elastic/plastic Indentation damage in ceramics: the median/radial crack system, Journal of the American Ceramic Society 63 (1980) 574.

[161] G. M. Pharr, Measurement of mechanical properties by ultra-low load indentation, Materials Science and Engineering A253 (1998) 151-159.

[162] A. Agüero, F. J. G. d. Blas, M. C. García, R. Muelas, A. Román, Thermal spray coatings for molten carbonate fuel cells separator plates, Surface and Coatings Technology 146-147 (2001) 578-585.

[163] J. Wagner, C. Mitterer, M. Penoy, C. Michotte, W. Wallgram, M. Kathrein, The effect of deposition temperature on microstructure and properties of thermal CVD TiN coatings, International Journal of Refractory Metals and Hard Materials 26 (2008) 120-126.

[164] T. Bell, K. Mao, Y. Sun, Surface engineering design: modelling surface engineering systems for improved tribological performance, Surface and Coatings Technology 108-109 (1998) 360-368.

[165] S. C. Lim, M. F. Ashby, Wear-mechanism Maps, Acta Metallurgica 35 (1987) 1-24.

[166] J. Jiang, R. D. Arnell, On the running-in behaviour of diamond-like carbon coatings under the ball-on-disk contact geometry, Wear 217 (1998) 190-199.

[167] V. Fridrici, Fretting d'un alliage de titane revêtu et lubrifié: application au contact aube/disque, Ph.D. thesis, Ecole Centrale de Lyon, 2002.

[168] A. Matthews, K. G. Swift, Intelligent knowledge-based systems for tribological coating selection, Thin Solid Films 109 (1983) 305-311.

[169] A. Matthews, A. Leyland, K. Holmberg, H. Ronkainen, Design aspects for advanced tribological surface coatings, Surface and Coatings Technology 100-101 (1998) 1-6.

[170] A. Matthews, K. Holmberg, S. Franklin, A methodology for coating selection, in: 19th Leeds-Lyon Symp. on Tribology: Thin films in tribology, Leeds, UK, 1992.

[171] A. Matthews, S. Franklin, K. Holmberg, Tribological coatings: contact mechanisms and selection, J. Phys. D: Appl. Phys. 40 (2007) 5463-5475.

[172] S. E. Franklin, J. A. Dijkman, The implementation of tribological principles in an expert-system ("PRECEPT") for the selection of metallic materials, surface treatments and coatings in engineering design, Wear 181-183 (1995) 1-10.

[173] S. E. Franklin, Coating selection and tribological testing for engineering equipment applications, TriboTest 14 (2008) 63-80.

[174] C. S. Syan, A. Matthews, K. G. Swift, Knowledge-based expert systems in surface coating and treatment selection for wear reduction, Surface and Coatings Technology 33 (1987) 105-115.

[175] L. A. Dobrzanski, J. Madejski, Prototype of an expert system for selection of coatings for metals, Journal of Materials Processing Technology 175 (2006) 163-172.

[176] D. Landru, Aides informatisées à la sélection des matériaux et des procèdes dans la conception de pièces de structure, Ph.D, Institut National Polytechnique de Grenoble, 2000.

[177] K. Schiffmann, M. Petrik, H. J. Fetzerb, S. Schwarz, A. Gemmler, M. Griepentrog, G. Reiners, INO – A WWW information system for innovative coatings and surface technology, Surface and Coatings Technology 153 (2002) 217-224.

[178] C. Langlade, B. Vannes, M. Taillandier, M. Pierantoni, Fretting behavior of low-friction coatings: contribution to industrial selection, Tribology International 34 (2001) 49-56.

[179] J. F. Carton, A. B. Vannes, G. Zambelli, L. Vincent, An investigation of the fretting behaviour of low friction coatings on steel, Tribology International 29 (1996) 445-455.

[180] H. C. Meng, K. C. Ludema, Wear models and predictive equations: their form and content, Wear 181-183 (1995) 443-457.

[181] S. M. Hsu, M. C. Shen, A. W. Ruff, Wear prediction for metals, Tribology International 30 (1997) 311-383.

[182] J. Alcock, O. Toft Sorensen, S. Jensen, P. Kjeldsteen, Comparative wear mapping techniques I. Friction and wear mapping of tungsten carbide/silicon carbide, Wear 194 (1996) 219-227.

[183] A. Skopp, M. Woydt, K. H. Habig, Tribological behavior of silicon nitride materials under unlubricated sliding between 22°C and 1000°C, Wear 181-183 (1995) 571-580.

[184] H. Chen, A. T. Alpas, Sliding wear map for the magnesium alloy Mg-9Al-0.9Zn (AZ91), Wear 246 (2000) 106-116.

[185] S. M. Hsu, M. C. Shen, Ceramic wear maps, Wear 200 (1996) 154-175.

[186] S. Wilson, A. T. Alpas, Effect of temperature and sliding velocity on TiN coating wear, Surface and Coatings Technology 94-95 (1997) 53-59.

[187] S. C. Lim, C. Y. H. Lim, Effective use of coated tools — the wear-map approach, Surface and Coatings Technology 139 (2001) 127-134.

[188] R. S. Fein, AWN - A proposed quantitative measure of wear protection, Lubr. Eng. 31 (1975).

[189] N. C. Welsh, The dry wear of steels I. The general pattern of behaviour, Philosophical Transactions of the Royal Society of London. Series A, Mathematical and Physical Sciences 257 (1965) 31-50.

[190] R. M. Matveevsky, The critical temperature of oil with point and line contact machines, Trans. ASTM 87 (1965) 754-760.

[191] M. A. Plint, The energy pulse: a new criterion and its relevance to wear in gear teeth and automotive engine valve trains, in: Proceeding of the XI NCIT, 1995.

[192] M. Z. Huq, J. P. Celis, Reproducibility of friction and wear results in ball-on-disc unidirectional sliding tests of TiN-alumina pairings, Wear 212 (1997) 151-159.

[193] S. Fouvry, P. Kapsa, H. Zahouani, L. Vincent, Wear analysis in fretting of hard coatings through a dissipated energy concept, Wear 203-204 (1997) 393-403.

[194] S. Fouvry, C. Paulin, T. Liskiewicz, Application of an energy wear approach to quantify fretting contact durability: Introduction of a wear energy capacity concept, Tribology International 40 (2007) 1428-1440.

[195] V. Fridrici, S. Fouvry, P. Kapsa, P. Perruchaut, Impact of contact size and geometry on the lifetime of a solid lubricant, Wear 255 (2003) 875-882.

[196] R. F. Smart, Selection of surfacing treatments, Tribology International 11 (1978) 97-104.

[197] M. Farrow, Selecting wear resistance surfaces, in: International Conference on Metallurgical coatings (ICMC 86), San Diego, USA, 1986.

[198] K.-H. Zum Gahr, Microstructure and Wear of Materials, Elsevier, Amsterdam, 1987.

[199] G. Barbezat, Application of thermal spraying in the automobile industry, Surface and Coatings Technology 201 (2006) 2028-2031.

[200] N. B. Dahotre, S. Nayak, Nanocoatings for engine application, Surface and Coatings Technology 194 (2005) 58-67.

[201] M. Dienwiebel, K. Pöhlmanna, M. Scherge, Origins of the wear resistance of AlSi cylinder bore surfaces studies by surface analytical tools, Tribology International 40 (2007) 1597-1602.

[202] Piston ring museum, RIKEN Corporation

[203] S. C. Tung, M. L. McMillan, Automotive tribology overview of current advances and challenges for the future, Tribology International 37 (2004) 517-536.

[204] A. Neville, A. Morina, T. Haque, M. Voong, Compatibility between tribological surfaces and lubricant additives — How friction and wear reduction can be controlled by surface/lube synergies, Tribology International 40 (2007) 1680-1695.

[205] http://www.aa1car.com/library/ar293.htm, AA1Car.

[206] H. L. MacLean, L. B. Lave, Evaluating automobile fuel/propulsion system technologies, Progress in Energy and Combustion Science 29 (2003) 1-69.

[207] M. Zhong, W. Liu, H. Zhang, Corrosion and wear resistance characteristics of NiCr coating by laser alloying with powder feeding on grey iron liner, Wear 260 (2006) 1349-1355.

[208] E. P. Becker, Trends in tribological materials and engine technology, Tribology International 37 (2004) 569-575.

[209] R. Gåhlin, M. Larsson, P. Hedenqvist, ME-C:H coatings in motor vehicles, Wear 249 (2001) 302-309.

[210] K. C. Radil, Test method to evaluate cylinder liner-piston ring coatings for advanced heat engines, NASA TM-107526 (1996).

[211] B. L. Ruddy, D. Dowson, P. N. Economou, A review of studies of piston ring lubrication, Proceedings of 9th Leeds-Lyon Symposium on Tribology: Tribology of Reciprocating Engines Paper V(i) (1982) 109-121.

[212] S. Uozato, K. Nakata, M. Ushio, Evaluation of ferrous powder thermal spray coatings on diesel engine cylinder bores, Surface and Coatings Technology 200 (2005) 2580-2586.

[213] T. S. Sudarshan, S. B. Bhaduri, Wear in cylinder liners, Wear 91 (1983) 269-279.

[214] K. Fursund, Wear in cylinder liners, Wear 1 (1957) 104-118.

[215] J. Keller, Etude de l'endommagement tribologique des chemises de moteurs Diesel poids lourds et optimisation des matériaux et états de surface, Ph.D thesis, Ecole Centrale de Lyon, 2006.

[216] J. R. G. Calow, S. R. Epton, Piston ring wear in the gasoline engine, in: Symposium on wear in the gasoline engine, Thornton Research Center, 1960.

[217] J. A. Picas, A. Forn, G. Matthäus, HVOF coatings as an alternative to hard chrome for pistons and valves, Wear 261 (2006) 477-484.

[218] F. Rastegar, D. E. Richardson, Alternative to chrome: HVOF cermet coatings for high horse power diesel engines, Surface and Coatings Technology 90 (1997) 156-163.

[219] R. Wei, E. Langa, C. Rincon, J. H. Arps, Deposition of thick nitrides and carbonitrides for sand erosion protection, Surface and Coatings Technology 201 (2006) 4453-4459.

[220] C. Friedrich, G. Berg, E. Broszeit, F. Rick, J. Holland, PVD Cr_xN coatings for tribological application on piston rings, Surface and Coatings Technology 97 (1997) 661-668.

[221] J. J. Truhan, J. Qu, P. J. Blau, A rig test to measure friction and wear of heavy duty diesel engine piston rings and cylinder liners using realistic lubricants, Tribology International 38 (2005) 211-218.

[222] H. Wang, W. Xia, Y. Jin, A study on abrasive resistance of Ni-based coatings with a WC hard phase, Wear 195 (1996) 47-52.

[223] M. B. Karamış, K. Yıldızlı, H. Çakırer, An evaluation of surface properties and frictional forces generated from Al–Mo–Ni coating on piston ring, Applied Surface Science 230 (2004) 191-200.

[224] G. Barbezat, Advanced thermal spray technology and coating for lightweight engine blocks for the automotive industry, Surface and Coatings Technology 200 (2005) 1990-1993.

[225] A. Edrisy, T. Perry, A. T. Alpas, Investigation of scuffing damage in aluminum engines with thermal spray coatings, Wear 259 (2005) 1056-1062.

[226] A. Skopp, N. Kelling, M. Woydt, L.-M. Berger, Thermally sprayed titanium suboxide coatings for piston ring/cylinder liners under mixed lubrication and dry-running conditions, Wear 262 (2007) 1061-1070.

[227] E. Buyukkaya, M. Cerit, Thermal analysis of a ceramic coating diesel engine piston using 3-D finite element method, Surface and Coatings Technology 202 (2007) 398-402.

[228] J. Vetter, G. Barbezat, J. Crummenauer, J. Avissar, Surface treatment selections for automotive applications, Surface and Coatings Technology 200 (2005) 1962-1968.

[229] P. J. Golden, M. J. Shepard, Life prediction of fretting fatigue with advanced surface treatments, Materials Science and Engineering A 468-470 (2007) 15-22.

[230] T. Nicholas, Critical issues in high cycle fatigue, International Journal of Fatigue 21 (1999) S221-S231.

[231] C. H. Hager-Jr, J. Sanders, S. Sharma, A. Voevodin, Gross slip fretting wear of CrCN, TiAlN, Ni, and CuNiIn coatings on Ti6Al4V interfaces, Wear 263 (2007) 430-443.

[232] S. Fouvry, P. Duó, P. Perruchaut, A quantitative approach of Ti–6Al–4V fretting damage: friction, wear and crack nucleation, Wear 257 (2004) 916-929.

[233] M. P. Szolwinski, J. F. Matlik, T. N. Farris, Effects of HCF loading on fretting fatigue crack nucleation, International Journal of Fatigue 21 (1999) 671-677.

[234] P. A. McVeigh, G. Harish, T. N. Farris, M. P. Szolwinski, Modeling interfacial conditions in nominally flat contacts for application to fretting fatigue of turbine engine components, International Journal of Fatigue 21 (1999) S157-S165.

[235] H. Murthy, D. B. Garcia, J. F. Matlik, T. N. Farris, Fretting fatigue of single crystal/polycrystalline nickel subjected to blade/disk contact loading, Acta Astronautica 57 (2005) 1-9.

[236] V. Fridrici, S. Fouvry, P. Kapsa, Fretting wear behavior of a Cu–Ni–In plasma coating, Surface and Coatings Technology 163-164 (2003) 429-434.

[237] P. J. Golden, A. Hutson, V. Sundaram, J. H. Arps, Effect of surface treatments on fretting fatigue of Ti–6Al–4V, International Journal of Fatigue 29 (2007) 1302-1310.

[238] H. Mohrbacher, B. Blanpain, J. P. Celis, J. R. Roos, L. Stals, M. V. Stappen, Oxidational wear of TiN coatings on tool steel and nitrided tool steel in unlubricated fretting, Wear 188 (1995) 130-137.

[239] V. Fridrici, S. Fouvry, P. Kapsa, Effect of shot peening on the fretting wear of Ti–6Al–4V, Wear 250 (2001) 642-649.

[240] D. Liu, B. Tang, X. Zhu, H. Chen, J. He, J.-P. Celis, Improvement of the fretting fatigue and fretting wear of Ti6Al4V by duplex surface modification, Surface and Coatings Technology 116-119 (1999) 234-238.

[241] Y. Fu, N. L. Loh, A. W. Batchelor, D. Liu, X. Zhu, J. He, K. Xu, Improvement in fretting wear and fatigue resistance of Ti–6Al–4V by application of several surface treatments and coatings, Surface and Coatings Technology 106 (1998) 193-197.

[242] L. Wu, B. C. Holloway, D. P. Beesabathina, C. Kalil, D. M. Manos, Analysis of diamond-like carbon and Ti–MoS_2 coatings on Ti–6Al–4V substrates for applicability to turbine engine applications, Surface and Coatings Technology 130 (2000) 207-217.

[243] C. H. Hager Jr, J. H. Sanders, S. Sharma, Unlubricated gross slip fretting wear of metallic plasma-sprayed coatings for Ti6Al4V surfaces, Wear 265 (2008) 439-451.

[244] B. Rajasekaran, S. G. S. Raman, S. V. Joshi, G. Sundararajan, Performance of plasma sprayed and detonation gun sprayed Cu–Ni–In coatings on Ti–6Al–4V under plain fatigue and fretting fatigue loading, Materials Science and Engineering A 479 (2007) 83-92.

[245] M. Shima, J. Okado, I. R. McColl, R. B. Waterhouse, T. Hasegawa, M. Kasaya, The influence of substrate material and hardness on the fretting behaviour of TiN, Wear 225-229 (1999) 38-45.

[246] Y. Fu, N. L. Loh, A. W. Batchelor, X. Zhu, K. Xu, J. He, Preparation and fretting wear behavior of ion-beam-enhanced-deposition CrN films, Materials Science and Engineering A265 (1999) 224-232.

[247] O. Jin, S. Mall, J. H. Sanders, S. K. Sharma, Durability of Cu–Al coating on Ti–6Al–4V substrate under fretting fatigue, Surface and Coatings Technology 201 (2006) 1704-1710.

[248] W. Ren, S. Mall, J. H. Sanders, S. K. Sharma, Evaluation of coatings on Ti–6Al–4V substrate under fretting fatigue, Surface and Coatings Technology 192 (2005) 177-188.

[249] K. J. Chun, J. H. Kim, J. S. Hong, A study of exhaust valve and seat insert wear depending on cycle numbers, Wear 263 (2007) 1147-1157.

[250] T. Hejwowski, Investigations of corrosion resistance of Fe-, Ni- and Co-based hardfacings, Vacuum 80 (2006) 1386-1390.

[251] T. Ootani, N. Yahata, A. Fujiki, A. Ehira, Impact wear characteristics of engine valve and valve seat insert materials at high temperature (impact wear tests of austenitic heat-resistant steel SUH36 against Fe-base sintered alloy using plane specimens), Wear 188 (1995) 175-184.

[252] R. Lewis, R. S. Dwyer-Joyce, G. Josey, An experimental approach to solving valve and seat wear problems, in: Proceedings of the 27th Leeds-Lyon Symposium on Tribology, Elsevier, Lyon, 2001.

[253] R. Lewis, R. S. Dwyer-Joyce, Combating automotive engine valve recession: a case study, Tribology and Lubrication Technology 59 (2003) 48-51.

[254] Y. S. Wang, S. Narasimhan, J. M. Larson, J. E. Larson, G. C. Barber, The effect of operating conditions on heavy duty engine valve seat wear, Wear 201 (1996) 15-25.

[255] K. Gebauer, Performance, tolerance and cost of TiAl passenger car valves, Intermetallics 14 (2006) 355-360.

[256] P. Kulu, T. Pihl, Selection criteria for wear resistant powder coatings under extreme erosive wear conditions, Journal Of Thermal Spray Technology 11 (2002) 517-522.

[257] X. M. Li, Y. Y. Yang, T. M. Shao, Y. S. Jin, G. Barbezat, Impact wear performances of Cr_3C_2-NiCr coatings by plasma and HVOF spraying, Wear 202 (1997) 208-214.

[258] J. G. Han, K. H. Nam, I. S. Choi, The shear impact wear behavior of Ti compound coatings, Wear 214 (1998) 91-97.

[259] S. Y. Yoon, S.-Y. Yoon, W.-S. Chung, K. H. Kim, Impact-wear behaviors of TiN and Ti–Al–N coatings on AISI D2 steel and WC–Co substrates, Surface and Coatings Technology 177-178 (2004) 645-650.

[260] A. A. Voevodin, R. Bantle, A. Matthews, Dynamic impact wear of TiC_xN_y and Ti-DLC composite coatings, Wear 185 (1995) 151-157.

[261] ASM, ASM Handbook. vol.13A. Corrosion: fundamentals, testing, and protection, ASM International, USA, 2003.

[262] http://stellite.com/ProductsServices/CoatingServices/tabid/218/Default.aspx, Deloro Stellite Group.

[263] http://www.sulzermetco.com/en/desktopdefault.aspx, Sulzer Metco Ltd.

[264] http://www.teercoatings.co.uk/index.php, Teer Coatings Ltd.

[265] J. Stallard, D. Mercs, M. Jarratt, D. G. Teer, P. H. Shipway, A study of the tribological behaviour of three carbon-based coatings, tested in air, water and oil environments at high loads, Surface and Coatings Technology 177-178 (2004) 545-551.

[266] http://www.gordonengland.co.uk/, Gordon England.

[267] http://www.brycoat.com/, BryCoat Inc.

[268] http://www.staff.ncl.ac.uk/s.j.bull/SENotes.html, Steve BULL.

[269] http://www.ionbond.com/dynasite.cfm?dsmid=84834, Ionbond.

[270] http://www.phelly.com/, Phelly Materials Inc.

[271] http://www.richterprecision.com/, Richter Precision Inc.

[272] http://www.wallcolmonoy.com/, Wall Colmonoy Corporation.

[273] K. Demmou, S. Bec, J.-L. Loubet, J.-M. Martin, Temperature effects on mechanical properties of zinc dithiophosphate tribofilms, Tribology International 39 (2006) 1558-1563.

[274] Y. Ye, J. Chen, H. Zhou, An investigation of friction and wear performances of bonded molybdenum disulfide solid film lubricants in fretting conditions, Wear 266 (2009) 859-864.

[275] S. Descartes, Y. Berthier, Rheology and flows of solid third bodies: background and application to an $MoS_{1.6}$ coating, Wear 252 (2002) 546-556.

ECOLE CENTRALE DE LYON

DIRECTION DE LA RECHERCHE

Liste des personnes Habilitées à Diriger des Recherches en poste à l'Ecole Centrale de Lyon

Nom-Prénom	*Corps grade*	Laboratoire ou à défaut département ECL	Etablissement
AURIOL Philippe	*professeur*	AMPERE	ECL
BEROUAL Abderrahmane	*professeur*	AMPERE	ECL
BURET François	*maître de conférences*	AMPERE	ECL
JAFFREZIC-RENAULT Nicole	*directeur de recherche*	AMPERE	CNRS/ECL
KRÄHENBÜHL Laurent	*directeur de recherche*	AMPERE	CNRS/ECL
MARTELET Claude	*professeur*	AMPERE	ECL
NICOLAS Alain	*professeur*	AMPERE	ECL
NICOLAS Laurent	*directeur de recherche*	AMPERE	CNRS/ECL
SIMONET Pascal	*chargé de recherche*	AMPERE	CNRS/ECL
THOMAS Gérard	*professeur*	AMPERE	ECL
VOLLAIRE Christian	*maître de conférences*	AMPERE	ECL
		Nbre Ampère 11	
HELLOUIN Yves	*maître de conférences*	DER EEA	ECL
LE HELLEY Michel	*professeur*	DER EEA	ECL
		Nbre DER EEA 2	
GUIRALDENQ Pierre	*professeur émérite*	DER STMS	ECL
VINCENT Léo	*professeur*	DER STMS	ECL
		Nbre DER STMS 2	
LOHEAC Jean-Pierre	*maître de conférences*	ICJ	ECL
MAITRE Jean-François	*professeur émérite*	ICJ	ECL
MARION Martine	*professeur*	ICJ	ECL
MOUSSAOUI Mohand	*professeur*	ICJ	ECL
MUSY François	*maître de conférences*	ICJ	ECL
ROUY MIRONESCU Elisabeth	*professeur*	ICJ	ECL
ZINE Abdel-Malek	*maître de conférences*	ICJ	ECL
		Nbre ICJ 7	
DAVID Bertrand	*professeur*	ICTT	ECL
		Nbre ICTT 1	
CALLARD Anne-Ségolène	*maître de conférences*	INL	ECL
CLOAREC Jean-Pierre	*maître de conférences*	INL	ECL
GAFFIOT Frédéric	*professeur*	INL	ECL
GAGNAIRE Alain	*maître de conférences*	INL	ECL
GARRIGUES Michel	*directeur de recherche*	INL	CNRS/ECL
GENDRY Michel	*directeur de recherche*	INL	CNRS/ECL
GRENET Geneviève	*directeur de recherche*	INL	CNRS/ECL
HOLLINGER Guy	*directeur de recherche*	INL	CNRS/ECL

JOSEPH Jacques	*professeur*	INL	ECL
KRAWCZYK Stanislas	*directeur de recherche*	INL	CNRS/ECL
LETARTRE Xavier	*chargé de recherche*	INL	CNRS/ECL
MARTIN Jean-René	*professeur émérite*	INL	ECL
O'CONNOR Ian	*maître de conférences*	INL	ECL
PHANER-GOUTORBE Magali	*professeur*	INL	ECL
ROBACH Yves	*professeur*	INL	ECL
SAINT-GIRONS Guillaume	*chargé de recherche*	INL	CNRS/ECL
SEASSAL Christian	*chargé de recherche*	INL	CNRS/ECL
SOUTEYRAND Eliane	*directeur de recherche*	INL	CNRS/ECL
TARDY Jacques	*directeur de recherche*	INL	CNRS/ECL
VIKTOROVITCH Pierre	*directeur de recherche*	INL	CNRS/ECL

Nbre INL 20

CHEN Liming	*professeur*	LIRIS	ECL

Nbre LIRIS 1

BAILLY Christophe	*professeur*	LMFA	ECL
BERTOGLIO Jean-Pierre	*directeur de recherche*	LMFA	CNRS/ECL
BLANC-BENON Philippe	*directeur de recherche*	LMFA	CNRS/ECL
BOGEY Christophe	*chargé de recherche*	LMFA	CNRS/ECL
CAMBON Claude	*directeur de recherche*	LMFA	CNRS/ECL
CARRIERE Philippe	*chargé de recherche*	LMFA	CNRS/ECL
CHAMPOUSSIN J-Claude	*professeur émérite*	LMFA	ECL
COMTE-BELLOT geneviève	*professeur émérite*	LMFA	ECL
FERRAND Pascal	*directeur de recherche*	LMFA	CNRS/ECL
GALLAND Marie-Annick	*maître de conférences*	LMFA	ECL
GODEFERD Fabien	*chargé de recherche*	LMFA	CNRS/ECL
GOROKHOVSKI Mikhail	*professeur*	LMFA	ECL
HENRY Daniel	*directeur de recherche*	LMFA	CNRS/ECL
JEANDEL Denis	*professeur*	LMFA	ECL
JUVE Daniel	*professeur*	LMFA	ECL
LE RIBAULT Catherine	*chargée de recherche*	LMFA	CNRS/ECL
LEBOEUF Francis	*professeur*	LMFA	ECL
PERKINS Richard	*professeur*	LMFA	ECL
ROGER Michel	*professeur*	LMFA	ECL
SCOTT Julian	*professeur*	LMFA	ECL
SHAO Liang	*chargé de recherche*	LMFA	CNRS/ECL
SIMOENS Serge	*chargé de recherche*	LMFA	CNRS/ECL
TREBINJAC Isabelle	*maître de conférences*	LMFA	ECL

Nbre LMFA 23

BENAYOUN Stéphane	*professeur*	LTDS	ECL
CAMBOU Bernard	*professeur*	LTDS	ECL
COQUILLET Bernard	*maître de conférences*	LTDS	ECL
DANESCU Alexandre	*maître de conférences*	LTDS	ECL
FOUVRY Siegfrid	*chargé de recherche*	LTDS	CNRS/ECL
GEORGES Jean-Marie	*professeur émérite*	LTDS	ECL
GUERRET Chrystelle	*chargé de recherche*	LTDS	CNRS/ECL
HERTZ Dominique	*past*	LTDS	ECL
ICHCHOU Mohamed	*maître de conférences*	LTDS	ECL
JEZEQUEL Louis	*professeur*	LTDS	ECL
JUVE Denyse	*ingénieur de recherche*	LTDS	ECL
KAPSA Philippe	*directeur de recherche*	LTDS	CNRS/ECL
LE BOT Alain	*chargé de recherche*	LTDS	CNRS/ECL

LOUBET Jean-Luc	*directeur de recherche*	LTDS	CNRS/ECL
MARTIN Jean-Michel	*professeur*	LTDS	ECL
MATHIA Thomas	*directeur de recherche*	LTDS	CNRS/ECL
MAZUYER Denis	*professeur*	LTDS	ECL
PERRET-LIAUDET Joël	*maître de conférences*	LTDS	ECL
SALVIA Michelle	*maître de conférences*	LTDS	ECL
SIDOROFF François	*professeur*	LTDS	ECL
SINOU Jean-Jacques	*maître de conférences*	LTDS	ECL
STREMSDOERFER Guy	*professeur*	LTDS	ECL
THOUVEREZ Fabrice	*professeur*	LTDS	ECL
TREHEUX Daniel	*professeur*	LTDS	ECL
VANNES André-Bernard	*professeur émérite*	LTDS	ECL
		Nbre LTDS 25	
	Total HdR ECL	91	

dernière page de la thèse

AUTORISATION DE SOUTENANCE

Vu les dispositions de l'arrêté du 7 août 2006,

Vu la demande du Directeur de Thèse

Monsieur Ph. KAPSA

et les rapports de

Monsieur A. RAMALHO
Professeur - Mechanical Engineering Department - Faculty of Sciences and Technology, Polo II
3030 Coimbra - Portugal

et de

Monsieur C. LANGLADE
Professeur - LERMPS - Université de Technologie de Belfort Montbéliard - 90010 BELFORT cedex

Monsieur LUO Dabing

est autorisé à soutenir une thèse pour l'obtention du grade de **DOCTEUR**

Ecole doctorale MATERIAUX

Fait à Ecully, le 17 septembre 2009

P/Le Directeur de l'E.C.L.
La Directrice des Etudes

ECOLE CENTRALE DE LYON
SCOLARITE
3ème Cycle
M-A. GALLAND